Functional characterization of the synaptic-activity regulated gene Synaptotagmin10

Dissertation

zur

Erlangung des Doktorgrades (Dr. rer. nat.)

der

Mathematisch-Naturwissenschaftlichen Fakultät

der

Rheinischen Friedrich-Wilhelms-Universität Bonn

vorgelegt von

Anne Maria Helena Woitecki

aus

Oberhausen

Bonn 2013

Angefertigt mit Genehmigung der Mathematisch-Naturwissenschaftlichen Fakultät

der Rheinischen Friedrich-Wilhelms-Universität Bonn

1. Gutachter: Prof. Dr. Susanne Schoch

2. Gutachter: Prof. Dr. Albert Haas

Tag der mündlichen Prüfung: 22.11.2013

Erscheinungsjahr: 2013

Diese Dissertation ist auf dem Hochschulschriftenserver der ULB Bonn

unter http:// hss.ulb.uni-bonn.de/diss_online elektronisch publiziert.

Erklärung

Diese Dissertation wurde im Sinne von § 4 der Promotionsordnung vom 17.6.2011 am Institut für Neuropathologie und Klinik für Epileptologie der Universität Bonn unter der Leitung von Frau Prof. Dr. Susanne Schoch angefertigt.

Hiermit versichere ich an Eides statt, dass ich die vorliegende Arbeit selbständig angefertigt habe und keine weiteren als die angegebenen Hilfsmittel und Quellen verwendet habe, die gemäß § 6 der Promotionsordnung kenntlich gemacht sind.

Bonn, den _____   _____

                                        Anne Woitecki

1 Introduction

1.1 Epilepsy, a neurodevelopmental disorder

Epilepsy is a neurodevelopmental disorder affecting almost 1 % of the population all over the world (Elger 2002; Fisher et al. 2005). Neurodevelopmental disorders comprise diseases that develop early in brain or as a consequence of head trauma, a tumor or an infection in the adult brain and span throughout life. Although the underlying etiology of the various disorders might be different, all of them lead to similar brain dysfunctions (defects of the sensory and motor system) and to comparable cognitive deficits in learning and memory. Epilepsy represents a complex and multifactorial disease which is accompanied by neuropathological changes (particular neuronal degeneration, structural reorganization) that accumulate during progression of the disorder (Elger 2002). Due to the multifactorial component it is not defined as one disorder but as a group of diverse conditions, leading into an enhanced predisposition to epileptic seizures. Epilepsy is nowadays demarcated as a condition with (1) a history of at least one seizure, (2) a persistent brain alteration (measured by electroencephalography (EEG)) with the probability of upcoming seizures and (3) the association with neurobiologic, cognitive, psychological and social impairments (Fisher et al., 2005). Epilepsies develop mostly in late childhood or adolescence starting with an initial insult (febrile seizures, head trauma, infections or tumors) resulting in a process called epileptogenesis (or latency period). This process, starting during the initial insult and ending with the occurrence of the first spontaneous seizure, is highly dynamic, leading to alterations in network excitability and to structural reorganization (reviewed by Pitkänen & Lukasiuk 2011).

1.2 Epilepsy animal models

For an efficient treatment of epilepsy it is essential to shed light on the molecular pathways underlying epileptogenesis. However, human tissue samples from patients that underwent surgery due to intractable epilepsy are obtained from the end stage of a long and complex treatment period. To overcome the lack of human tissue samples from the stage of epileptogenesis and the absence of human control tissue samples, many animal models have developed over the years. The widely used animal models to study temporal lobe epilepsy (TLE), which is the most common type of partial

complex seizures in adulthood (Hauser et al., 1996; Wieser & Häne, 2004), are post-status epilepticus (SE) models. Self-sustained SE is induced (1) by persistent electrical stimulation of the hippocampus or (2) by injection of epileptogenic compounds at convulsant doses (pilocarpine or kainic acid). The acquired changes lead to segmental neuronal cell loss in the hippocampus and to the occurrence of spontaneous recurrent seizures after a latency period of 3-4 weeks after SE (reviewed by Majores et al. 2007; reviewed by Löscher 2002). However, there are differences in the neuropathological changes observed after pilocarpine compared to kainic acid-induced SE: Neuronal injury seems to be different in extent and regional distribution within the hippocampal formation (CA1 or CA3/CA4) and appears to be less variable after the use of pilocarpine compared to kainic acid (KA) (reviewed by Majores et al. 2007). Yet, epileptogenesis occurs after both, pilocarpine and kainic acid-induced SE.

1.3 Epileptogenesis

Epileptogenesis describes a process in which an initial insult triggers multiple cellular and molecular changes finally resulting in recurrent spontaneous seizures. The occurrence of various acquired alterations includes structural reorganization, neurodegeneration, blood-brain barrier disruption, recruitment of inflammatory cells into brain tissue and cellular plasticity (Figure 1.1). Due to the multifactorial nature of the disease, many investigators try to unravel the molecular pathways underlying the circuitry reorganization by analyzing gene expression at the whole transcriptome level. Most of the studies vary among each other regarding the animal model for epilepsy, the time point after SE or the array platform used. Nevertheless, there are genes that are commonly altered, which possess rather general functions (signal transduction or transcription) but also specific functions associated with epileptogenesis (ion transport, synaptic transmission and plasticity, inflammation, channel/receptor function and neurotransmitter metabolism) (reviewed by Pitkänen & Lukasiuk 2011).
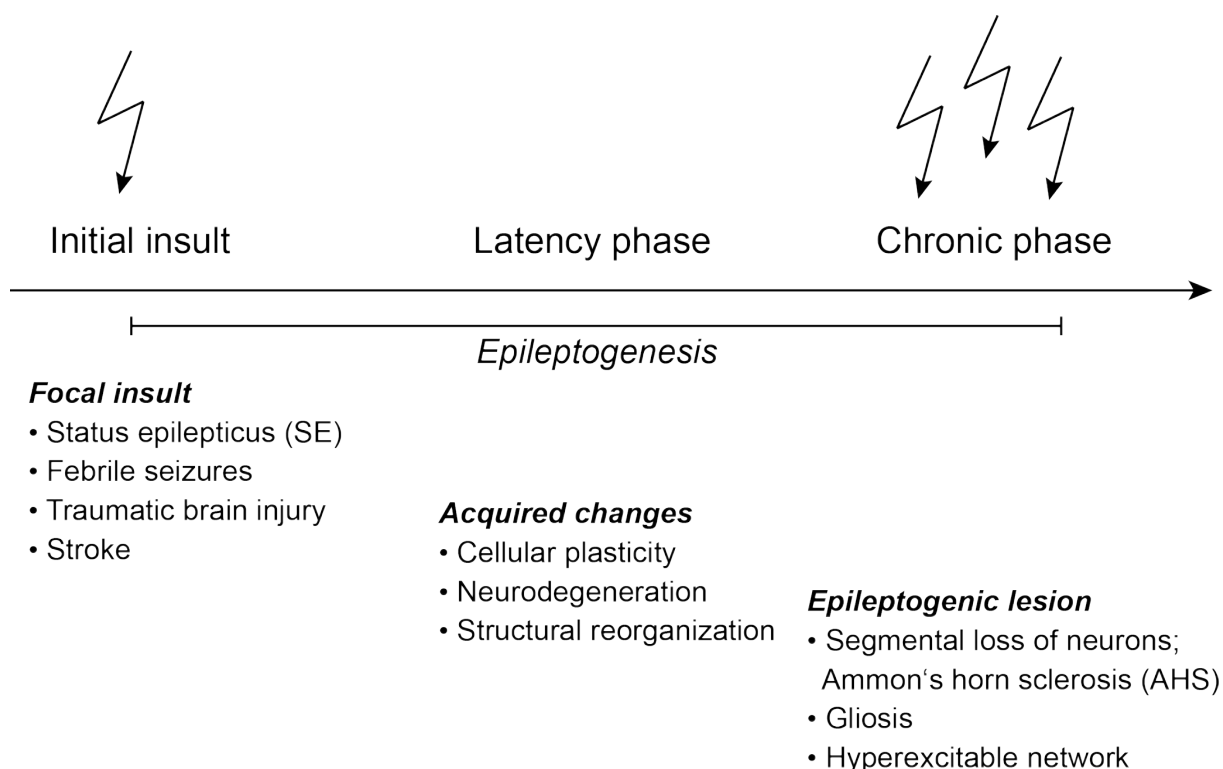
Figure 1.1 Pathogenetic concept of temporal lobe epilepsy (TLE). Schematic drawing of different stages in the pathogenesis of TLE and of the corresponding hallmarks. Modified from Majores et al., 2007.

1.4 Mechanisms underlying epileptogenesis

1.4.1 Transcriptional regulation

Changes in gene expression are an important link between external stimuli and intracellular responses. Through binding of *trans*-acting transcription factors to *cis*-acting DNA regions, such as enhancers and promoters, regulated gene expression can mediate developmental changes, cell survival and division (Figure 1.2). In mature neurons, altered activity levels might induce long-lasting changes in neuronal gene expression, forming the molecular basis for synaptic plasticity. Common sequence elements like a TATA box or an initiator sequence and binding sites for general transcription factors are found in most of the promoters and might be considered as characteristics for a so called core promoter. These elements are important for recruitment of the transcription machinery to the transcription start site (TSS) and lead to basal activity of a promoter (Figure 1.2 Step 1). Enhancers, which are usually located upstream or downstream of the TSS, also contain transcription factor binding sites. However, when DNA sequence specific transcription factors bind to *cis*-elements in the proximal part of the promoter, general transcription is

enhanced by stabilizing the binding of general factors via site-specific factors (Figure 1.2 Step 2). Further stimulation of a promoter is achieved by binding of site-specific factors to an enhancer region (Figure 1.2 Step 3). Another interaction, which is thought to enhance promoter activity in a cell-type specific manner, is the interaction of cell-type specific co-activators with bound factors. A more favorable chromatin environment (by histone acetylation) is achieved through these factors, which leads either to recruitment of histone-modifying enzymes (i.e. histone acetyltransferase (HAT)) (Figure 1.2 Step 4) or to recruitment of a kinase and subsequent phosphorylation of RNA polymerase II followed by stimulation of elongation (Figure 1.2 Step 5). Not only activating factors bind to *cis*-elements, there are also repressing factors leading to interference with activator binding or to repressive chromatin structures (reviewed by Farnham 2009).
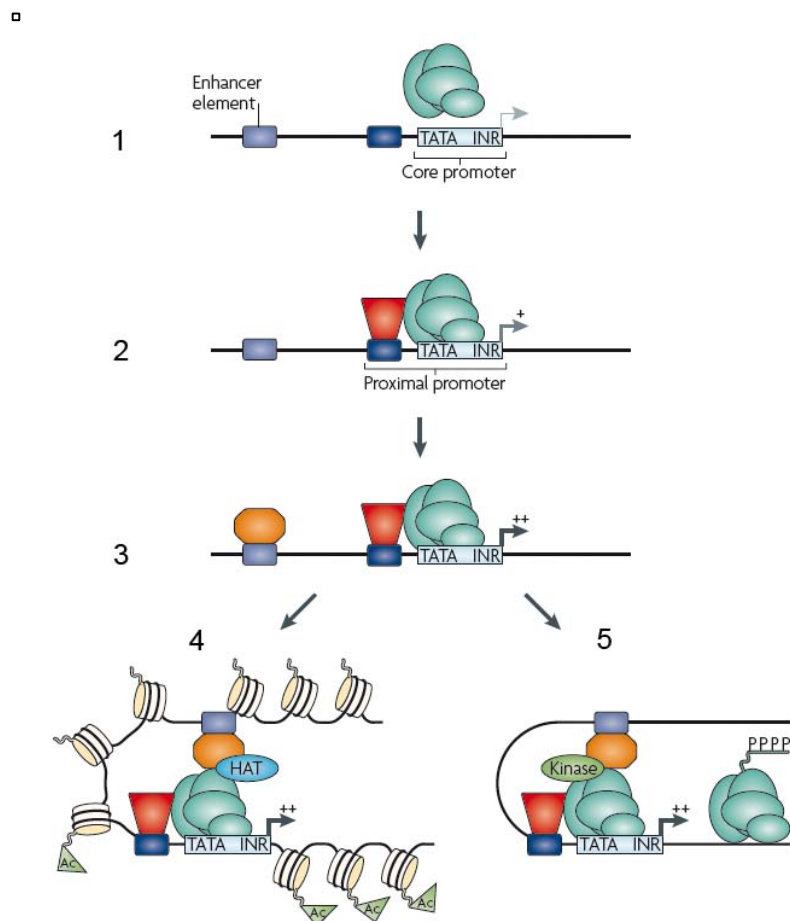
Figure 1.2 Mechanism of transcriptional regulation by promoters and enhancers. Diagram depicts distinct states of promoter regulation. Step 1: Basal transcription with universal transcription factors (green spheres) bound to the core promoter. Step 2: Increased transcription (+) through stabilization of the transcription machinery via bound site-specific factors (red triangle) to *cis* elements (dark blue box). Step 3: Further enhanced transcription (++) by binding of site-specific factors (orange box) to enhancers (light blue box). Stimulation of transcription by Step 4: Recruitment of histone acetyltransferase (HAT) or by Step 5: Phosphorylation of RNA polymerase II via a kinase and subsequent elongation. TATA: TATA box, INR: initiator, P: Phosphorylation, Ac: histone acetylation. Modified from Farnham 2009.

1.4.2 Mechanisms of activity-dependent gene transcription

Two of the most extensively studied activity-regulated genes are Brain-derived neurotrophic factor (*BDNF*) and Activity-regulated cytoskeletal protein (*Arc/Arg3.1*). *BDNF* reacts to neural activity with expression of *BDNF* mRNA in the activated brain area and thereby regulates local secretion of BDNF protein and transport of the BDNF receptor to the plasma membrane. BDNF is essential for neuronal differentiation and growth, synapse formation and plasticity and higher cognitive functions (Park & Poo, 2013). Therefore, the function of BDNF depends strongly on the exact temporal and spatial control of BDNF expression. Recently, the promoter underlying this tight control mechanism has been characterized in numerous studies (reviewed by Lyons & West 2011). Transcription factors mediating the induction of neuronal activity regulated Exon I of the rat *BDNF* gene are CREB, USFs, MEF2D, NFkB and additionally for the human *BDNF* gene NPAS4 was identified (Tabuchi et al., 2002; Lubin et al., 2007; Flavell et al., 2008; Pruunsild et al., 2011).

Transcription of *Arc* is increased by synaptic activity that is mediated by a proximal promoter and a distal enhancer element named synaptic activity response element (SARE). Some transcription factors regulating *Arc* transcription have already been identified namely Egr1/3 binding the proximal promoter and SRF binding with co-activator a ternary complex factor (TCF) the serum response element (SRE) (Posern & Treisman, 2006). A possible role for MAL acting as another co-activator of SRE has been postulated recently (Zaromytidou et al., 2006). Besides a SRE, a cAMP response element (CRE) site, a myocyte enhancer factor 2 (MEF2) site and a Zeste-like response element (ZRE) have been identified and binding of CREB and MEF2 are confirmed (Kawashima et al., 2009; Pintchovski et al., 2009). However, besides the yet unknown binding factors acting through the novel ZRE, there might be other unknown transcription factors regulating the transcription of Arc (reviewed by Korb & Finkbeiner 2011).

Altered transcription of a given gene has an impact on disease progression as it may lead to changes in intrinsic and synaptic plasticity. Many genes have been identified as differentially expressed during epilepsy.

1.4.3 Altered transcription during epilepsy

Whole transcriptome studies have revealed a large number of genes that are differentially expressed during epileptogenesis. However, only few candidate genes have been studied in further detail concerning their functional significance in epileptogenesis. One differentially changed gene that has been studied in detail with regard to epileptogenesis is the $GABA_A$ receptor. Brooks-Kayal et al. analyzed in 1998 $GABA_A$ receptor subunit expression in dentate granule cells via single cell mRNA amplification and found that $GABA_A$ receptor subunit expression was altered in pilocarpine-treated rats. This change was already observed at the latent phase (before the onset of spontaneous seizures) indicating that altered $GABA_A$ receptor subunit expression may influence epileptogenesis. Functional analyses from the same study suggested that these dentate granule cells reveal a higher sensitivity to zinc indicating that the GABA-mediated inhibition is altered during epilepsy and that these changes are essential for the process of epileptogenesis (Brooks-Kayal et al., 1998).

The T-type Ca^{2+}-channel $Ca_v3.2$ is another channel with a transient up-regulation on the mRNA and protein level in pilocarpine-treated rats leading to functional changes in the intrinsic burst firing and an increase in cellular T-type Ca^{2+}-currents (Becker et al. 2008). Recently, the underlying transcriptional changes mediating the induction of $Ca_v3.2$ after SE were uncovered (van Loo et al., 2012). The promoter driving $Ca_v3.2$ expression was found to be regulated bi-directionally by the transcription factors early growth factor 1 (Egr1) (activation) and repressor element 1-silencing transcription factor (REST) (repression) resulting in increased Ca^{2+}-currents in neuroblastoma NG108-15 cells overexpressed with Egr1. Understanding the mechanisms regulating epileptogenesis represents a possibility to interfere with the phenotype that might have an essential role in epileptogenesis.

1.4.4 Membrane trafficking

Structural reorganization during epileptogenesis is dependent on the insertion and removal of membranous organelles. To accommodate the changing intracellular distribution of a wide range of proteins, vesicles and other membranous organelles move along distinct pathways and finally fuse with the plasma membrane or with other components in a process known as membrane trafficking. The distinct steps of this process include cargo selection, budding and fission of vesicles from a donor

organelle, transport of cargo via microtubules and actin filaments, association of vesicles with the exact target membrane and finally fusion of vesicles with the target via requisite SNARE proteins (Hutagalung & Novick, 2011).

In eukaryotic cells, two major pathways of membrane traffic exist: (A) the secretory pathway from the Endoplasmatic Reticulum (ER) to *cis*-Golgi membranes via the ER to Golgi Intermediate Compartment (ERGIC) and (B) the endocytic pathway where endocytosed material is transported to early sorting endosomes. From there, organelles are either delivered back to the plasma membrane, are sorted by slow transport processes to the plasma membrane via recycling endosomes or are degraded in lysosomes (reviewed by Blackstone et al., 2011).

Trafficking in neurons is even more complex given that protein cargo needs to be sorted and transported long distances to their target, to the active zone or to dendrites. To achieve maintenance of dendrites by local biosynthesis of lipids and proteins, the ER extends into all dendrites but the Golgi Apparatus is outposted only to several dendrites (Hanus & Ehlers, 2008). Axon outgrowth is accomplished differently due to the lack of Golgi outposts in axons (reviewed by Horton & Ehlers, 2003; Ye et al., 2007). Sorting of synaptic vesicle (SV) proteins relies on signal sequences for axonal transport and different proteins use distinct pathways indicating that the transport mechanism might be unique for its protein cargo.

Communication of neurons occurs at highly specialized sites of the synapse. For this, an additional form of membrane traffic is essential, the synaptic vesicle exocytosis. This unique form of Ca^{2+}-ion triggered fast membrane fusion can be categorized into distinct steps, the SV loading, docking of SVs to the site of fusion, priming, which renders the SVs competent to fuse, and finally fusion. Two forms of exocytosis exist, namely synaptic exocytosis of small SVs in presynaptic nerve terminals and hormonal (endocrine) exocytosis of large dense core vesicles (LDCVs) in endocrine cells. The machinery of this complex process involves proteins specialized for distinct steps of the synaptic vesicle cycle. One class of proteins that is critically involved in the fusion of the two membranes is the Synaptotagmin (Syt) family, a class of Ca^{2+}-binding proteins (reviewed by Südhof, 2002, 2012; reviewed by Chapman, 2008). Influx of Ca^{2+}-ions into the presynaptic bouton triggers the binding of e.g. Syt1 to membrane lipids and SNARE proteins. Consequently, full assembly of the partially zippered SNARE-complex leads to fusion pore opening and to complete fusion of the vesicle membrane with the plasma membrane. As calcium sensors, Syts are crucial

for the synaptic vesicle cycle and due to the complexity of the Syt family, it is thought that they facilitate different forms of membrane trafficking pathways (Dean, et al. 2012).

1.5   Synaptotagmin gene family

Syts comprise a large family of membrane trafficking proteins that are evolutionary conserved (Craxton, 2001, 2004). First, Syt1 was described in 1981 as a vesicle-specific membrane protein, p65, localized to SVs and LDCVs in neurons and neuroendocrine cells, identified by a screen for synaptic proteins with monoclonal antibodies (Matthew et al., 1981). Later, two C_2-domains were identified in Syt1 and these domains were suggested to function as Ca^{2+}-sensors for vesicle exocytosis (Perin et al. 1990). Subsequently, other Syts were described in vertebrates. Whereas in Drosophila, seven Syt isoforms have been identified (Syt1, 4, 7, 12, 13, 16 and Syt alpha), only four isoforms were found in *Caenorhabditis elegans* (Syt1, 4, 7, and Syt alpha) (Craxton, 2010). According to bioinformatical analyses, mammalian Syts comprise 17 isoforms (Syt1-17) (Craxton, 2010). However Pang et al. included only 16 isoforms into the mammalian Syt gene family due to the lack of a transmembrane domain in Syt17 (reviewed by Pang & Südhof 2010). Since many members of the Syt gene family were discovered in recent years, there is a constant change of nomenclature. For example, the latest members of the Syt family, Syt16 and 17 (which is still debated), were formerly referred to as Strep 14 (Syt14-related protein) and B/K protein (brain/kidney protein), respectively (reviewed by Gustavsson & Han 2009).

1.5.1   Synaptotagmin protein domain structure

Syts share a common protein structure including an N-terminal intraluminal domain, an extracellular tail, a central variable linker and two C-terminal tandem C_2-domains (Perin et al. 1991) (Figure 1.3 A).

A

Synaptotagmin
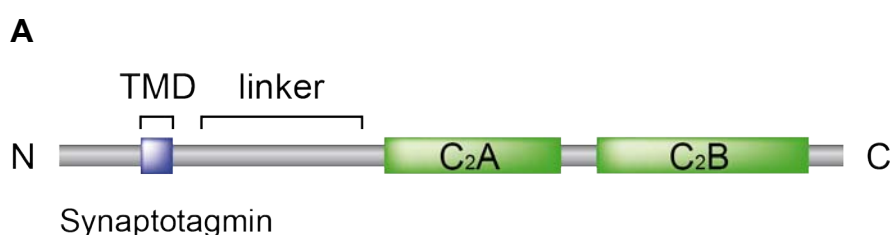
B
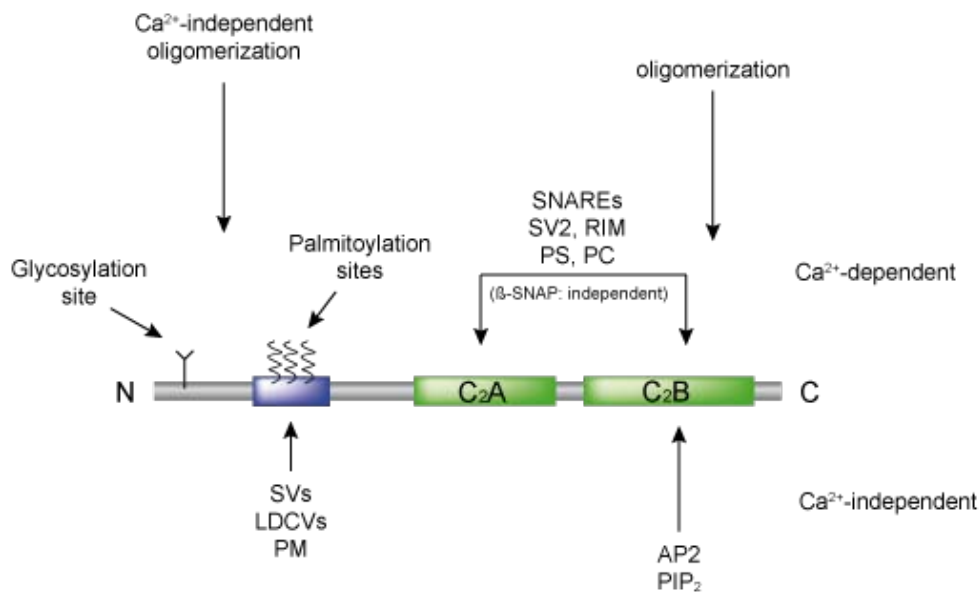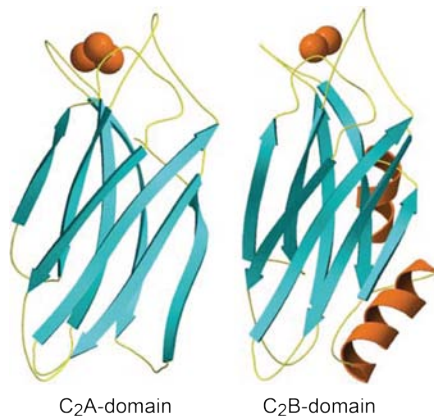
C   **D**
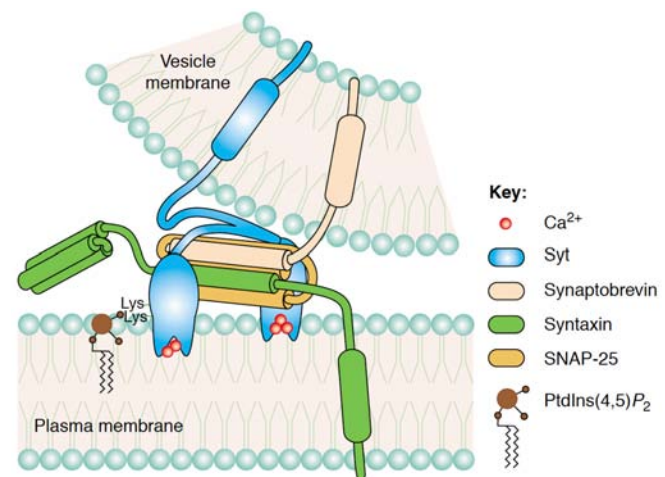
Figure 1.3 Syt domains, crystal structure and the Ca^{2+}-activated membrane fusion complex. (A) Schematic drawing of structural protein domains of Syts. N: N-terminus, TMD: transmembrane domain, C$_2$A: C$_2$A domain, C$_2$B: C$_2$B domain, C: C-terminus. Scaling based on the isoform Syt10. (B) Interaction sites and binding partners of Syt1. Note that interactions vary between different Syt isoforms and have to be studied in detail for others. SVs: synaptic vesicles, LDCVs: Large dense core vesicles, PM: plasma membrane, SNAREs: Soluble NSF-attachment protein receptor, SV2: synaptic vesicle protein 2, PS: phosphatidylserine, PC: phosphatidlycholine, PIP$_2$: phosphatidylinositol 4,5-bisphosphate, AP2: clathrin assembly (adapter) protein 2. (C) Atomic structure of the Syt1 C$_2$ domains formed by an eight-stranded ß-sandwich. The C$_2$A and the C$_2$B domain contain 3 and 2 bound Ca^{2+}-ions, respectively (red spheres). Picture was taken from Südhof 2012. (D) Model for the Ca^{2+}-activated membrane fusion complex. In response to Ca^{2+} the C$_2$A and C$_2$B binding loops insert into the bilayer and directly interact with the SNARE complex (Synaptobrevin, Syntaxin, SNAP-25). SNAP-25: synaptosome-associated protein of 25 kDa. Picture was taken from Bai and Chapman, 2004.

The N-terminal transmembrane domain serves to anchor the Syt proteins in synaptic, secretory vesicles or plasma membranes whereas the C$_2$-domains form binding pockets for Ca^{2+} (Brose et al. 1992; Davletov & Südhof 1993; Chapman & Jahn

1994). The central linker region varies in each Syt isoform and is the region with the highest sequence dissimilarity among the different isoforms. The different protein domains of Syts form contacts with distinct binding partners and thus exhibit diverse functions (Figure 1.4 B).

The N-terminus was shown to vary among the isoforms and therefore exhibits interactions that are not common to all Syt isoforms. Syt1 and Syt2 possess sites for N-glycosylation, which was shown in rat pheochromocytoma (PC12) cells to direct Syt1 to secretory vesicles and to be important for the readily releasable pool of SVs in neurons (Han et al. 2004). In non-neuronal cells, N-terminal O-glycosylation seems to mediate sorting of Syt1 and 2 to secretory vesicles (Atiya-Nasagi et al. 2005; Kanno & Fukuda 2008). However, a contradictory report showed that neither N- nor O-glycosylation is important for the sorting of Syt1 to SVs (Kwon & Chapman 2012). Another posttranslational modification shown to be important for Syts is palmitoylation (Figure 1.4 B). It has been proposed that it facilitates targeting of Syts to SVs (Prescott et al., 2009). There is evidence that Syt1 and Syt7 are targeted by palmitoylation to SVs and lysosomes, respectively (Veit et al. 1996; Heindel et al. 2003; Flannery et al. 2010). If not palmitoylated, these Syts are transported and anchored in the plasma membrane via their transmembrane domain.

Some of the Syts contain a cluster of cysteine residues specifically at the N-terminus (Syts 3, 5, 6, 10) (Fukuda et al. 1999a) or at the transmembrane region (Fukuda et al. 2001a) and might thereby be palmitoylated. Disulfide-bonded homodimerization as well as heterodimerization has been found to depend on cysteine residues in a subgroup of Syts, namely comprising Syts 3, 5, 6 and 10 (Fukuda et al. 1999a). Furthermore, it has been shown that both the TMD (Lewis et al., 2001) and the linker region (Fukuda et al. 2001b) are critical for Ca^{2+}-independent oligomerization but neither of the domains is sufficient (reviewed by Tucker & Chapman 2002). The most conserved protein domains of Syts are the C_2-domains that are composed of ß-sheets connected by loops (Rizo & Südhof 1998) (Figure 1.3 C). The Syt1 C_2A domain binds three Ca^{2+}-ions with an evident affinity of ~60-75 µM, ~400-500 µM and more than 1 mM (Ubach et al., 1998) and the C_2B domain of Syt1 forms two binding pockets for Ca^{2+}-binding with a similar affinity in the range of ~300-600 µM (Fernández-Chacón et al. 2001) (Figure 1.3 C). However, the Ca^{2+}-affinity of the C_2-domains is distinct in the different Syt isoforms. Both C_2-domains bind to phospholipids in a Ca^{2+}-dependent manner (Davletov & Südhof 1993; Fernández-

Chacón et al. 2001) and to SNARE proteins (Figure 1.3 D) (Bennett et al. 1992; Chapman et al. 1995; Li 1995). Whereas both C_2-domains bind to phosphatidlycholine (PC) and phosphatidylserine (PS), only the C_2B domain binds to phosphatidylinositol 4,5-bisphosphate (PI(4,5)P2) (Radhakrishnan et al., 2009).

The exact mode of C_2-domain function is still unclear. There is evidence from Doc2 proteins, that the C_2B domain blocks synchronous exocytosis whereas blocking Ca^{2+}-binding to the C_2A-domain decreases exocytosis only by approximately 40 % thus indicating that the C_2B-domain is more relevant for exocytosis (Pang et al., 2011). Oppositional results demonstrate that Syt's C_2A domain is essential for synchronous synaptic transmission whereas the C_2B domain only serves for fine-tuning of this process (Striegel et al., 2012). It is thought, however, that the C_2-domains function cooperatively (reviewed by Südhof 2012). Both C_2-domains have been shown to bind the clathrin assembly (adapter) protein 2 (AP2) and thereby function as a dual Ca^{2+}-sensor for both, exo- and endocytosis (Zhang et al. 1994; Yao et al. 2012). In a Ca^{2+}-dependent manner, C_2A and C_2B domains bind to SV2 (Schivell et al. 1996; Schivell et al. 2005; Lazzell et al. 2004) and to RIM (Coppola et al., 2001).

1.5.2 Classification of Synaptotagmins

The highly homologous family of Syt proteins can be divided in subgroups and they can be classified based on their ability to bind Ca^{2+} or by their sequence homology. Regarding their binding properties, Syts can be divided into Ca^{2+}-dependent isoforms, namely Syt1, 2, 3, 5, 6, 7, 9, 10. From this subgroup, only Syts 3, 5, 6 and 10 contain evolutionary conserved disulfide-bonded cysteine residues. Syts 4, 8 and 11-16 comprise a group of Ca^{2+}-independent Syts. The Ca^{2+}-independent Syts can be further divided into conserved isoforms (Syt4 and 11 and 14-16) and into a heterogeneous subgroup of non-conserved isoforms (Syt8, 12 and 13) (reviewed by Südhof 2012). In an evolutionary genomics approach, Syts were grouped by means of gene duplications trying to determine the phylogenetic relationships between vertebrate and invertebrate isoforms (Craxton, 2010). The classification described here, however, relies on protein structure similarities. Other multiple C_2-domain proteins (with and without a transmembrane domain) have been described and it has been suggested that, due to their structural homology, they might be good candidates for exocytotic Ca^{2+}-sensors. Besides Syts, three other protein classes of multiple C_2-domains with a transmembrane domain are encoded in the mammalian

genome: (1) extended Syts (E-Syt1-3), (2) Multiple C_2-transmembrane proteins (MCTPs) and (3) ferlins. Moreover, a large group of soluble C_2-domain proteins lacking a transmembrane domain was identified, consisting of Copines and Syt-like proteins (SLPs) (reviewed by Pang & Südhof 2010).

1.5.3 Expression of Synaptotagmins

Except for Syts 8, 14 and 15, that lack expression in the brain, mRNA expression of all Syts has been detected in the rodent brain in distinctive expression patterns (Fukuda 2003b, a; Mittelsteadt et al., 2009). Syts 1, 3, 4, 5, 7, 11, 12 and 13 are universally expressed in most brain areas, whereas the remaining isoforms Syt2, 6, 9 and 10 are restricted to distinct regions of the brain. Syt2 is mainly expressed in the hindbrain and brainstem, Syt6 and 10 are specifically enriched in the olfactory bulb, the cerebellum and the hippocampus. However, strong Syt10 expression is found mainly in the olfactory bulb. Finally, Syt9 expression is detected in the cerebellum, the olfactory bulb, the thalamus and the putamen (Mittelstaedt et al., 2009).

Similar to the distinct distribution of Syts throughout the brain, likewise the subcellular localization of the isoforms is very specific. Syts 1, 2, 9 and 12 were shown to be localized on SVs (Matthew et al. 1981; Poser et al. 1997; Xu et al. 2007; Maximov et al. 2007). Based on pHluorin experiments, Syt9 and 12 were suggested to localize on distinct vesicle subtypes (Dean, et al. 2012a). The above mentioned isoforms (1, 2, 9, 12) are also present on secretory granules in neuroendocrine cells (reviewed by Südhof 2012). Syt1 was found additionally in LDCVs of neuroendocrine PC12 cells where Syts 4, 7 and 9 are expressed as well (Fukuda et al. 2004a, b; Wang et al. 2003; Wang & Chicka 2005). Syt2, besides Syts 3, 5 and 9 (Melicoff et al. 2009; reviewed by Baram et al. 2001; Haberman et al. 2007; Grimberg 2002) was identified as the major isoform present on lysosomes of mast cells (Baram et al., 1999). In addition to LDCVs, Syt4 was found to localize to the Golgi complex (Ibata et al., 2000; Matsuoka et al., 2011), to postsynaptic organelles in Drosophila (Adolfsen et al., 2004), to peptidergic nerve terminals and to neurotrophin-containing dense-core vesicles in hippocampal neurons (Zhang et al. 2009; Dean et al. 2009). Besides Syt1 and 9, Syt7 is the predominant isoform in granules of rat adrenal chromaffin cells (Matsuoka et al., 2011).

The subcellular localization of Syts 3 and 6 remains uncertain as they are thought to be enriched at the plasma membrane (Butz et al., 1999; Saegusa et al., 2002) but

were also identified on secretory granules (Brown et al., 2000; Gao et al., 2000; Falkowski et al., 2011), the Golgi/ER complex (Fukuda et al. 1999b) and on endosomal compartments. Syt5 is localized to phagosomes (Vinet et al., 2008) and to LDCVs in PC12 cells (Saegusa et al., 2002). Until recently, the localization of Syt10 was uncertain. It has been reported, that Syt10 is present on secretory vesicles containing insulin-like growth factor 1 (IGF-1) in olfactory bulb mitral neurons (Cao et al., 2011). As Syt10, also IGF-1 is intensely expressed in the olfactory bulb (Rotwein et al., 1988). Moreover, Syt10 mRNA expression is also detected in pancreas, lung and kidney (Zhao et al., 2003). The exact localization of the remaining Syt isoforms still remains to be clarified.

1.5.4 Function of Synaptotagmins

Syt1, the best-characterized Syt isoform, was shown to be present on SVs and LDCVs where it functions as a Ca^{2+}-sensor for fast synaptic transmission and endocrine exocytosis, respectively (Geppert et al. 1994; Diantonio & Schwarz 1994; Littleton et al. 1994; Voets et al. 2001; Sørensen et al. 2003). In addition to Syt1, Syt2 and 9 function as Ca^{2+}-sensors for fast synchronous neurotransmitter release in cortical neurons (Xu et al. 2007). Previous studies already observed that Syt2 plays a role in fast synchronous release (Stevens & Sullivan 2003; Nagy et al. 2006). However, in a systematic analysis regarding rescue capacity of all Syt isoforms, Syt9 was found also to rescue the Syt1 knockout (KO) phenotype of abolished synchronous release in neurons (Xu et al. 2007). Interestingly, Syt2 and 9 exhibit distinct kinetics for synchronous release whereby Syt2 constitutes the fastest and Syt9 the slowest Ca^{2+}-sensor for fast synchronous release. Additionally, Syt2 acts as the major Ca^{2+}-sensor for exocytosis in non-neuronal and non-endocrine cells, namely in mast cells (Melicoff et al., 2009).

Intriguingly, Syt7 was not sufficient to rescue the Syt1 KO phenotype even though it has been described to localize to the synapse and to regulate Ca^{2+}-dependent exocytosis in endocrine cells, such as PC12 cells, fibroblasts, adrenal chromaffin cells and pancreatic cells (Martinez et al. 2000; Sugita et al. 2001; Wang & Chicka 2005; Li et al. 2007; Schonn et al. 2008; Gustavsson et al. 2008; Gustavsson & Han 2009). Nevertheless, deletion of Syt1 and Syt7 in chromaffin cells impairs the fast or the slow component of LDCV exocytosis, respectively; deletion of both isoforms abolishes both phases. Thus, both isoforms are functionally overlapping but the

reason for the selectivity to the fast or slow component remains uncertain (Sugita et al. 2002).

Syt4 is a Syt isoform whose function and localization is under debate in the literature. In PC12 cells and rat brain, Syt4 is induced by depolarization as an immediate early gene (Vician et al. 1995) and Syt4 KO mice showed impairment in memory and motor performance (Ferguson et al. 2000). Despite the lack of the conserved amino acid aspartate in the Ca^{2+} -binding loop of the C_2A domain in mice (von Poser et al., 1997), the C_2A domain of Drosophila carrying the same substitution has the potential to bind Ca^{2+}/phospholipids (Dai et al. 2004; Wang & Chapman 2010). Indeed, Syt4 is sufficient to rescue neurotransmitter release of the Syt1 KO in Drosophila (Robinson et al., 2002) suggesting a positive role for the C_2A domain in Ca^{2+} -binding. The role of the C_2B domain regarding its ability to function as a Ca^{2+} -sensor remains controversial due to one report indicating that the C_2B domain of Syt4 is sufficient to promote glutamate release in astrocytes (Zhang et al. 2004) and another work reporting that the C_2B domain does not bind Ca^{2+} *in vitro* (Dai et al., 2004). In contrast to the predominant localization of Syt4 in astrocytes found by Zhang et al. 2004, Syt4 expression was found at low levels in astrocytes and at high levels in pyramidal neurons of the hippocampus (Mittelstaedt et al., 2009). In mouse hippocampal neurons Syt4 negatively regulates the release of BDNF containing vesicles in axons and dendrites (Dean et al. 2012b; Dean et al. 2009) and overexpression of Syt4 in PC12 cells showed inhibition of evoked hormone secretion from dense core vesicles (Wang et al. 2001; Machado et al. 2004; Zhang et al. 2010). In posterior pituitary nerve terminals, high levels of Ca^{2+} lead to Syt4-mediated Ca^{2+} -dependent exocytosis, whereas at low levels Syt4 inhibits this exocytosis (Zhang et al. 2009).

The function of Syts 3, 5, 6 and 8 is widely unknown, even though reports have described that Syt6 and 8 are involved in acrosomal exocytosis in the sperm head (Michaut et al., 2001; Hutt et al., 2002) and that Syt3 functions as a plasma membrane Ca^{2+} -sensor for exocytosis in PC12 cells (Sugita et al. 2002).

1.6 Synaptotagmin10

1.6.1 Synaptotagmin10 native expression

Compared to Syt1, the overall Syt10 expression throughout the brain is very low (Figure 1.4 A, B) (Mittelstaedt et al., 2009). The only regions where Syt10 is highly expressed are the olfactory bulb (OB) and the suprachiasmatic nucleus (SCN) (Figure 1.4 C) (Mittelstaedt et al., 2009; Husse et al., 2011). In the OB, Syt10 expression is not restricted to a specific layer but expressed in all three layers, the glomerular, the mitral and the granule cell layer. In contrast, in the neocortex, overall Syt10 expression is low and specifically restricted to layers II, V and VI. Mittelstaedt et al (2009) observed that Syt10 expression in the hippocampus is restricted to single cells as revealed by a punctate labeling. Moreover, within the HC, Syt10 is nearly exclusively detected in the dentate gyrus (DG). The ventral pallidum is the only region of the striatum that exhibits Syt10 expression.
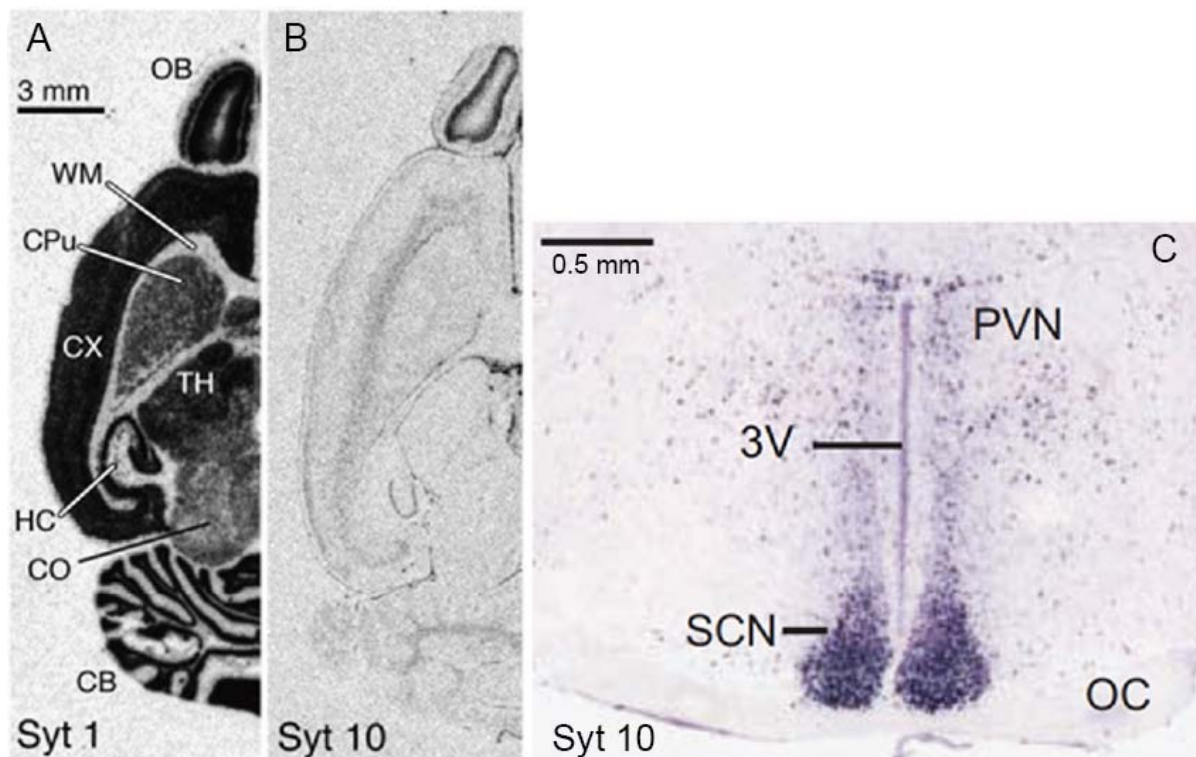
Figure 1.4 Differential expression pattern of Syt1 and Syt10. (A), (B) Horizontal sections of P28 rat brains. Via radioactive in situ hybridization with ^{35}S-labeled oligonucleotides specific for Syt1 and Syt10 gene expression levels were analyzed. (A) Expression of Syt1 is distributed throughout the whole brain. (B) In contrast, Syt10 shows low gene expression in the brain. The OB is the only region with high levels of Syt10. Olfactory bulb (OB), white matter regions (WM), caudate putamen (CPu), cortex (Cx), thalamus (TH), hippocampus (HC), colliculus (CO), cerebellum (CB) (modified from Mittelstaedt et al., 2009). (C) Syt10 expression in the suprachiasmatic nucleus. Coronal section of mouse brains labeled with digoxigenin-tagged riboprobes specific for Syt10. In situ hybridization shows strong Syt10 expression in the SCN. Paraventricular nucleus of the hypothalamus (PVN), third ventricle (3V), suprachiasmatic nucleus (SCN), optic chiasm (OC) (modified from Husse et al., 2011).

No specific labeling of Syt10 could be detected in the cerebellum, the midbrain and diencephalon. Similar to most other Syt isoforms, Syt10 expression levels in the brainstem are low.

Recently, Dean et al. (2012a) analyzed the subcellular localization and kinetics of Syt1 to 17 in pHluorin experiments. In this functional screen, they found Syt10 to be localized to the axonal plasma membrane of hippocampal neurons under resting conditions. Depolarization of the neuronal membrane did not lead to an alteration in fluorescence, indicating that no exo- or endocytosis of Syt10 containing vesicles occurred. The authors concluded that a weak stimulus is not sufficient to induce a change in Syt10 localization but conceivably strong synaptic activity may alter the kinetics and localization of Syt10.

1.6.2 Synaptotagmin10 localization to IGF1 containing vesicles

Until recently, the functional role of Syt10 remained undetermined. However, Cao et al. (2011) identified Syt10 to completely co-localize with IGF1 in somatic and dendritic vesicles of OB neurons via immunofluorescence of overexpressed tagged proteins (Cao et al., 2011). Analyzing Syt10 KO mice, Cao et al., 2011 found that synaptic transmission was impaired in mitral cells from Syt10 KO mice and that the size of Syt10 KO neurons was decreased as measured by a higher input resistance and a decrease in cell capacitance. IGF1 immunoassay revealed an impairment in the activity-dependent IGF1 secretion in Syt10 KO mice that resulted in smaller neurons. Strikingly, the Syt10 KO phenotype could not be rescued by the Syt10 related Syt isoforms Syt3, 5 and 6 but by application of exogenous IGF1. These results indicate that the Syt10-dependent exocytosis is a distinct pathway that is independent of Syt1-mediated exocytosis of synaptic vesicles (Figure 1.5). Furthermore, it suggests the occurrence of two different vesicle exocytosis pathways in the same neuron.
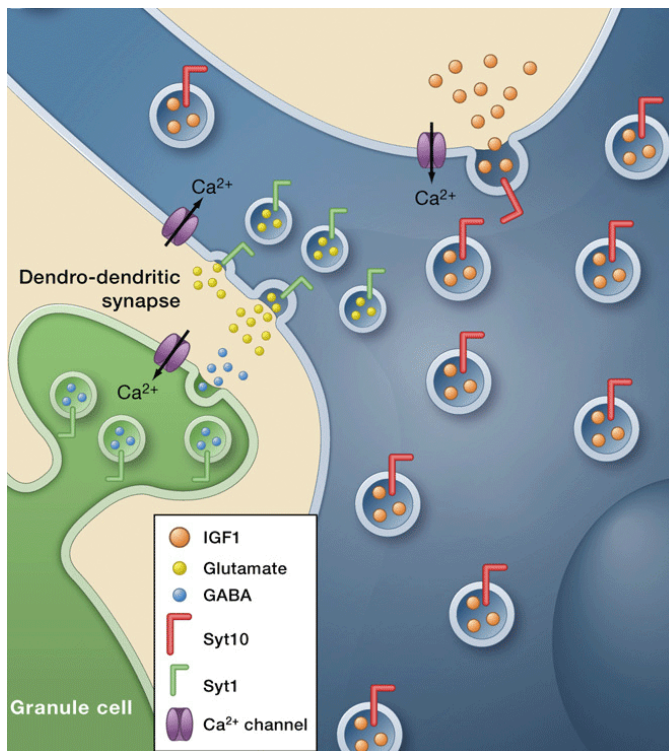
Figure 1.5 Schematic drawing of Syt10-mediated IGF1 exocytosis. The picture summarizes Syt1 and Syt10-mediated exocytosis. Syt10 is located to IGF1 containing vesicles and acts there as the calcium sensor for release of IGF1 from non-synaptic vesicles. The parallel existing pathway of Syt1-mediated exocytosis is shown as well. Syt1 functions as a Ca^{2+}-sensor for release of neurotransmitters into the synaptic cleft where they bind to their receptors. Note that the distinct types of exocytosis can occur in the same neuron (Kononenko & Haucke, 2011).

1.6.3 Synaptotagmin10, a seizure-induced gene

In 1997, Babity et al. first identified Syt10 by differential display (Babity et al., 1997). Syt10 mRNA expression was increased in the hippocampus 3 hours (h) after seizures evoked by systemic KA administration into adult rat (Figure 1.6 A). Peak expression of Syt10 was observed 6 h after seizure activity and declined 12 h following kainic acid treatment. In the piriform cortex, basal Syt10 mRNA expression was stronger compared to basal expression in the hippocampus. Following seizure activity, Syt10 expression was elevated in the piriform cortex at 3-6 h and decreased at 12 h after KA administration.

The parietal cortex served as a control region since it is a tissue in which seizure-induced neurodegeneration is not observed. In fact, no up-regulation of Syt10 expression was observed in this region after seizure activity. Using *in situ* hybridization Babity et al. (1997) confirmed Syt10 mRNA expression to be more abundant 6 h after seizure activity in the granule cell layer of the dentate gyrus and layer II of the piriform cortex (Figure1.6 B).

A

B

control   6 h kainic acid
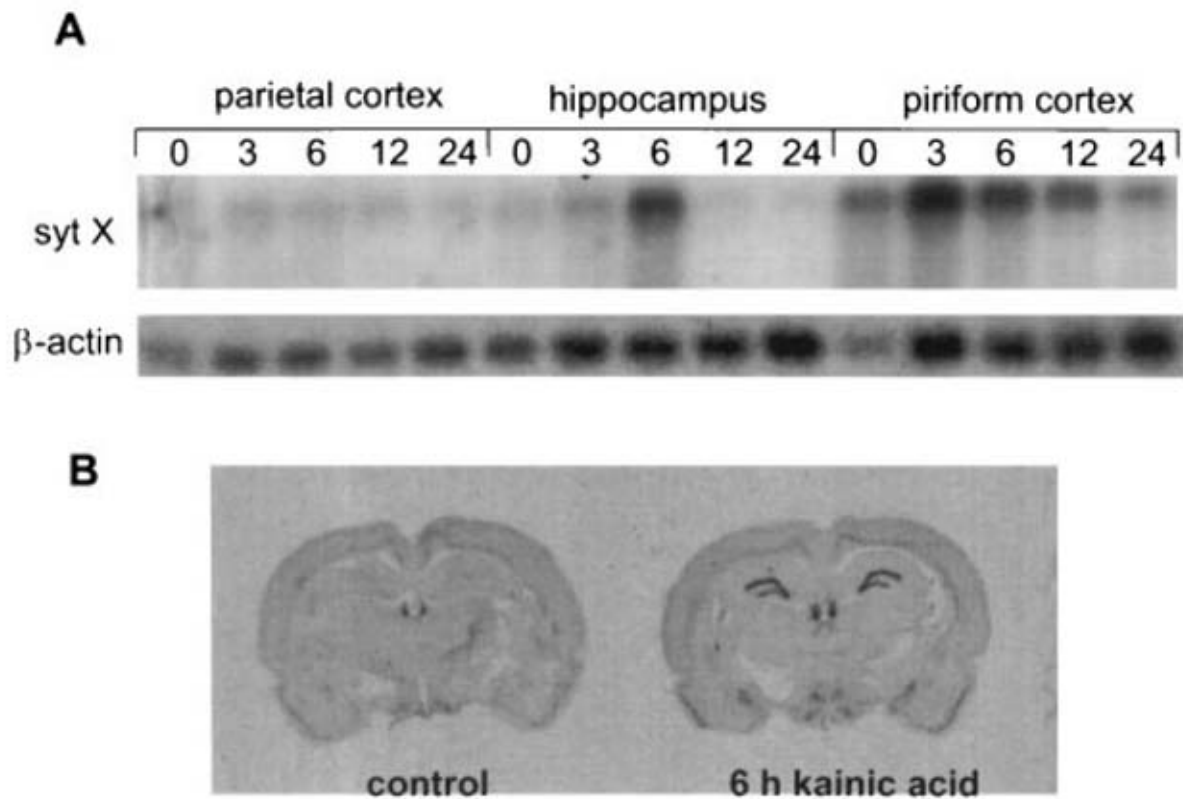
Figure 1.6 Induction of Syt10 gene expression following systemic administration of KA. (A) Northern blot analysis of Syt10 expression in KA administered rats at different time points following seizure activity. Induction of Syt10 expression was observed in the hippocampus and the piriform cortex but not in the parietal cortex. (B) *In situ* hybridization of rat brain coronal sections using olignucleotides specific for Syt10. Compared to the control, gene expression was induced in the hippocampus of seizure-experienced rats (Babity et al., 1997).

As mentioned above, Syt10 is expressed at high levels in the OB where it is crucial for IGF1 release. During development, IGF1 is distributed ubiquitously but in the adult brain it is restricted to the OB as well (Rotwein et al., 1988). In the OB, IGF-1 regulates axon guidance and neuronal migration (Scolnick et al., 2008; Hurtado-Chong et al., 2009), which may be important for neuronal repair.

In addition, IGF1 mRNA expression was described to be increased at 3 days (d), 7 d and in the chronic phase after pilocarpine-induced SE (Okamoto et al., 2010). IGF1 protein expression levels are more abundant 2 d after SE (Choi et al., 2008). Furthermore, IGF1 plays a role in epileptogenesis as it is important for progenitor cell proliferation in the subgranular zone of the dentate gyrus 2 d following pilocarpine-induced SE (Choi et al., 2008). Hence, expression of IGF1 and Syt10 is altered in response to seizure activity but Syt10 is not the only Synaptotagmin gene family member that is altered during neurodegeneration. To understand the different pathways of Syt-dependent vesicle exocytosis and their potential interactions, it is essential to understand the role of Syts in neurodegeneration.

1.7   The role of Synaptotagmins in neurodegeneration

There is growing evidence that membrane trafficking underlies pathophysiological and adaptive changes in neurodegeneration, neuronal plasticity and glial activation. Given that Syts are membrane trafficking proteins, Syt expression may be altered during the process of plasticity. Neurodegenerative changes are characterized by malfunctions of synaptic connections and/or loss of neurons within specific regions in the CNS. These alterations can appear after epileptic seizures, cerebrovascular insults or neurodegenerative diseases, namely Alzheimer's disease, Parkinson's disease or Huntington's disease. Even though the underlying pathophysiological processes between distinct neurodegenerative diseases may differ, all lead to cell death either by apoptosis, leakage of detrimental cytoplasmic contents (necrosis) or membrane disruption (reviewed by Glavan et al. 2009).

Numerous reports show that Syts are important for plasmalemmal and axolemmal repair and that this resealing is mediated by Ca^{2+} -regulated exocytosis (Detrait et al. 2000b; Detrait & Eddleman 2000a; Bi et al. 1995; Reddy et al. 2001; Miyake & McNeil 1995; Steinhardt et al. 1994). It is therefore tempting to speculate that Syts are involved in remodeling after neuronal cell loss and in the repair of degenerating neurons.

In Parkinson's disease, four Syts exhibited altered expression, namely Syts 2, 4, 7 and 10. In an animal model for Parkinson's disease Syt2 mRNA was decreased whereas the expression of Syt10 mRNA was increased (Glavan & Zivin, 2005). In response to anti-Parkinson drug treatment, Syt4 and 7 mRNA expression levels were increased indicating that these Syts might be involved in pathophysiological alterations of synaptic transmission. A role for Syt11 in Parkinson's disease was suggested due to binding of Syt11 to the parkin protein (Huynh et al., 2003).

In rat hippocampus, Syt4 mRNA expression is more abundant 24 h after transient global cerebral ischemia (Yokota et al., 2001) whereas using a different method, mRNA expression levels of Syt4 were described to be increased at a later time point (21 d) (Krüger et al., 2006). This discrepancy may result from different brain ischemia models used in the studies.

The only Syt isoform that was reported to be less abundant in the context of Alzheimer's disease is Syt1 (Masliah et al. 2001; Reddy et al. 2001; Sze et al. 2000; Yoo & Cairns 2001; Mufson et al. 2002).

Epilepsy is another disease that induces morphological plasticity, i.e. mossy fiber sprouting and reactive gliosis in the hippocampus. Cell death occurs in the CA1 and CA3 region and in hilar cells of the dentate gyrus (Nadler 2003; Tauck & Nadler 1985; Dashtipour et al. 2002). Several Syt isoforms are differentially regulated in epilepsy, namely Syts 1, 3, 4 and 10. In patients with mesial temporal lobe epilepsy (MTLE), a decrease of Syt1 protein was detected based on two-dimensional gel electrophoresis (2-DE) combined with mass spectrometry (Yang et al. 2006). The reduction of Syt1 protein is consistent with a down-regulation of Syt1 mRNA in CA1 and CA3 subfields of the hippocampus in adult rats with KA-induced seizures (Tocco et al., 1996). Recently, it has been reported that spontaneous epileptic rats (SER), which exhibit tonic convulsions and absence seizures after 6 weeks of age, express Syt1 protein at lower levels in frontal piriform and entorhinal cortices and in the inner molecular layer of the dentate gyrus compared to Wistar rats (Hanaya et al., 2012). Decreased Syt1 probably leads to impaired SV exocytosis and consequently to GABAergic dysfunction, thus resulting in expression and propagation of epileptic seizures in SERs. Moreover, Syt1 is thought to play a role in refractory epilepsy as protein expression of patients with refractory epilepsy is more abundant. Furthermore mRNA and protein expression levels of Syt1 are augmented in kindled rats with phenytoin-resistance (Xiao et al. 2009; Zeng et al. 2009). These results indicate that Syt1 might play a role in the strengthening of refractory epilepsy by increased SV trafficking.

Two more Syts are altered in response to seizures, (a) Syt3 mRNA expression was found to be decreased in hippocampus following electroconvulsive seizures (Elfving et al., 2008) and (b) Syt4 expression was altered after kainate injection. In situ hybridization of adult rats revealed a peak increase of Syt4 mRNA 4 h after seizure onset in the dentate gyrus and 8 h after seizure onset in CA1, CA3 and piriform cortex. This transient up-regulation decreased in all regions 30 h post seizure onset. A similar time course of mRNA increase after KA injection was observed in rats analyzed for Syt10 expression. As mentioned above, both Syt10 mRNA as well as IGF1 mRNA expression levels are augmented in the hippocampus after SE (Babity et al., 1997; Choi et al., 2008; Okamoto et al., 2010). Hence, Syt10 and IGF-1 play a role in epileptogenesis but to date it remains to be defined whether they are regulated simultaneously and subsequently function together in the hippocampus.

2 Aims of the study

Epileptogenesis describes a process of multiple cellular and molecular changes in the brain finally resulting in the occurrence of recurrent spontaneous seizures. It involves alterations leading to morphological changes of neuronal connections and circuits in the brain and to functional modifications of the cellular network. Understanding the mechanisms underlying these modifications is essential for new and efficient treatment possibilities. Analyzing changes in gene expression during epileptogenesis is a first step in this direction. One gene that is rapidly and transiently up-regulated in the rat hippocampus early after the experimental induction of SE but is barely detectable under native conditions is Syt10. It was therefore suggested that Syt10 might be involved in cerebral changes influencing the process of epileptogenesis or act neuroprotectively. However, to date, little is known about the function of Syt10 in health and disease conditions especially in the hippocampus.

In order to gain further insight into the signaling cascades mediating Syt10 expression and to resolve the function of Syt10 the following aims will be pursued:

Firstly, define the mechanisms regulating the Syt10 expression in the hippocampus. Therefore, the Syt10 promoter and genomic regulatory regions will be bioinformatically and functionally characterized. Next, using Luciferase assays and quantitative RT-PCR the signaling cascades controlling basal and activity-induced transcription will be further examined.

Secondly, resolve, in which subcellular compartment Syt10 is present. Isoform-specific antibodies will be generated to comparatively analyze the distribution of Syt10 and the related Syt isoforms 3, 5 and 6 using immunocytochemistry and overexpression of GFP-tagged proteins in neurons. Next, different Syt10 sequences will be probed for their relevance in subcellular targeting.

Thirdly, establish a procedure to identify Syt10 containing organelles and protein complexes. This approach will allow the isolation of the respective Syt10 complexes or organelles from the hippocampus after SE.

Fourthly, examine the role of Syt10 in epileptogenesis. The time course of Syt10 expression in response to pilocarpine-induced SE will be examined in mice. In the same model functional changes of Syt10 KO mice in the hippocampus will be studied.

In summary, this study will provide novel insights into key mechanisms controlling Syt10 gene expression in response to transient hyperexcitability as well as into the functional role of Syt10 in the normal and epileptic brain.

3   Materials

3.1   Equipment

Table 3.1: List of equipment used for this study

Application	Model	Company
Acrylamid electrophoresis system	Mini-PROTEAN 3 Electrophoresis System	BioRad
Agarose electrophoresis system	SUB-CELL GT	BioRad
Analytical balance	BP210S	Sartorius
Analytical balance	Toledo	Mettler
Autoclave	Varioclav 75T	H + P
Balance	SBC53	SCALTEC
Capillary Sequencer	3130/xl/Genetic Analyzer	Applied Biosystems
Cell-culture hood	MSC-Advantage	Thermo Scientific
Cell-culture hood	HERA SAFE KS	Thermo Scientific
Centrifugation concentrator	Amicon Ultra-4 / Ultra-15 100K	Millipore
Centrifuge	Function line	Heraeus
Centrifuge	5415C	Eppendorf
Centrifuge	Mikro 22R	Hettich
Centrifuge	Mikro 200R	Hettich
Centrifuge	Rotina 220R	Hettich
Centrifuge	Megafuge 1.0R	Heraeus
Confocal laser scanning microscope	LSM710	Zeiss
Confocal laser scanning microscope	Eclipse T*i*	Nikon
Confocal laser scanning microscope	Leica TCS	Leica
Controller	Micro4 Controller, 4-Channel	World Precision Instruments
Cryostat	FV300	MICROM
Gel documentation system	AlphaImager	Alpha Innotech
Heparin column	HiTrap Herparin HP	GE Healthcare
Incubator	TH 30 / TH 15	Edmund Bühler GmbH
Incubator		Binder
Incubator (cells/cell culture)	HERAcell 150 / 150i	Thermo Scientific
Incubator (media/cell culture)	Modell 100	Memmert
Incubator small	Inkubator 1000, Unimay 1010	Heidolph
Incubator small	Incubating Mini shaker	VWR

Table 3.1 (continued)

Application	Model	Company
Infrared imaging system	Odyssey	Li-cor
Inverse microscope	Axio Observer 1A	Zeiss
Luminometer	Glomax 96 microplate luminometer	Promega
Micro pump	UltraMicroPump III	World Precision Instruments
PCR-Cycler	UNOII	Biometra
PCR-Cycler	T3	Biometra
PCR-Cycler	T3000	Biometra
pH-meter	pHMeter 766 Calimatic	Knick
Precision Syringe	Nanofil Hamilton 10µl	World Precision Instruments
Quick-seal tubes	26.3ml 25x89mm	Beckman Coulter
Real time PCR (Taqman)	9700HT	ABI Prism
Rotor	Type 70 Ti	Beckman Coulter
Shaker plate	Polymax 1040	Heidolph
Spectrophotometer	ND-1000	NanoDrop
Thermo shaker	MKR13	HLC
Thermo shaker	Thermomixer compact	Eppendorf
Transfer System	Mighty Small Transphor/Hoefer TE22	Amersham
Ultrasonic Processor	UP50H	Hielscher
Vibratom	Microm HM 650V	Thermo Scientific
Vortex	Vortex-Genie 2	Scientific Industries
Vortex	Reax control	Heidolph
Water bath	Shake Temp SW23	Julabo

3.2 Materials and reagents

3.2.1 Antibodies

Table 3.2: Primary antibodies

Name	Assay	Dilution	Company
anti-rat biotin cross SP	IHC	1:165	Jackson Immuno Research Laboratories Inc.
BrdU	IHC	1:150	AbD Serotec
FLAG	WB	1:5000	Sigma-Aldrich
GFAP	ICC	1:2000	Dako
GM130	ICC	1:500	BD Transduction Laboratories
HA	ICC	1:100	Covance
HA	ICC	1:100	Sigma-Aldrich
MAP2	ICC	1:500	Chemicon
PSD95	ICC	1:200	Chemicon
ß-actin	WB	1:10000	Abcam
Synapsin	ICC	1:100	Synaptic Systems
Syt1	ICC	1:200	Synaptic Systems
Syt10 1D3	ICC	1:2-5	Helmholtz Zentrum Dr. Kremmer
Syt10 2A9	ICC	1:2-5	Helmholtz Zentrum Dr. Kremmer
Syt10 poly 150 T3	ICC/WB	1:250	Pineda
vGAT	ICC	1:500	Synaptic Systems

Table 3.3: Secondary antibodies

Name	Assay	Dilution	Company
anti-mouse Cy3	ICC	1:400	Jackson Immuno Research Laboratories Inc.
anti-mouse Cy5	ICC	1:400	Jackson Immuno Research Laboratories Inc.
anti-mouse FITC	ICC	1:400	Jackson Immuno Research Laboratories Inc.
anti-rabbit Cy3	ICC	1:400	Jackson Immuno Research Laboratories Inc.
anti-rabbit FITC	ICC	1:400	Jackson Immuno Research Laboratories Inc.
Cy3-Streptavidin	IHC	1:160	Jackson Immuno Research Laboratories Inc.
IRDye anti-mouse 800nm	WB	1:20000	Licor
IRDye anti-rabbit 680nm	WB	1:20000	Licor

3.2.2 Enzymes

Table 3.4: Enzymes used in this study

Enzyme	Company
GoTaq® Flexi DNA Polymerase	Promega
DNase I	Roche
Lipofectamine™ 2000 Transfection Reagent	Life technologies
Pfu DNA Polymerase	Thermo Scientific
T4 Ligase	Thermo Scientific
Trypsin	GIBCO BRL
Restriction Enzymes	
MluI, SalI, XhoI, KpnI, HindIII, EcoRI, BamHI, MfeI, XbaI	Thermo Scientific
StuI	New England Biolabs

3.2.3 Chemicals

Table 3.5: Chemicals used in this study

Chemical	Company
4',6-diamidino-2-phenylindole, dihydrochloride (DAPI)	Life technologies
5-bromo-2'-deoxyuridine (BrdU)	Sigma-Aldrich
Arabinofuranosyl cytidine (Ara-C)	Sigma-Aldrich
Bovine serum albumin (BSA)	Sigma-Aldrich
cOmplete Protease Inhibitor Cocktail Tablets	Roche
Diazepam	Ratiopharm
dimethyl sulfoxide (DMSO)	Roth
Fetal calf serum (FCS)	Life technologies
Gelatin from cold water fish skin	Sigma-Aldrich
glucose solution 5 %	Fresenius
Iodixanol OptiPrep	Nycomed Pharma
Isofluran	Forene
Kainic acid (KA)	Abcam
N,N-Bis-(2-hydroxyethyl)-2-amino-ethansulfonic acid (BES)	Roth
Normal goat serum (NGS)	GIBCO BRL
Paraformaldehyd (PFA)	Merck
Pilocarpine hydrochloride	Sigma-Aldrich
Poly-L-lysine	Sigma-Aldrich
Scopolamine methyl nitrate	Sigma-Aldrich
Triton X-100	Sigma-Aldrich

3.2.4 Diverse material

Table 3.6: Diverse products used in this study

Product	Company
Nitrocellulose membrane (Protran® 0,45 µm pore size)	Watman, GE Healthcare
Nylon cell strainer 100µm	BD Biosciences
Tissue tek	Sakura Finetek
Vectashield Hard Set Mounting Medium	Axxora

3.2.5 Cell culture media

Table 3.7: Cell culture media used in this study

Cell culture medium	Company
B27	Gibco
Basal Medium Eagle (BME)	Life technologies
Dulbecco's Modified Eagle's Medium (DMEM)	Gibco
Fetal calf serum (FCS)	Life technologies
Glucose	Sigma-Aldrich
Hank's Buffered Salt Solution (HBSS)	Gibco
Iscove's Modified Dulbecco's Medium (IMDM)	Gibco
L-Glutamine	Gibco
minimum essential medium (MEM)	Sigma-Aldrich
Opti-MEM	Gibco
Papain	Sigma-Aldrich
Penicillin-Streptomycin	Gibco
Phospate saline buffer (PBS)	Gibco
Poly-D-Lysin	Sigma-Aldrich
sodium bicarbonate	Invitrogen Life technologies
sodium hypoxanthine, aminopterin, thymidine (HAT)	Life technologies

3.2.6 Kits

Table 3.8: Kits used in this study

Kit	Company
BigDye® Terminator v3.1 Cycle Sequencing Kit	Applied Biosystems
Cell viability imaging kit	Roche
DNA Clean and Concentration kit	Zymo Research
Dual-Luciferase® Reporter Assay System	Promega
DyeEx 2.0 (Purification of Sequencing)	Qiagen
Dynabeads® mRNA DIRECT™ Micro Kit	Life technologies
EndoFree Plasmid Maxi Kit	Quiagen
GeneJET™ Plasmid Miniprep Kit	Thermo Scientific
High Capacity cDNA Reverse Transcription Kit	Applied Biosystems
Maxima™ SYBR Green/ROX qPCR Master Mix (2X)	Thermo Scientific
PureLink™ HiPure Plasmid Filter Maxiprep Kit	Life technologies
PureLink™ HiPure Plasmid Filter Midiprep Kit	Life technologies
QuickChangeII XL Site Directed Mutagenesis kit	Stratagene
RevertAid First Strand cDNA Synthesis Kit	Thermo Scientific
TOPO vectors	Life technologies
Zymoclean Gel DNA recovery kit	Zymo Research

3.3 Oligonucleotides

3.3.1 Cloning

Table 3.9: Primers used for cloning of full-length Syts and IGF1. #: primer number of the lab internal primer list; RE: restriction enzymes that were used for cloning of fragments into the corresponding vectors. Fw: forward; rev: reverse

Gen	Direction	#	5'-SEQUENCE-3'	RE
GFP	fw	1309	GCGGTCGACGGGGGCGGCGGAATGGTGAGCAAGGGCGAG	SalI
GFP	rev	1310	GCGAGATCTTACTTGTACAGCTCGTCCATG	BglII
mCherry	fw	1309	GCGGTCGACGGGGGCGGCGGAATGGTGAGCAAGGGCGAG	SalI
mCherry	rev	1310	GCGAGATCTTACTTGTACAGCTCGTCCATG	BglII
mRFP	fw	2152	GCGGTCGACATGGCCTCCTCCGAGGACGT	SalI
mRFP	rev	2153	GCGAGATCTTTAGGCGCCGGTGGAGTGGC	BglII
Syt10	fw	1449	GCGGAATTCACCATGAGTTTCCGCAAGGAGG	EcoRI
Syt10	rev	1798	GCGGGATCCGCCTCCAGGGCCTCCTGGTGTGGACGGTGGC	BamHI
Syt10	fw	1449	GCGGAATTCACCATGAGTTTCCGCAAGGAGG	EcoRI
Syt10	rev	1796	GGATCCTTATGGTGTGGACGGTGG	BamHI
Syt10	fw	1449	GCGGAATTCACCATGAGTTTCCGCAAGGAGG	EcoRI
Syt10	rev	1497	GCGGGATCCCCCTGGTGTGGACGGTGGC	BamHI
Syt3	fw	1463	GCGCAATTGACCATGTCTGGGGACTACGAAGATG	MfeI
Syt3	rev	1382	GCGGTCGACCTCTGAATTCTCTTTCTCTGACAATC	SalI
Syt5	fw	1383	GCGGAATTCACCATGCCCGGGGCCAGGGACGC	EcoRI
Syt5	rev	1384	GCGCGTCGACTCGTTTCTCCAGCAGAGAGTG	SalI
Syt6	fw	1385	GCGGAATTCGGCATGAGCGGAGTTTG	EcoRI
Syt6	rev	1386	GCGCGTCGACCAACCGGGGGGTTCCC	SalI
IGF1	fw	1949	GAATTCACCATGACCGCACCTGCAATAA	EcoRI
IGF1	rev	1951	GGATCCGCCTCCAGGGCCTCCGCCCAGTCTTTTTTCTCTGG	BamHI

Table 3.10: Primers used for cloning of chimeric Syts. #: primer number of the lab internal primer list; RE: restriction enzymes that were used for cloning of fragments into the corresponding vectors. Fw: forward; rev: reverse

Gen	Domain	Direction	#	5'-SEQUENCE-3'	RE
Syt10	TMD to C-terminus	fw	1449	GCGGAATTCACCATGAGTTTCCGCAAGGAGG	EcoRI
Syt10	TMD to C-terminus	rev	1610	GCGGAATTCAGGCCTGTTAGCGGTTGTTGTAAGC	BamHI
Syt3	N-terminus	fw	1611	GCGACCATGTCTGGGGACTACGAAGATG	blunt
Syt3	N-terminus	rev	1677	CTGTCTGCATCCGGACC	blunt
Syt5	N-terminus	fw	1613	GCGACCATGCCCGGGGCCAG	blunt
Syt5	N-terminus	rev	1678	CTATCTGGGTCGCGGAGC	blunt
Syt6	N-terminus	fw	1615	GCGACCATGAGCGGAGTTTGGGGG	blunt
Syt6	N-terminus	rev	1679	CTGACAGAGGTGCCTGAGTC	blunt

Table 3.11: Primers used for cloning of promoter fragments. #: primer number of the lab internal primer list; RE: restriction enzymes that were used for cloning of fragments into the corresponding vectors. Fw: forward; rev: reverse

region	Direction	#	5'-SEQUENCE-3'	RE	genomic position (bp) relative to the start ATG
pGL3-306	fw	1472	GCGACGCGTTCAGGAAGGTGTGTGGGAA	MluI	-306 to 0
pGL3-306	rev	1473	GCGGTCGACCTTGGCTTCTGCTCGCAG	SalI	-306 to 0
pGL3-1036	fw	1476	GCGACGCGTGGGGTAACTTTACCATAACCTGG	MluI	-1036 to 0
pGL3-1036	rev	1473	GCGGTCGACCTTGGCTTCTGCTCGCAG	SalI	-1036 to 0
pGL3-4713	fw	1480	GCGACGCGTAGTGATTTGTAGAAAAGACCACATGA	MluI	-4713 to 0
pGL3-4713	rev	1473	GCGGTCGACCTTGGCTTCTGCTCGCAG	SalI	-4713 to 0
RR-IN	fw	1541	GCGGGATCCTAAAGGGACAAGCTTGGGCT	XhoI	152 to 3034
RR-IN	rev	1542	GCGGGTCGACAAAATTCTTGATAAATACTTGCTGAA	BglII	152 to 3034
RR-5'	fw	1682	GCGGGTACCTCTTCAGGCTCAAAATTAGTGG	KpnI	-33755 to -32055
RR-5'	rev	1683	GCGGGTACCCAAACTTCAAAAACATCATGCTA	KpnI	-33755 to -32055

Table 3.11 (continued)

region	Direction	#	5'-SEQUENCE-3'	RE	genomic position (bp) relative to the start ATG
RR-3'	fw	1884	GTCGACGTTCTTCTCGCAGAGCCTCA	SalI	-63567 to- 63029
RR-3'	rev	1885	GTCGACAAGTCGGGGAAAGGGATTATT	SalI	-63567 to -63029
RR-1	fw	1952	GCGGGTACCAGAAGTTTACCCAGCTCACCA	KpnI	-4344 to -3675
RR-1	rev	1953	GCGGGTACCACTCACTGTGGTAAGCATTCATT	KpnI	-4344 to -3675
RR-2	fw	1954	GCGGGTACCCTGCCCAGACTGTAGATAAACG	KpnI	-4054 to -3675
RR-2	rev	1953	GCGGGTACCACTCACTGTGGTAAGCATTCATT	KpnI	-4054 to -3675
RR-3	fw	1952	GCGGGTACCAGAAGTTTACCCAGCTCACCA	KpnI	-4344 to -4054
RR-3	rev	1955	GCGGGTACCTTATCTACAGTCTGGGCAGAACA	KpnI	-4344 to -4054
Exon 1	fw	c64	GCGCTCGAGTACCTGTGCCACCTCCG	XhoI	0 to 149
Exon 1	rev	c65	GCGAAGCTTAGTTTCCGCAAGGAGGAC	HindIII	0 to 149
Del I	fw	1472	GCGACGCGTTCAGGAAGGTGTGTGGGAA	MluI	-306 to -108
Del I	rev	c154	GCGCTCGAGGACGGACGCTGCTGC	XhoI	-306 to -108
Del II	fw	1472	GCGACGCGTTCAGGAAGGTGTGTGGGAA	MluI	-306 to -76
Del II	rev	c151	GCGCTCGAGGTTGGCAAGGGCGCA	XhoI	-306 to -76
Del III	fw	c153	GCGACGCGTTCCCAGTCACGAGTCATGAT	MluI	-724 to 0
Del III	rev	c265	GCGCTCGAGCTTGGCTTCTGCTCGCAG	XhoI	-724 to 0
Del IV	fw	c152	GCGACGCGTGGAATCAAGTGGTGCCTCC	MluI	-740 to 0
Del IV	rev	c265	GCGCTCGAGCTTGGCTTCTGCTCGCAG	XhoI	-740 to 0
Del V	fw	c264	GCGACGCGTGTAGGCAGTAGCTTGACTTCTCCA	MluI	-2165 to 0
Del V	rev	c265	GCGCTCGAGCTTGGCTTCTGCTCGCAG	XhoI	-2165 to 0

Table 3.12: Primers used for cloning constructs for tandem affinity purification. #: primer number of the lab internal primer list; RE: restriction enzymes that were used for cloning of fragments into the corresponding vectors. Fw: forward; rev: reverse

Gen	Direction	#	5'-SEQUENCE-3'	RE
SF-TAP	fw	1543	GCGGGATCCCCCGGACCCTGGAGCCACCCTCAGTTC	SalI
SF-TAP	rev	1437	GCGGTCGACTCATTTATCATCATCATCTTTATAATCC	HindIII
SF-TAP	fw	1544	GCGGAATTCACCATGGATTATAAAGATGATGATG	EcoRI
SF-TAP	rev	1545	GCGGGATCCTGGTCCTGGTTTCTCGAACTGCGGGTG	BamHI
Syt10	fw	1449	GCGGAATTCACCATGAGTTTCCGCAAGGAGG	EcoRI
Syt10	rev	1497	GCGGGATCCCCCTGGTGTGGACGGTGGC	BamHI
Syt6	fw	1385	GCGGAATTCGGCATGAGCGGAGTTTG	EcoRI
Syt6	rev	1768	GCGGGATCCCCAACCGGGGGGGTTCCC	BamHI
Syt10	fw	c24	GCGGGATCCAAGTTGTGCTGGCCATGCT	BamHI
Syt10	rev	c25	GCGTCTAGATTATGGTGTGGACGGTGGC	XbaI
Syt6	fw	c26	GCGGGATCCAAGCTGTGCTGGATGCCC	BamHI
Syt6	rev	c27	GCGTCTAGATTACAACCGGGGGGGTTCCC	XbaI

3.3.2 Diverse oligos

Table 3.13: Sequencing primers. #: primer number of the lab internal primer list; Fw: forward; rev: reverse

Template	Direction	#	5'-SEQUENCE-3'	Position (bp)
pCMV ß-Globin Intron	fw	1461	GAGTCCAAGCTAGGCCCTTT	1197
pSyn	fw	1379	GCGAGATAGGGGGGCACG	518
Syt10	fw	1797	CTTGGGAGAGACCATTGGAA	1426
pGL3	fw	1455	CTAGCAAAATAGGCTGTCCC	4760
pGL3	rev	1456	CTTTATGTTTTTGGCGTCTTCCA	89
mCherry	rev	1462	AAGCGCATGAACTCCTTGAT	37

3.3.3 Site directed mutagenesis

Table 3.14: Primers used for site directed mutagenesis. #: primer number of the lab internal primer list; Fw: forward; rev: reverse

Template	Direction	#	5'-SEQUENCE-3'	aa exchange
pAAV-Syn-Syt10-GFP	fw	1617	GTGTGAGCAGCCTGGCCCAGAAGGCGCTGC	C13-->A
pAAV-Syn-Syt10-GFP	rev	1618	GCAGCGCCTTCTGGGCCAGGCTGCTCACAC	C13-->A
pAAV-Syn-Syt10-GFP	fw	1619	TCATCACCGAGCTGGCCTTCGCGGGTCAGG	C24-->A
pAAV-Syn-Syt10-GFP	rev	1620	CCTGACCCGCGAAGGCCAGCTCGGTGATGA	C24-->A
pAAV-Syn-Syt10-GFP	fw	1621	GGTGGAGTGGGACAAGGCTTCGGGCATCTTTCCA	C34-->A
pAAV-Syn-Syt10-GFP	rev	1622	TGGAAAGATGCCCGAAGCCTTGTCCCACTCCACC	C34-->A

3.3.4 Quantitative RT-PCR

Table 3.15: Primers used for quantitative RT-PCR. #: primer number of the lab internal primer list; Fw: forward; rev: reverse

Gene	Direction	#	5'-SEQUENCE-3'	position (bp)
Syp	fw		TCAGGACTCAACACCTCAGTGG	580 to 653
Syp	rev		AACACGAACCATAAGTTGCCAA	580 to 653
rNPAS4	fw	q97	GGTGTCTCAACATTCCCCTA	2333 to 2432
hNPAS4	rev	q55	GTTCCCCTCCACTTCCATCT	2333 to 2432
IGF1	fw	q111	TTGCGGGGCTGAGCTGGTG	142 to 240
IGF1	rev	q112	GCCCTCCGAATGCTGGAGCC	142 to 240
rSyt10	fw	753	GTGTCGAACTGGACTTGACG	1398 to 1463
rSyt10	rev	754	TGATAGGCCAGCATTTCA	1398 to 1463
mSyt10	fw	q129	TCCCTCCAGAGAATGTGGAC	1404 to 1503
mSyt10	rev	q130	AGTCCAGTTCGACACACGCCT	1404 to 1503

3.4 Vectors and vector construction

3.4.1 Multiple cloning sites (MCS)

CMV/Syn-MCS:

```
     ClaI      EcoRI          BamHI  XbaI    SalI          HindIII                                    BglII
      |          |              |     |       |               |                                        |
5' ATCGATTGAATTCCCCGGGGATCCTCTAGAGTCGACCTGCAGAAGCTTGCCTCGAGCAGCGCTGCTCGAGAGATCT
   +|+++++|+++++|+++++|+++++|+++++|+++++|+++++|+++++|+++++|+++++|+++++|+++++|+++++|+
3' TAGCTAACTTAAGGGGCCCCTAGGAGATCTCAGCTGGACGTCTTCGAACGGAGCTCGTCGCGACGAGCTCTCTAGA
```

pGL3 basic-MCS:

```
      Acc65I        SacI              Xmal    XhoI
        |    KpnI      |      MluI  NheI  |  SmaI  |    BglII              HindIII
        |    |         |      |     |     |  |     |    |                    |
   5' GGTACCGAGCTCTTACGCGTGCTAGCCCGGGCTCGAGATCTGCGATCTAAGTAAGCTT
      +|+++++|+++++|+++++|+++++|+++++|+++++|+++++|+++++|+++++|+++++|+
   3' CCATGGCTCGAGAATGCGCACGATCGGGCCCGAGCTCTAGACGCTAGATTCATTCGAA
```

Additional information about the backbone vectors that were used for cloning is given in the appendix (Supplementary Figures 1 - 6).

3.4.2 Generated constructs

Table 3.16: List of all generated constructs

Name	Insert	Template	Vector	Enzymes
TOPO-constructs				
pcDNA3.1 TOPO Syt3	Syt3 (rat)	pCMV-Syt3	pcDNA3.1 TOPO	-
pcDNA3.1 TOPO Syt5	Syt5 (rat)	pCMV-Syt5	pcDNA3.1 TOPO	-
pcDNA3.1 TOPO Syt6	Syt6 (rat)	pCMV-Syt6	pcDNA3.1 TOPO	-
pcDNA3.1 TOPO Syt10	Syt10 (mouse)	cDNA	pcDNA3.1 TOPO	-
fluorescent reporter protein constructs				
pSyn-GFP Cterm.	GFP	EGFP	pSyn-MCS	SalI/BglII
pSyn-mCherry Cterm.	mCherry	mCherry	pSyn-MCS	SalI/BglII
pAAV-Syn-mRFP	mRFP	mRFP	pAAV-Syn-MCS	SalI/BglII
Syt/IGF constructs				
pSyn-Syt3-GFP	Syt3	pcDNA3.1 TOPO Syt3	pSyn-GFP Cterm.	MfeI/SalI
pSyn-Syt5-GFP	Syt5	pcDNA3.1 TOPO Syt5	pSyn-GFP Cterm.	EcoRI/SalI
pSyn-Syt6-GFP	Syt6	pcDNA3.1 TOPO Syt6	pSyn-GFP Cterm.	EcoRI/SalI
pSyn-Syt10-GFP	Syt10	pcDNA3.1 TOPO Syt10	pSyn-GFP Cterm.	EcoRI/BamHI
pAAV-Syn-Syt10-mRFP	Syt10	pcDNA3.1 TOPO Syt10	pAAV-Syn-mRFP	EcoRI/BamHI
pAAV-Syn-IGF1-mRFP	IGF1	pAAV-IGF1	pAAV-Syn-mRFP	EcoRI/BamHI
chimeric constructs				
pAAV-Syn-Syt10-TMD to C-terminus-GFP	Syt10-TMD to C-terminus	pcDNA3.1 TOPO Syt10	pAAV-Syn-GFP	EcoRI/BamHI
pAAV-Syn-Syt3/10-GFP	Syt3 N-terminus	pcDNA3.1 TOPO Syt3	pAAV-Syn-Syt10-TMD to C-terminus-GFP	StuI/blunt
pAAV-Syn-Syt5/10-GFP	Syt5 N-terminus	pcDNA3.1 TOPO Syt5	pAAV-Syn-Syt10-TMD to C-terminus-GFP	StuI/blunt
pAAV-Syn-Syt6/10-GFP	Syt6 N-terminus	pcDNA3.1 TOPO Syt6	pAAV-Syn-Syt10-TMD to C-terminus-GFP	StuI/blunt

Table 3.16 (continued)

Name	Insert	Template	Vector	Enzymes
promoter constructs				
pGL3-306	fragment -306	genomic DNA (rat)	pGL3 basic	MluI/SalI
pGL3-1036	fragment -1036	genomic DNA (rat)	pGL3 basic	MluI/SalI
pGL3-4713	fragmant -4713	genomic DNA (rat)	pGL3 basic	MluI/SalI
pGL3-IN	fragment Intron	genomic DNA (rat)	pGL3 basic	XhoI/BglII
pGL3-306+RR5'	fragment RR5'	genomic DNA (rat)	pGL3-306	KpnI
pGL3-306+RR3'	fragment RR3'	genomic DNA (rat)	pGL3-306	SalI
pGL3-306+RR-1	fragment RR-1	pGL3-4713	pGL3-306	KpnI
pGL3-306+RR-2	fragment RR-2	pGL3-4713	pGL3-306	KpnI
pGL3-306+RR-3	fragment RR-3	pGL3-4713	pGL3-306	KpnI
pGL3-306+ExonI	fragment Exon 2. half	genomic DNA (rat)	pGL3-306	XhoI/HindIII
pGL3-DelI	fragment DelI	pGL3-4713	pGL3 basic	MluI/XhoI
pGL3-DelII	fragment DelII	pGL3-4713	pGL3 basic	MluI/XhoI
pGL3-DelIII	fragment DelIII	pGL3-4713	pGL3 basic	MluI/XhoI
pGL3-DelIV	fragment DelIV	pGL3-4713	pGL3 basic	MluI/XhoI
pGL3-DelV	fragment DelV	pGL3-4713	pGL3 basic	MluI/XhoI
TAP constructs				
pAAV-CMV-C-TAP	SF-TAP Cterm.		pAAV-CMV-MCS	SalI/HindIII
pAAV-CMV-N-TAP	SF-TAP Nterm.		pAAV-CMV-MCS	EcoRI/BamHI
pAAV-CMV-Syt6-TAP	Syt6	pcDNA3.1 TOPO Syt6	pAAV-CMV-C-TAP	EcoRI/BamHI
pAAV-CMV-Syt10-TAP	Syt10	pcDNA3.1 TOPO Syt10	pAAV-CMV-C-TAP	EcoRI/BamHI
pAAV-CMV-Syt6-TAP without Nterm.+TMD	Syt6	pcDNA3.1 TOPO Syt6	pAAV-CMV-N-TAP	EcoRI/BamHI
pAAV-CMV-Syt10-TAP without Nterm.+TMD	Syt10	pcDNA3.1 TOPO Syt10	pAAV-CMV-N-TAP	EcoRI/BamHI

Table 3.16 (continued)

Name	Insert	Template	Vector	Enzymes
site-directed mutagenesis constructs				
pAAV-Syn-Syt10-Mut1-GFP	-	pAAV-Syn-Syt10-GFP	-	-
pAAV-Syn-Syt10-Mut2-GFP	-	pAAV-Syn-Syt10-GFP	-	-
pAAV-Syn-Syt10-Mut3-GFP	-	pAAV-Syn-Syt10-GFP	-	-
pAAV-Syn-Syt10-Mut1+2-GFP	-	pAAV-Syn-Syt10-GFP	-	-
pAAV-Syn-Syt10-Mut1+3-GFP	-	pAAV-Syn-Syt10-GFP	-	-
pAAV-Syn-Syt10-Mut2+3-GFP	-	pAAV-Syn-Syt10-GFP	-	-
pAAV-Syn-Syt10-Mut1+2+3-GFP	-	pAAV-Syn-Syt10-GFP	-	-

Plasmids kindly provided by other labs

pcDNA3.1-hNPAS4, pcDNA3.1-hUSF1, pcDNA3.1-hUSF2, pcDNA3.1-Arnt2-V5: Prof. Tõnis Timmusk (Tallinn University of Technology, Tallinn, Estonia).

pCMV-CREB: PD Dr. Bernd Evert (University of Bonn Medical Center).

pcDNA cJun-FLAG: Dr. Marc Piechaczyk (Insitute of Molecular Genetics, Montpellier, France)

pcDNA3-MEF2A-FLAG, pcDNA3-MEF2C: Dr. Eric N. Olson (University of Texas, Southwestern Medical Center)

pcDNA3.1-Per1: Prof. Gregor Eichele / Prof. Henrik Oster (Max Planck Institute for Biophysical Chemistry, Göttingen)

pAAV-IGF1: Prof. S. Ramakrishnan (University of Minnesota Medical School, Minneapolis, USA)

TfR-GFP, NPY-GFP: Prof. Casper C. Hoogenraad (Cell Biology, Faculty of Science, Utrecht University, Utrecht, The Netherlands)

4 Methods

4.1 Bioinformatics

4.1.1 Promoter analysis

The databases UCSC (http://genome.ucsc.edu/) and the ECR browser of rvista 2.0 (http://rvista.dcode.org/) were used for multiple alignments to search for evolutionary conserved regions. Searches for transcription factor binding sites were carried out using the Genomatix database (http://www.genomatix.de/) and multiTF of rvista 2.0 (http://rvista.dcode.org/). Prediction of the transcription start site (TSS) was performed using Eponine TSS from Wellcome Trust Sanger Institute (http://www.sanger.ac.uk/resources/software/eponine/), whereas the CpG islands were predicted with the platform CpGPlot from EMBL-EBI (http://www.ebi.ac.uk/Tools/emboss/cpgplot/).

4.2 Molecular biology methods

4.2.1 RNA extraction and cDNA synthesis

mRNA from primary hippocampal neurons and from microdissected hippocampal subregions was isolated using Dynabeads® mRNA DIRECT Micro Kit (Life technologies, Karlsruhe, Germany,) and cDNA was synthesized using RevertAid™ First Strand cDNA Synthesis Kit (Fermentas) both carried out according to the manufacturer's specifications.

4.2.2 PCR

Table 4.1: Standard PCR thermal profile

Step	Temperature	Time	Cycle
1	95 °C	10 min	
2	95 °C	15 sec	
3	59 °C	60 sec	
4	72 °C	40 sec	40 cycles step 2-4
5	4 °C	∞	

General amplification protocol

For all amplifications from plasmid DNA, *Pfu* polymerase was used with the standard PCR thermal profile.

Genomic DNA amplification protocol:

Amplifications from genomic DNA carried out for the promoter fragments were performed using *Taq* polymerase with 1/3 *Pfu* polymerase for proofreading activity, 2.5 mM DMSO, 1.5-2 mM $MgCl_2$ and the standard PCR thermal profile with 60 °C annealing temperature. Primers used for the amplification are listed in table 3.11.

4.2.3 Real-time PCR

For quantitative RT-PCR, the Maxima SYBR Green qPCR Master Mix/ROX (Fermentas) was used according to the following protocol:

Table 4.2: Real-time PCR protocol

Reaction component	Volume
Master Mix	3.125 µl
cDNA	1.25 µl
primer fw (10 pmol/ml)	0.1875 µl
primer rev (10 pmol/ml)	0.1875 µl
DEPC-H_2O	1.5 µl
Σ	6.25 µl

Table 4.3: Real-time PCR thermal profile

Step	Temperature	Time	Cycle
1	95 °C	10 min	
2	95 °C	15 sec	
3	59 °C	60 sec	
4	72 °C	40 sec	40 cycles step 2-4

Experiments were performed in triplicates on an ABI Prism 9700HT system (PE Applied Biosystems, Foster City, CA, USA) and analysis was carried out according to

the $\Delta\Delta C_t$ method. Expression of the housekeeping gene Synaptophysin was used to normalize expression. Primers used for real time PCR are listed in table 3.15.

4.2.4 Vector construction

For all cloning strategies, DNA was amplified by PCR and separated on an agarose gel to verify the correct size of the PCR product. Subsequently, the band of interest was cut out and purified (Zymoclean Gel DNA recovery kit). The PCR fragment and vector were cut with the respective restriction enzymes and purified (Zymoclean DNA clean and concentrator kit). The ligation reaction was carried out at 37 °C for 1 h. All generated constructs are listed in table 3.16.

4.2.5 Site directed mutagenesis

Primers (Table 3.14) were designed following the instructions of the QuickChange Primer Design Program (https://www.genomics.agilent.com/). Mutations were introduced with QuickChange II XL Site-Directed Mutagenesis Kit using the standard conditions as recommended by the manufacturer with the following variation: 10 ng Plasmid DNA and additional 2 µl Quick Solution were added to the PCR reaction and 2 min/kb DNA was chosen as elongation time with a final elongation of 7 min.

4.2.6 Sequencing

The PCR reaction for sequencing of plasmid DNA was prepared using the BigDye Terminator v3.1 cycle sequencing kit with template specific primers (Table 3.13). The sequencing PCR reactions were purified through a gel filtration spin column (DyEx 2.0 spin kit) or with the DNA clean and concentrator kit and run on a capillary sequencer. Subsequent analysis of the results was performed with the help of the Lasergene 8 software SeqMan.

4.3   Biochemical methods

4.3.1 Polyclonal peptide antibody generation

An epitope-specific antibody was raised in rabbits against the following peptide: CKEVEENEKPAPKAIEPAIK (mSyt10). The localization of the peptide is shown in figure 5.15. Using the immunizing peptide, the antibody was affinity purified

according to standard procedures. Generation and purification of the antibody was performed by Pineda antibody service (http://www.pineda-abservice.de).

4.3.2 Monoclonal peptide antibody generation

Two antibodies were generated in mice against the following peptide: DSQGSAbuSSPRPPS. Figure 5.15 shows the localization of the peptide in the C-terminus of Syt10. A cysteine was added to the N-terminus for coupling. Generation and purification of the antibody was carried out by the service platform of the Helmholtz Zentrum Munich (Dr. Kremmer, Institute of Molecular Immunology, Helmholtz Zentrum, Munich).

4.3.3 Western blotting

Preparation of protein extracts

Tissue and cells were lysed under denaturing conditions with 1x PBS containing 1 % SDS and 10 mM EDTA pH 8.0 followed by sonification. HEK293T cells used for lysis under native conditions were prepared in the respective lysis buffer containing 1-2 % detergent and Complete Protease Inhibitor Cocktail. The lysis reaction was incubated on a rotating wheel at 4 °C for 1 h. Cell debris was separated from the lysed supernatant by 10 min centrifugation at 14,000 rpm and 4 °C.

Electrophoresis and blotting

Samples were loaded with 6x loading buffer (378 mM Tris/HCl (pH 6.8), 30 % Glycerol, 12 % SDS, 0.06 % Bromphenol blue) containing 8 % ß-Mercaptoethanol and were heated at 95 °C for 5 min. 50-100 µg protein was loaded on 12 % SDS-polyacrylamide gels and transferred to a Whatman® Protran® nitrocellulose membrane. For immunolabeling, membranes were blocked 1 h with 2 % fish gelatin in 1x PBS at room temperature. Next, membranes were incubated with the respective primary antibody at 4 °C overnight in PBS with 0.1 % Tween. After three washing steps with 1x PBS, the secondary antibody was used on the subsequent day in PBS with 0.1 % Tween and 0.01 % SDS for 1 h at room temperature. The secondary antibodies were IR-labeled (Licor) and were visualized with an infrared

imaging System (Odyssey, Licor). Quantification of Western Blots was carried out using the software AIDA.

4.4 Cell culture

4.4.1 HEK293T cell culture

HEK293T cells were maintained in Dulbecco's Modified Eagle's Medium with sodium pyruvate (DMEM) supplemented with 10 % (v/v) heat inactivated fetal calf serum (FCS) (Hyclone), 100 units/ml penicillin/streptomycin (pen/strep) and 2 mM glutamine at 37 °C and 5 % CO_2. Cells were passaged every 2-3 days in a 1:10 dilution.

4.4.2 Transfection of HEK293T cells

HEK293T cells were transfected with lipofectamine to obtain protein lysates of overexpressed Syts for antibody characterization using immunoblots.

For Syt10 antibody characterization in immunocytochemistry, HEK293T cells were transfected based on the DNA/Ca^{2+}-phosphate precipitation method in 48-wells. The same method on a larger scale (10 cm plates) was used to overexpress Syt10 and Syt6 in HEK293T cells to study Syt10 binding partners.

Therefore, HEK293T cells were transfected at approximately 70 % confluency. Before transfection, the medium was exchanged by Iscove's Modified Dulbecco's Medium (IMDM) containing 5 % FCS. DNA and $CaCl_2$ were mixed and 2x HEBS was added dropwise while using a vortex mixer and the precipitate was given directly to the cells. The cells with the mixture were incubated at 5 % CO_2 and 37 °C overnight. On the following morning, cells were washed once with 1x PBS to remove the precipitate and then kept in DMEM supplemented with 10 % FCS and penicillin/streptomycin (pen/strep). 36-48 h after transfection, cells were harvested or fixed.

Buffer (2x HEBS)
50 mM HEPES
280 mM NaCl
1.5 mM Na_2HPO_4
pH 7.05 – pH 7.10

Table 4.4: Components of the HEK293T transfection protocol

24-well plate		10 cm plate	
DNA	500 ng (≈0.5 µl)	DNA	6-8 µg (≈5-8 µl)
250 mM CaCl$_2$	30 µl	2.5 M CaCl$_2$	145.2 µl
-	-	H$_2$O	1,056 µl
2x HEBS	30 µl	2x HEBS	1,320 µl

4.4.3 NG108-15 cell culture

NG108-15 cells were maintained in DMEM without sodium pyruvate supplemented with 1.5 g/L sodium bicarbonate, 10 % (v/v) FCS, 100 units/ml pen/strep, 2 mM glutamine and 1x HAT (sodium hypoxanthine, aminopterin, and thymidine; Life technologies, Karlsruhe, Germany) at 37 °C and 5 % CO$_2$. Cells were passaged every 2-3 days in a 1:3.5 dilution.

4.4.4 Transfection of NG108-15 cells

Transfection of NG108-15 cells was performed in 48-well cell culture plates in triplicates using lipofectamine (Life technologies, Karlsruhe, Germany) according to the manufacturer's protocol. Cells were transfected at approximately 70 % confluency. During transfection, DMEM was replaced by reduced serum medium (OPTI-MEM) containing the transfection solution and cells were kept at 37 °C and 5 % CO$_2$. The transfection mixture contained 50 ng of the pGL-promoter construct expressing firefly luciferase, 12 ng pRL-TK with the *Renilla* gene (Promega), the indicated amount of overexpression plasmid for the respective transcription factor, and 0.5 µl lipofectamine in 25 µl OPTI-MEM. The mixture was incubated at room temperature for 20 min and then added to the wells. The DNA/Lipofectamine mixture in OPTI-MEM was replaced by serum containing medium 12 h after transfection and the cells were collected 48 h following transfection.

4.4.5 Primary neuronal cell culture

Solutions

- Borate buffer containing 0.1 mg/ml Poly-D-Lysin

- DNase I (0.001 g/ml)

- BME:

  500 ml BME containing

  10 % FCS

  2 % B-27

  1 % glucose 45 %

  1.2 ml L-glutamine (200 mM)

Cover slip and well treatment

For optimal adhesion of primary neurons, the coverslips or wells were treated as follows. Coverslips were baked for approximately 12 h at 200 °C. 24-wells with or without and 6-wells without sterile coverslips were coated overnight with poly-D-lysine (0.1 mg/ml in borate buffer) at 37 °C. Subsequently, wells were washed with sterile water and after an incubation for approximately 2 h at 37 °C, two additional washing steps were carried out.

Preparation of primary neurons

A pregnant rat or mouse was sacrificed, and the uterus containing the embryos (E16-E19) was removed. The embryo heads were dissected in HBSS and placed in a Petri dish with ice-cold HBSS. Then, the hippocampus and cortex of every pup were isolated and collected separately in a 3.5 cm Petri dish. The cortices were cut into approximately 1 mm thick pieces and all collected tissue was transferred into a 15 ml falcon tube. The tissue was washed 3-5 times with HBSS and trypsin solution (0.025 g/ml trypsin) was added. The incubation was performed for 20 min at 37 °C followed by 3-5 washing steps with HBSS. Afterwards, the tissue was transferred into 2 ml tubes and the remaining DNA was digested with DNase I (0.001 g/ml) in approximately 1 ml HBSS. Next, the tissue was dissociated using cannulas (three times 0.9 mm x 40 mm; three times 0.45 mm x 23 mm). The solution from rat tissue was given through a Nylon cell strainer (100 µm) and the mesh was rinsed with 4-

10 ml Basal Medium Eagle (BME) supplemented with 1 % glucose, 10 % FCS, 2 % B-27, and 0.5 mM L-glutamine to collect all cells. Tissue from mice was resuspended by pipetting up and down repeatedly with a 1 ml pipette. After counting in a Neubauer chamber, the cells were plated on a 24-well cell culture plate at densities listed in table 4.5. One to 24 h after seeding, the medium was replaced by fresh BME. Neurons were cultured in a humidified incubator at 37 °C and 5 % CO_2. Olfactory bulbs from newborn mouse pups (P0-3) or from embryos were isolated according to the same protocol with the following modifications. Dissociation was performed by papain digestion (10 U/ml, with 1 µM Ca^{2+} and 0.5 µM EDTA). Neurons that were analyzed regarding their survival following KA stimulation were supplemented with 5 µM Arabinofuranosyl cytidine (Ara-C) from DIV3 to the time point of analysis to limit glial cell division.

Table 4.5: Cell numbers plated

Well	Cell number
24-well (low density)	40,000
24-well (high density)	70,000
6-well	300,000

4.4.6 Transfection of neurons for promoter studies

Rat hippocampal neurons were transfected in 24-well cell culture plates in triplicates at DIV5 (OB neurons at 7 DIV) using lipofectamine (Life technologies, Karlsruhe, Germany) according to the manufacturer's protocol. During transfection, BME medium was replaced by OPTI-MEM containing the transfection solution and cells were kept at 37 °C and 5 % CO_2. After 2 h, OPTI-MEM was substituted for the original BME-Medium. The transfection mixture contained 0.1 µg of the pGL-promoter construct expressing firefly luciferase, 0.025 µg pRL-TK with the *Renilla* gene (Promega), the indicated amount of overexpression plasmid for the respective transcription factor, and 1 µl lipofectamine in 50 µl OPTI-MEM. The mixture was incubated at room temperature for 20 min and then added to the wells.

4.4.7 Transfection of neurons for localization studies

For localization studies, transfection of mouse cortical and hippocampal neurons was carried out using a protocol based on DNA/Ca^{2+} -phosphate co-precipitation (Köhrmann et al., 1999). Neurons were transiently transfected on DIV5-7. The original medium of the neurons was exchanged for minimum essential medium (MEM) and was kept in the incubator for the transfection procedure. Per 24-well, 2 µg endotoxin-free plasmid DNA was used. A mixture of DNA, 60 µl CaCl$_2$ and 60 µl 2x BES buffered saline (2x BBS) was prepared for two wells. After using a vortex mixer for 20 s the precipitate was directly added to the wells and the plate was incubated at 2.5 % CO$_2$ at 37 °C for 30-40 min. Formation of the amount of precipitate was monitored under the microscope. Subsequently, neurons were washed twice with 1x HBS and twice with BME and then the original medium was added back to the cells.

Buffers

- 2x BBS

    280 mM NaCl

    1.5 mM Na$_2$HPO$_4$

    50 mM BES

    pH 7.1

- HEPES buffered saline (1x HBS)

    135 mM NaCl

    4 mM KCl

    1 mM Na$_2$HPO$_4$

    2 mM CaCl$_2$

    1 mM MgCl$_2$

    10 mM glucose

    20 mM HEPES

    pH 7.35

4.4.8 Stimulation of neurons

For stimulation of primary neurons with potassium chloride (KCl) or kainic acid (KA), half of the original medium was removed and mixed with the respective concentration of the stimulant. Then, the other half of the medium was removed well by well and

the mixture containing the stimulant was added directly to the well, to ensure that the neurons were always covered by medium. After stimulation, the cells were washed 2-3 times with 1x PBS and subsequently, the second half of the medium was added back to the neurons. The medium of the control cells was exchanged as often as the one of stimulated neurons followed by the same washing steps. All stimulations were carried out in 24-well cell culture plates in triplicates.

4.5   rAAV virus production

Transfection of HEK293T cells

For high titer purified rAAV preparations (Serotype 1/2 or 8), HEK293T cells were plated on 10 x 15 cm culture dishes per rAAV construct and transfected at approximately 70 % confluency. Three hours before transfection, the medium was exchanged by IMDM containing 5 % FCS. The transfection procedure was carried out as described in chapter 4.4.2. Cells were harvested approximately 72 h following transfection.

Table 4.6: Components of the rAAV transfection protocol (Mix for 5 x 15cm dishes)

AAV-Serotype 1/2	AAV-Serotype 8
62.5 µg rAAV construct of interest	25 µg rAAV construct of interest
125 µg pFdelta6	50 µg pFdelta6
31.25 µg pRV1	25 µg pNLrep
31.25 µg pH21	-
1650 µl 2.5 M CaCl$_2$	1650 µl 2.5 M CaCl$_2$
10500 µl H$_2$O	10500 µl H$_2$O
+ 12000 µl 2xHEBS	+ 12000 µl 2xHEBS

Harvesting cell lysates

Cells were scraped off in the culture medium and centrifuged 20 min at 2000 rpm and 4 °C. The pellet was resuspended in 45 ml 150 mM NaCl, 20 mM Tris-HCl, pH 8.0 and stored over night at -20 °C. On the following day, cell pellets were incubated with Benzonase endonuclease (50 U/ml) and sodium deoxycholate (0.5 %) for 1-2 h. After 30 min, 1M NaCl was added only to cell lysates for serotype 8 purification and

incubated another 30 min at 56 °C. After centrifugation at 4500 rpm for 20 min at 4 °C, the supernatant was stored at -20 °C over night.

Purification of Serotype 1/2

The cell lysate was thawed at room temperature and centrifuged at 4500 rpm for 20 min at 10 °C. Meanwhile the HiTrap Heparin column for purification was calibrated as follows: 10 ml 150 mM NaCl, 20 mM Tris-HCl, pH 8.0 was run through the column by an automatic pump at 60 ml/h. Sample loading was carried out with an Omnifix LuerLock 50 ml syringe at a rate of 60 ml/h. Afterwards, the following washing and elution steps were performed. Only the first washing step was carried out using the pump, the other ones were performed manually.

Washing

- 20 ml 100 mM NaCl, 20 mM Tris-HCl. pH 8.0
- 1 ml 200 mM NaCl, 20 mM Tris-HCl, pH8.0
- 1 ml 300 mM NaCl, 20 mM Tris-HCl, pH8.0

Elution

(fractions were collected in a sterile 15 ml tube)
- 1.5 ml 400 mM NaCl, 20 mM Tris-HCl, pH 8.0
- 3 ml 450 mM NaCl, 20 mM Tris-HCl, pH 8.0
- 1.5 ml 500 mM NaCl, 20 mM Tris-HCl, pH 8.0

The virus was concentrated using an Amicon Ultra-4 100K column at 4 °C and a maximum speed of 3200 rpm. The sample was concentrated to a volume as small as possible. Then, the column was washed two times with 1x PBS and finally concentrated to approximately 500 µl. The purified virus was stored at 4 °C. Purification of the virus was examined by loading 15 and 7.5 µl of purified virus on a 10 % SDS-PAGE and subsequent Coomassie staining. Highly purified virus should reveal only viral protein bands at 60, 70 and 80 kDa.

Purification of Serotype 8

After thawing, centrifugation was carried out using an ultracentrifuge with a JA-20 rotor (Beckman) at 7000 rpm for 30 min at 4 °C. Then, 2 cycles of freezing (with an isopropanol/dry ice bath) and thawing with the same centrifugation step in between as before. Discontinuous iodixanol step gradients were formed in quick-seal tubes (25 x 89 mm, Beckman) by underlaying and displacing the less dense cell lysate (15 ml) with iodixanol. The solution was prepared using a 60 % sterile solution of iodixanol OptiPrep (Nycomed) and 1x PBS supplied with 1 mM $MgCl_2$ and 2.5 mM KCl (PBS-MK). The gradient consists of (from the bottom) 3 ml 54 %, 3 ml 40 %, 4 ml 25 % and 7 ml 15 %; the 15 % density step also contained 1 M NaCl. On the top, 7.5 ml of the virus was added, tubes were sealed and centrifuged in a JA-20 rotor at 60.000 g for 90 min at 18 °C (without setting the brake). The 40 % phase was aspirated with a syringe and the virus was concentrated using an Amicon Ultra-15 100K. For this, the sample was adjusted with PBS-MK to 15 ml and centrifuged at 2000 g for 2 min at 4 °C. The refilling to 15 ml and centrifugation was repeated four times. Afterwards, the virus was concentrated to approximately 500 µl and stored at 4 °C. Purification of the virus was examined by loading 15 and 7.5 µl of purified virus on a 10 % SDS-PAGE and subsequent Coomassie staining. Highly purified virus should reveal viral protein bands at 60, 70 and 80 kDa.

4.6   P0-3 virus injection

Newborn C57/Bl6 mice (P0) were anesthetized 45 s on ice and intracerebral injection of viral particles in the ventricles and in the OB was performed using a 10 µl Hamilton syringe at a rate of 451 nl/sec. The injection was performed on both hemispheres on three consecutive days (P0-3). Six to eight weeks after injection, mice were deeply anesthetized with Isofluran and subsequently sacrificed via perfusion with 4 % PFA. After this, the mice were decapitated and the brain was removed. Using a vibratome, 20 µm thick slices were prepared and viral injection was examined using an epifluorescence microscope. All experiments were performed in accordance with the guidelines of the University of Bonn Medical Center Animal Care Committee.

4.7 Promoter analysis methods

4.7.1 Luciferase assay

For luciferase measurements, cells were washed with 1x PBS and subsequently lysed with passive lysis buffer (PLB). Lysis of 24-well plates (primary neurons) was performed in 100 µl/well PLB and of 48-well plates (NG108-15 cells) in 50 µl/well PLB. During lysis, cells were incubated 20 min at room temperature on a shaking plate. Before lysis incubation, neurons were carefully scraped off the wells with a scraper. Meanwhile, luciferase assay reagent, which provides the substrate for the luciferase measurement and Stop and Glo, which quenches the luciferase luminescence and contains the *Renilla* substrate, were freshly prepared. The measurement was carried out with 50 µl of each substrate using a Glomax Luminometer (Promega). Duration of luciferase measurement was 10 s with a 2 s delay between luciferase and *Renilla* luminescence measurement.

4.8 Immunochemical methods

4.8.1 Immunocytochemistry

Primary hippocampal and cortical neurons at DIV14-16 were fixed for 10 min with 4 % paraformaldehyde (PFA), washed three times in 1x PBS and permeabilized with 0.3 % TritonX-100 in 1x PBS for 10 min. Then, neurons were incubated over night with primary antibodies at 4 °C in blocking solution (1 % BSA, 10 % NGS, 0.1 % Triton X-100 in 1x PBS). On the following morning, cells were washed three times with 1x PBS and incubation with the secondary antibody was performed in blocking solution for 45 min at room temperature in the dark. Cover glasses were mounted in Mowiol.

4.8.2 Immunohistochemistry

Mouse brains were perfused with 4 % paraformaldehyde (PFA) and incubated on a shaker plate at 4 °C overnight in PFA. On the following day, the right hemisphere was embedded in freezing medium (Tissue-Tek). 50 µm thick cryosections were cut on a cryostat and every second of 10 sections were stained against BrdU. Sections sections were kept in sterile 1x PBS and incubated in 24-wells in 2 N HCl for 30 min at 35 °C in a waterbath. After four washing steps in TBS, sections were incubated

overnight at 4 °C with primary antibody (BrdU) in 1x TBS containing 0.6 % Triton X-100 (1x TBST). On the following day, sections were washed four times with 1x TBS and the incubation with the anti-rat biotin antibody was performed in 1x TBST for three hours at 35 °C in the waterbath. Following four washing steps, the secondary antibody (Cy3-Streptavidin) was added to the wells in 1x TBST and was incubated 3 h at 35 °C in the dark. After extensive washing with 1x TBS, sections were mounted in Vectashield hard set mounting medium.

4.9 Pilocarpine injection

Male C57/BL6 mice, ordered from Charles River, as well as male Syt10 wildtype (WT) and Syt10 knockout (KO) mice (all ≥ 60 d old; weight ≥ 20 g) were housed under a 12 light/dark cycle with food and water *ad libitum*. Administration of pilocarpine, a muscarinic agonist, was used to induce sustained seizures in these experimental animals. First, animals received a low dose of 1 mg/kg scopolamine methyl nitrate subcutaneously (s.c.). After 20 min, mice were injected with 335 mg/kg pilocarpine hydrochloride (s.c.) to induce SE. Series of continuous generalized tonic-clonic seizures were defined as SE and represent the seizure description stage V. Treatment of sham-injected control animals was identical except for the injection of an isotonic NaCl solution instead of pilocarpine. To terminate seizures, 4 mg/kg (s.c.) diazepam was administered to the mice 40 min after onset of SE. After SE, animals were fed with soaked rodent food and with a 5 % glucose solution. For subsequent analysis, only those of the pilocarpine-injected animals were used that developed SE. All experiments were performed in accordance with the guidelines of the University of Bonn Medical Center Animal Care Committee.

4.10 BrdU injection

Syt10 WT and Syt10 KO control and SE-experienced mice received a single dose of 300 mg/kg Bromodeoxyuridine (BrdU) intraperitoneally 2 d after SE. Two hours following BrdU-injection mice were deeply anesthetized with Isofluran and subsequently sacrificed via perfusion with 4 % PFA.

4.11 Imaging

Labeled sections were imaged with an epifluorescence microscope (Zeiss Axiovert Observer 1A). For high magnification of cells, imaging was performed with a confocal microscope (Leica TCS, Zeiss LSM710 and Nikon Eclipse T*i*).

4.12 Statistical analysis

Results were tested for statistical significance using Student's *t*-test or One-Way Analysis of Variance followed by Tukey's Posthoc Test. Values were considered significantly at $p < 0.05$. All results were plotted as mean ± SEM.

5   Results

Syts comprise a large family of membrane trafficking proteins that are evolutionary conserved (Craxton, 2001, 2004). However, the function of many Syt family members remains enigmatic, especially in disease conditions. To gain first insights into the role of this gene family in epilepsy, Syts were screened for differential expression in the hippocampal formation following status epilepticus (SE) induced in rats (unpublished data by T. Mittelstaedt). One Syt isoform was less abundant (Syt3) in response to SE but two family members, namely Syt6 and Syt10 showed a rapid and transient up-regulation of their mRNA in all hippocampal subregions (data not shown). The strong increase of Syt10 mRNA 6 h after SE (5-fold in the dentate gyrus and the CA3 region, 4-fold in the CA1 region) returned near to basal levels 5 d following SE. This was an intriguing finding as Syt10 was only barely expressed in the native brain. However, as the function and localization of Syt10 in the hippocampus are unknown, its role in epileptogenesis remains enigmatic.

5.1   Analysis of signaling pathways regulating Syt10 gene expression

5.1.1   Identification of the Syt10 core promoter

Syt10 mRNA levels are rapidly and transiently augmented in response to kainic acid-induced SE in rat (Babity et al., 1997). Intriguingly, this transcriptional up-regulation is limited to the hippocampus and the piriform cortex. The restricted expression of Syt10 to the olfactory bulb (OB) under native conditions indicates the presence of an intricate control mechanism that hasn't been resolved yet. In order to delineate the transcriptional mechanisms mediating the transcriptional response of the Syt10 gene to SE the Syt10 promoter region was bioinformatically analyzed. For this purpose, the sequence 355 bp upstream and 320 bp downstream of the translation start site of the Syt10 rat gene was examined for characteristics typically associated with core promoter regions: a) the presence of CpG-islands, b) a high level of conservation between species, and c) transcription start sites (TSS) (Figure 4.1 A). In the Syt10 gene a CpG island of 423 bp was found around the first exon, with 286 bp upstream and 137 bp downstream of the start ATG. Six transcription start sites were detected

at 63 bp, 100 bp, 125 bp, 138 bp, 198 bp and 232 bp upstream of the start ATG (Figure 5.1 A).
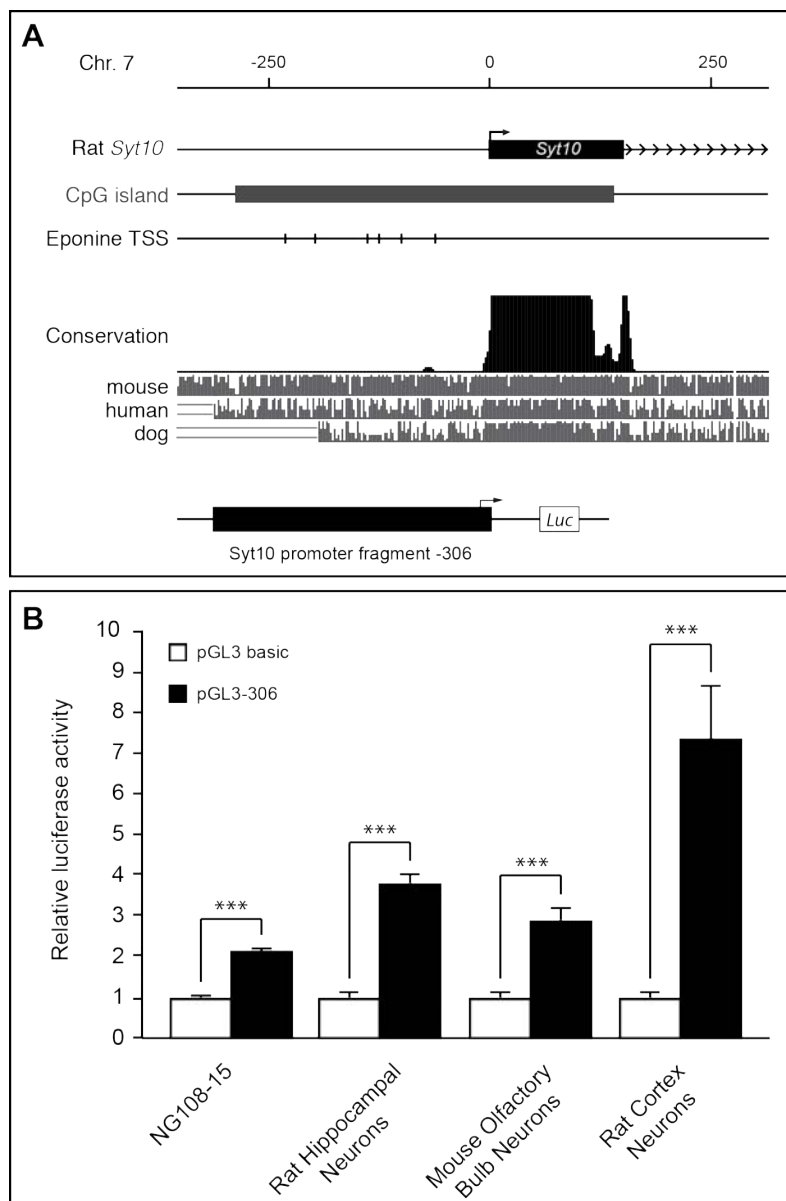
Figure 5.1 Identification of the Syt10 core promoter. (A) Graphic representation of the rat Syt10 gene (Chromosome 7: 355 bp up- and 320 bp downstream of the start ATG). The identified CpG island (423 bp around the start ATG), the level of conservation and six transcription start sites (TSS) are indicated. The lower grey bars represent pairwise alignments between the indicated species. (B) Basal luciferase activity of the predicted Syt10 core promoter in NG108-15 cells, rat hippocampal neurons, mouse olfactory bulb neurons and rat cortical neurons. A construct containing *Renilla* luciferase under control of a standard promoter was used for standardization and the results are presented as Firefly/*Renilla* relative luciferase units (RLUs). The core promoter fragment -306 was active in all four cell types compared to the pGL3 basic vector. All values were normalized to the pGL3 basic vector and statistical analysis was carried out using Student's *t*-test (*** $p \leq 0.001$). Results are presented as mean +/- SEM.

To examine whether the bioinformatically identified core promoter indeed showed promoter activity the corresponding genomic fragment (-1 to -306, relative to the start ATG) was cloned into a luciferase reporter vector (pGL3 basic) and the luciferase

activity was measured in NG108-15 cells, primary rat hippocampal (RH) and cortical (RC) neurons and in mouse olfactory bulb (MOB) neurons. The presence of the core promoter fragment -306 increased the luciferase activity relative to the promoterless control pGL3 basic 2-fold in NG108-15 cells, 4-fold in rat hippocampal neurons, 3-fold in mouse olfactory bulb neurons and 7-fold in rat cortical neurons (each $p \le 0.001$) (Figure 5.1 B). These results indicate that the bioinformatically identified core promoter contains promoter characteristics leading to functional promoter activity.

5.1.2 Bioinformatic analysis of potential regulatory elements

Activity of a promoter is often regulated by enhancers and repressors. These regulatory elements are frequently located distally from a gene as shown for the Arc/Arg3.1 promoter, which is regulated by the synaptic activity-responsive element (SARE) (Kawashima et al., 2009). To search for putative regulatory regions the analysis was extended to 40 kb upstream and 70 kb downstream of the start ATG. Comparative sequence analysis between the rat reference sequence and human, mouse and dog orthologs revealed five regions conserved among all four species and one region that was conserved between rat, mouse and human orthologs. The promoter region analyzed in the subsequent experiments is depicted in figure 5.2 as black box and regulatory regions as grey boxes.
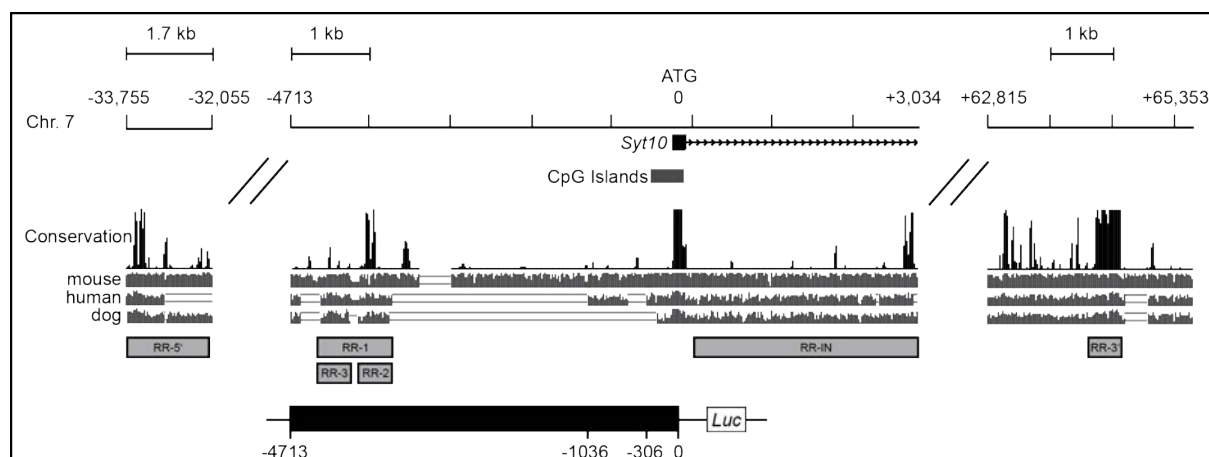
Figure 5.2 Bioinformatic analysis of the Syt10 gene. (A) Graphic representation of the rat Syt10 gene (Chromosome 7). Using UCSC, 50 kb up- und 70 kb downstream of the start ATG were analyzed. The conservation track was based on PhastCons (black bars). The lower grey bars represent pairwise alignments between the indicated species. Regions with high homology were identified and according to their position, they were named regulatory region-5' (RR-5'), regulatory region-Intron (RR-IN), regulatory region-3' (RR-3') and regulatory region-1, -2 and -3 (RR-1, -2, -3). Grey boxes and black box with positions (-306, -1036, -4713) indicate the fragments that were subcloned in the pGL3 basic vector carrying a luciferase reporter gene.

5.1.3 Functional characterization of activating and repressing regions within the Syt10 promoter

To determine whether the promoter fragments of varying length and the regulatory regions contain activating or/and repressing elements, the corresponding sequences were cloned into a luciferase reporter vector and their transcriptional activity was tested in NG108-15 cells and in primary hippocampal, olfactory bulb and cortical neurons. Compared to the core promoter an increase in activity was only observed for fragment -1036 in hippocampal neurons indicating the presence of a cell-type specific enhancer or the absence of a repressor (Figure 5.3, right diagram). Furthermore, compared to the other cell types promoter activity in NG108-15 cells was lower for most fragments, but roughly the same for the other cell types (Figure 5.3, left diagram). As plasmid -306/RR-IN exhibited a promoter activity even lower than the one of the promoterless control plasmid pGL3 basic, it was not further examined.
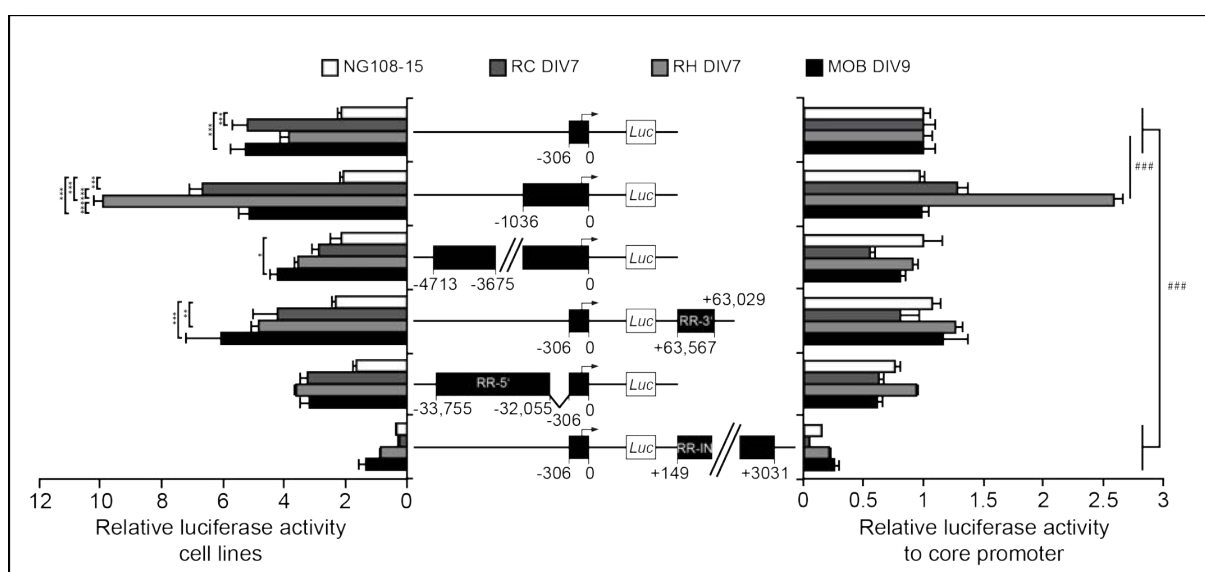
Figure 5.3 Functional analysis of regulatory regions of the Syt10 gene. Basal luciferase activity of different Syt10 promoter constructs in NG108-15 cells (white bars), rat cortical neurons (RC; dark grey bars), rat hippocampal neurons (RH; light grey bars) and mouse olfactory bulb neurons (MOB; black bars). RH and RC neurons were transfected on DIV5, MOB neurons on DIV7 and NG108-15 cells 24 h after seeding. 48 h later, cells were lysed for luciferase measurements. Firefly/*Renilla* relative units are normalized to pGL3 basic (left diagram) and to the Syt10 core promoter fragment -306 (right diagram). Analysis of basal luciferase activity revealed a specifically higher activity of Syt10 promoter fragment -1036. This result indicates the presence of a potential hippocampus specific activating region or a repressing region that is not functional in the hippocampus. Results are presented as mean +/- SEM and statistical analysis was performed using a One-way ANOVA followed by Tukey posthoc test (* $p \leq 0.05$, ** $p \leq 0.01$, *** $p \leq 0.001$; ### $p \leq 0.001$).

The region identified as the core promoter (chapter 5.1.1), -306, increased the promoter activity relative to the promoterless control pGL3 basic in all tested cell

types (Figure 5.1). Furthermore, even though the fragment -4713 comprises a longer region upstream of the first exon, its promoter activity was not higher compared to the core promoter (Figure 5.4, right diagram). Intriguingly, the fragment -4713 contains a region that is highly conserved among species (RR-1; genomic position -4344 to -3675 relative to the start ATG, Figure 5.2). This region can be further sub-divided into two smaller regions, one that has a higher degree of conservation (RR-2; -4054 to -3675 upstream of the start ATG) than the other one (RR-3; -4344 to -4054 relative to the start ATG) (Figure 5.2). To test these fragments for their activating or repressing properties, their luciferase activity was analyzed in the four cell types used before and the results were normalized to pGL3 basic (Figure 5.4, left diagram) or to the core promoter, -306 (Figure 5.4, right diagram). The fragment -306/RR-1 resulted in a higher promoter activity compared to the core promoter and compared to -4713. Furthermore, in hippocampal neurons luciferase assays revealed the presence of an activating element in the fragment -306/RR-2 whereas the presence of the fragment -306/RR-3 decreased the promoter activity to levels of -306/RR-1 (Figure 5.4, right diagram). These results indicate that the region RR-2 is a hippocampus specific regulatory element, which is, similar to -1036, suppressed in the genomic context.
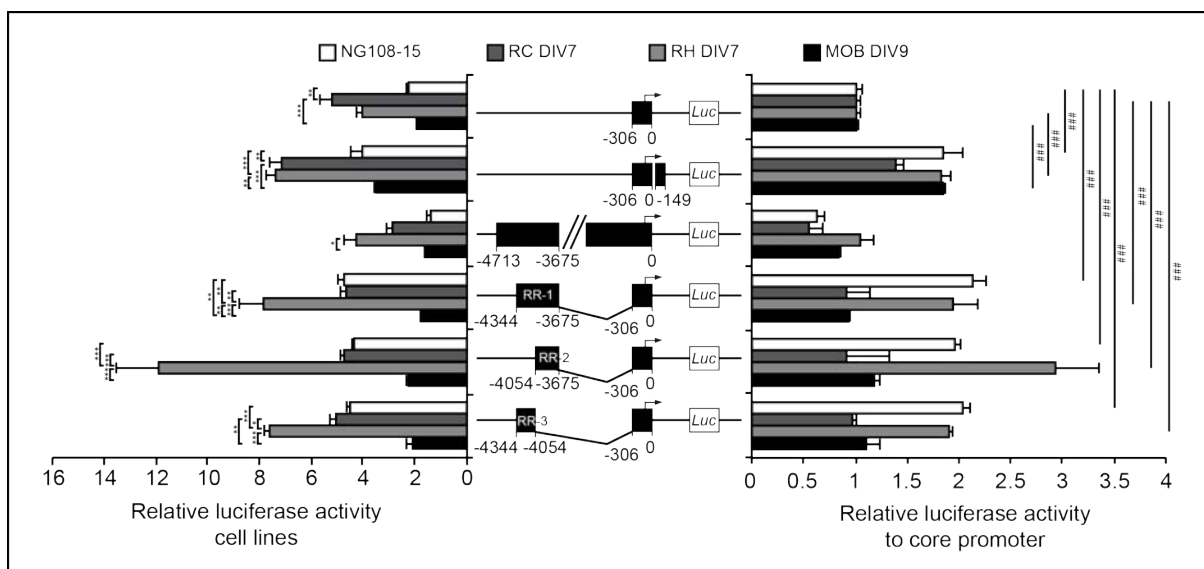
Figure 5.4 Active regulatory regions within the Syt10 promoter. Basal luciferase activity of different Syt10 promoter constructs in NG108-15 cells (white bars), rat cortical neurons (RC; dark grey bars), rat hippocampal neurons (RH; light grey bars) and mouse olfactory bulb neurons (MOB; black bars). RH and RC neurons were transfected on DIV5, MOB neurons on DIV7 and NG108-15 cells 24 h after seeding. 48 h later, cells were lysed for luciferase measurements. Firefly/*Renilla* relative units are normalized to pGL3 basic (left diagram) and to the Syt10 core promoter fragment -306 (right diagram). Combined fragments consisting of -306 and the complete first exon (without ATG) or RR1, 2 and -3 show stronger luciferase activity in NG108-15 cells and in rat hippocampal neurons. Results are presented as mean +/- SEM and statistical analysis was performed using a One-way ANOVA followed by Tukey posthoc test (* $p \leq 0.05$, ** $p \leq 0.01$, *** $p \leq 0.001$; ### $p \leq 0.001$).

Due to the presence of a CpG island and putative binding sites for transcription factors, the first exon might be an important element of the Syt10 promoter. To test this hypothesis, a luciferase plasmid was generated containing the genomic sequence -306 to +149 that however did not contain the start ATG (-306/149). With the exception of cortical neurons fragment -306/149 showed a stronger luciferase activity compared to the core promoter in all cell types indicating that this region contains positive regulatory elements. The higher activity of the complete exon I compared to the core promoter indicates that the first exon is important for the basal activity of the Syt10 promoter.

5.1.4 The Syt10 promoter harbors functional binding sites for activity-regulated transcription factors

To assess which transcription factors might contribute to the up-regulation of Syt10 following SE, first a bioinformatic analysis using different algorithms (Genomatix, rVISTA) was performed. The focus was on transcription factors, which are known to be differentially expressed after synaptic activity, namely cAMP responsive element binding protein (CREB), activator protein 1 (AP1), myocyte enhancer factor 2A (MEF2A), neuronal PAS domain protein 4 (NPAS4) and upstream stimulatory factor 1 and 2 (USF1 and 2).

DNA-binding sites were predicted in the Syt10 promoter for all of these factors. Most of the binding sites were observed within the region -4713 bp upstream of the ATG (Figure 5.5 A). However, none of these factors were overrepresented in the Syt10 promoter sequence as assessed by the RegionMiner (Genomatix) algorithm for the search of overrepresented transcription factors binding sites in the Syt10 promoter (Appendix, supplementary table 1). To determine the functionality of the putative transcription factor binding sites on the Syt10 promoter fragments, NG108-15 cells, which are often used to assess the activating potential of transcription factors, were used. These cells were co-transfected with expression plasmids coding for the predicted transcription factors (MEF2A, MEF2C, NPAS4, cJun, USF1 and USF2) and with the promoter fragments -306, -1036, -4713, -306/RR3' and -306/RR5'. Analyzing luciferase activity in NG108-15 cells clearly revealed no alteration of the promoter fragments with the transcription factors MEF2A and MEF2C compared to mock transfected cells (Figure 5.5 B).
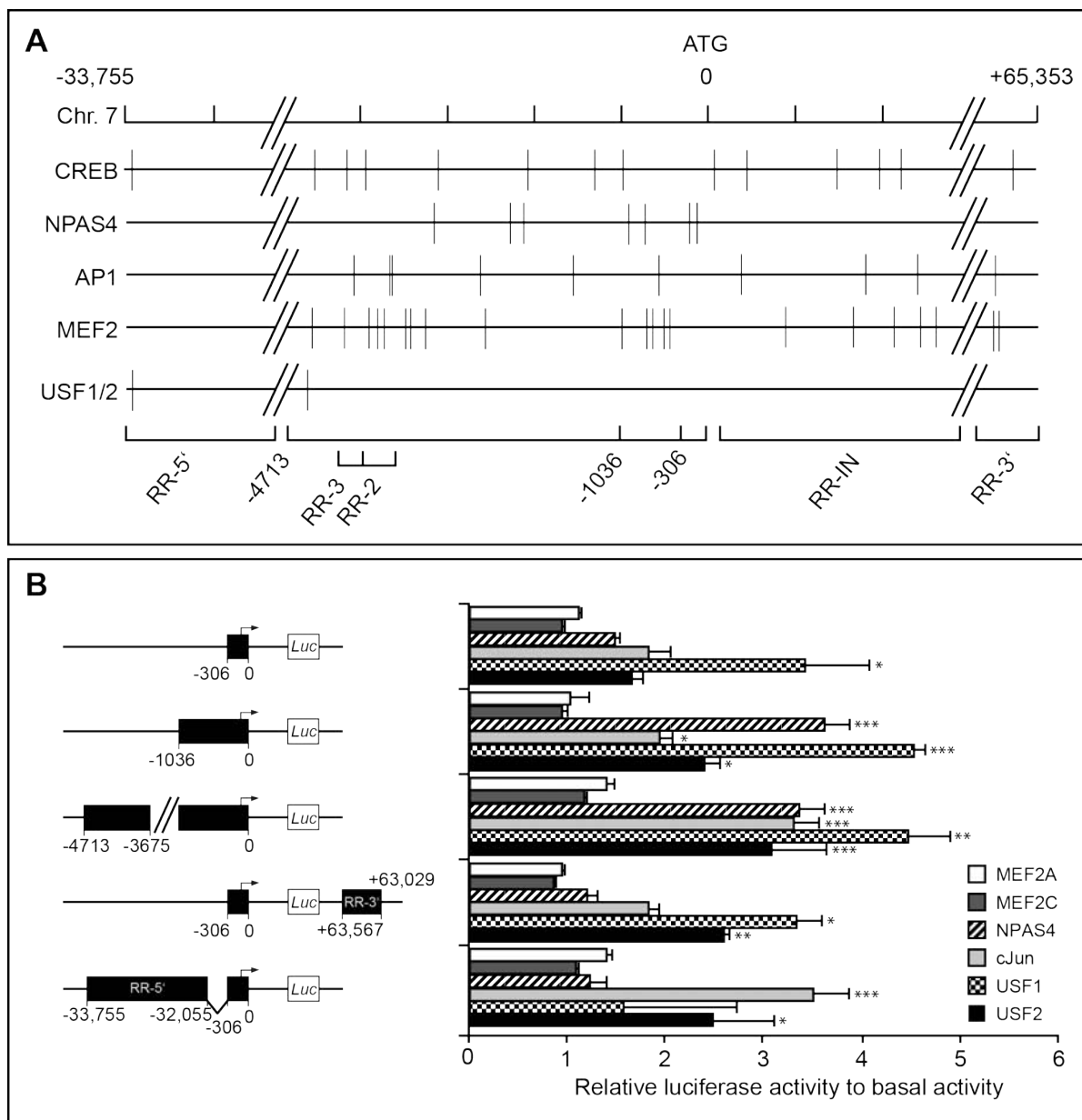
Figure 5.5 The Syt10 gene harbors functional binding sites for activity-regulated transcription factors. (A) Graphic representation of the rat Syt10 gene with predicted transcription factor binding sites of factors known to be involved in differential expression after synaptic activity (CREB1, NPAS4, AP1, MEF2, USF1/2). (B) Luciferase activity in NG108-15 cells of the promoter fragments with overexpressed transcription factors (MEF2A/C, NPAS4, cJun, USF1/2). A construct containing *Renilla* luciferase under control of a standard promoter was used for standardization and the results are presented as Firefly/*Renilla* relative luciferase units (RLUs). All values were normalized to the respective control condition (not shown) and statistical analysis was performed using One-way ANOVA followed by Tukey posthoc test (* $p \leq 0.05$, ** $p \leq 0.01$, *** $p \leq 0.001$). Results are presented as mean +/- SEM.

In NPAS4-transfected samples, measurement of luciferase activity showed a clear activation of the promoter fragment -1036 (3.6-fold, $p \leq 0.001$) and -4713 (3.4-fold, $p \leq 0.001$) (Figure 5.5 B). The transcription factor cJun induced the promoter fragments -1036 (1.9-fold, $p \leq 0.05$), -4713 (3.3-fold, $p \leq 0.001$) and -306/RR5'

(3.5-fold, p ≤ 0.001) (Figure 5.5 B). The other AP1 transcription factors tested, JunB and JunD, also strongly activated the Syt10 promoter in NG108-15 cells (Data not shown). USF1 and USF2 transfected cells showed a similar activation of the promoter fragments with the difference that USF1 induction of the promoter was stronger compared to USF2. Whereas USF1 increased the promoter fragment -306 (3.4-fold, p ≤ 0.05) (and not USF2) -306/RR5' was only induced by USF2 (2.5-fold, p ≤ 0.05) (and not by USF1). Taken together, these results indicate that not all of the predicted transcription factor binding sites lead to a functional activation of the Syt10 promoter in NG108-15 cells (MEF2A, MEF2C), whereas some factors strongly alter the promoter activity (NPAS4, cJun, USF1, USF2).

5.1.5 Activity-regulated transcription factors induce endogenous Syt10 gene expression in primary neurons

Using quantitative real-time RT-PCR, the ability of the transcription factors that increase the Syt10 promoter activity in NG108-15 cells was examined to effect endogenous Syt10 expression in primary neurons. Rat hippocampal neurons were therefore transfected on DIV5 with NPAS4, USF2 and cFos and the cells were lysed for extraction of mRNA at DIV6-7 (indicated as 24 or 48 h after transfection). Even though only less than 30 % of neurons were transfected, overexpression of NPAS4, USF2 and cFos resulted in a robust increase of endogenous Syt10 expression in hippocampal neurons (each p ≤ 0.05) (Figure 5.6). Neurons transfected with cJun did not show an augmented Syt10 mRNA expression (0.8-fold, p > 0.05, Figure 5.6), which indicates that either the transfection efficiency was to low or that cJun does not affect the Syt10 promoter in neurons.
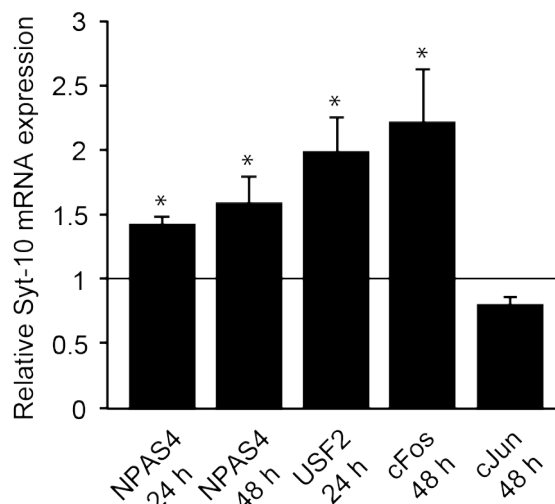
Figure 5.6 Activity-regulated transcription factors activate endogenous Syt10 gene expression. Quantitative RT-PCR on mRNA from rat hippocampal neurons transfected with an empty vector or with the indicated transcription factors on DIV5. Cells were lysed 24 or 48 h after transfection and Synaptophysin was used as housekeeping gene. Overexpression of NAPS4, USF2 and cFos but not of cJun led to augmented Syt10 mRNA expression levels. All values were normalized to the respective control condition (black line) and statistical analysis was performed using Student's *t*-test (* $p \leq 0.05$). Results are presented as mean +/- SEM.

5.1.6 NPAS4 activates the Syt10 promoter

NPAS4 is an interesting candidate transcription factor to be involved in the regulation of Syt10 gene expression as it is up-regulated in the hippocampus in response to seizure activity (Flood et al., 2004). Since NPAS4 markedly augmented the promoter activity of Syt10 in NG108-15 cells and was sufficient to robustly increase endogenous Syt10 expression, it was next examined if NPAS4 also activates the Syt10 promoter in neurons. Therefore, primary hippocampal neurons were co-transfected at DIV5 with the Syt10 promoter fragment -4713 and with or without NPAS4 and the cells were lysed 48 h later for analyzing luciferase activity. NPAS4 showed a markedly increase of luciferase activity of the promoter fragment -4713 (2.5-fold, $p \leq 0.001$) (Figure 5.7).
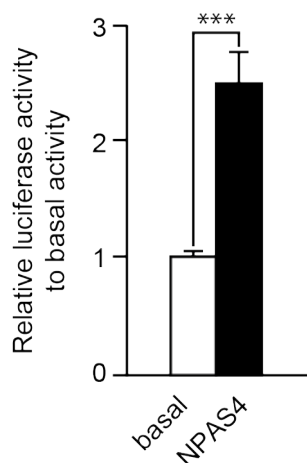
Figure 5.7 Transcription factor NPAS4 activates the Syt10 promoter. The transcription factor NPAS4 increased the luciferase activity of the Syt10 promoter fragment -4713. RH neurons were transfected on DIV5 with either an empty vector or 25 ng NPAS4 and 48 h later, cells were lysed for luciferase measurements. Firefly relative units are normalized to the basal values (mock transfected cells). Statistical analysis was performed using the Student's *t*-Test (*** $p \leq 0.001$). Results are presented as mean +/- SEM.

5.1.7 Analysis of NPAS4 binding sites mediating activation of the Syt10 promoter

NPAS4 strongly activated the Syt10 promoter in NG108-15 cells and in rat hippocampal neurons (Figure 5.5 and 5.7). To delineate the exact NPAS4 binding sites in the Syt10 promoter that increase the activity of the promoter, deletion constructs covering the distinct predicted binding sites were designed (Figure 5.8 A). Fragments of different lengths were cloned into the pGL3 basic vector and were transfected on DIV5 into rat hippocampal neurons. To assess all predicted binding sites for NPAS4, the deletion constructs were compared to the promoter fragments -306, -1036 and -4713. Lysis of transfected neurons was carried out 48 h later for subsequent luciferase assays. Figure 5.8 B depicts the luciferase activity of these fragments in rat hippocampal neurons that were co-transfected with an empty vector (basal values) or 50 ng NPAS4 and were normalized to basal values (not shown). Due to the finding that the Syt10 promoter was saturated with NPAS4 at a concentration of 50 ng (Appendix, supplementary Figure 7), this concentration was used in further experiments. NPAS4 increased the promoter activity of the deletion constructs I, II and fragment -306, which cover the first two predicted binding sites (Figure 5.8 B).
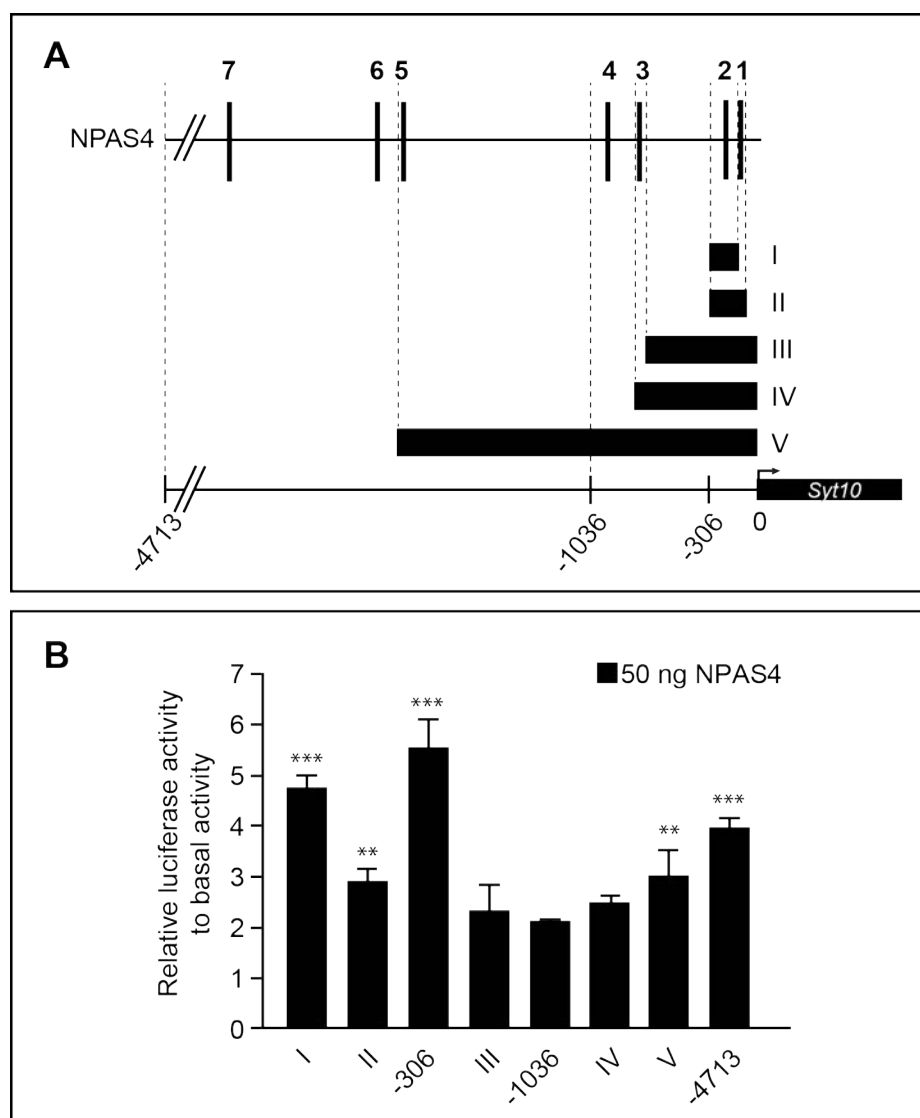
Figure 5.8 Analysis of the key NPAS4 binding sites mediating the activation of the Syt10 promoter via deletion constructs. (A) Schematic drawing of deletion constructs covering the distinct bioinformatically predicted NPAS4 binding sites that are indicated by the black lines. NPAS4 binding sites are numbered from 1-7 starting with the one closest to the start ATG. (B) Rat hippocampal neurons were transfected on DIV5 with either an empty vector or 50 ng NPAS4 and 48 h later, cells were lysed for luciferase assays. The Luciferase/*Renilla* values were normalized to the respective basal values (not shown) and plotted into the diagram. The deletion constructs covering NPAS4 binding sites 1, 2 and 5-7 showed a strong increase in the luciferase activity compared to basal values. Statistical analysis was performed using a One-way ANOVA followed by Tukey posthoc test (** $p \leq 0.01$, *** $p \leq 0.001$). Results are presented as mean +/- SEM.

Deletion constructs III, IV and fragment -1036 did not show induced promoter activity indicating that there might be a repressing region that overrules the activity of the first two NPAS4 binding sites in the Syt10 promoter. This repressing activity was not found in the luciferase activity of deletion constructs V and fragment -4713, which were activated by NPAS4 (Figure 5.8 B). This indicates that NPAS4 binding sites 5-7 might reverse the repressing activity in the middle part (genomic position -306 to -1036 relative to the start ATG) of the Syt10 promoter.

5.1.8 NPAS4 and Per1 double the activity of the NPAS4 induced Syt10 promoter

NPAS4 forms heterodimers with other basic helix-loop-helix Per-Arnt-Sim (bHLH-PAS) transcription factors, for example members of the Arnt family (Ooe et al., 2009b; Pruunsild et al., 2011). Arnt2 has recently been found to activate the BDNF promoter as an Arnt2:NPAS4 heterodimer (Pruunsild et al., 2011). Therefore, it was next tested, if heterodimer formation would affect the stimulatory ability of NPAS4. The promoter fragments -306, -1036 and -4713 were co-transfected into primary hippocampal neurons with either 25 ng of an empty vector, 25 ng NPAS4, 25 ng Arnt2 or a combination of both, NPAS4 and Arnt2 (25 ng each). The amount of transfected DNA was adjusted in each sample with the empty vector to a total amount of 50 ng. Transfection of NPAS4 increased the activity of the core promoter (3-fold, $p \leq 0.001$) and fragment -4713 (4-fold, $p \leq 0.001$) as seen above in figure 5.8. Overexpression of Arnt2 alone did not affect the Syt10 promoter activity. Co-transfection of NPAS4 and Arnt2 increased the luciferase activity of -4713 2-fold compared to the basal values ($p \leq 0.05$). These results indicate that instead of exhibiting a synergistic function together with NPAS4 Arnt2 presumably represses NPAS4 (Figure 5.9).
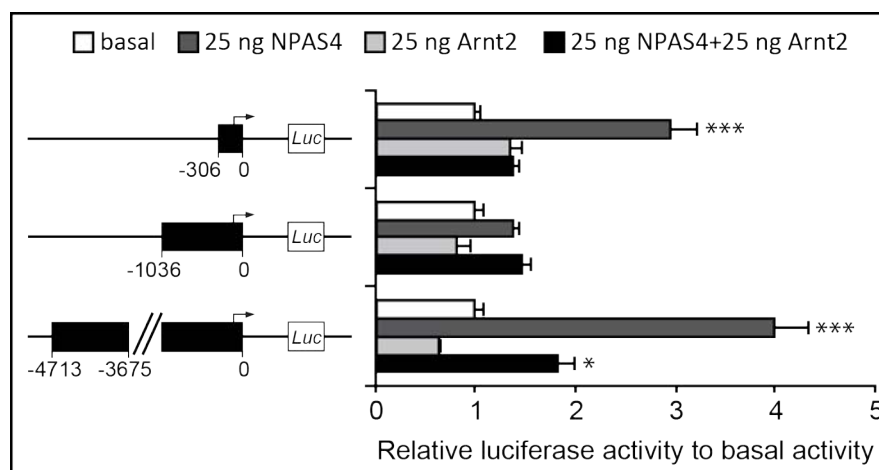
Figure 5.9 Arnt2 represses the stimulatory ability of NPAS4. The promoter fragments -306, -1036 and -4713 were transfected into rat primary hippocampal neurons together with an empty vector, 25 ng NPAS4, 25 ng Arnt2 or both transcription factors together (25 ng each). Neurons were lysed for luciferase assays 48 h later and the Luciferase/*Renilla* values were normalized to the basal values. When transfected alone, NPAS4 increased the luciferase activity of fragments -306 and -4713. Arnt2 alone did not affect the Syt10 promoter activity. When transfected with NPAS4 Arnt2 seemed to repress the activity of NPAS4. Statistical analysis was performed using a One-way ANOVA followed by Tukey posthoc test (* $p \leq 0.05$, *** $p \leq 0.001$). Results are presented as mean +/- SEM.

Nevertheless, bHLH-PAS transcription factors can form heterodimers via their bHLH-domain and homodimers through PAS-PAS interactions (Hirose et al., 1996; Huang

et al., 1995; Ooe et al., 2004; Pongratz et al., 1998). Recently, Husse et al. observed Syt10 expression in the SCN (Husse et al., 2011), the brain region, in which clock genes are expressed in an oscillatory manner. One of the clock genes is a bHLH-PAS transcription factor named Period1 (Per1). Moreover, Per1 expression was found to be more abundant in the hippocampus in response to kainic acid-induced SE and to electroconvulsive seizures (Eun et al., 2011).

Luciferase measurement of transfected rat hippocampal neurons revealed that this transcription factor induced the activity of the longest promoter fragment, -4713 (Appendix, supplementary Figure 7). To elucidate whether Per1 could heterodimerize with NPAS4 and thereby could further increase the Syt10 promoter activity the longest promoter fragment -4713 was co-transfected into rat hippocampal neurons on DIV5 with either an empty vector (100 ng), NPAS4 (50 ng), Per1 (50 ng) or a combination of both, NPAS4 and Per1 (50 ng each). The amount of transfected DNA in each sample was adjusted with the empty vector to a total amount of 100 ng. Transfection of both, NPAS4 and Per1 alone, led to a 2.5-fold increased luciferase activity ($p \leq 0.01$) compared to basal values. Co-transfection of NPAS4 and Per1 nearly doubled the luciferase activity to 5-fold compared to basal values ($p \leq 0.001$) (Figure 5.10). Hence, NPAS4 and Per1 might act as heterodimers on the Syt10 promoter.
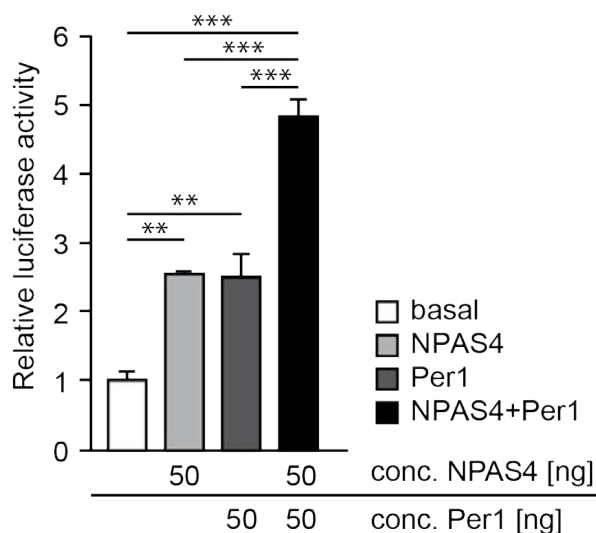
Figure 5.10 NPAS4 and Per1 increase Syt10 promoter activity as putative heterodimers. Rat hippocampal neurons were transfected with the longest promoter fragment, -4713, and an empty vector, 50 ng NPAS4, 50 ng Per1 or both transcription factors together (50 ng each). Neurons were lysed for luciferase measurements 48 h later and the Luciferase/*Renilla* values were normalized to the basal values. When transfected alone, both NPAS4 and Per1, lead to a 2.5-fold increase of the luciferase activity. Transfection of both factors together revealed a doubled increase (nearly 5-fold) compared to the factors alone. Statistical analysis was performed using a One-way ANOVA followed by Tukey posthoc test (** $p \leq 0.01$, *** $p \leq 0.001$). Results are presented as mean +/- SEM.

5.2 Stimulation protocols to mimic epilepsy-mediated up-regulation of Syt10

5.2.1 Membrane depolarization induces Syt10 expression

One hallmark of epileptogenesis is the occurrence of a hyperexcitable network (reviewed by Pitkänen & Lukasiuk, 2011). To mimic this strong synaptic activity *in vitro,* rat primary hippocampal neurons were depolarized on DIV7 for 8 h with 25 mM KCl and first Syt10 gene expression was analyzed using quantitative RT-PCR. Relative Syt10 mRNA expression levels were 2.1-fold increased after stimulation of rat hippocampal neurons compared to the control condition ($p \leq 0.001$) (Figure 5.11 A). Rat cortical neurons were stimulated following the same protocol. Here, Syt10 mRNA expression was not elevated compared to basal values (Figure 5.11 A).
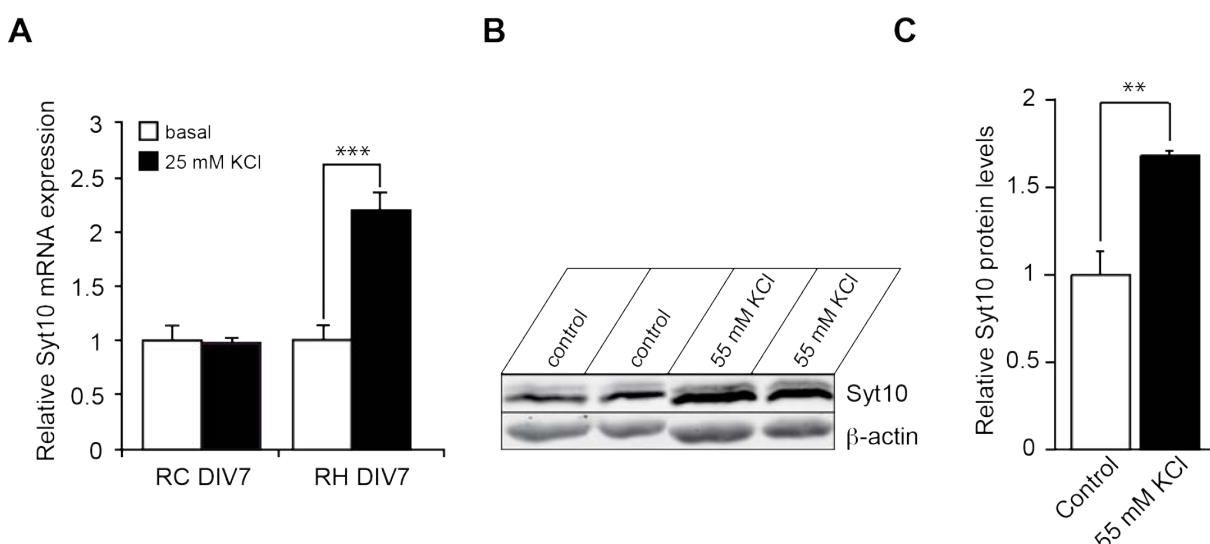
Figure 5.11 Membrane depolarization with potassium chloride induces Syt10 expression. (A) Relative mRNA expression levels of rat hippocampal (RH) and rat cortical (RC) neurons on DIV7. Neurons were stimulated with 25 mM KCl for 8 h and subsequently lysed for quantitative RT-PCR. Up-regulation of Syt10 gene expression was restricted to RH neurons (2-fold increase) and was not observed in RC neurons. For quantitative RT-PCR experiments expression of the house keeping gene Synaptophysin was used to normalize gene expression. (B) Representative immunoblot of RH neurons that were stimulated at DIV14 with 55 mM KCl for 15 min. Cells were harvested 24 h later for Western Blot analysis. Here, beta-actin was used to normalize protein expression. (C) Western Blot analysis of stimulated RH neurons as shown in (B). Quantification of Western Blots was carried out using the software AIDA. Strong depolarization revealed a 1.7-fold increase in Syt10 protein expression. All values were normalized to the respective control condition and statistical analysis was performed using Student's *t*-test (** $p \leq 0.01$, *** $p \leq 0.001$).

To evaluate whether the increase obtained on the mRNA expression level translates into higher levels of Syt10 protein following membrane depolarization, rat hippocampal neurons were stimulated on DIV13 for 15 min with 55 mM KCl and were

harvested 24 h after washing for Western blot analysis. The immunoblots were probed with a Syt10 specific antibody (described in chapter 5.3.1) and an antibody for the internal standard ß-actin (Figure 5.11 B). Quantification of the immunoblots revealed that Syt10 protein expression was increased significantly after treatment of cultured hippocampal neurons with 55 mM KCl (1.7-fold up-regulation, $p \leq 0.01$; Figure 5.11 B and C). Taken together, both Syt10 mRNA and protein levels of rat hippocampal neurons were elevated in response to membrane depolarization by KCl.

5.2.2 Analysis of Syt10 promoter activity following membrane depolarization

Next, to examine if the transcriptional regulatory elements mediating the response to membrane depolarization are located in the above characterized Syt10 promoter, transfection of primary neurons was carried out on DIV5 with the promoter fragments -306, -1036 and -4713. Following established protocols (Flavell and Greenberg, 2008; Kim et al., 2010; Eun et al., 2011; Pruunsild et al., 2011; Ramamoorthi et al., 2011), the neurons were depolarized at 7 DIV with 25 mM KCl for 8 h (controls were treated equally) and were directly lysed for analyzing luciferase activity. Membrane depolarization only increased the relative luciferase activity of the promoter fragment -4713 (2.8-fold, $p \leq 0.001$; Figure 5.12 A).

One transcription factor, NPAS4, is known to function as an activity-regulated transcription factor (Lin et al., 2008; Zhang et al., 2009a; Pruunsild et al., 2011; Ramamoorthi et al., 2011) and results showed that NPAS4 markedly increased both, the Syt10 promoter and endogenous Syt10 expression (chapter 5.1). Due to the finding that membrane depolarization activates the Syt10 promoter as well, it was tested whether NPAS4 acts activity-dependent on the Syt10 promoter.

Therefore, primary neurons were transfected at 5 DIV with the indicated promoter fragments and with/without NPAS4 and depolarization was carried out at 7 DIV with 25 mM KCl for 8 h (controls were treated equally). Subsequently, neurons were lysed for measuring luciferase activity and the results were compared with the basal activity of these fragments. Depolarization with KCl alone induced only fragment -4713 (Figure 5.12 A). A synergistic effect was observed when neurons contained both, transfected NPAS4 and 25 mM KCl. Under this condition, all Syt10 promoter fragments were augmented 4-5-fold but their activity was stronger than with NPAS4 alone ($p \leq 0.001$). Taken together these findings indicate that NPAS4 increases the Syt10 promoter in an activity-dependent manner.
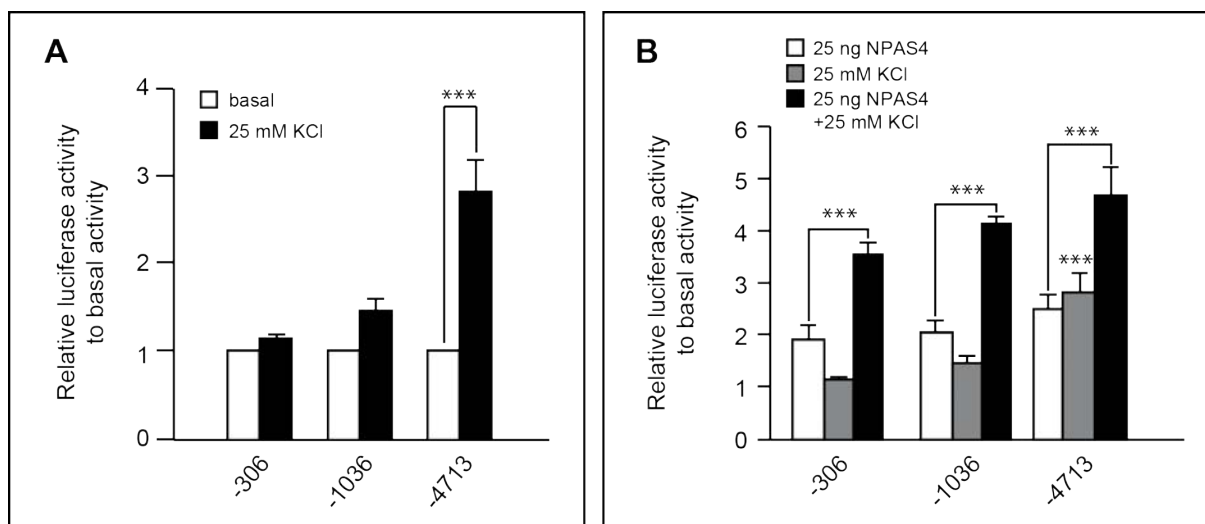
Figure 5.12 Syt10 promoter fragments are stimulated by membrane depolarization and by the activity-regulated transcription factor NPAS4. (A) Rat hippocampal (RH) neurons were transfected with the indicated promoter fragments on DIV5. 40 h later cells were stimulated with 25 mM KCl for 8 h and lysis was performed directly after stimulation revealing an induction of promoter fragment -4713 following KCl stimulation (2.8-fold). (B) Luciferase activity of RH neurons that had been transfected with the indicated promoter fragments and with 25 ng NPAS4 followed by KCl stimulation. Note that luciferase activity of all promoter fragments carrying a binding site for NPAS4 was up-regulated when NPAS4 and KCl were present, indicating that NPAS4 acts as an activity dependent transcription factor on the Syt10 promoter. RH neurons were transfected on DIV5 with either an empty vector or 25 ng NPAS4 and 40 h later, cells were stimulated with 25 mM KCl for 8 h or were treated as controls. Following stimulation, cells were lysed for luciferase measurements and Firefly units were normalized to the basal values (mock transfected cells). Statistical analysis was performed using a One-way ANOVA followed by Tukey posthoc test (*** $p \leq 0.001$).

5.2.3 Syt10 gene expression is induced by kainic acid stimulation

Expression of Syt10 seems to be tightly controlled and *in vivo* has only in the hippocampus been observed after SE, induced either by kainate or pilocarpine injection. Thus, it was investigated whether kainic acid (KA) can induce the Syt10 expression in primary neurons. Therefore, rat hippocampal neurons were stimulated with KA using different stimulation durations and the time between stimulation and lysis of the cells was varied as indicated in the diagram in figure 5.13 A-C. Subsequently, Syt10-, IGF1-, Synaptophysin to control for cell death, and NPAS4-gene expression levels were determined using quantitative RT-PCR. Relative Syt10 gene expression was strongly augmented by two different stimulation conditions. Constant stimulation of neurons with 50 µm KA for 24 h increased relative Syt10 gene expression 9.3-fold (p ≤ 0.001) compared to basal values and a stronger stimulation with 150 µm KA (1/2 h, harvested 24 h later) led to an even slightly higher augmentation (11-fold, p ≤ 0.001) compared to values of non-stimulated samples (Figure 5.13 A).

IGF1 mRNA expression paralleled the one observed for Syt10 but with a stronger increase (19-fold and 40-fold, $p \leq 0.001$; figure 5.13 B). As NPAS4 regulated Syt10 expression, NPAS4 gene expression levels after KA stimulation were analyzed as well. Significant increases in NPAS4 expression were observed with a constant stimulation (24 h) of neurons with 25 µM (4-fold, $p \leq 0.001$) or 50 µM KA (5.5-fold, $p \leq 0.001$) (Figure 5.13 C).
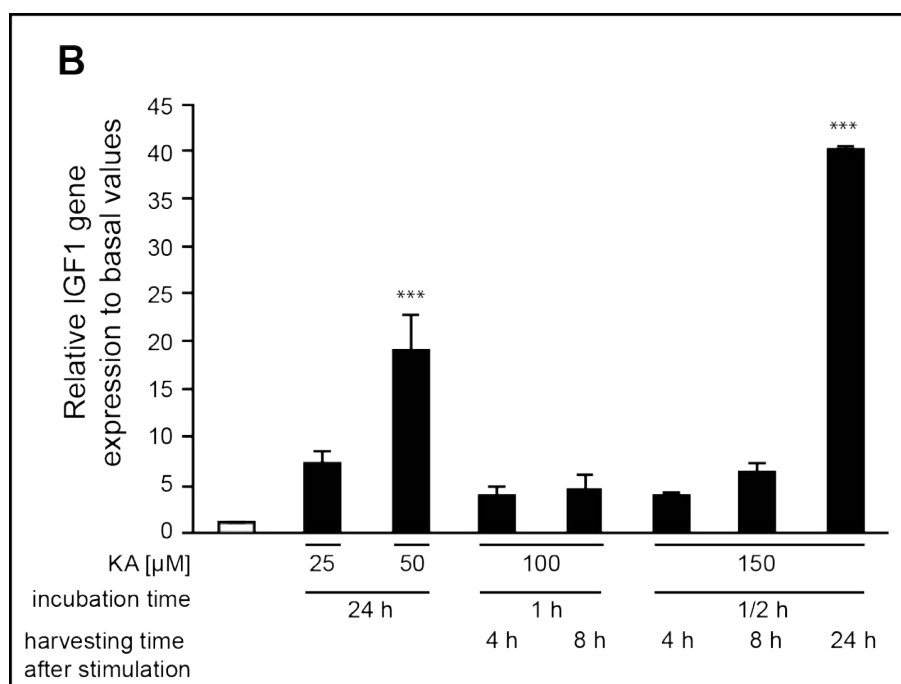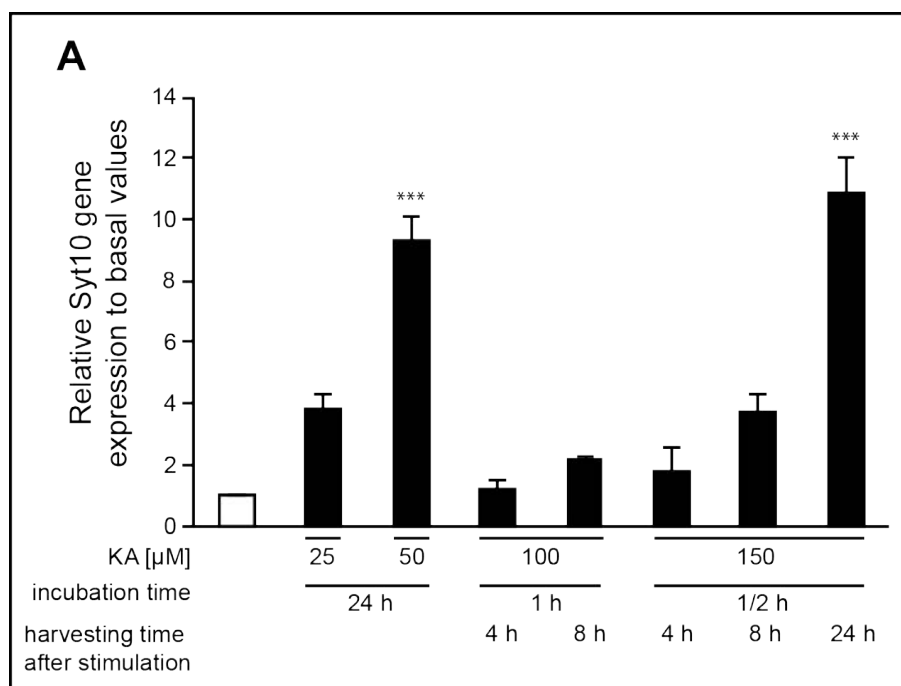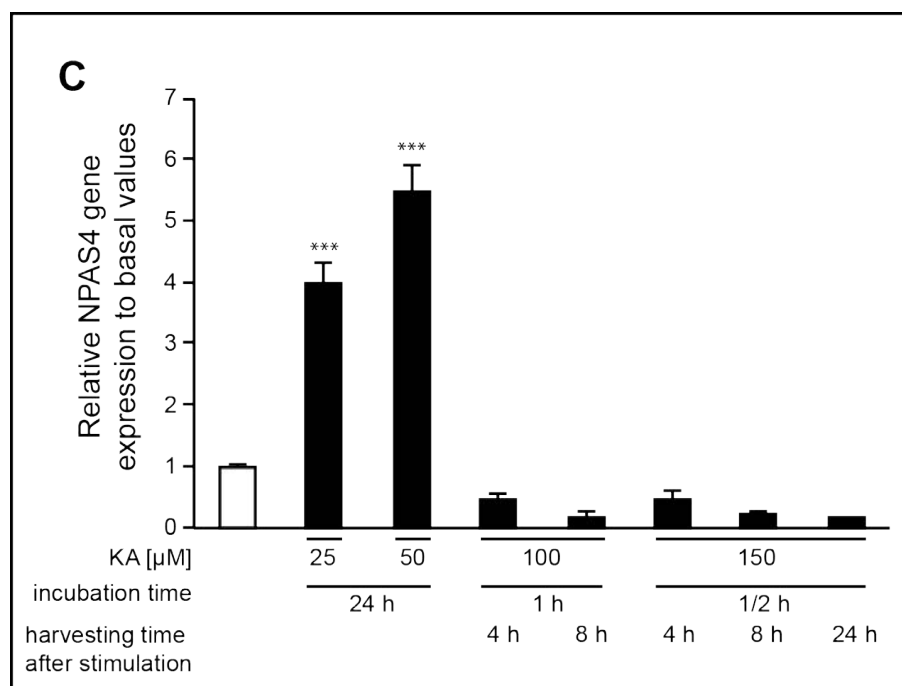
Figure 5.13 Altered gene expression of rat hippocampal neurons following KA stimulation. Quantitative RT-PCR on mRNA extracted from non-stimulated rat hippocampal neurons on DIV14 (white bar) and from rat hippocampal neurons stimulated with KA. The amount of KA, the incubation duration and the harvesting time after incubation are indicated under each diagram. (A) Syt10 gene expression after continuous (24 h) KA stimulation with 50 µM KA revealed a significant increase as well as 1/2 h stimulation with 150 µM KA and a time period until harvesting of 24 h compared to non-stimulated controls. (B) The same conditions as observed for Syt10 increased IGF1 gene expression levels compared to non-stimulated controls. (C) NPAS4 mRNA expression was up-regulated compared to controls after continuous (24 h) KA stimulation with 25 µM or 50 µM KA. For all measurements Synaptophysin was used for standardization, all values were normalized to the control condition (white bar) and statistical analysis was performed using a One-way ANOVA followed by Tukey posthoc test (*** $p \leq 0.001$). Results are presented as mean +/- SEM.

5.2.4 Survival of neurons after KA stimulation is affected by Syt10 loss

Due to the finding that Syt10, IGF1 and NPAS4 gene expression was up-regulated in response to KA stimulation, the functional role of this induction was investigated. Since the IGF1 signaling pathway is known to be important for neuroprotection (Sansone et al., 2013) it was investigated if knockout of Syt10 that controls the Ca^{2+}-dependent release of IGF1-containing vesicles, alters survival of neurons after stimulation with KA. Therefore, primary hippocampal neurons from Syt10 knockout (KO) and wildtype (WT) mice littermates were stimulated on DIV13 with KA using two stimulation conditions that augmented IGF1 (7.4-fold and 6.5-fold, $p > 0.05$) and Syt10 (3.8-fold and 3.7-fold, $p > 0.05$) mRNA expression levels (see figure 5.13 A, B), 25 µM KA for 24 h and 150 µM KA for 1/2 h fixed 8 h later. Although the mRNA expression levels were more abundant under these conditions they were only

detected as significantly altered using Student's *t*-test (not shown) but not using One-Way ANOVA followed by Tukey posthoc test.

Subsequently, these neurons were labeled with microtubule-associated protein 2 (MAP2), a marker for dendrites, astrocytes with glial fibrillary acidic protein (GFAP) and cell nuclei were labeled with DAPI. Figure 5.14 A shows representative images of neurons from Syt10 WT and KO animals under basal condition (Figure 5.14 A, upper panel) and stimulated with 25 µM KA for 24 h that were processed directly after stimulation (Figure 5.14 A, lower panel). The images showed that the number of neurons were not different in unstimulated cultures between Syt10 WT and KO (Figure 5.14 A, upper panel). However, the images revealed that the loss of Syt10 led to a decrease in neuronal cell survival when cultures were stimulated with 25 µM KA for 24 h (Figure 5.14 A, lower panel).

Quantification using the ImageJ software was carried out and results were analyzed as a ratio of GFAP or MAP2 positive cells versus the total cell number (DAPI) of the respective image. For the two genotypes, the values were normalized to the respective basal values (100 %, not shown) and the means are shown in the diagram (Figure 5.14 B). It was observed that stimulation for 24 h with 25 µM KA decreased the number of MAP2 positive Syt10 KO neurons compared with Syt10 WT neurons (52 % versus 38 %, $p \leq 0.05$) whereas the number of GFAP positive astrocytes was not different in both genotypes (90 % versus 96 %, $p > 0.05$). Following the second stimulation protocol tested (150 µM KA for 30' harvested 8 h later) the number of surviving neurons was lower. The number of MAP2 positive neurons decreased to 4 % and 2 % in Syt10 WT and KO cultures, respectively. But neither the rate of MAP2 positive nor of GFAP positive cells (WT: 94 % versus KO: 119 %) was significantly different between both genotypes ($p > 0.05$).

Taken together, these results indicate that the loss of Syt10 significantly decreased the number of surviving neurons but not of astrocytes after a 24 h stimulation with 25 µM KA. When stimulated with 150 µM KA for 1/2 h and processed 8 h later, no significant difference between the two genotypes was observed in either cell types.

A

Basal

WT   **KO**

GFAP
MAP2
DAPI

25 µM KA 24 h

B

□ WT   ■ KO

KA [µM]	25	150	25	150
incubation time	24 h	1/2 h	24 h	1/2 h
harvesting time after stimulation		8 h		8 h
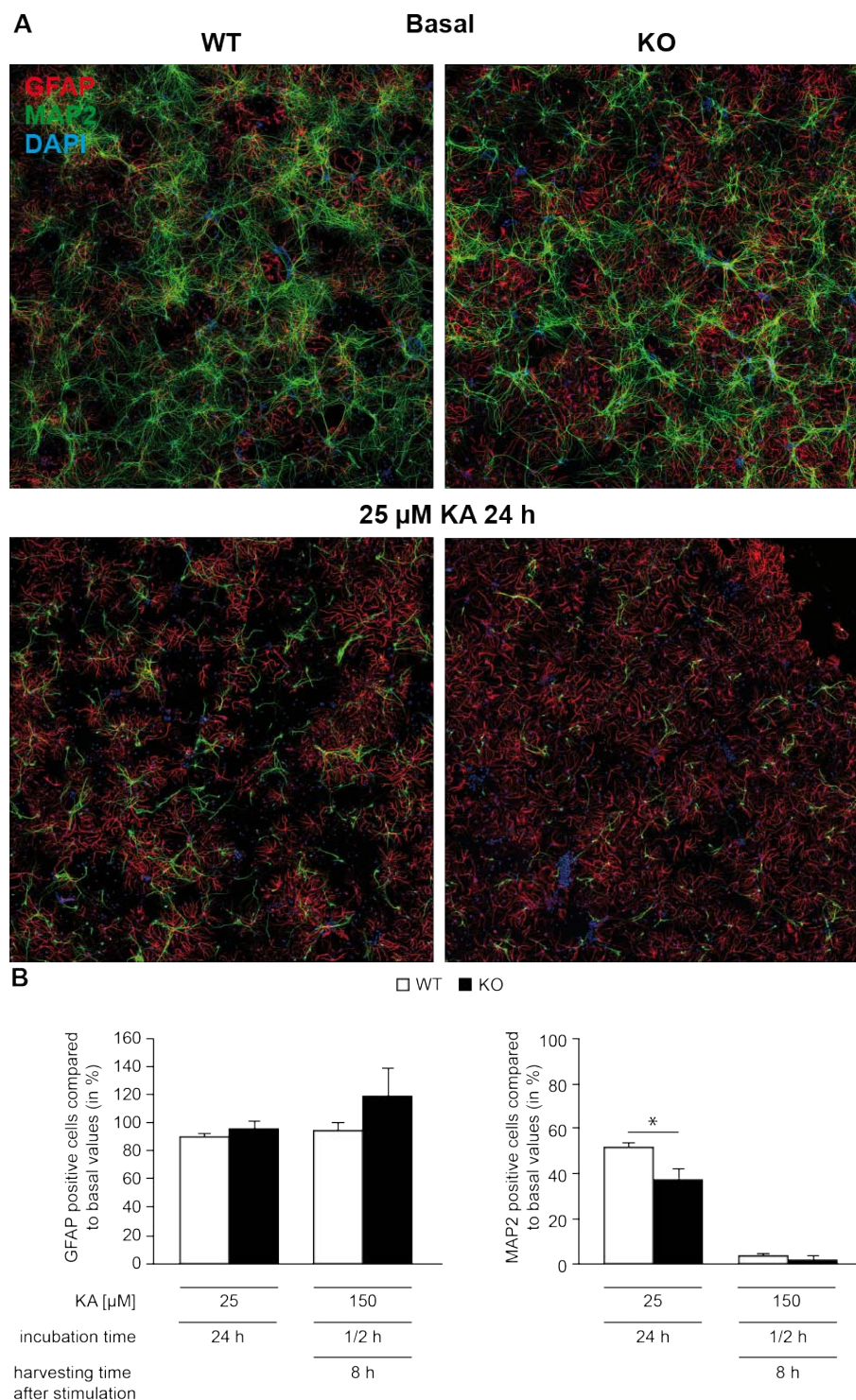
Figure 5.14 Loss of Syt10 decreases the survival rate of neurons after KA stimulation.
Dissociated hippocampal Syt10 KO or WT neurons were stimulated following two protocols that elevated IGF1 and Syt10 gene expression (shown in figure 5.13), 25 µM KA for 24 h and 150 µM KA for 1/2 h fixed 8 h later. Cells were stained for the neuronal marker MAP2, the astrocytic marker GFAP and for cell nuclei (DAPI). (A) Representative images of control Syt10 WT and KO neurons under basal conditions and following stimulation for 24 h with 25 µM KA. Following this stimulation condition less MAP2 positive neurons were visible in cultures from Syt10 KO animals (lower panel, right image) compared with cultures from WT animals (lower panel, left image), whereas the number of neurons under basal conditions were equal (upper panel). Scale bar: 500 µm. (B) Quantification of the two stimulation conditions shown below the diagram. Cells that were positive for MAP2 or GFAP were counted with ImageJ and were normalized to the total cell number (DAPI). Then, all values were normalized to the basal values for each genotype (WT or KO). Statistical analysis was performed using Student's *t*-test (* $p \leq 0.05$). Results are presented as mean +/- SEM.

5.3 Analysis of cellular and subcellular expression patterns of Syt10

5.3.1 Generation and characterization of isoform-specific antibodies

To date, nothing is known about the cellular and subcellular localization of Syt10 protein in the hippocampus, mainly due to the lack of a Syt10-specific antibody. To study the cellular distribution of Syt10, isoform-specific antibodies were raised. A polyclonal antibody was generated using a peptide residing in the Syt10 linker region and the monoclonal antibodies were raised with a peptide located in the Syt10 C-terminus (Figure 5.15 A, B). All peptides were coupled to a carrier protein in order to increase their immunogenicity. Due to the strong sequence homology of Syt10 with Syts 3, 5, and 6, it was essential to verify the specificity of the Syt10 antibodies.

By immunoblotting, it could be shown that the polyclonal antibody specifically recognized Syt10 as seen in the OB sample from WT mice and in the overexpressed Syt10 HEK293T cell lysate. The calculated molecular weight of Syt10 was about 62 kDa and the band that appeared at around 125 kDa corresponds to the Syt10 homodimers. The Syt10 specific bands neither appeared in the lysate from Syt10 KO olfactory bulbs nor in the untransfected HEK293T cell lysate sample. In addition, cross reactivity could not be detected as HEK293T cell lysates transfected with the evolutionary conserved isoforms Syt3, 5 and 6 were lacking a corresponding band (Figure 5.15 C). Monoclonal antibody clones from rats (23 clones) and mice (15 clones) were examined by immunoblotting as well. In contrast to the polyclonal antibody, no specific signal could be observed using the monoclonal antibodies (data not shown). Immunoblotting of homogenates from various brain regions revealed that Syt10 had the strongest expression in olfactory bulb, pons and cerebellum. In the other brain regions examined, including the striatum, hippocampus, cortex and pituitary gland, Syt10 was only very weakly expressed (Figure 5.15 D).

A

B

C

D
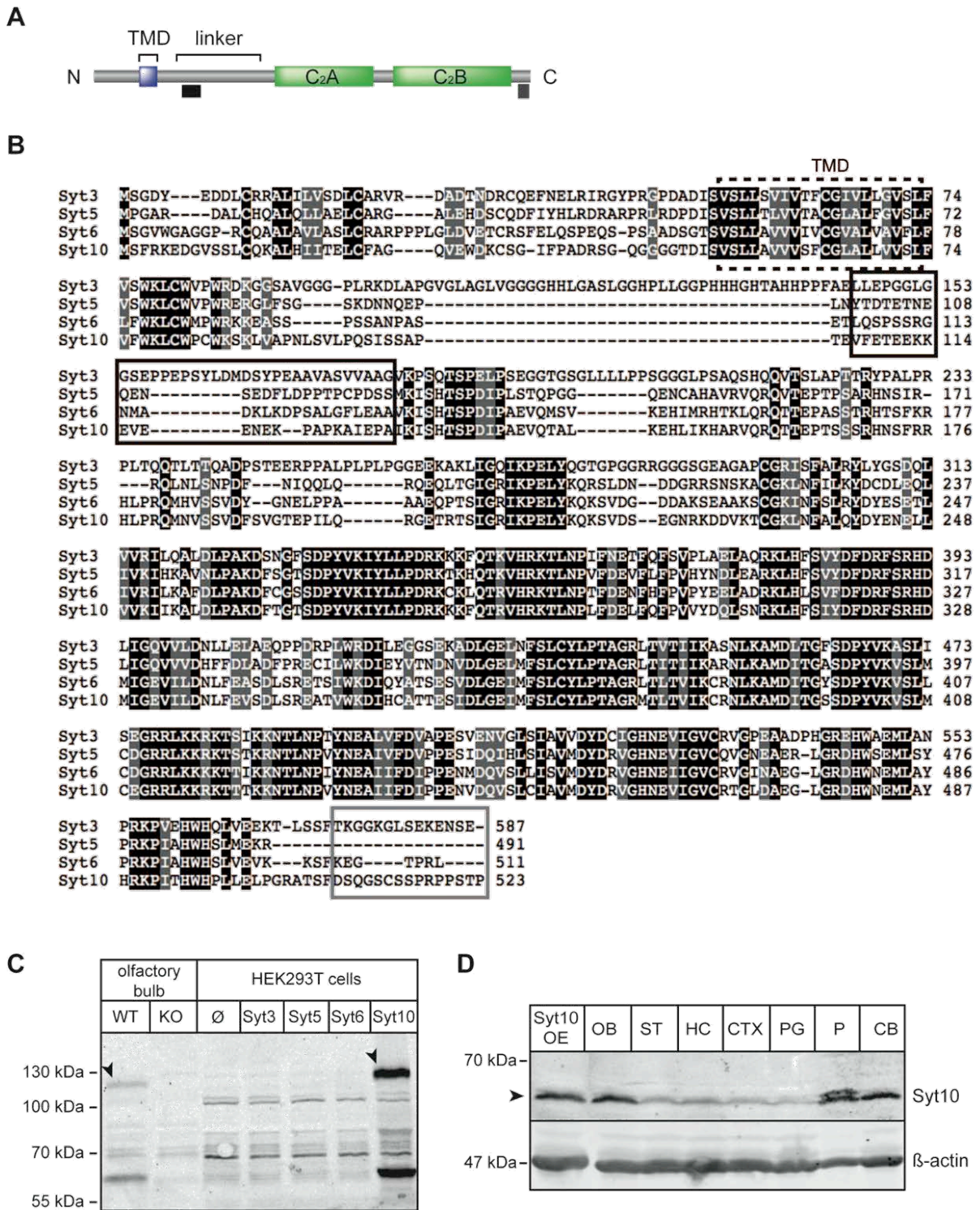
Figure 5.15 Characterization of Syt10 isoform specific antibodies. (A) Protein domain structure of Syt10. The black box depicts the epitope region of the polyclonal antibody; the grey box illustrates the epitope region of the monoclonal antibody. (B) Multiple alignment of the mouse Syt isoforms Syt3, 5, 6 and 10. Sites with two or three identical amino acids are highlighted in grey, amino acid positions with complete sequence similarities are highlighted in black. The transmembrane domain (TMD) is marked with a dotted line, the epitope region of the polyclonal antibody is marked in black and the grey line assigns the epitope region of the monoclonal antibodies. (C) Protein lysates of OB from Syt10 WT and KO mice as well as from HEK293T cells transfected with Syts 3, 5, 6 and 10 or untransfected (∅) were analyzed by immunoblotting with the polyclonal Syt10 antibody (Syt10 150 T3) at a dilution of 1:250. Syt10 molecular weight: 62 kDa. (D) Immunoblot showing the distinct distribution of Syt10 in several brain subregions. Syt10 was labeled with the polyclonal Syt10 antibody and the housekeeper ß-actin was used as a loading control.

Figure 5.15 (continued) Arrowheads indicate the Syt10 specific protein band. Syt10 OE: Syt10 overexpression in HEK293T cells; OB: olfactory bulb; ST: striatum; HC: hippocampus; CTX: cortex; PG: pituitary gland; P: pons; CB: Cerebellum.

To test if the antibodies were suitable for immunocytochemistry, first the newly generated antibodies (Figure 5.15) were characterized in HEK293T cells. Therefore, HEK293T cells were transfected with constructs carrying the CMV promoter and coding for Syt10-GFP, GFP alone or an empty vector (Figure 5.16 A). Next, cells were labeled with the polyclonal and the two monoclonal antibodies and analyzed by microscopy. All three antibodies (antibody 2A9 not shown) exhibited a strong fluorescent signal that was co-localized with overexpressed Syt10-GFP (Figure 5.16 A and B a, d, g). This signal was absent in either GFP transfected cells (Figure 5.16 A and B b, e, h) or cells transfected with an empty vector (Figure 5.16 A and B c, f, i). Taken together, the newly generated antibodies specifically recognized overexpressed Syt10 in HEK293T cells.
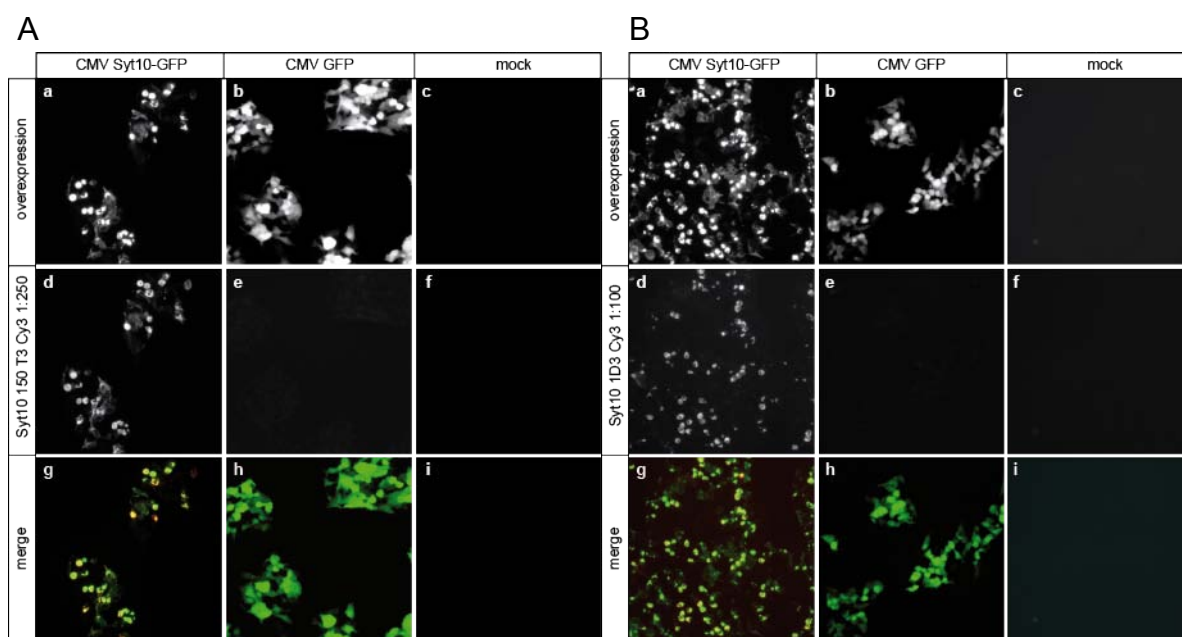
Figure 5.16 The polyclonal and monoclonal antibodies specifically recognize overexpressed Syt10. HEK293T cells were transfected with Syt10-GFP, GFP and an empty vector (mock) under the control of the CMV promoter. Two days after transfection, the cells were fixed and stained with the polyclonal antibody 150 T3 (A) or the monoclonal antibody 1D3 (B). Both antibodies label overexpressed Syt10-GFP, whereas no unspecific staining of GFP alone or the empty vector could be detected.

Some members of the Syt family, e.g. Syt1, 2 and 9, are known to function as regulators for vesicle release in neurons. To investigate the distribution of Syt10 in primary neurons, the newly generated Syt10 antibodies were characterized in mouse hippocampal neurons (Figure 5.17). Neurons were transfected with Syt10-GFP,

untagged Syt10 or GFP alone, all under control of the synapsin promoter, or with an empty vector under control of the CMV promoter. The polyclonal Syt10 antibody 150 T3 specifically labeled overexpressed Syt10-GFP, shown by overlap of the two fluorescent signals (Figure 5.17 A a, e, i). The labeling of untagged Syt10 showed a staining pattern similar to overexpressed Syt10-GFP indicating that the GFP-tag does not lead to a change of the subcellular Syt10 localization (Figure 5.17 A b, f, j). No signal was detected in neurons overexpressing GFP (Figure 5.17 A c, g, k) or in mock transfected neurons (Figure 5.17 A d, h, l). The specificity of the monoclonal antibodies 1D3 (Figure 5.17 B) and 2A9 (Figure 5.17 C) was similar to the polyclonal antibody 150 T3. In summary, the newly generated antibodies could be used to specifically label Syt10 in protein lysates or in Syt10 overexpressing neurons.

A

B

	Syn Syt10GFP	Syn Syt10	GFP	mock
overexpression	a	b	c	d
Syt10 1D3 Cy3 1:2	e	f	g	h
merge	i	j	k	l

C

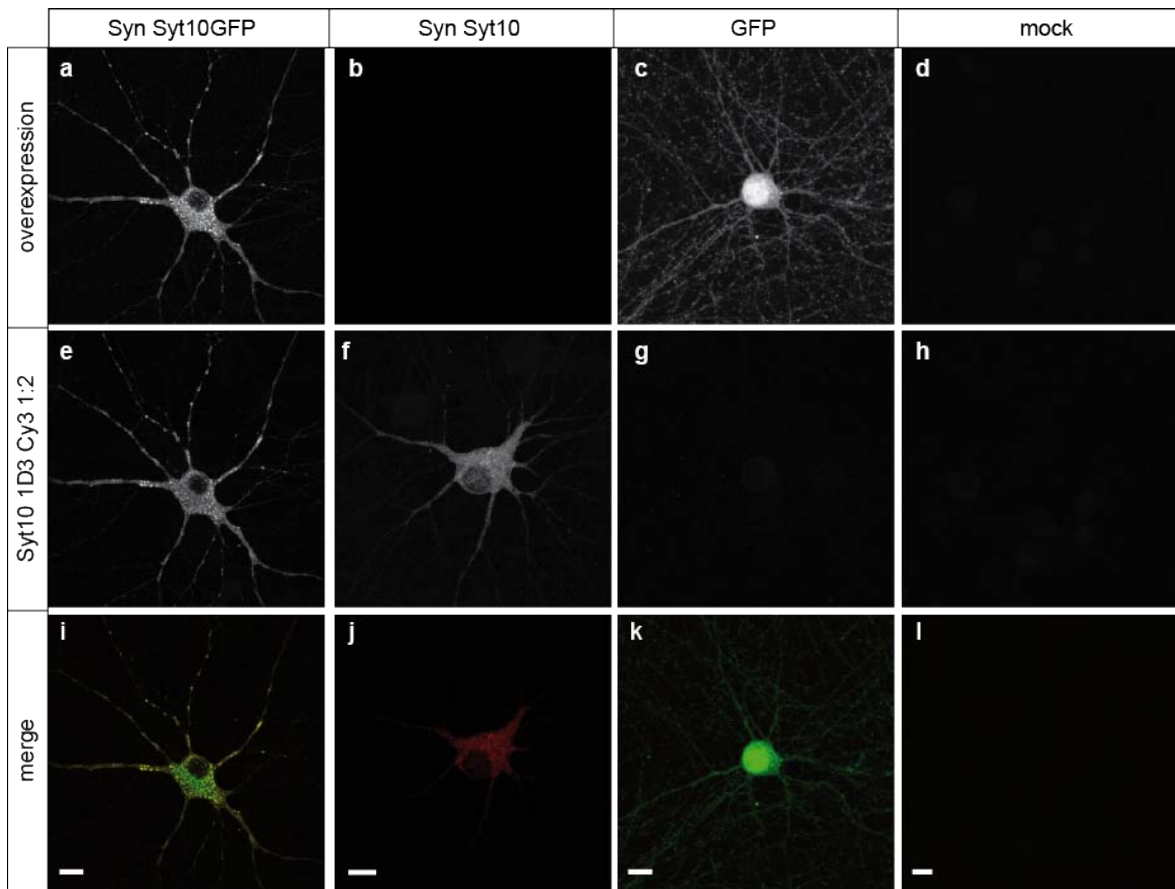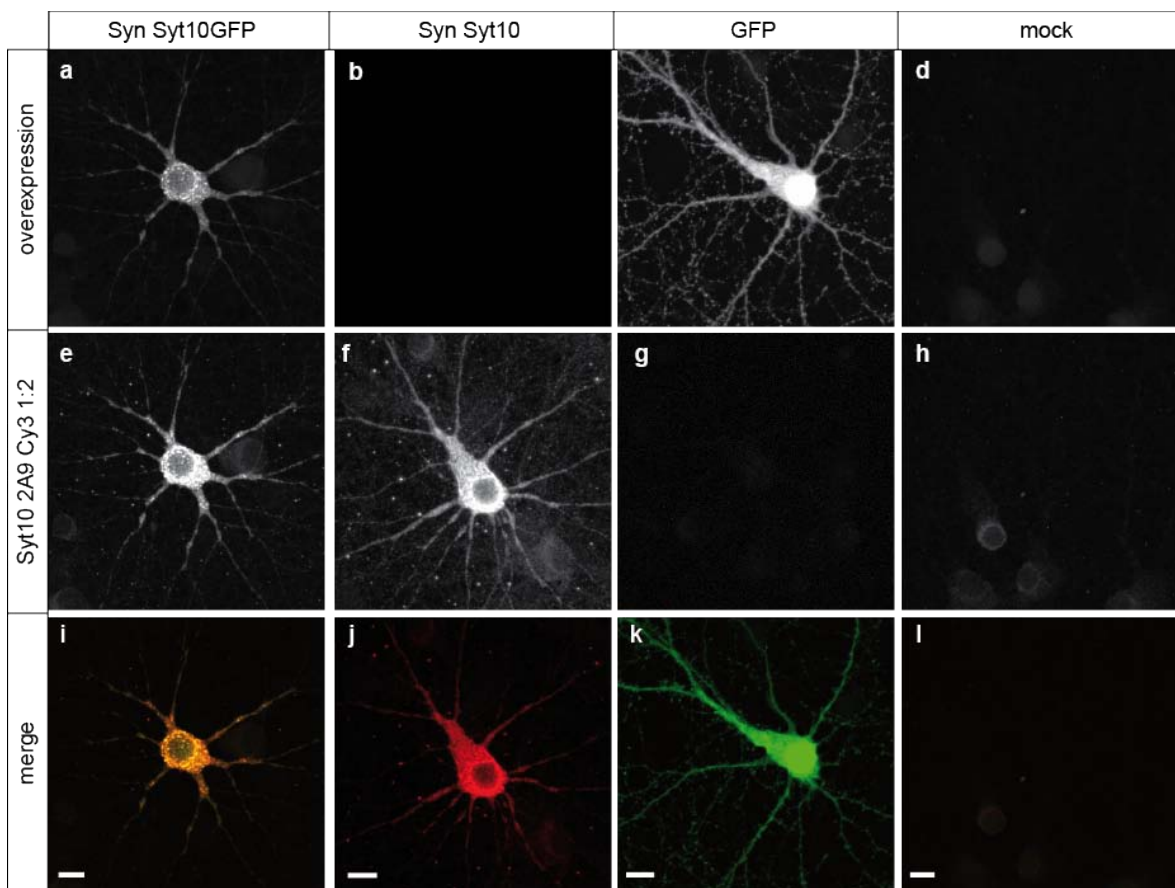|	Syn Syt10GFP	Syn Syt10	GFP	mock
overexpression	a	b	c	d
Syt10 2A9 Cy3 1:2	e	f	g	h
merge	i	j	k	l
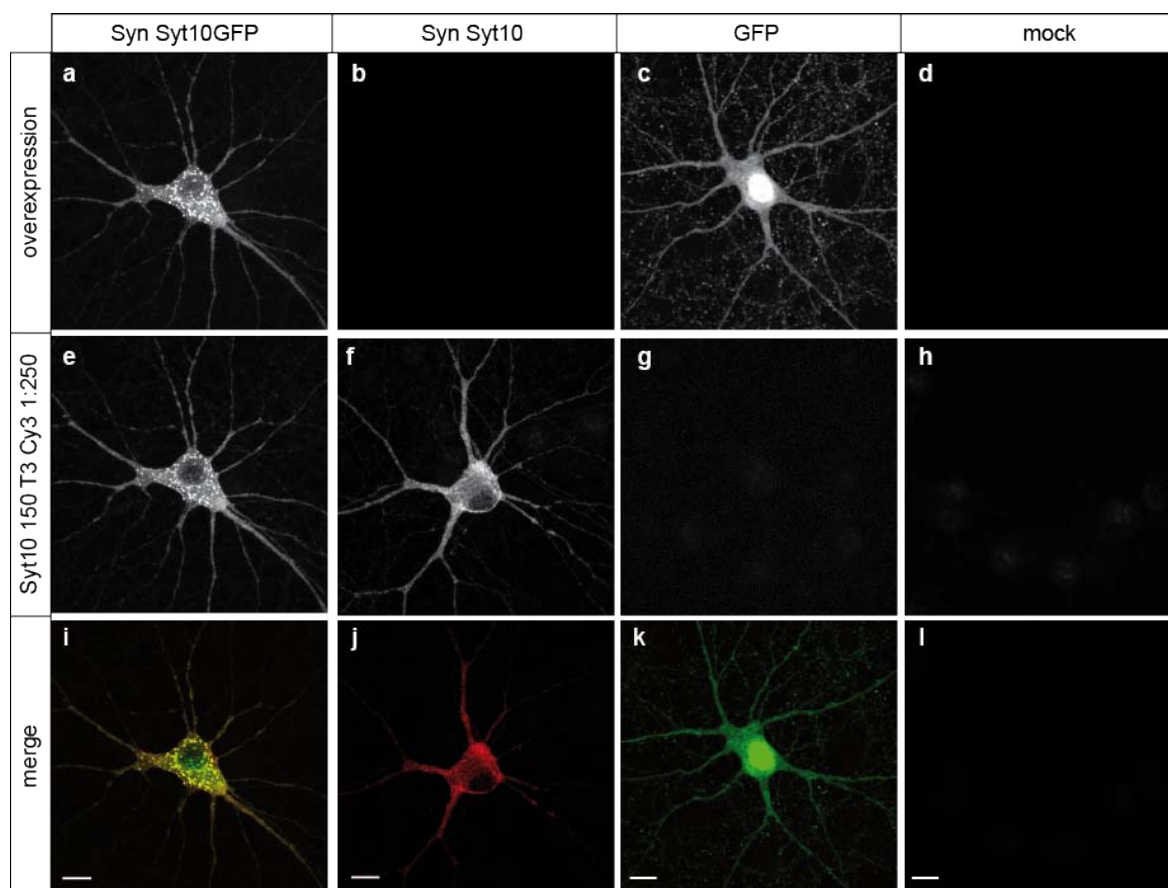
Figure 5.17 In neurons, the polyclonal antibody and the monoclonal antibodies specifically detect overexpressed Syt10. Mouse hippocampal neurons were transfected with constructs coding for Syt10-GFP, Syt10 without a tag, GFP alone, all under the control of the synapsin promoter, or an empty vector under the control of the CMV promoter. (A) The polyclonal antibody led to a strong fluorescence signal in neurons overexpressing Syt10-GFP (a, e, i) and Syt10 (b, f, j). This signal was absent in GFP-overexpressing neurons (c, g, k) or mock transfected neurons (d, h, l). An identical labeling pattern was observed with the monoclonal antibodies 1D3 and 2A9. Note that the overall fluorescence intensity was weaker in B. Scale bar: 10 µm.

5.4 Syt10 subcellular localization in PC12 cells and in neurons using overexpression

Neuroendocrine rat pheochromocytoma PC12 cells possess two types of vesicles, synaptic vesicles (SVs) and large dense core vesicles (LDCVs) (Greene and Tischler, 1976). Therefore, the use of this cell line to study the subcellular localization of proteins that are involved in vesicular exocytosis is well established. Indeed, the localization of some Syts has been described in PC12 cells. Syt1 has been identified to be present on synaptic vesicles whereas there are confounding reports about the localization of Syt7. Sugita et al. 2001 reported that Syt7 was located at the plasma membrane (Han et al., 2004; Sugita et al., 2001), while other studies show a localization of Syt7 at LDCVs (Fukuda et al., 2004a; Wang & Chicka, 2005). However, to date, the subcellular localization of Syt10 in PC12 cells has not been investigated. Analysis of the subcellular localization of Syt10 in PC12 cells could reveal whether the protein is localized to any of the two vesicles types, to the plasma membrane or to other subcellular compartments.

5.4.1 Distinct localization of Syt isoforms in PC12 cells

To gain insights into the subcellular localization of Syt10, overexpression plasmids were generated containing full-length Syt10 fused to a C-terminal fluorescent reporter (mCherry or GFP) under the control of the synapsin promoter. As tags can affect the protein localization, first the distribution of Syt10-GFP was compared to the one of the untagged Syt10 protein (Figure 5.17 A, B, C). From Syt1 and Syt7 it is known that Syt1 localizes to synaptic vesicles in neurons/small vesicles in PC12 cells and that Syt7 is present at the plasma membrane (Han et al., 2004). Overexpression of Syt1-GFP and Syt7-GFP confirmed these subcellular localizations in PC12 cells. Due to the strong sequence similarity of Syts 3, 5, 6 and 10, it was hypothesized that their proteins might be present at similar subcellular compartments. To test this, the

subcellular localization of these evolutionary conserved Syts was examined in PC12 cells as well. Consistent with Sugita et al. 2002, overexpressed Syt3-GFP was clearly localized at the plasma membrane in PC12 cells (Figure 5.18) (Sugita et al., 2002). Overexpression of Syt6-GFP showed a punctate expression pattern distributed throughout the cytoplasm (Figure 5.18). An enrichment of Syt6-GFP at the plasma membrane could not be observed. Similar to Syt6-GFP, the Syt5-GFP expression pattern in PC12 cells was punctate (Figure 5.18). Overexpressed Syt10-GFP in PC12 cells was localized distinct to the plasma membrane expression of Syt3- and Syt7-GFP. Expression of Syt10-GFP was distributed throughout the cytoplasm with a punctate expression pattern similar to Syt5- and Syt6-GFP.
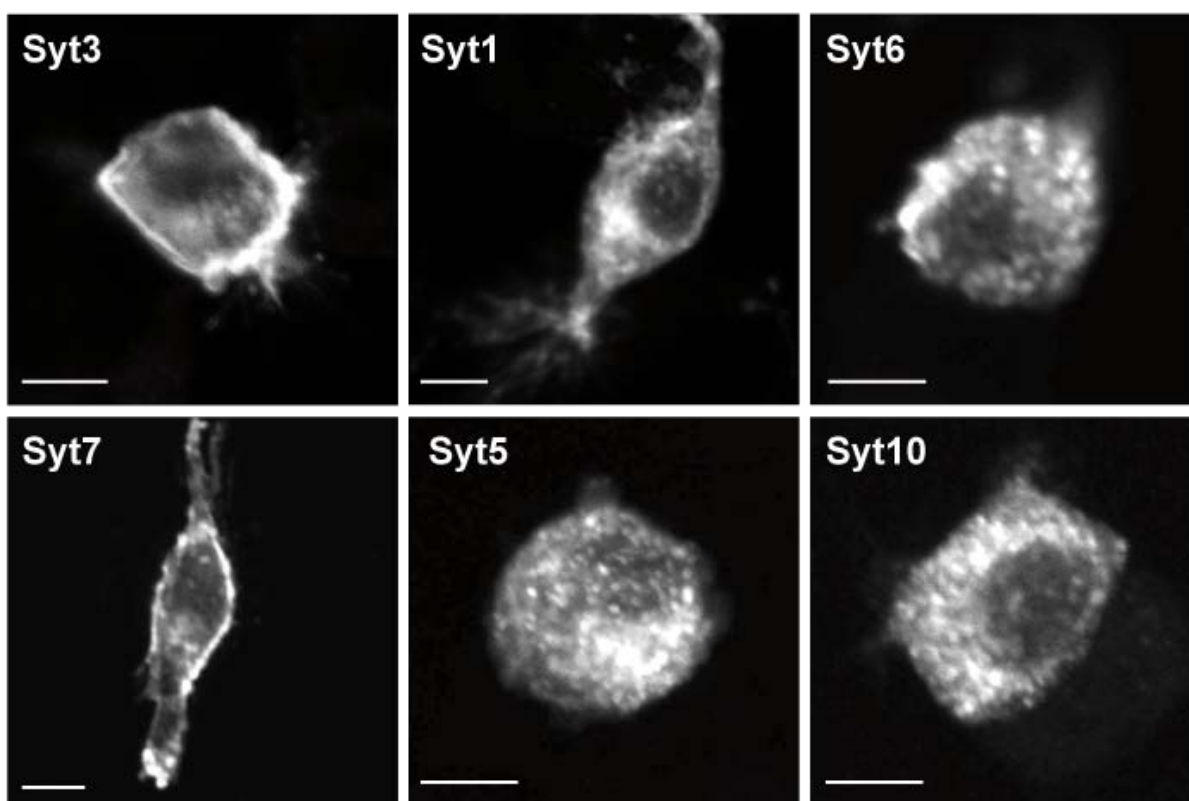
Figure 5.18 Subcellular localization of overexpressed Syts in PC12 cells. Syts are localized differentially in PC12 cells as shown by overexpression of Syt proteins fused to a C-terminal GFP. Whereas Syts 3 and 7 are located at the plasma membrane, Syts 1, 5, 6 and 10, exhibited a punctate expression pattern in the cytoplasm. PC12 cells were analyzed by confocal microscopy 48 h after transfection. Scale bar: 5 µm.

5.4.2 Syt10 does not co-localize to closely related isoforms in PC12 cells

Phylogenic analysis revealed a close relationship between Syts 3, 5, 6 and 10 (Marquèze et al., 2000). It has been postulated that Syts form heterodimers via their unique cysteine binding sites and thereby increase their functional repertoire (Fukuda et al., 1999a). To test whether those Syts change their subcellular localizations upon

putative heterodimerization, co-transfection of Syt10 with Syts 3, 5 and 6 tagged with a fluorescent reporter was carried out in PC12 cells. As a comparison, single transfections of the constructs are given in the appendix (Supplementary figure 8). When co-expressed with Syt10, Syt3 was localized at the plasma membrane. Syts 5, 6 and 10 were distributed throughout the cytoplasm showing punctate expression but only Syt5-mCherry expression partially overlapped with Syt10-GFP. No change of the distribution pattern upon co-expression was observed in those cells (Figure 5.19).
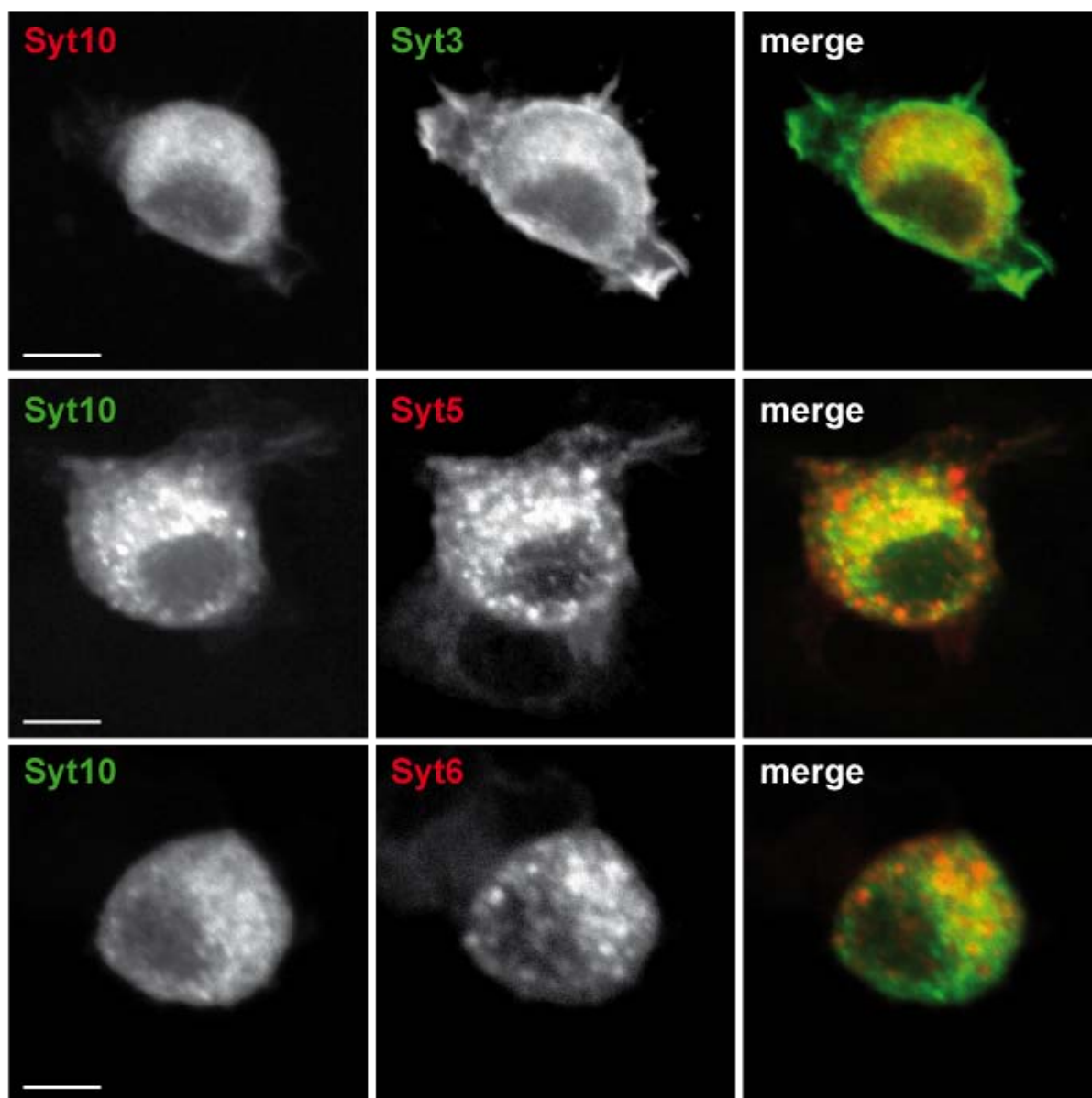
Figure 5.19 Co-transfection of Syt10 with Syts 3, 5 and 6 in PC12 cells. PC12 cells were co-transfected with Syt10 and the closely related Syt isoforms Syt3, 5 and 6, and fixed for imaging 48 h after transfection. While Syt3-GFP was localized to the plasma membrane, Syt10-mCherry did not co-localize with Syt3-GFP. Partial overlap of co-expressed Syt10-GFP and Syt5-mCherry was observed with a punctate expression pattern near the nucleus. Syt10-GFP and Syt6-mCherry did not show an overlap in the punctate expression pattern. Scale bar: 5 µm.

5.4.3 Syt10 expression in neurons

The subcellular localization of Syt10 remains unresolved in cortical or hippocampal neurons to date. Therefore, primary neurons were transfected with a construct coding for Syt10 tagged with a fluorescent reporter on DIV5-6 and fixed for subsequent immunostainings on DIV13-14. Confocal imaging of these neurons revealed an expression of Syt10-GFP that was mainly concentrated to the soma, showing a punctate pattern. Syt10-GFP distribution along neurites was weaker and bit more diffuse compared to the soma (Figure 5.20 A). But even in neurites, Syt10-GFP overexpression still appeared punctate. To further identify this subcellular expression pattern, several markers were used to label synapses and dendrites. Co-labeling of Syt10-GFP overexpressed neurons with microtubule-associated protein 2 (MAP2), a marker for dendrites, showed that Syt10-GFP was distributed along the dendrites. Even though Syt10-GFP expression was punctate, a subcellular localization to synapses as examined by co-labelings with Syt1 and synapsin, was not observed. Furthermore, Syt10-GFP was not co-localized with the vesicular GABA transporter (vGAT) indicating that Syt10 is not present on SVs containing GABA (Figure 5.20 B).

A
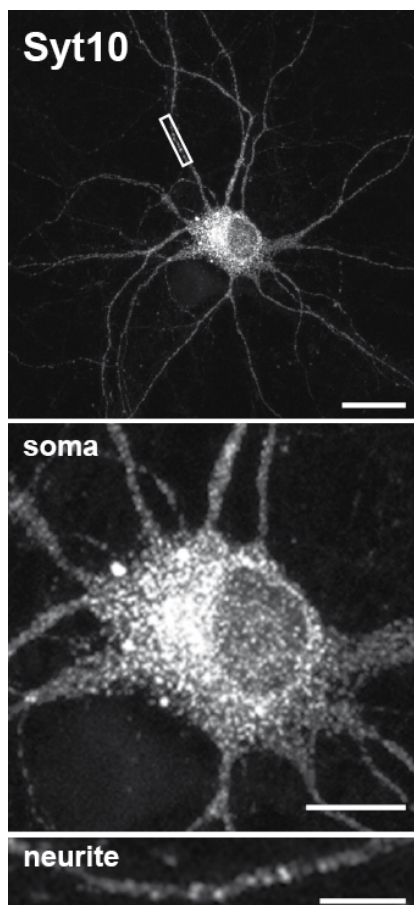
Figure 5.20 Subcellular localization of Syt10-GFP in primary neurons DIV13-14. (A) Confocal images showing that overexpression in mouse cortical neurons Syt10-GFP was distributed along the soma and neurites. Localization of Syt10-GFP in the branches was less pronounced compared to the strong punctate expression in the soma. In the two lower panels, higher magnifications of the soma and a neurite are shown from the same neuron presented in the upper panel. Scale bars: 20 μm (whole neuron), 10 μm (soma), 5 μm (neurite). (B) Subcellular localization of Syt10 in primary neurons. Inhibitory neurons were labeled by vGAT, dendrites by MAP2 and synapses by Syt1 and Synapsin. Scale bar: 5 μm

B
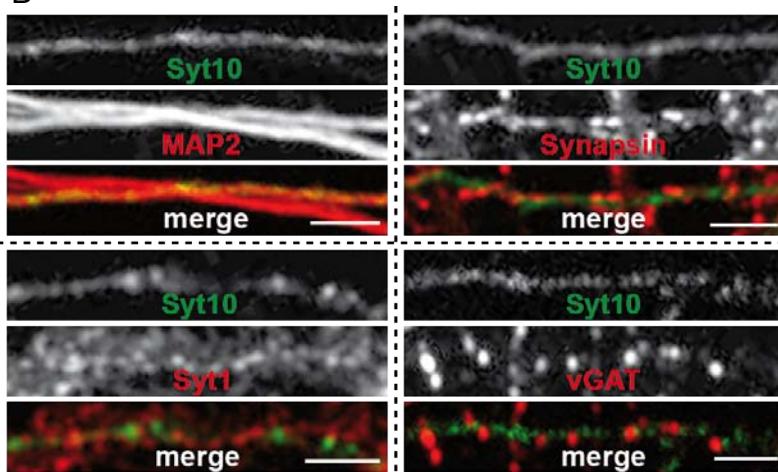
5.4.4 Examination of Syt10 localization in the ER-Golgi trafficking pathway

Since other Syts were described to be localized to the Golgi (Fukuda et al., 2004b; Fukuda et al., 2003c; Matsuoka et al., 2011) and due to the expression pattern of Syt10-GFP observed in PC12 cells (Figure 5.19) and in neurons (Figure 5.20), it was next analyzed whether Syt10 is present on intracellular compartments. To unravel, whether Syt10 could be localized on intracellular compartments, PC12 cells were transfected with Syt10-mCherry and a plasmid coding for the Transferrin Receptor (TfR) fused to a fluorescent reporter (TfR-GFP). Transferrin binds to the TfR and both the ligand and receptor are internalized into the cell via clathrin-mediated endocytosis and are sorted via early and recycling endosomes to the plasma membrane (reviewed by Mayle et al., 2012). Overexpressed Syt10-mCherry did not show a high degree of co-localization to TfR-GFP indicating that Syt10 does not localize to endosomal compartments in PC12 cells (Figure 5.21 A). For comparison with the co-transfections, the distribution pattern of all single transfections in PC12 cells is shown in the appendix (Supplementary figure 8).

To analyze whether Syt10 is present on other compartments of the Golgi ER trafficking pathway, vesicle trafficking in the Golgi was inhibited via treatment with 2 µM Brefeldin A (BFA) and the localization of Syt10-GFP transfected PC12 cells was analyzed with a counterstain against the Golgi matrix protein 130 (GM130), a marker for the Golgi apparatus. BFA interrupts the anterograde transport of vesicles from the Endoplasmatic Reticulum (ER) to the Golgi Apparatus leading to an accumulation of proteins in the ER and a collapse of the typical Golgi stacks (Klausner et al., 1992; Pelham, 1991). Under control conditions, Syt10-GFP showed a slight accumulation near the nucleus where the Golgi Apparatus could be identified by a staining with GM130 revealing the characteristic organization of the Golgi stacks. Overnight treatment with BFA exhibited the collapse of the Golgi as seen by disorganization of the Golgi stacks. However, no change in the Syt10-GFP expression was observed indicating that Syt10-GFP is neither trapped in the ER nor in the ER to Golgi Intermediate Compartment (ERGIC) following BFA treatment (Figure 5.21 B).

A
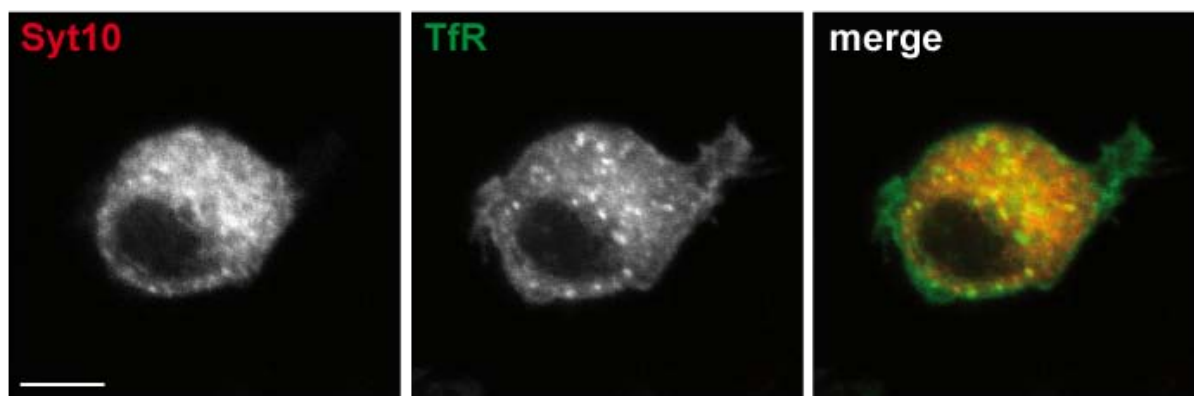
B
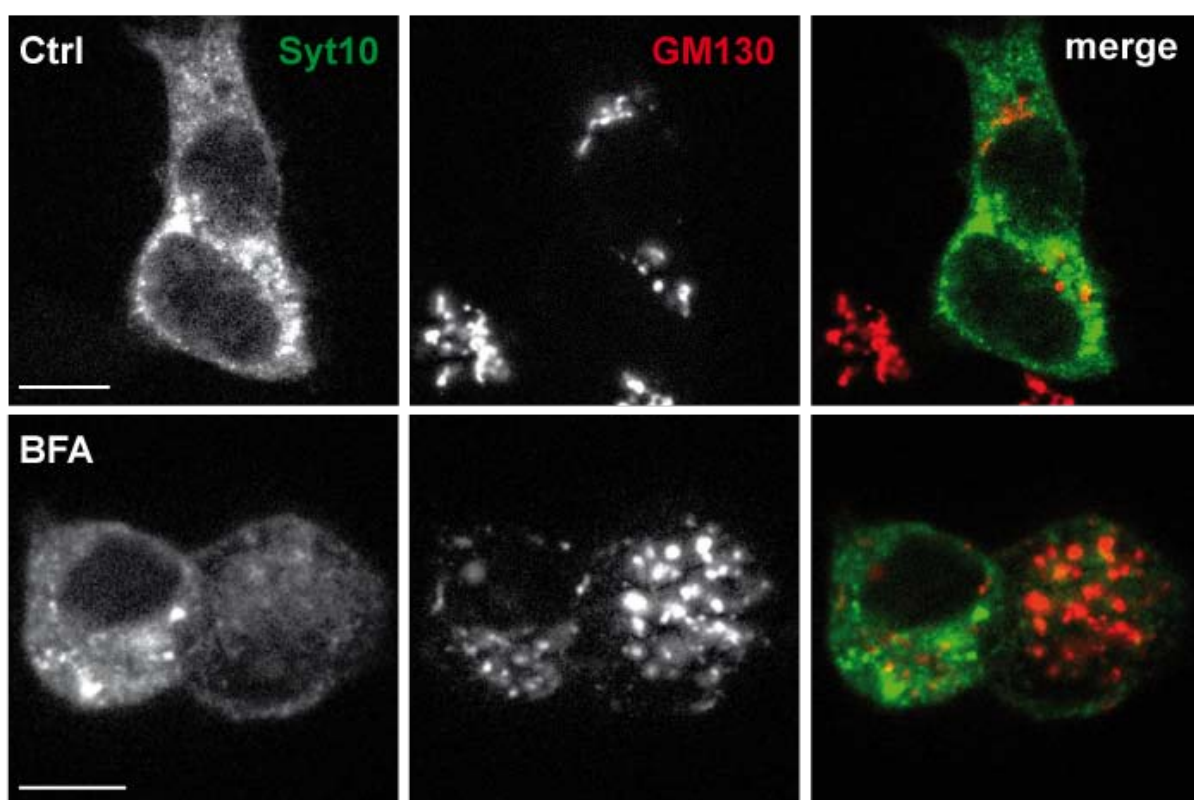
Figure 5.21 Syt10 is not concentrated in Golgi-compartments and endosomes in PC12 cells. PC12 cells were transfected and fixed for imaging 48 h after transfection. (A) Co-expression of Syt10-mCherry and a GFP-tagged TfR-GFP, which is a marker for early endosomes, showed that Syt10-mCherry was not expressed at the same endosomal compartments. (B) Overexpression of Syt10-GFP and counterstaining against GM130, a Golgi matrix protein, showed that Syt10-GFP was a resident Golgi protein. Treatment with BFA did not change Syt10-GFP localization indicating that the disassembly of the Golgi does not influence Syt10-GFP localization. Scale bar: 5 µm.

As analyzed in PC12 cells, a putative localization of Syt10-mCherry in the ER/Golgi complex was examined by co-expression with TfR-GFP in primary neurons. Similar to Syt10-GFP, Syt10-mCherry expression was weak throughout the branches but stronger in the soma. Higher magnification of the soma shows that Syt10-mCherry was co-localized to a certain degree with TfR-GFP. This co-localization was

restricted to the soma and not found in the branches (Figure 5.22 A). A similar overlap but to a lesser extend was observed for Syt10-GFP when co-labeled with chromogranin A, a neuroendocrine secretory protein which was located at secretory vesicles in neurons and neuroendocrine cells (Data not shown). For comparison with the co-transfections, the distribution pattern of all single transfections in neurons is shown in the appendix (Supplementary figure 9).

A
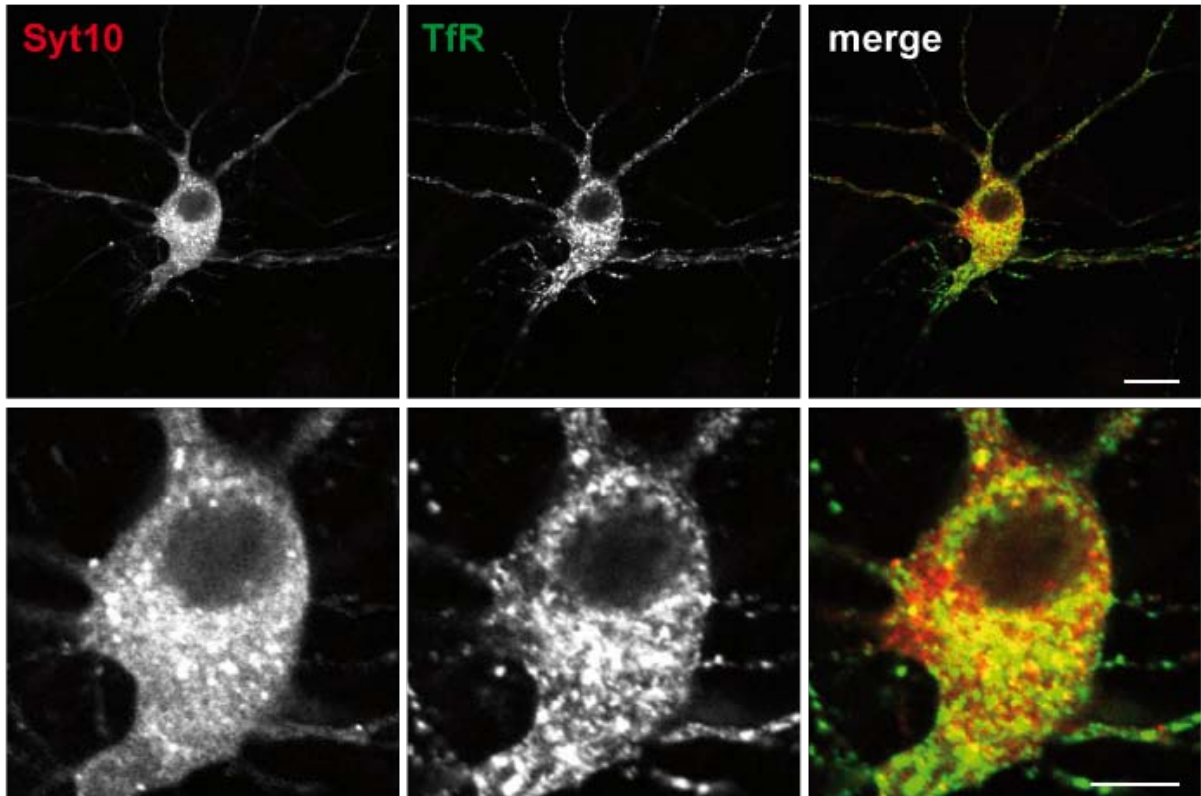
B
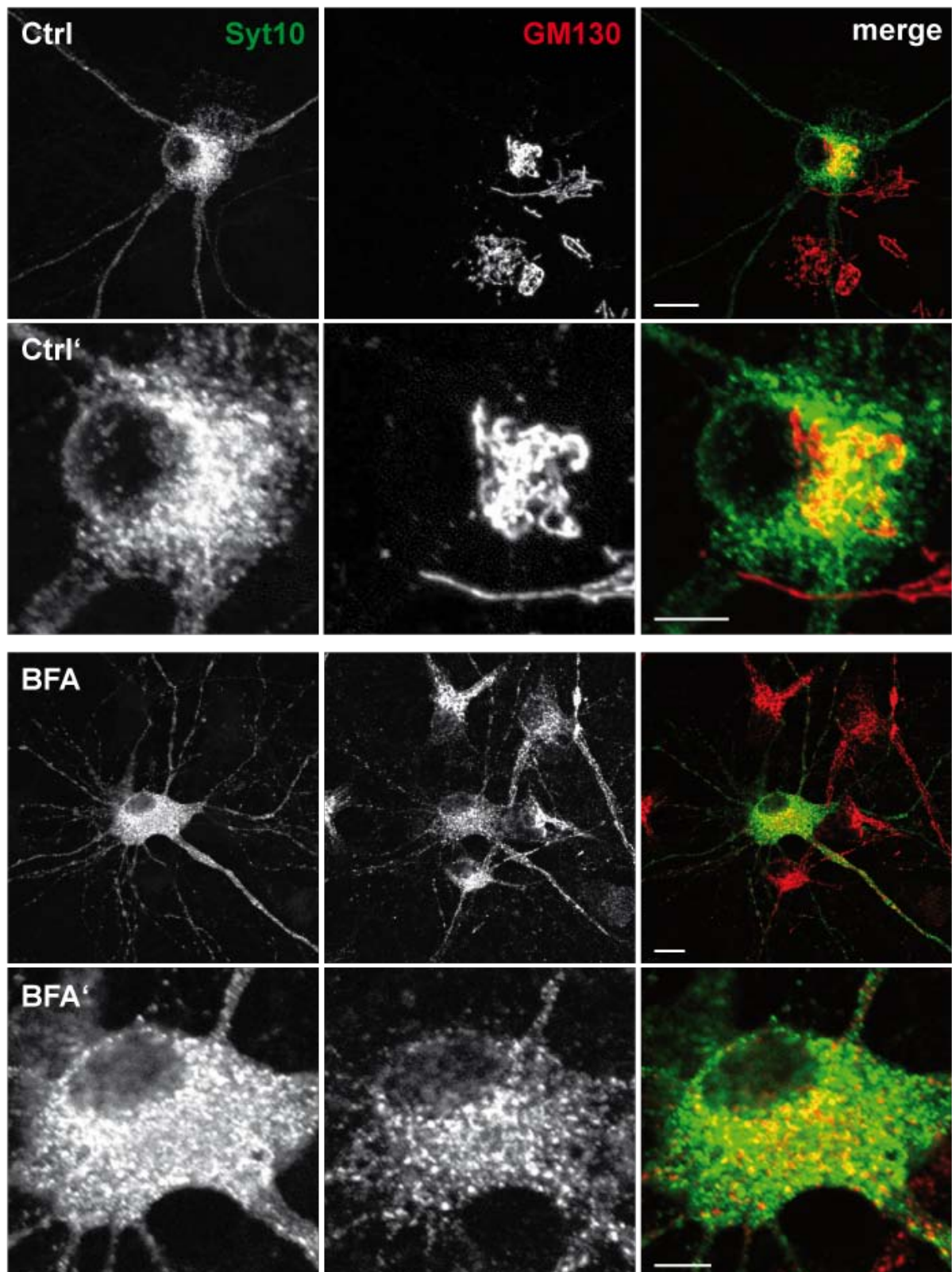
Figure 5.22 Syt10 is not concentrated in the ER-Golgi pathway. Mouse hippocampal neurons transfected at DIV5-6 and fixed with PFA for immunolabeling at DIV14. (A) Neurons overexpressing Syt10-mCherry and TfR-GFP co-localized in the soma. (B) Golgi Apparatus labeled with GM130 of control neurons as well as BFA-treated neurons. Syt10-GFP expressing neurons exhibited a partially overlapping localization with GM130 under control conditions. Disrupted vesicle traffic led to a collapse of the Golgi cisternae as demonstrated by GM130 labeling.

Figure 5.22 (continued) However, the localization of Syt10-GFP did not change following the stimulation. Scale bar upper rows: 10 µm; lower rows: 5 µm.

To unravel, whether Syt10 is part of the ER/Golgi traffic in neurons, a putative localization of Syt10-GFP to the Golgi Apparatus was examined by counterstaining of Syt10-GFP transfected neurons with GM130. Overlap of Syt10-GFP was observed with the localization of the Golgi matrix protein (Figure 5.22 B upper row). In addition, treatment with BFA induced the collapse of Golgi cisternae, as monitored by the change of GM130 staining pattern, but did not lead to a change of Syt10-GFP localization in primary hippocampal neurons. The results obtained from PC12 cells and from primary neurons indicate that in both cell types Syt10 is not a resident Golgi protein.

5.4.5 Syt10 is partially localized to neuropeptide Y containing vesicles

To study the punctate localization of Syt10 in more detail, it was first examined if Syt10-mRFP is localized to NPY, a marker for peptide vesicles. Primary neurons were co-transfected on DIV5-6 with a construct coding for Syt10-mRFP and a vector containing NPY-GFP and cells were prepared for confocal imaging on DIV16. Overlap of Syt10-mRFP and NPY-GFP was mainly observed in the soma of these neurons, which could not be detected in the branches of overexpressed neurons (Figure 5.23 A-C). To exclude that the overexpressed mRFP-tag changes the correct localization of Syt10, primary neurons were overexpressed on DIV5-6 with NPY-GFP and untagged Syt10 and staining against Syt10 with the polyclonal Syt10 antibody 150 T3 was carried out on DIV14. Similar to the results obtained with Syt10-mRFP, a stronger overlap of the proteins was found in the soma and less co-localization could be detected in the neurites (Figure 5.23 C-E). These results indicate that the two proteins might be present on the same vesicles.
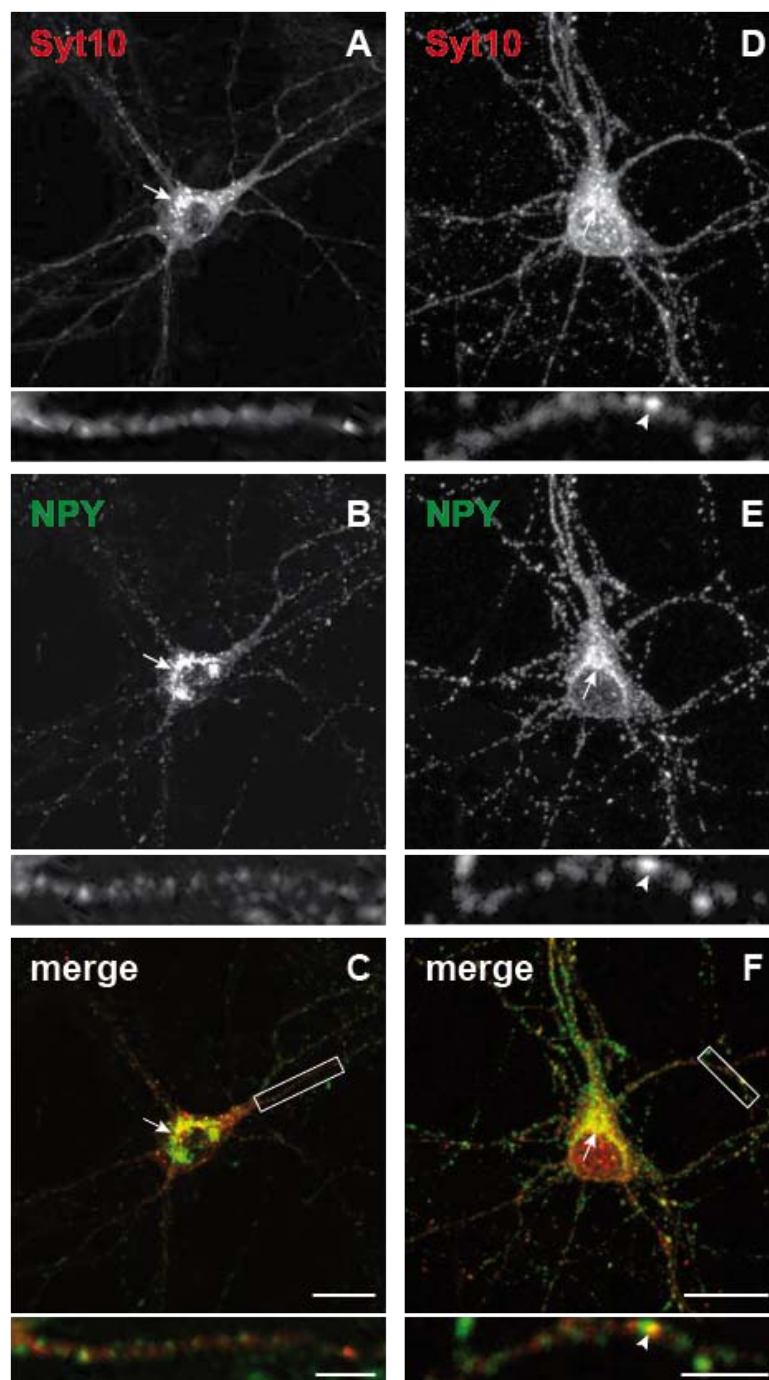
Figure 5.23 Co-transfection of Syt10-mRFP or untagged Syt10 with NPY-GFP. Confocal images of mouse cortical neurons transfected on DIV5-6 and fixed for confocal imaging on DIV14-16. (A-C) Neurons overexpressing Syt10-mRFP and NPY-GFP. Overlapping expression of the two proteins could only be detected in the soma (white arrows). (D-F) Neurons that were transfected with NPY-GFP and untagged Syt10 were stained with the polyclonal Syt10 antibody 150 T3. Similar to the mRFP-tagged fusion protein, untagged Syt10 and NPY-GFP exhibited only a low degree of co-expression in the neurites (white arrowheads) but showed a stronger overlap in the soma of hippocampal primary neurons (white arrows). Scale bar: 20 µm; magnification: 5 µm.

5.4.6 Distribution of Syt10 and IGF1 in hippocampal neurons

Olfactory bulb neurons overexpressing pHluorin-tagged Syt10 and FLAG-tagged IGF1 analyzed by immunocytochemistry were found to exhibit almost 100 % co-

localization (Cao et al., 2011). It was therefore speculated whether in primary cortical or hippocampal neurons, Syt10 is also localized to IGF1 containing vesicles and could thereby function in these cell types as Ca^{2+}-sensor for IGF1 release as well. To address this hypothesis, mouse cortical neurons were transfected on DIV5 with Syt10-GFP and IGF1-mRFP and on DIV14 the neurons were fixed for confocal imaging. Figure 5.24 shows a neuron overexpressing both constructs. In the soma as well as in the branches, there were overlapping expression punctae although the degree of overlap was not 100 % (Figure 5.24 A).

Due to its size GFP might interfere with the correct localization of a fusion protein. Hence, a putative co-expression of Syt10 and IGF1 was analyzed in neurons by transfection of constructs coding for proteins with a smaller tag or without a tag. Consequently, Syt10 and IGF1-HA were co-transfected into mouse hippocampal neurons on DIV5 and the cells were immunolabeled following fixation on DIV14 with the monoclonal antibody 2A9 and an antibody specific for the HA-tag. The fluorescent signal of the HA and Syt10 staining was more diffusely and weaker distributed along the soma and branches compared to fluorescently tagged fusion proteins (compare Figure 5.24 A and B). Analysis of Syt10 and IGF1 distribution in the dendrites revealed a rather low degree of co-localization although Syt10 was localized to a few IGF1-HA positive punctae (Figure 5.24 B, 2). An identical pattern was observed using different Syt10 antibodies (Appendix, supplementary figure 10).

A
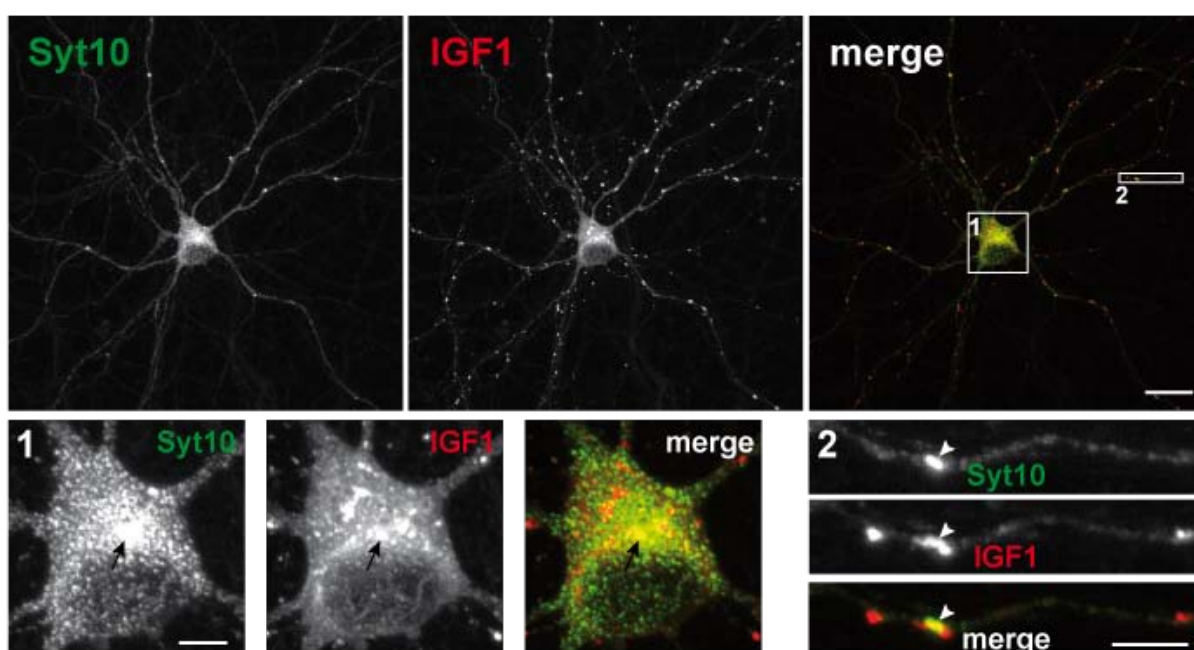
B
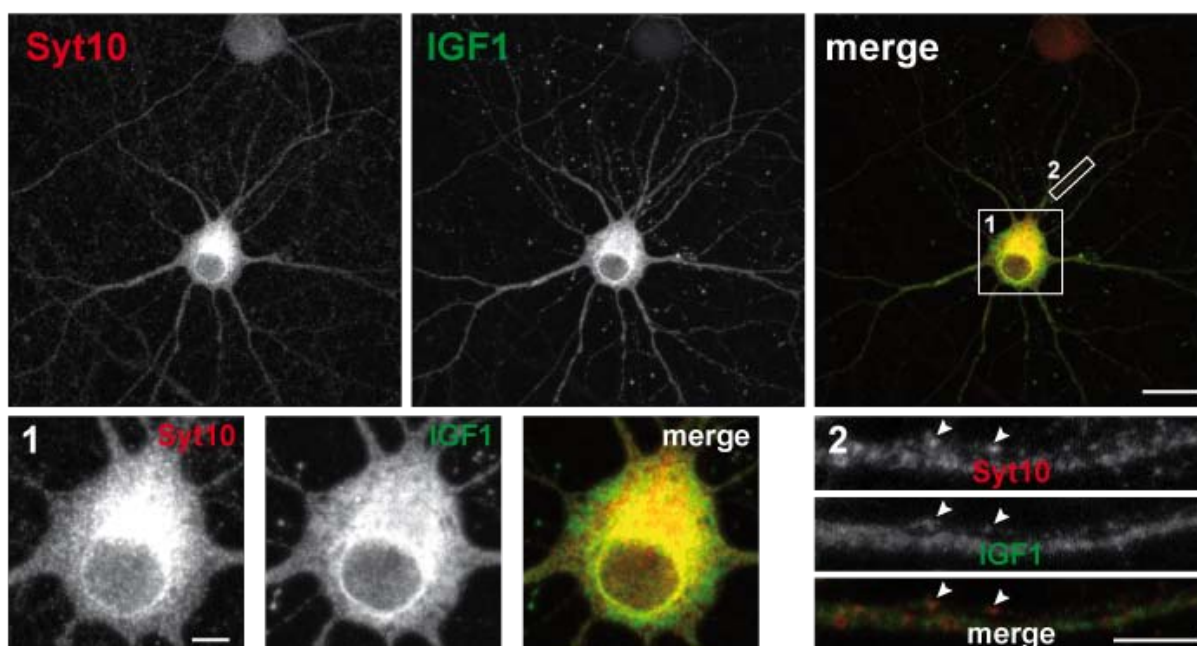
Figure 5.24 Partial overlap of overexpressed Syt10 and IGF1 in mouse primary neurons. (A) Co-transfection of mouse cortical neurons on DIV5 with constructs coding for Syt10-GFP and IGF1-mRFP. Neurons were fixed for subsequent confocal imaging on DIV14. Overlapping expression of the two proteins could only be detected near the nucleus (black arrows) and at the branches (white arrowheads) although the degree of overlap was not 100 %. (B) Co-transfection of untagged Syt10 and IGF1 fused to a C-terminal HA-tag. Mouse hippocampal neurons were fixed on DIV14 for subsequent immunolabeling with the monoclonal Syt10 antibody 2A9 and an antibody specific for HA. Similar to the GFP-tagged fusion proteins, Syt10 and IGF1-HA did not exhibit a high degree of co-expression in the neurites (white arrowheads) but in the soma of hippocampal primary neurons. Numbers in the upper right image indicate the boxes with higher magnifications of the soma (1) and of one neurite (2). Scale bar: 20 µm, magnifications: 5 µm.

5.4.7 Subcellular distribution of closely related Synaptotagmins in neurons

Syts 3, 5, 6 and 10 exhibit a high degree of sequence similarity and only differ in their TMD, the linker region and the very end of the C-terminus. Nevertheless, these isoforms vary in their subcellular localization as shown in PC12 cells and in neurons (Saegusa et al., 2002). To study the subcellular localization of the different isoforms with regard to Syt10, primary neurons were transfected with constructs coding for Syts 3, 5 and 6 fused to GFP on DIV5 and fixed for subsequent confocal microscopy on DIV14. Syt3-GFP, Syt5-GFP and, to a higher degree, Syt6-GFP were widely distributed in the soma and the neurites with a punctate expression along the branches and the soma (Figure 5.25).
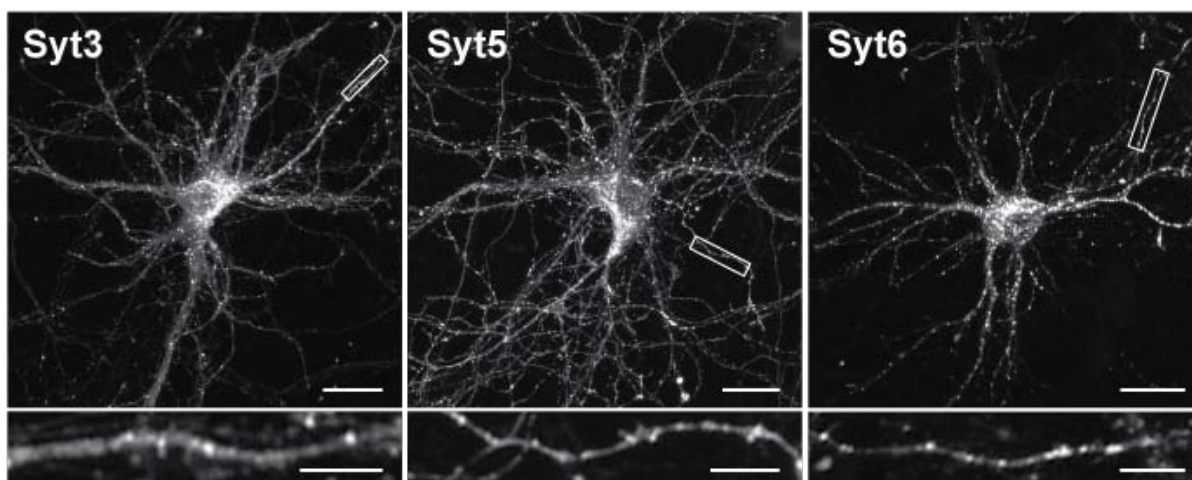
Figure 5.25 Localization of overexpressed Syt3, 5 and 6 fusion proteins in primary neurons. Confocal images of hippocampal neurons transfected with constructs coding for Syts 3, 5 and 6 fused to GFP. Syt6 was strongly distributed throughout the soma and along neurites showing a punctate expression. Overexpression of Syt3 and 5 revealed a similar pattern but with a lesser degree of punctae. White boxes indicate magnification of branches below the respective image. Scale bar: 20 μm; magnification: 5 μm.

5.4.8 Co-expression of Syt10 with closely related isoforms

Syts 3, 5, 6 and 10 are known to form homo- and heterodimers via evolutionary conserved cysteine residues indicating a potential co-localization of those isoforms (Fukuda et al., 1999a). To examine, whether Syt10 is co-localized with one of these isoforms in primary neurons, co-transfections of Syt10-mCherry with Syt3, 5 and 6-GFP were carried out on DIV5-6. Neurons were fixed for confocal imaging on DIV13-14. For comparison with the co-transfections, the distribution pattern following single transfection of individual Syt isoforms is shown in figure 5.25 and supplementary figure 9 (Appendix).

Overlap of Syt3-GFP and Syt10-mCherry (Figure 5.26 left row) as well as of Syt5-GFP and Syt10-mCherry (Figure 5.26 middle row) was mostly restricted to the soma and not present in neurites. In contrast, Syt6-GFP co-transfected with Syt10-mCherry showed a strong overlap in the soma that was also found in the branches (Figure 5.26 right row). Moreover, co-transfection of Syt10-mCherry with Syt6-GFP seemed to have an effect on the overall localization of Syt10-mCherry in primary neurons since its co-transfection with Syt6-GFP exhibited a more punctate expression pattern (Figure 5.26 right row).
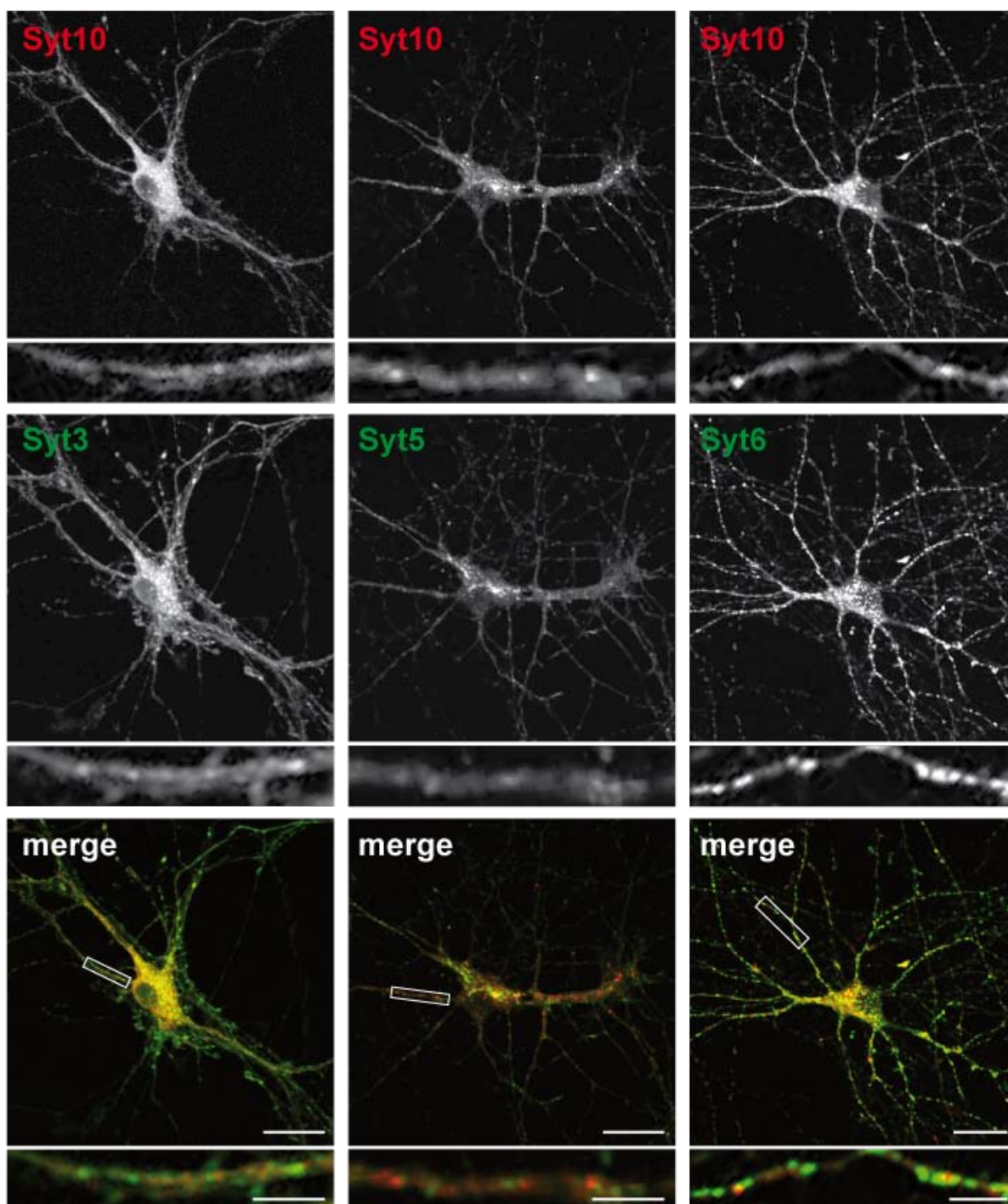
Figure 5.26 Confocal images of mouse primary neurons showing Syt10-mCherry co-transfected with Syt3, 5 and 6-GFP. Neurons transfected on DIV5-6 and fixed for microscopy on DIV13-14. Left row: Overexpressed Syt3-GFP was co-localized with Syt10-mCherry in the soma but less in the neurites. Middle row: Overlap of Syt10-mCherry expression with Syt5-GFP was restricted to a small part near the nucleus. Right row: Overexpressed Syt10-mCherry overlapped with expression of Syt6-GFP in the soma and partially in the neurites. Scale bar: 20 μm, magnification: 5 μm.

5.4.9 Distribution of co-expressed Syt6-mCherry and Syt10-GFP

Confocal analysis of the distribution patterns of co-expressed Syt10-GFP and Syt6-mCherry indicated that the expression pattern of Syt10-GFP in the branches was altered in the presence of Syt6-mCherry. Due to this finding the subcellular distribution of Syt6 was further investigated using several markers to label synapses and dendrites. As observed for Syt10, Syt6 was distributed along dendrites but no overlap with a pre- or postsynaptic marker could be detected (Appendix, supplementary figure 11).

To further analyze the phenomenon mentioned above, primary neurons were co-transfected with Syt10-GFP and Syt6-mCherry with different DNA ratios on DIV5 and the cells were fixed on DIV14 for subsequent analysis via confocal microscopy. The results revealed a change of Syt10-GFP localization following co-transfection with 4-fold excess of Syt6-mCherry. As described in chapter 5.4.3, single transfection of Syt10-GFP revealed punctate expression in the soma but a weaker and more diffuse distribution in the neurites. In contrast, neurons transfected with Syt6-mCherry and Syt10-GFP at a ratio of 4:1, showed more punctae in the branches where Syt6-mCherry and Syt10-GFP exhibited a strong overlap (Figure 5.27). If Syt10-GFP and Syt6-mCherry were transfected at a ratio of 4:1, this phenomenon was not observed. This result might indicate that both isoforms form heterodimers in neurons in the presence of higher amounts of Syt6 protein and that the heterodimer might be targeted to the Syt6 subcellular localization.
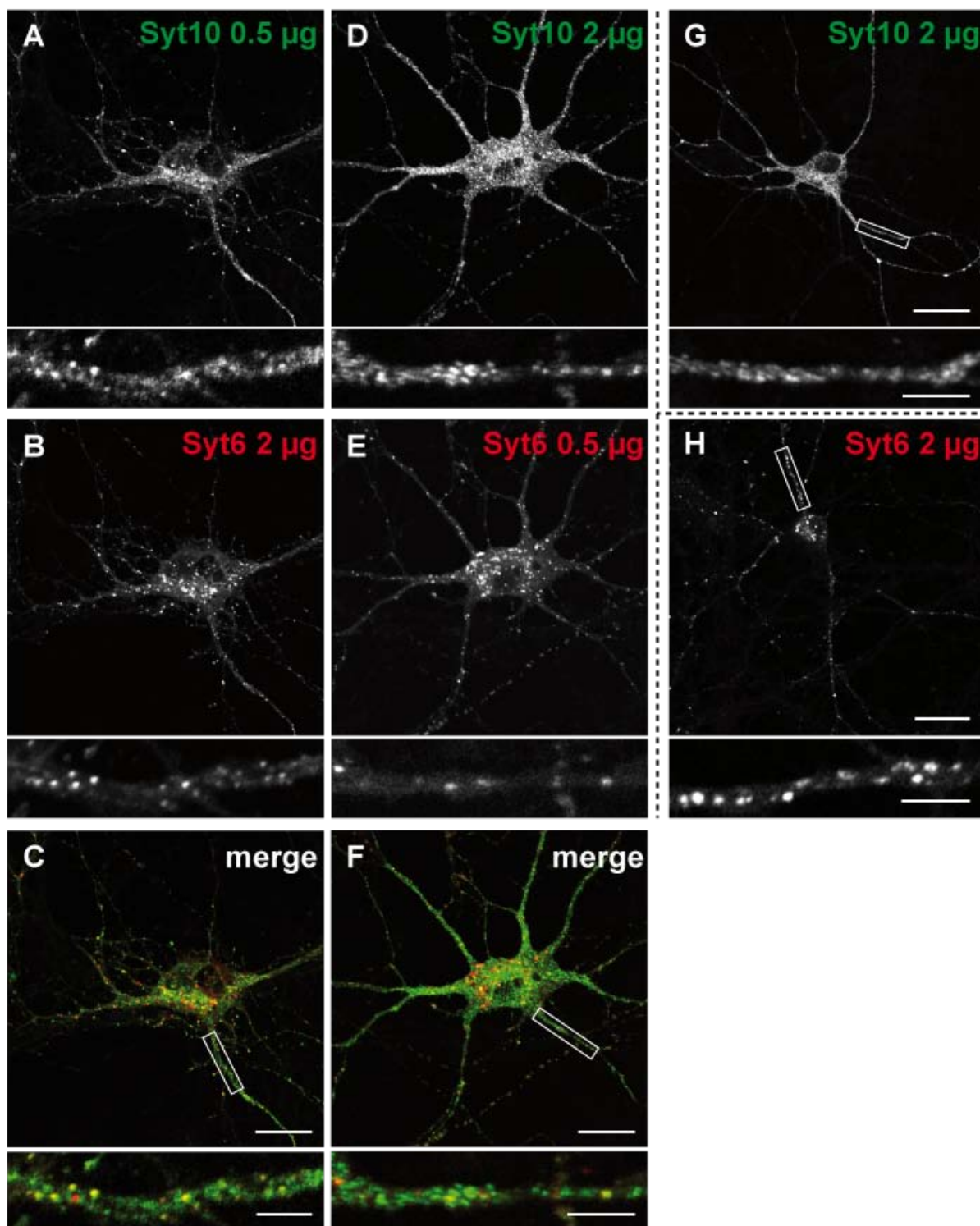
Figure 5.27 Co-expression of Syt10-GFP with Syt6-mCherry changes the subcellular distribution of Syt10. Confocal images of cortical neurons transfected on DIV5 with different concentrations of Syt10-GFP and Syt6-mCherry. (A)-(C) DNA was transfected at a ratio of 1:4 (Syt10-GFP:Syt6-mCherry). (D)-(F) Ratio of transfected DNA was 4:1 (Syt10-GFP:Syt6-mCherry). (G), (H) single transfections of Syt10-GFP and Syt6-mCherry (both 2 μg DNA). Scale bar: 20 μm, higher magnification: 5 μm.

5.4.10 Characterization of Syt10 N-terminal targeting sequences

Targeting signal sequences in the N-terminus or posttranslational modifications, i.e. N- and O-glycosylation or palmitoylation mostly determine the localization of a given protein (Han et al., 2004; Flannery et al., 2010; Kwon and Chapman, 2012). Han et al., 2004, identified that the N-terminus of Syt1 is important for Syt1 localization to synaptic vesicles. Furthermore, Syts 3, 5, 6 and 10 possess evolutionary conserved cysteine residues in their N-terminus that are known to be important for homo- and heterodimerization of those isoforms (Fukuda et al., 1999a) or that might be palmitoylation target sites. As a first step to identify the Syt10 targeting sequences, it was probed if the N-terminus of those isoforms or the cysteine residues of Syt10 are needed for the correct targeting of the respective proteins in neurons.

For this, the respective cysteine residues in the Syt10 full-length sequence were mutated into alanine (Mutation 1: C13A, Mutation2: C24A, Mutation3: C34A) and chimeras were constructed that are composed of either a Syt3, 5 or 6 N-terminus combined with the TMD, linker and C_2-domains of Syt10 (Figure 5.29 A and B).
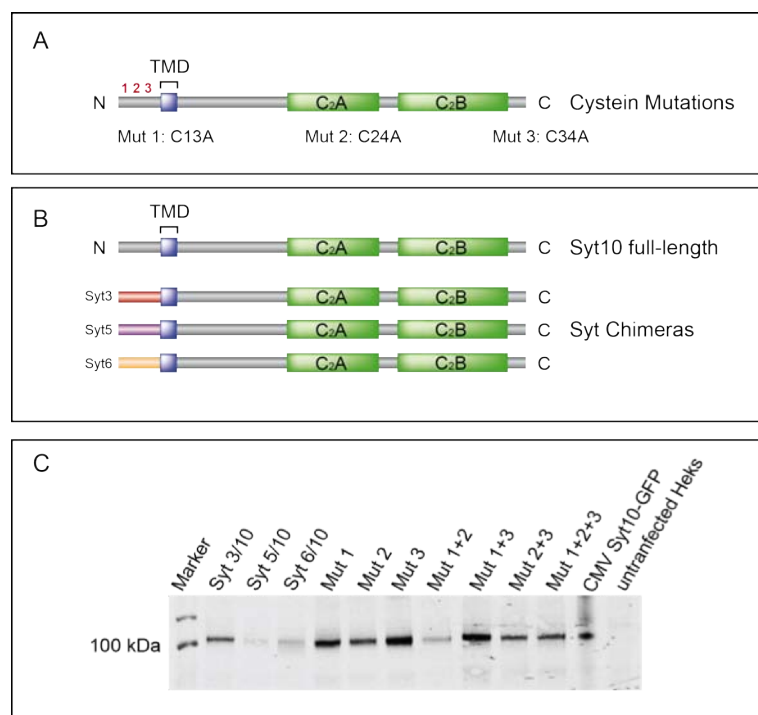
Figure 5.28 Schematic drawing and immunoblot of mutated cysteine residues and Syt10 chimeras. (A) Cartoon of full-length Syt10 with cysteine residues indicated by red numbers. Cysteine residues are located at amino acid positions 13, 24 and 34, and are mutated by site-directed mutagenesis into alanine. (B) Picture of the chimera design showing the Syt10 full-length domain structure as a reference and the chimeras Syt3/10 (red N-terminus), Syt5/10 (violet N-terminus) and Syt6/10 (yellow N-terminus). The Syt10 N-terminus is exchanged by the N-terminus of the respective closely related isoforms. (C) Immunoblot of HEK293T cell lysates with overexpressed chimera and mutation proteins. Labeling with the polyclonal Syt10 antibody 150 T3 revealed the expected size of 100 kDa in all protein lysates.

First, it was tested whether the DNA sequence of the chimeric and mutated GFP-tagged proteins were translated into proteins of the correct size. HEK293T cells were transfected with constructs coding for the chimeric and mutated proteins and subsequent immunoblotting of the protein lysates was carried out using the polyclonal antibody against Syt10. All chimeric and mutated proteins showed the expected size of 100 kDa (Figure 5.28 C).

To probe if the N-terminal cysteines are required for proper targeting, these residues in the Syt10-GFP construct were mutated into alanine as schematically shown in figure 5.28 A and were transfected into primary neurons.

Mutation 1: C13A

Mutation 2: C24A

Mutation 3: C34A
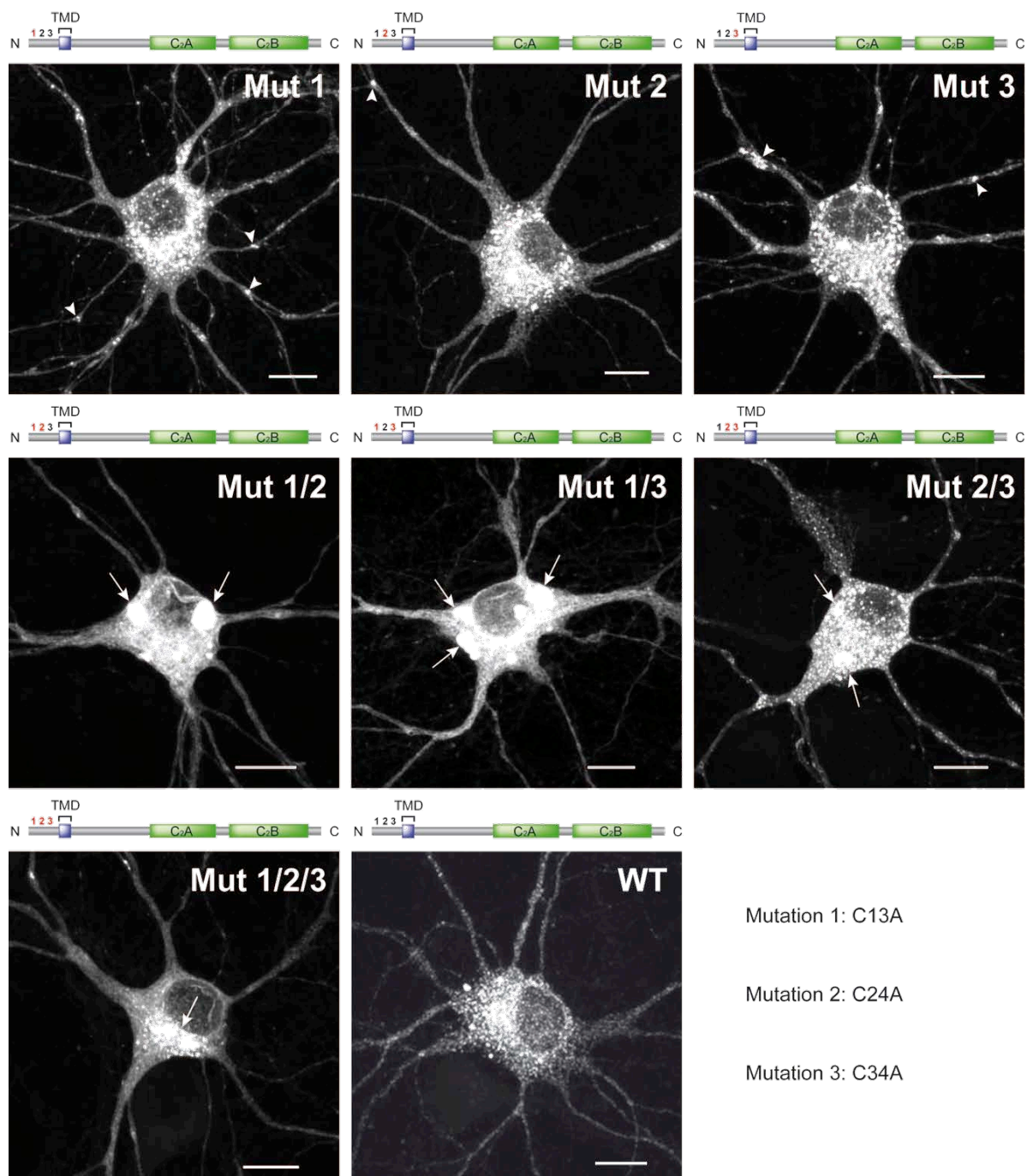
Figure 5.29 Mutated cysteine residues in the Syt10 N-terminus changes the subcellular localization in neurons. Confocal images of cortical neurons transfected on DIV5 with constructs carrying mutated cysteine to alanine residues at the amino acid positions indicated by red numbers (Mutation 1: C13A, Mutation 2: C24A, Mutation 3: C34A) in the Syt10 full-length sequence fused to GFP. WT: full-length Syt10 without mutations. Insertion of one mutation increased the number of large dendritic punctate structures (white arrowheads). As two or more cysteines were mutated simultaneously larger aggregates were observed in the soma (white arrows). Scale bar: 10 µm.

Confocal imaging of cortical neurons revealed that neurons transfected with either Syt10 Mut1, 2 or 3 exhibited more and larger punctae in the branches compared to WT Syt10 (Figure 5.29 upper row). Simultaneous mutation of two cysteines resulted in large fluorescence intense aggregates in the soma of transfected neurons (Figure 5.29 middle row). Mutation of all three cysteine residues led to complete retention of Syt10 into the soma (Figure 5.29 lower row). These results indicate that mutation of cysteine residues leads to an accumulation of Syt10 protein in both, branches and the soma of cortical neurons. The more sites were changed to alanine simultaneously, the higher the observed degree of Syt10 protein contained in aggregates in the soma.

To test if, as for Syt1, targeting signals located in the N-terminus are relevant for the correct targeting of Syt10 and the isoforms of the same subclass, chimeric constructs were made consisting of the Syt3, 5 or 6 N-terminus fused to the remaining Syt10 full-length protein domains as depicted in figure 5.28 B. Primary neurons were transfected with chimeric proteins on DIV5 and fixed for confocal imaging on DIV14. Different from the respective Syt3, 5 and 6 full-length proteins (Figure 5.30 F-H), the fluorescent signal from all chimeric proteins (Figure 5.30 C-E) was more diffuse and widely distributed along the branches and less punctate in the soma.

The expression pattern of the chimeric proteins was more similar to the Syt10 full-length protein than to the corresponding Syt3, 5 and 6 full-length proteins. This indicates that besides the Syt10 N-terminus another protein domain appears to be important for the correct targeting of the Syt10 full-length protein.
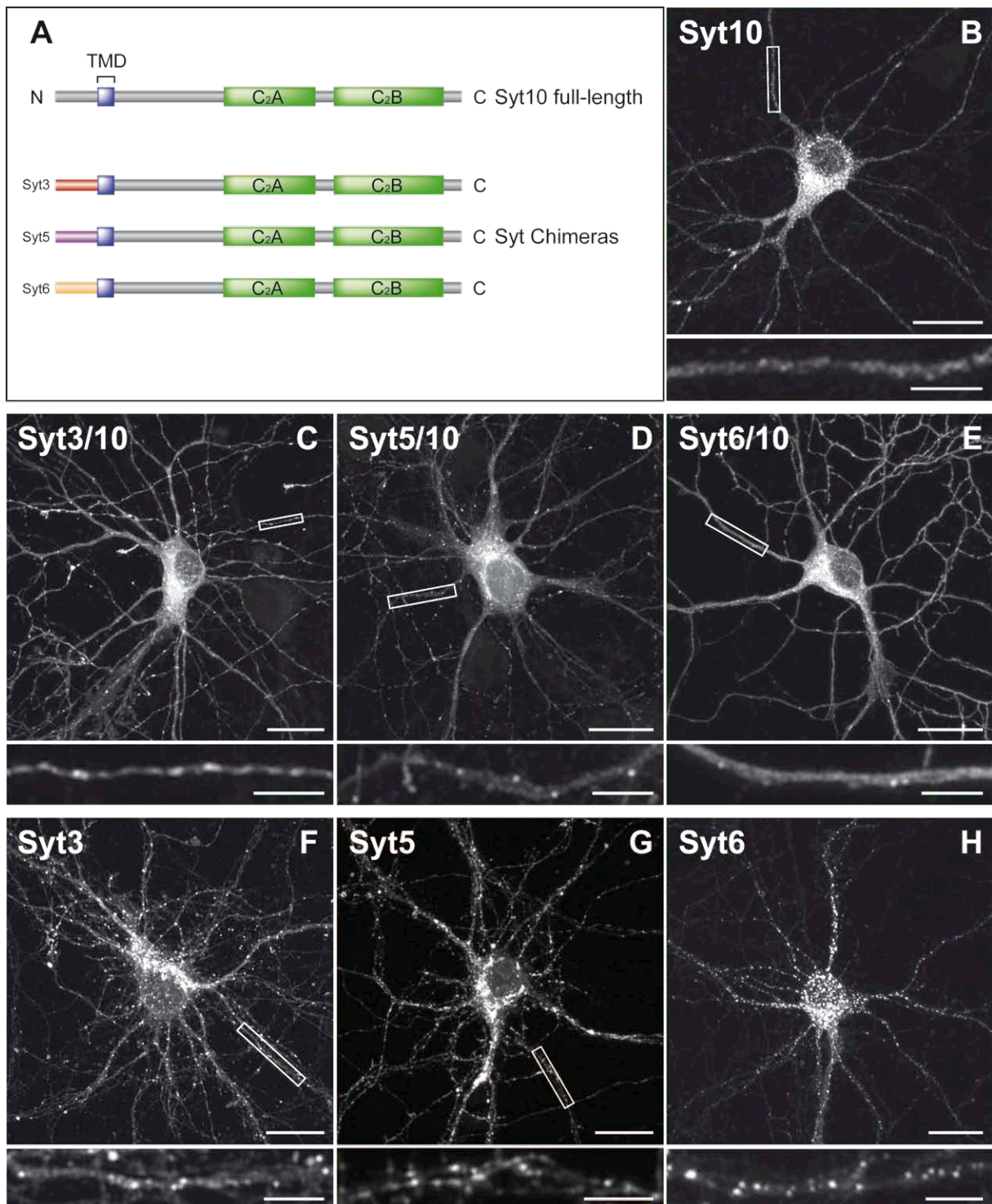
Figure 5.30 Localization of chimeric Syt10 constructs compared to full-length Syts 3, 5, 6 and 10 in neurons at DIV14. (A) Schematic drawing of full-length Syt10 and the chimeric constructs. Note that all proteins shown in (A) and the corresponding full-length Syt3, 5, and 6 are fused to GFP. (B)-(H) Mouse cortical neurons were transfected on DIV5 with full-length Syt10 or chimeric proteins (Syt3/10, Syt5/10, Syt6/10) or the corresponding full-length Syts 3, 5 and 6 and were fixed for confocal imaging on DIV14. Scale bar: 20 µm; higher magnification (white box): 5 µm.

5.5 Establishment of a technical approach to characterize Syt10 containing organelles and protein complexes

5.5.1 Extraction of the Syt10 protein under native conditions

Although it has been reported that Syt10 is localized on IGF1 containing vesicles in OB neurons (Cao et al., 2011), the nature of Syt10 containing organelles in the hippocampus is still unresolved. As in the hippocampus Syt10 is only highly expressed after seizures, an *in vivo* approach (e.g. purification of synaptosomes from SE-experienced mice) might be suitable for the characterization of Syt10 containing organelles. To this end, interaction partners of Syt10 could be identified via streptavidin/FLAG-tandem affinity purification (SF-TAP) and subsequent analysis using mass spectrometry. To preserve *in vivo* interactions, the 3-D structure of the proteins has to be maintained, meaning that the protein folding may not be disrupted by the use of denaturing conditions.

To control for the correct size of the proteins, first all plasmids were transfected coding for either Syt10 or Syt6 fused to a SF-TAP tag using the Ca^{2+}-phosphate method in HEK293T cells. Lysis of the samples under denaturing conditions was carried out 48 h later and the immunoblot was stained with the polyclonal Syt10 antibody 150 T3 and with a FLAG antibody. The signals from both antibodies completely overlapped and the expected size of the TAP fusion proteins was observed (Syt10: 69 kDa, Syt6: 66 kDa; Appendix, supplementary figure 12).

Next, different approaches were tried to solubilize Syt10 under native conditions. For this purpose, HEK293T cells were transfected with either Syt10- or Syt6- TAP plasmids. To visualize the transfection efficiency before lysis, cells were transfected in parallel with a Syt10-GFP construct. Lysis was performed 48 h following transfection with lysis buffer 1 containing 30 mM Tris-HCl, 150 mM NaCl and 1 % of detergent. Non-denaturing detergents known not to interfere with the following tandem affinity purification were chosen (Triton X-100, DTT, CHAPS, DDM, NP40, Cholat). Subsequent immunoblotting was performed using an antibody that specifically recognized the FLAG-tag. Figure 5.32 A shows the immunoblot of samples treated with SDS as a positive control as well as two samples for each of the non-denaturing detergents: (1) 'pellet after lysis' represents the cell debris that could contain unsolubilized Syt10 protein, (2) 'supernatant' means the sample after lysis possibly containing solubilized Syt10 protein. By comparison of the two

samples, the amount of non-solubilized versus solubilized protein was determined for each detergent tested. As shown in figure 5.31 A, none of the detergents was able to completely solubilize Syt10. Bands were only visible in the cell debris sample (pellet after lysis) (Figure 5.31 A). A similar result was observed for Syt6-TAP protein. In contrast, a Syt10-GFP fusion protein was to some degree extracted with all tested detergents (Figure 5.31 A). However, a TAP tag is indispensable for the analysis of binding partners given that the GFP protein might raise the probability for unspecific binding. Therefore, only TAP fusion constructs were used for further analysis. Due to the observed insufficient solubilization, the investigation was extended to other detergents and the ionic strength of the lysis buffer 2 was increased (30 mM Tris-HCl, 300 mM NaCl, 2.5 mM EGTA and 1 % detergent if not otherwise indicated). Two detergents (n-Octyl-ß-D-glucopyranoside and Zwittergent 3-14) showed the potential to get Syt10 into solution (Figure 5.31 B). Nevertheless, the corresponding Syt10 protein band was still very faint.

A

B

	Syt10-TAP												
kDa	denaturing condition	Pellet after lysis			supernatant			denaturing condition	Pellet after lysis			supernatant		
	PBS+SDS	CL91	CL114	5% Triton X-100	CL91	CL114	5% Triton X-100	PBS+SDS	Zwittergent 3-14	n-Octyl-ß-D-glucopyranoside	n-Octyl-ß-D-thioglucopyranoside	Zwittergent 3-14	n-Octyl-ß-D-glucopyranoside	n-Octyl-ß-D-thioglucopyranoside
130 –														
100 –														
70 –														
55 –														
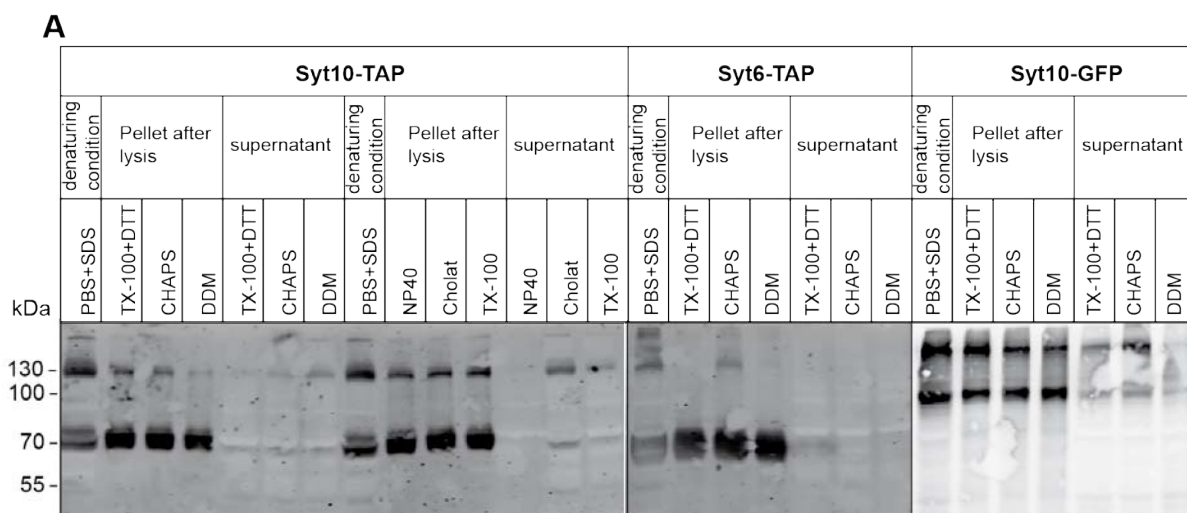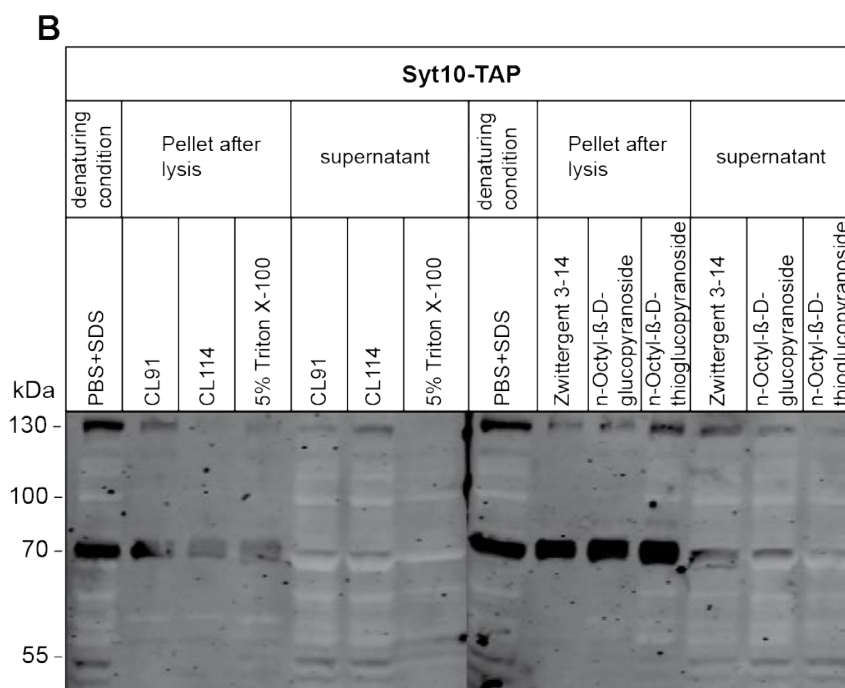
Figure 5.31 Extraction of Syt10 from HEK293T cells under native conditions. HEK293T cells were either transfected with a SF-TAP-tagged Syt10 or Syt6 construct or with a Syt10-GFP plasmid and were collected after 48 h later. The sample containing SDS served as a positive control, and both, the pellet and supernatant were obtained after 1 h of lysis and subsequent centrifugation. The amount of Syt10 protein in the lysate was determined by immunoblotting with a FLAG antibody. (A) Here, lysis buffer 1 was used. In the supernatants of cells transfected with Syt10-GFP a weak band was visible, whereas no Syt10-TAP protein was detected in other supernatants. (B) Using lysis buffer 2 a faint band in the supernatant lysed with Zwittergent 3-14 and n-octyl-ß-D-glucopyranoside was detected.

5.5.2 Syt10 and Syt6 without a TMD exhibit an altered solubility

It could be hypothesized that the difficulties regarding the extraction of Syt10 might be due to the presence of the TMD. To examine whether deletion of the Syt10 or Syt6 N-terminus and TMD might alter the solubility of the protein, TAP fusion constructs lacking these domains were designed. Here, lysis buffer was composed of 30 mM Tris-HCl, 300 mM NaCl and 10 mM EGTA at pH 7.4 and one percent of detergent. Surprisingly, deleting the TMD decreased the amount of solubilized Syt10 protein in the supernatant (Figure 5.32). In contrast, the missing TMD of Syt6 led to an increase of the Syt6 protein solubility (Figure 5.32). As Syt10 is not endogenously expressed in HEK293T cells, the results might suggest that Syt10 overexpressed in this cell line formed aggregates that could not be solubilized.

To probe if solubility could be increased in neuronal cells, the Syt10-TAP plasmid was transfected into the neuroblastoma/glioma NG108-15 cell line, and it was examined whether the Syt10 protein concentration on the immunoblot was higher compared to samples obtained from HEK293T cells. Even though NG108-15 cells

are neuron-like, Syt10 extraction from this cell line was not more efficient than compared to HEK293T cells (Data not shown).
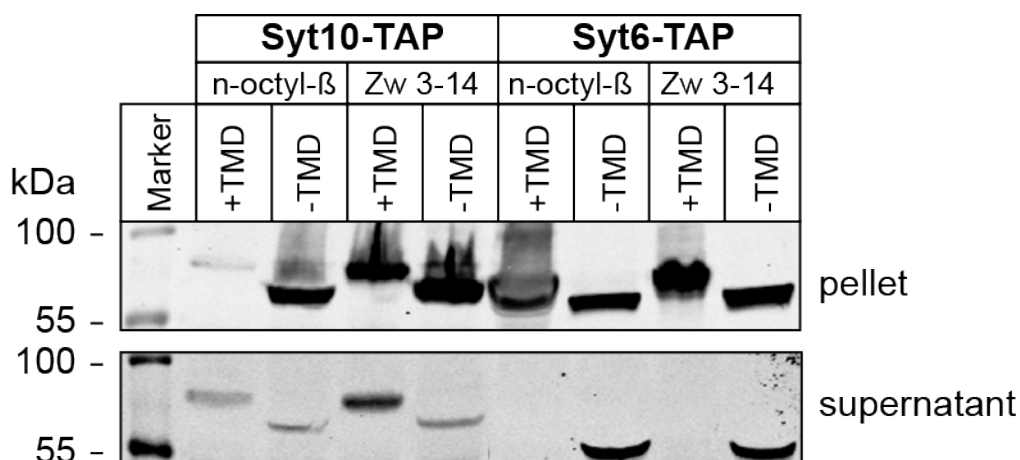
Figure 5.32 Deletion of the transmembrane domain (TMD) alters the Syt10 and Syt6 protein solubility. HEK293T cells were either transfected with a SF-TAP-tagged Syt10 or Syt6 construct containing (+TMD) or lacking (-TMD) a transmembrane domain. 48 h later, samples were lysed for 1 h with differentially composed lysis buffers. One percent of two detergents, n-octy-ß-D-glucopyranoside (n-octyl-ß) and Zwittergent 3-14 (Zw 3-14), were tested separately in lysis buffer (see text above). Both, the pellet containing unsolubilized protein and the supernatant were obtained after 1 h of lysis and subsequent centrifugation. The amount of Syt10 protein in the lysate was determined by immunoblots using a FLAG antibody. The Syt10 protein solubility was decreased when the TMD was lacking. Conversely, no Syt6 protein was detected when the TMD was present but was enriched in the samples lacking the TMD.

5.5.3 *In vivo* expression of GFP in the olfactory bulb and hippocampus after rAAV transduction

As mentioned above, formation of aggregates might cause the difficulties extracting Syt10 from HEK293T and NG108-15 cells. To overcome this problem, a different approach extracting native Syt10 protein was initiated. The olfactory bulb is the brain region in which Syt10 is expressed under native conditions. In this region, putative binding partners of Syt10 and the vesicle type that Syt10 is present on, are existent. Hence, overexpression of Syt10 in the OB might not result in the formation of aggregates. To test if the injection of rAAV particles results in a strong and broad infection of the OB, rAAV particles (serotypes 1/2 and 8) encoding the GFP protein were delivered into the OB and HC of newborn C57/Bl6 mice at three consecutive days (P0-3). Three weeks after injection, PFA perfused brains were cut horizontally into 30 µm thick vibratome slices. High numbers of infected neurons were found in all layers of the OB except for the external plexiform layer (EPL) that only contains a small number of tufted cells (Figure 5.33 A). Targeting the hippocampus resulted in

an efficient viral infection of all hippocampal subregions, dentate gyrus (DG), Cornu Ammonis 3 (CA3) and Cornu Ammonis 1 (CA1) (Figure 5.33 B). Taken together, these results show, that the viral injection into P0-3 day old mice was suitable for stable infection of neurons in the OB and the hippocampus. This method raises the possibility to study Syt10 binding partners *in vivo* after delivery of rAAV particles encoding the Syt10-TAP fusion protein. With this tool, it could be questioned if a change in the set of Syt10 binding partners would occur in response to seizure activity in the hippocampus.
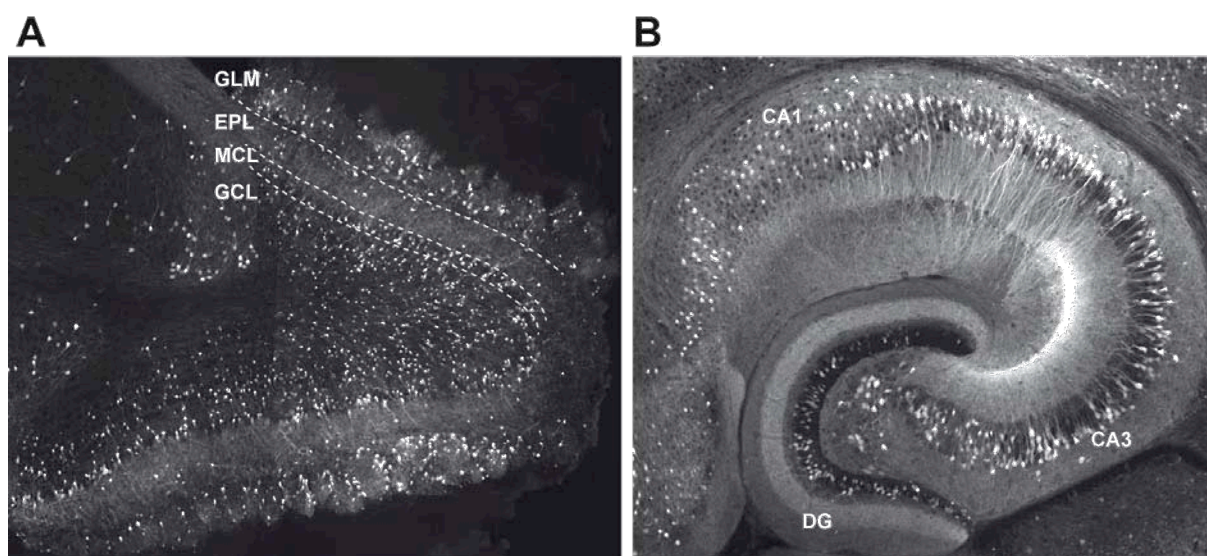
Figure 5.33 Sufficient targeting of neurons in the mouse brain by P0-3 injection of rAAV particles into the OB and HC. C57/Bl6 mice were injected P0-3 with serotype 1/2 and 8 viral particles purified from HEK293T cells transfected with an rAAV construct coding for GFP under the control of the human synapsin promoter. Three weeks after injection, mice were sacrificed by PFA perfusion and 30 µm thick brain vibratom slices were prepared. (A) Broad viral infection in the OB layers. EPL: external plexiform layer; GCL: granule cell layer; GLM: glomerular layer; MCL: mitral cell layer. (B) GFP positive neurons are distributed along all subregions of the hippocampus. DG: dentate gyrus; CA3: Cornu Ammonis 3; CA1: Cornu Ammonis 1.

5.6   Functional role of Syt10 during epileptogenesis

5.6.1 Pilocarpine-induced SE increases expression of Syt10-, IGF1- and NPAS4 mRNA

As mentioned above, Babity et al., 1997, found in rats that kainate injection leads to a rapid and transient up-regulation of Syt10 in the piriform cortex and in the hippocampus, with a peak expression 6 h after SE (Babity et al., 1997). Due to the fact that not all processes can be mimicked by stimulations *in vitro*, Syt10 gene expression was further characterized in mice that experienced SE.

To elucidate whether in mice, Syt10 induction after SE is observed with a similar time course as seen in Babity et al., 1997 mice were subjected to pilocarpine-induced SE and the hippocampal subregions DG, CA3 and CA1 were microdissected 2 h, 6 h, 12 h, 24 h, 36 h, 72 h and 28 d after SE (total hippocampus was prepared at 2 h following SE). The different time points reflect distinct stages of epileptogenesis: The acute phase (2 h, 6 h, 12 h), the latency stage (24 h, 36 h, 72 h) and the chronic epileptic phase (28 d). By quantitative real-time RT-PCR, mRNA levels of Syt10, IGF1 and NPAS4 were assessed using Synaptophysin as a reference gene to account for neuronal cell loss (n = 5 for all groups; 2 h SE, n = 8; chronic control, n = 4).

Surprisingly, the time course of Syt10 induction following SE differed from the one in rats. Whereas a significant down-regulation of Syt10 in DG was observed at five time points (2 h, 6 h, 36 h, 72 h and 28 d), an up-regulation in the CA3 region was detected at 12 h (2.4-fold, $p \leq 0.01$), 24 h (1.9-fold, $p \leq 0.01$) and 36 h (2.3-fold, $p \leq 0.01$) following SE (Figure 5.34 A). After SE, Syt10 mRNA expression in the CA1 region was significantly more abundant at 12 h (1.8-fold, $p \leq 0.05$) and 24 h (1.7-fold, $p \leq 0.05$) and peaked to a strong increase at 36 h (5-fold, $p \leq 0.01$). In contrast to Syt10 mRNA levels in the DG, IGF1 mRNA expression in the DG were constantly augmented beginning 6 h after SE (1.7-fold, $p \leq 0.05$), showing a peak expression 72 h (3.8-fold, $p \leq 0.01$) following SE and declining near to control values in the chronic phase (1.8-fold, $p \leq 0.05$) (Figure 5.34 B). IGF1 was more abundant in the CA3 and the CA1 region at all time points examined, however with an overall stronger IGF1 increase in the CA3 region 72 h after SE (12-fold, $p \leq 0.001$) and a strong augmentation in the CA1 region 72 h following SE (6.3-fold, $p \leq 0.01$). The immediate early gene NPAS4 showed an early response to SE with a very strong up-regulation 2 h following SE (128-fold, $p \leq 0.001$) which was transient and decreased to near control values between 36 h and 72 h after SE (Figure 5.34 C).
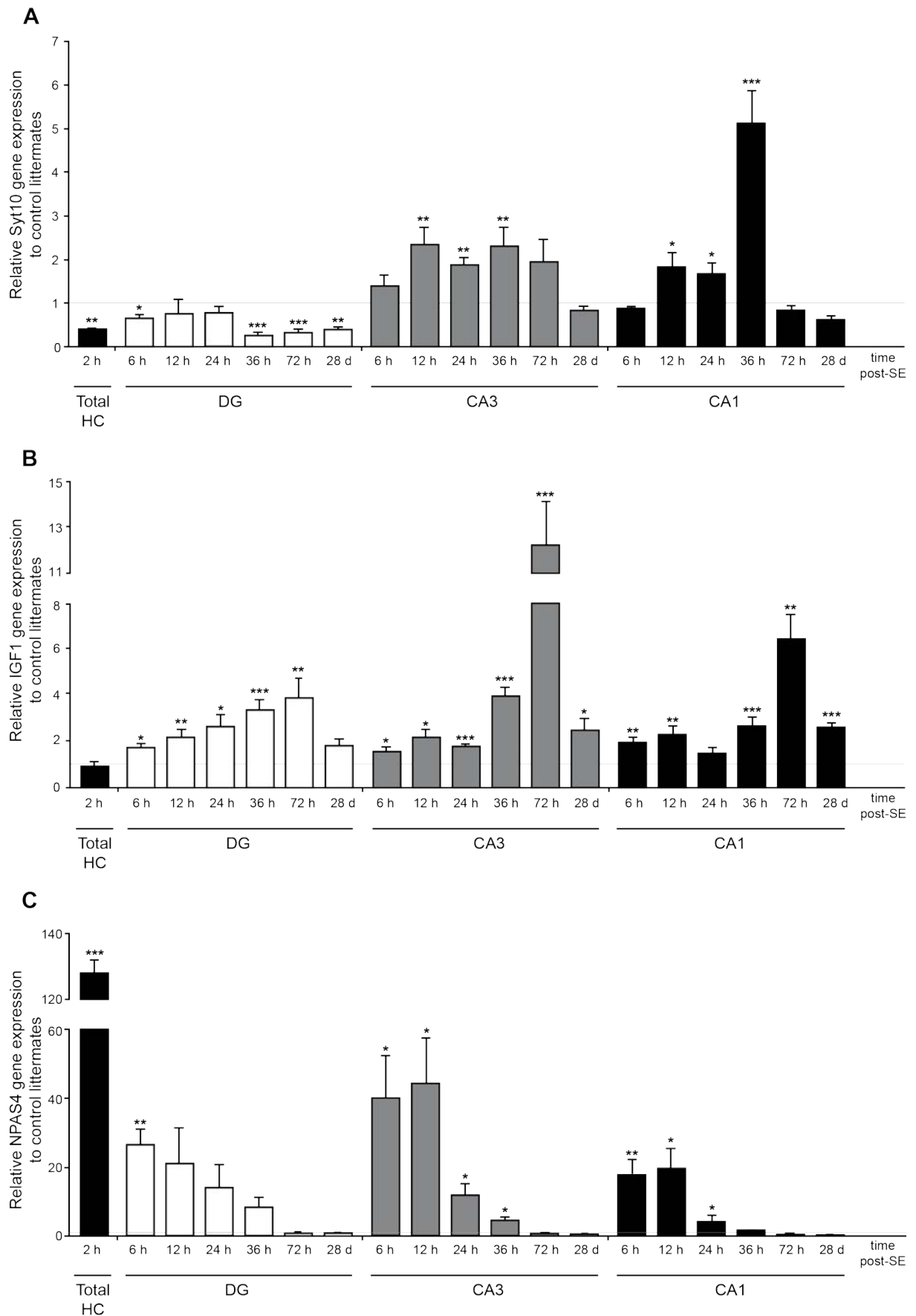
Figure 5.34 Pilocarpine-induced SE increases functional expression of Syt10-, IGF1- and NPAS4 mRNA. (A)-(C) Syt10-, IGF1 and NPAS4-mRNA expression levels in hippocampal subregions of mice (C57/Bl6) microdissected 2 h, 6 h, 12 h, 24 h, 36 h, 72 h and 28 d following

Figure 5.34 (continued) pilocarpine-induced SE compared to control littermates (black line) as assessed by quantitative RT-PCR. (A) Syt10 mRNA expression levels of the hippocampal subregions dentate gyrus (DG), CA3 and CA1 of SE-experienced mice shown relative to control littermates. Note that there is a peak up-regulation of Syt10 at 36 h after SE in the CA1 region (5.14 +/- 0.73). (B) Relative IGF1 mRNA expression of SE-experienced mice compared to control littermates exhibited an increase in all subregions of the hippocampus reaching its peak expression at 72 h following SE (DG 72 h: 3.81 +/- 0.78; CA3: 12.31 +/- 1.96; CA1: 6.25 +/- 1.10). (C) NPAS4 mRNA expression presented as fold change of SE-experienced mice compared to control littermates showing a peak up-regulation 2 h after SE (128.05 +/- 3.71) that declined in all subregions to baseline at 72 h after SE. The housekeeping gene Synaptophysin was used to normalize gene expression and statistical analysis was carried out using Student's t-test (*p ≤ 0.05, ** p ≤ 0.01, *** p ≤ 0.001) (n = 5 for all groups; 2 h SE, n = 8; chronic control, n = 4). Results are presented as mean +/- SEM.

5.6.2 Progenitor cell proliferation in the subgranular zone following SE is dependent on Syt10

Adult neurogenesis occurs in the subgranular zone (SGZ) of the hippocampus and the subventricular zone (reviewed by Curtis et al., 2012; Eriksson et al., 1998; Ming & Song, 2005). One hallmark of epilepsy is the aberrant network reorganization that is caused apart from other factors by increased neurogenesis (Parent et al., 1997; Parent et al., 2006; Parent et al., 2006). Recently, it was found that progenitor cell proliferation after SE is coupled to IGF1 and that Syt10 is localized to IGF-containing vesicles in the olfactory bulb (Cao et al., 2011; Choi et al., 2008).

As a first step to elucidate if Syt10 is also involved in mediating IGF1 release in the hippocampus after SE, pilocarpinized Syt10 WT and Syt10 KO animals were injected with a single dose of BrdU (300mg/kg of bodyweight) two days after SE to label newly proliferating cells (Figure 5.35 A). Two hours later, mice were perfused with 4 % PFA and processed for cryosections on the following day. Slices of 50 μm thickness were immunostained against BrdU for subsequent fluorescence imaging of the hippcampus. Figure 5.35 B shows representative images of the subregion dentate gyrus of one animal per experimental group. The granule cell layer (GCL) can be distinguished by the light grey background from the hilus (H). The subgranular zone is located between the GCL and the hilus. The representative images showed that SE led to a strongly augmented number of BrdU-positive cells (Figure 5.35 B). The quantification of the overall number of BrdU-positive cells counted in the GCL and the hilus verified the increase in total BrdU-positive cells after SE in WT animals (Figure 5.35 C). To study specifically the neurogenic niche of the hippocampus, BrdU-positive cells were counted in the subgranular zone. To correct for differs in the variable hippocampus sizes, the cell number was normalized to the length of the corresponding subgranular zone. This quantification revealed a significant up-

regulation in the rate of cell proliferation (2.5-fold, p ≤ 0.001) in WT mice but not in KO mice (1.5-fold, p ≤ 0.05) after SE relative to control animals (Figure 5.35 C). No significant difference in BrdU-positive cells was obtained in WT versus KO mice in the control situation. Interestingly, after SE the loss of Syt10 led to a 1.7-fold (p ≤ 0.01) decreased rate of cell proliferation (5.5 cells/mm) compared to WT mice (9.7 cells/mm) (Figure 5.35 C). Hence, Syt10 is crucial for an SE-mediated increase in the rate of cell proliferation.

C
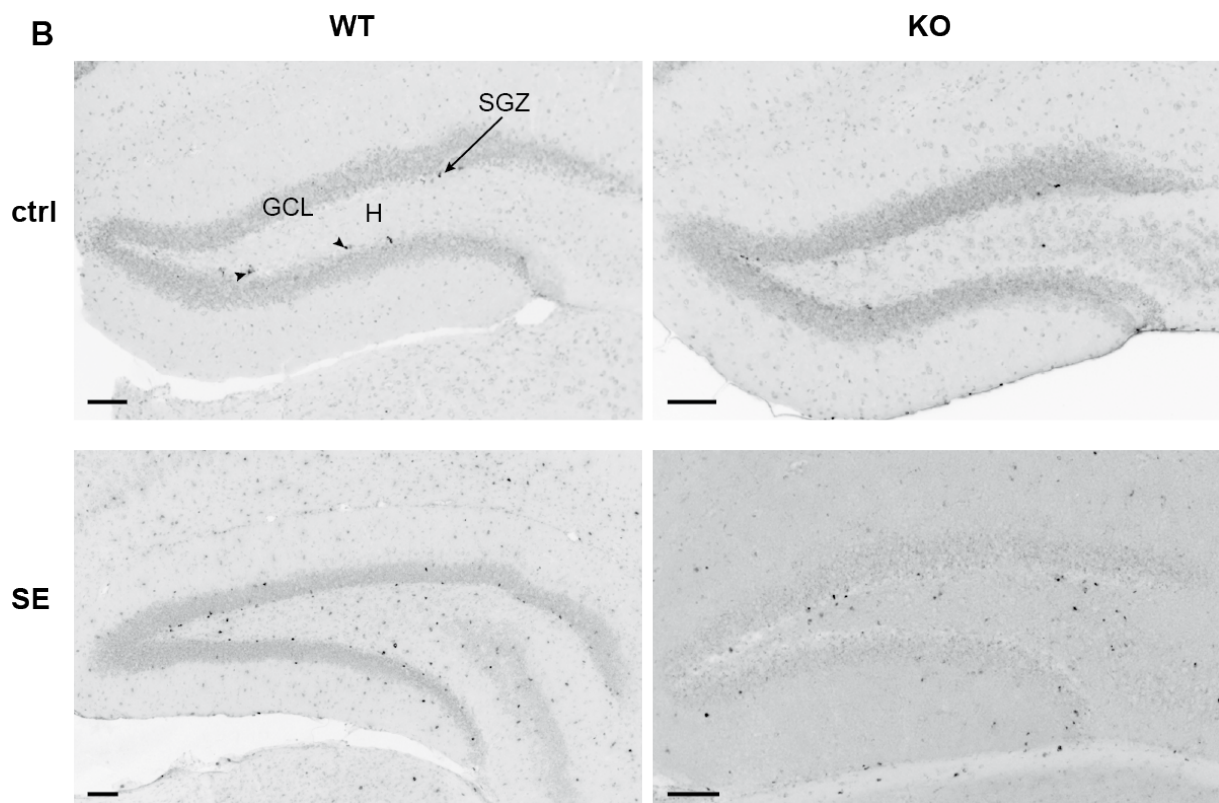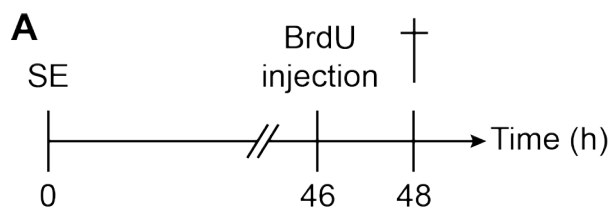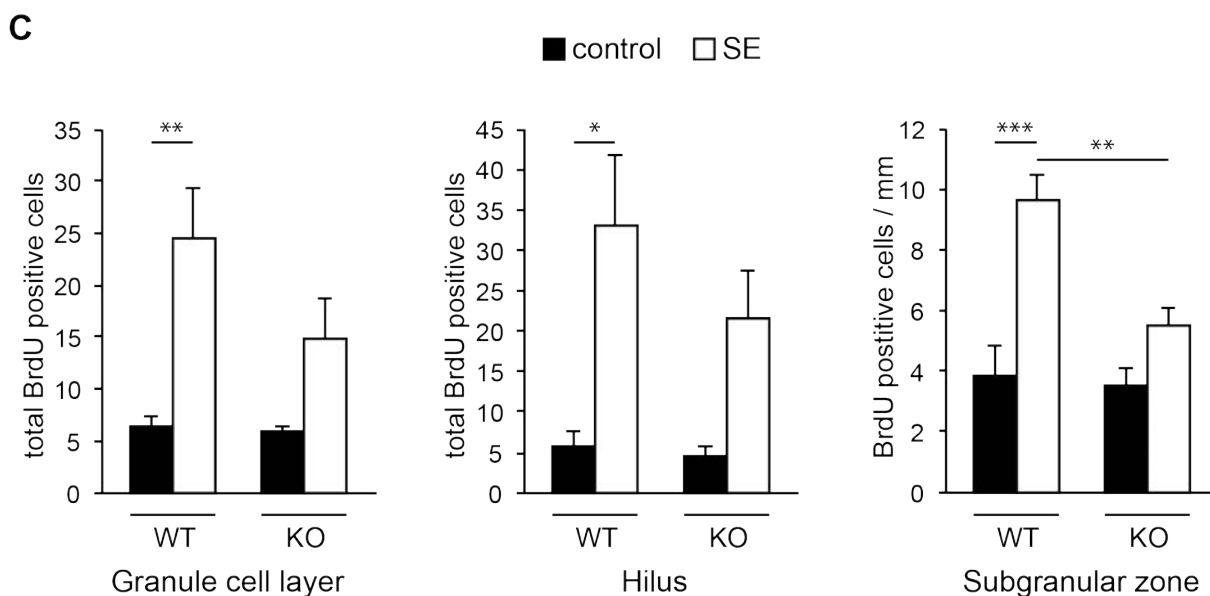
Figure 5.35 Decreased progenitor cell proliferation in Syt10 KO animals following SE.
(A) Schematic drawing of the experimental design. Syt10 KO and WT mice experienced pilocarpine-induced SE or were treated as controls (ctrl). Two days after SE, mice were injected with BrdU and were sacrificed 2 h after the injection. Subsequent immunolabeling against BrdU labels newly proliferating cells. (B) Representative images of the dentate gyrus (DG) from SE and ctrl Syt10 KO and WT mice. The granule cell layer (GCL), the hilus (H) and the subgranular zone (SGZ) of the dentate gyrus are indicated. The SGZ was defined as two cell layers between the GCL and the hilus. Per animal, five sections of the right hippocampus were labeled against BrdU. Scale bar: 100 µm. (C) Quantification of total BrdU positive cells counted in the GCL and in the hilus. The same samples were used for the quantification of BrdU-positive cells in the SGZ. Here, BrdU-positive cells were counted specifically in the SGZ and were normalized to the length of the SGZ. In all regions, an increase in the BrdU-positive cell number was observed in mice experienced SE compared to controls. Interestingly, Syt10 KO mice exhibit significantly less BrdU positive cells in the SGZ following SE compared to WT mice. Ctrl WT (n = 5), ctrl KO (n = 4), SE WT (n = 5), SE KO (n = 6). For quantification ImageJ was used, statistical analysis was carried out using One-way ANOVA followed by Tukey posthoc test (* $p \leq 0.05$; ** $p \leq 0.01$; *** $p \leq 0.001$) and results are presented as mean +/- SEM.

6 Discussion

Epileptogenesis describes a process of multiple cellular and molecular changes in the brain resulting in the occurrence of recurrent spontaneous seizures. One member of the synaptotagmin family, Syt10, is rapidly and transiently increased in the hippocampus after kainic acid-induction of status epilepticus (SE) (Babity et al., 1997).

The aim of this thesis was to gain novel insights into the signaling mechanisms controlling Syt10 gene expression in response to transient hyperexcitability as well as to resolve the function of Syt10 in the normal and epileptic brain.

Consequently, this study provided the first fundamental bioinformatic and functional characterization of the Syt10 promoter and genomic regulatory regions in different cell lines.

An insight into the putative function of Syt10 in hippocampal neurons was given by the analysis of the subcellular distribution of Syt10 in hippocampal neurons and in a neuronal cell line and was compared with Syt members belonging to the same Syt protein subclass.

Furthermore, the time course of Syt10 mRNA expression in mice as a response to SE was analyzed, which was different compared to rats. Functional changes of Syt10 KO mice in the hippocampus were studied. Thereby, alterations in the progenitor cell proliferation following SE in Syt10 KO mice were demonstrated.

6.1 Functional characterization of the activity-regulated Syt10 promoter

Under basal conditions, high levels of Syt10 mRNA expression were only detected in the olfactory bulb (OB) and in the suprachiasmatic nucleus (SCN) (Husse et al., 2011; Mittelstaedt et al., 2009). A transient and local increase of Syt10 was reported upon SE (Babity et al., 1997), indicating that Syt10 is under tight spatial and temporal control. In recent years, studies have identified the transcriptional machinery that promotes control of activity-dependent genes (reviewed by Lyons & West, 2011; van Loo et al., 2012). To gain insights into upstream regulatory mechanisms mediating the activity-induced expression of Syt10, potential transcriptional regulatory elements in the Syt10 gene were examined.

6.1.1 Identification and functional characterization of the Syt10 promoter

The bioinformatic analysis of the Syt10 gene carried out in the present study revealed characteristics commonly associated with a core promoter as well as evolutionary conserved potential regulatory elements. By using Luciferase assays these regions were examined in different primary neurons and a neuronal cell line (NG108-15) regarding their promoter activity. Thereby, activating and inhibitory elements within the Syt10 gene were identified, which are summarized in figure 6.1.
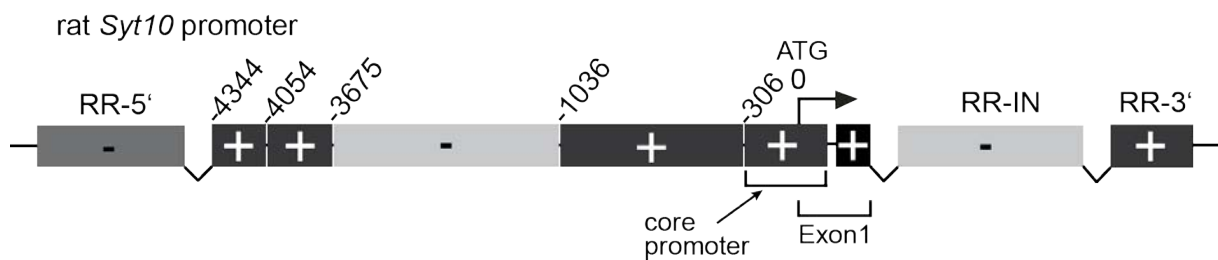
Figure 6.1 Graphic summary of activating and repressing regions of the Syt10 promoter. Measurements of basal luciferase activity revealed putative activating (+) or repressing (-) regulatory elements in the Syt10 gene.

Two interesting regulatory regions were uncovered. Firstly, the evolutionary conserved part of the first Syt10 intron (RR-IN) exhibited a lower basal promoter activity than the core promoter. Therefore, this region represents a strongly inhibiting promoter control motif. Intriguingly, the corresponding human intron region was predicted as a heterochromatin-withstanding region (UCSC), referring to a part of the Syt10 gene that has low transcriptional activity. The second region comprising 1036 bp to 306 bp upstream of the start codon strongly enhanced the activity of the core promoter only in hippocampal neurons. This part of the Syt10 gene might represent a region that could mediate the hippocampus-specific induction of Syt10 following SE (Babity et al., 1997; this thesis). Cell-type specific promoters are well established and are used as tools to generate transgenic animals and for gene therapy (reviewed by Boulaire et al., 2009 and Walther & Stein, 1996). The identification of a Syt10 promoter fragment that exhibits hippocampus specific activity could be used to express target cDNAs only in this brain region e.g. by viral gene transfer.

As reported for the well characterized promoter of the *Arc/Arg3.1* gene, regulatory elements can reside far away from the core promoter (Kawashima et al., 2009; Pintchovski et al., 2009). Therefore, the bioinformatic analysis was extended to regions that were 50 kb up- und 70 kb downstream of the start ATG and conserved

putative regulatory regions (RR-5' and RR-3') were identified. However, these regions did not display a significant increase in promoter activity compared to the core promoter indicating that they do not contain elements that positively affect the basal Syt10 promoter activity. In addition, highly conserved regions (RR1-3) were subcloned and analyzed residing in the fragment 4713 bp upstream of the start ATG and were combined with the core promoter. Interestingly, together with the core promoter, these regions revealed a higher promoter activity than the full -4713 bp fragment. This finding suggests that there might be a repressing region located between 1036 bp and 3675 bp upstream of the start ATG. However, only RR-2 exhibited a higher promoter activity specifically in hippocampal neurons.

Taken together, these results indicate that in accordance with low basal expression levels of Syt10 large negative regulatory regions could be identified. Furthermore, these findings suggest that the identified positive regulatory elements can be activated by relevant stimuli.

6.1.2 Activity-regulated transcription factors mediating Syt10 gene expression

The promoters of the activity-regulated genes *BDNF* and *Arc/Arg3.1* have been extensively studied and transcription factors regulating their activity have been identified (Kawashima et al., 2009; Kim et al., 2010; Lyons et al., 2012; Pintchovski et al., 2009; Pruunsild et al., 2011). However, to date the promoter of Syt10 and its regulatory mechanisms have not been resolved yet.

Using different algorithms, several binding sites for transcription factors were predicted in the Syt10 promoter region that were also important for the activity-dependent regulation of the BDNF and/or the Arc promoter. Luciferase assays in NG108 cells showed that some of these transcription factors did not induce the Syt10 promoter (MEF2A, 2C) whereas others (AP1-factors, USF1/2 and NPAS4) strongly increased the promoter activity of Syt10. Functionally relevant transcription factors should also affect endogenous Syt10 expression levels. To test, which of the transcription factors that have putative binding sites, also impact Syt10 expression *in vivo*, rat hippocampal neurons were transfected with transcription factors and Syt10 expression levels were analyzed using quantitative real-time PCR. NPAS4, USF2 and cFos augmented endogenous Syt10 expression levels. Further analysis revealed that USF2 and cFos were not sufficient to activate the characterized Syt10 promoter fragments in luciferase measurements of primary hippocampal neurons. This

discrepancy suggests that the promoter fragments might not contain the respective functional binding sites for USF2 and cFos. Whereas in contrast, NPAS4 was the only transcription factor that increased both, Syt10 endogenous expression and Syt10 promoter activity as examined by luciferase assays in NG108-15 cells and neurons. Although the observed level of up-regulation of Syt10 mRNA expression after NPAS4 transfection in neurons is relatively weak (approx. 2-fold), it has to be taken into account that the transfection efficiency of primary neurons is not very high (less than 30 %). Therefore, the actual increase in transfected neurons is higher. As NPAS4 was up-regulated in the hippocampus following PTZ-induced seizure activity (Flood et al., 2004), after kainate (Ooe et al., 2009a) and pilocarpine injection (this thesis), it is a putative factor to induce Syt10 expression in response to SE.

As NPAS4 is upstream of multiple transcription factors (Lin et al., 2008) it remained unclear if the observed effect on the Syt10 promoter is direct or indirect. Therefore, as a first step, the responsive NPAS4 binding sites were identified. Due to the finding that the Syt10 promoter contains several potential sites in the longest fragment, deletion reporter plasmids were generated. Deletion constructs carrying binding sites 1, 2 and 3 (constructs I, II, -306) led to a strong increase of the Syt10 promoter that was not found in the region between the conserved elements (constructs III, IV and -1036), whereas the two longest fragments (constructs V and -4713) were strongly activated by NPAS4. Thus, unknown factors in the region between the conserved elements repress the activation by NPAS4 binding to the core promoter. However, if the binding sites in construct V and -4713 are also present, the repression is overruled resulting in a stronger activation.

Taken together, these results indicate that for the activity of the Syt10 promoter, NPAS4 binding sites 1, 2 and 5 and/or 6, 7 are most important. To test, whether this effect was due to direct binding of NPAS4 to the Syt10 promoter, an *in vitro* binding assay could be carried out.

6.1.3 The Syt10 promoter is controlled by heterodimerization of bHLH-transcription factors

As a bHLH-PAS transcription factor, NPAS4 might form homo- as well as heterodimers with other members belonging to this transcription factor family (Hirose et al., 1996; Huang et al., 1993; Huang et al., 1995; Ooe et al., 2009a, b; Ooe et al.,

2004; Pongratz et al., 1998). An interesting candidate for the formation of a functional heterodimer with NPAS4 is the transcription factor Arnt2.

Luciferase assays of rat hippocampal neurons transfected with Arnt2 alone did not result in a stimulation of the Syt10 promoter. Moreover, co-transfection of Arnt2 with NPAS4 rather caused a decrease than a positive synergistic effect on Syt10 promoter activity. It could be further investigated if Arnt2 acts as a heterodimer with NPAS4 to reverse the activating function of NPAS4. Thereby, this heterodimer could be involved in the regulation of Syt10 gene expression.

The mammalian homologue of the Drosophila clock gene and bHLH-PAS transcription factor Period1 (Per1) is expressed in the SCN, where Syt10 is expressed as well at high levels (Tei et al., 1997; Husse et al., 2011). Given that epileptic seizures induce Per1 and Syt10 expression levels, respectively, (Babity et al., 1997; Eun et al., 2011), it was hypothesized that this transcription factor has an influence on Syt10 promoter activity alone or as a heterodimer with NPAS4.

Luciferase assays of rat hippocampal neurons transfected with Per1 revealed that the Syt10 promoter was indeed activated by Per1. Furthermore, co-transfection of NPAS4 and Per1 resulted in a synergistic effect.

Besides in the SCN, Per1 is also expressed in the hippocampus. In addition, multiple reports about Per1 rhythmicity in the hippocampus stated that it is expressed in an oscillatory manner (Balsalobre et al., 2000; Gilhooley et al., 2011; Golini et al., 2012; Jilg et al., 2010; Reick et al., 2001). Taken together, these results suggest a role for NPAS4 and Per1 in regulating Syt10 transcription in the hippocampus. Given that both transcription factors were altered in response to seizures and that Per1 is expressed in a circadian rhythm in both, hippocampus and SCN, there is evidence that these transcription factors play a role in induced Syt10 expression, conceivably in an oscillatory manner.

6.2 Stimulus-induced activation of Syt10

Injection of kainic acid (KA) into rats as well as of pilocarpine into mice revealed an increase of Syt10 mRNA *in vivo* (Babity et al., 1997; present study). However, SE activates multiple downstream signaling cascades leading to altered neuronal activity and to an induction of multiple immune cascades. To study the consequences of synaptic activity on transcription, it is well established to induce membrane depolarization *in vitro* (Kim et al., 2010; Pruunsild et al., 2011). Furthermore,

treatment of organotypic slice cultures with KA was widely used to examine epileptiform activity in the hippocampus (Bausch & McNamara, 2004; Reid et al., 2008; Routbort et al., 1999; Tinnes et al., 2011). Hence, different stimulation protocols were applied *in vitro* to study the effect of altered activity in neurons on Syt10 expression.

6.2.1 Membrane depolarization increases Syt10 promoter activity

Development of a hyperexcitable network is one of the hallmarks of epilepsy and recent studies examined changes in gene expression following SE in genome-wide analyses (Hendriksen et al., 2001; Becker et al., 2003; Gorter et al., 2006; Aronica and Gorter, 2007; Laurén et al., 2010; Okamoto et al., 2010). To screen for factors that might be important for the regulation of the Syt10 gene and its protein function, this hyperexcitable state was mimicked with strong membrane depolarization.

Indeed, both Syt10 mRNA and protein expression were induced by stimulation with potassium chloride (KCl). Furthermore, the identical stimulation protocol also increased the activity of the promoter fragment -4713 indicating that this region may be centrally relevant for the endogenous Syt10 up-regulation following KCl treatment. NPAS4, which activated the Syt10 promoter under basal conditions, has been reported to be induced by synaptic activity (Lin et al., 2008; Kawashima et al., 2009; Pruunsild et al., 2011; Ramamoorthi et al., 2011). Luciferase experiments showed that stimulation of neurons co-transfected with promoter fragments -306, -1036, -4713 and NPAS4 led to a strong increase in promoter activation compared to both, NPAS4 and KCl treatment alone. Interestingly, following membrane depolarization, an increase of mRNA levels of NPAS4 and Per1 could be observed as well (Data not shown).

Taken together, these experiments suggest that the transcription factors NPAS4 and Per1 are involved in mediating the up-regulation of Syt10 expression levels following synaptic activity. Previous studies reported that Per1 and NPAS4 mRNA expression is increased following strong synaptic activity further supporting this hypothesis (Eun et al., 2011; Rodríguez-Tornos et al., 2013). Figure 6.2 summarizes the Syt10 promoter regulation by NPAS4, Per1 and by membrane depolarization.
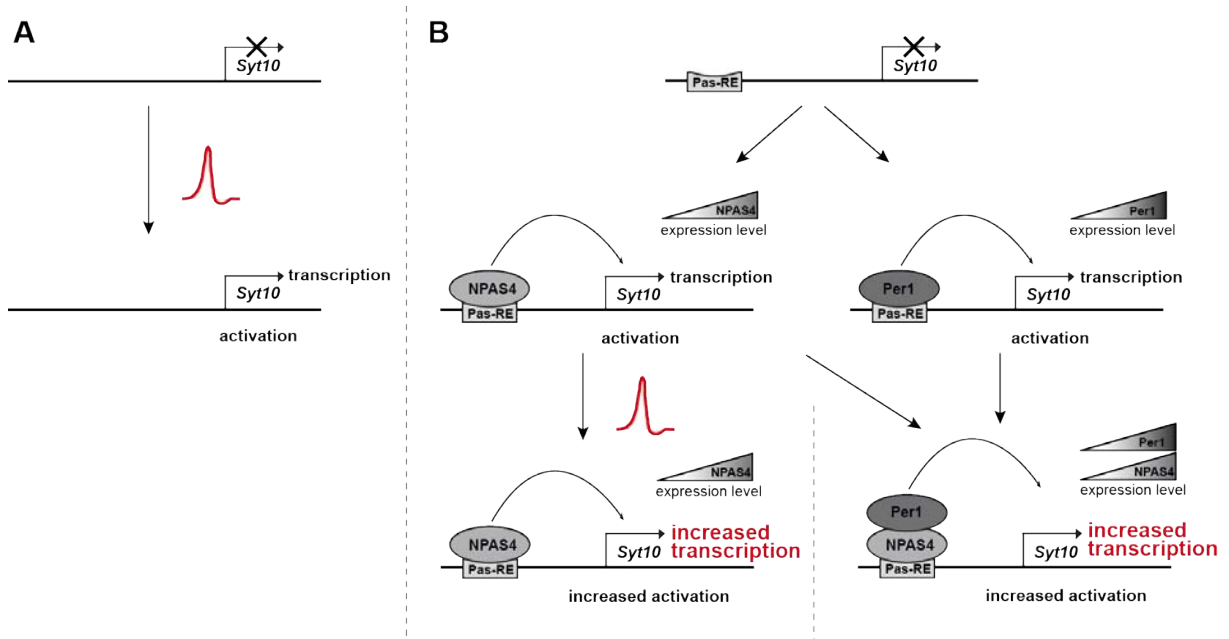
Figure 6.2 Model of Syt10 promoter regulation by depolarization, NPAS4 and Per1. (A) Membrane depolarization results in the activation of the Syt10 promoter. (B) Increases in NPAS4 or Per1 levels alone activate the Syt10 promoter as well. NPAS4 activation of the Syt10 promoter can be further influenced by membrane depolarization or subsequent addition of Per1, both resulting in a stronger activity of the Syt10 promoter.

6.2.2 Activation of kainate receptors increases endogenous Syt10 expression

Membrane depolarization is a more general stimulation to mimic synaptic activity (Kawashima et al., 2009; Kim et al., 2010; Pruunsild et al., 2011) but does not match all characteristics of changes following epileptic seizures. KA is a neurotoxic stimulus used to generate epileptic seizures leading to epilepsy-specific changes, like mossy-fiber sprouting *in vivo* and *in vitro* (Bausch & McNamara, 2004; Ben-Ari et al., 1979; Routbort et al., 1999; Simantov et al., 1999). Administration of KA to hippocampal neurons and subsequent analysis of mRNA expression revealed that endogenous Syt10 and IGF1 levels were significantly increased by identical conditions (chapter 5.2.3). The similarity in the time course of augmented mRNA expression argues in favor of a correlation of the two proteins as described previously (Cao et al., 2011, 2013). In contrast, NPAS4 expression was only increased by a 24 h stimulation at 25 µM and 50 µM KA but not by the 15 min stimulation at 150 µM KA that increased IGF1 and Syt10 expression. This result was in line with the finding that NPAS4 is an immediate early gene, which is up-regulated rapidly, already 5 minutes after synaptic activity, and transiently, returning to basal levels one hour after synaptic activity (Ramamoorthi et al., 2011). Following pentylenetetrazol (PTZ) injection an

augmented NPAS4 expression was reported as early as one hour after generalized seizures (Flood et al., 2004).

IGF1 is known for its role in neuroprotection in health and disease (Cheng et al., 2001; Guan et al., 1996; Miltiadous et al., 2010; Selvamani et al., 2012; Wine et al., 2009) and was up-regulated in response to KA, in parallel to Syt10 (this thesis).

To probe if there was a correlation between IGF1 and Syt10, it was examined whether Syt10 knockout (KO) neurons are more vulnerable to KA-induced neurotoxic effects. To address this question, Syt10 KO and WT neurons were subjected to two kainate stimulation protocols that induced Syt10 and IGF1 mRNA expression levels. Loss of Syt10 significantly decreased the number of surviving neurons but not of astrocytes after a 24 h stimulation with 25 µM KA.

This result indicates that Syt10 *in vitro* might play a role in neuroprotection. Interestingly, the survival rate of WT neurons was only higher compared to KO neurons following the KA stimulation protocol that up-regulated both, IGF1 and NPAS4 in parallel to Syt10. Hence, following KA stimulation NPAS4 might induce Syt10 expression and together with IGF1 these proteins might account for neuronal cell survival.

In line with this hypothesis, a neuroprotective function for NPAS4 has been reported. Overexpression of NPAS4 was described to inhibit cell death *in vitro* induced by different apoptosis protocols. RNAi-mediated knock-down of NPAS4 reversed the neuroprotective effect in hippocampal neurons. Intriguingly, overexpression of NPAS4 *in vivo* via viral gene transfer provides neuroprotection in response to KA-induced cell death assessed three days following SE (Zhang et al., 2009a).

Furthermore, IGF1 was reported to be essential for hippocampal cell survival, as IGF1 null mice exhibit a higher rate of dentate granule cell death (Cheng et al., 2001). Moreover, the damage caused by administration of intrahippocampal injection of KA such as astrogliosis, microgliosis and increased hippocampal neurogenesis as well as seizure severity can be decreased by simultaneous injection of IGF1 into mice and rats (Miltiadous et al., 2010, 2011).

Taken together, a neuroprotective role for Syt10 and IGF1 mediated by NPAS4 induction appeared to be plausible. However, the fact that stimulation with 150 µM KA for 30 min and fixation 8 h later did not exhibit significant changes between the genotypes might be due to the high KA concentration. This may lead to a dramatic cell death that could not be attenuated by endogenous Syt10 or IGF1 levels.

By using Enzyme-linked immunosorbent assay (ELISA) it could be clarified whether the IGF1-release is different between Syt10 KO and WT hippocampal neurons after KA stimulation. So far, this difference has only been reported for native OB neurons (Cao et al., 2011, 2013).

6.3 Characterization of the subcellular localization of Syt10

Members of the Syt protein family are key players in the regulation of different fusion processes. Some members have been identified to function as calcium sensors for synaptic vesicle and dense core vesicle release (Geppert et al., 1994; Nagy et al., 2006; Stevens & Sullivan, 2003; Sørensen et al., 2003; Voets et al., 2001; Xu et al., 2007). Nevertheless, the subcellular distribution of Syt isoforms is highly diverse and has not been identified for all isoforms to date (Cao et al., 2011; Dean et al., 2012a; Saegusa et al., 2002; reviewed by Südhof, 2002). Recently, Syt10 was reported to be localized to IGF1-containing vesicles in OB neurons. However, the subcellular localization of Syt10 in other neuronal subtypes remained unknown. Moreover, to understand its function it is essential to know whether Syt10 is localized on specific organelles. To shed further light on this matter, a detailed analysis of the subcellular distribution of Syt10 was carried in PC12 cells and hippocampal and cortical neurons.

6.3.1 Subcellular localization of Syt10 in PC12 cells and neurons

PC12 cells are often used to study components of the release machinery due to their vesicular content, comprising synaptic-like microvesicles (SLMVs) and large dense core vesicles (LDCVs). In the present study, to examine the localization of Syt10, this cell line and primary hippocampal and cortical neurons were used.

A punctate expression pattern of overexpressed Syt10-GFP was detected in PC12 cells as well as in primary hippocampal and cortical neurons. Immunolabeling of primary neurons overexpressed with Syt10-GFP revealed that Syt10 was present on dendrites as analyzed with an antibody against MAP2, a microtubule associated protein. However, a localization of Syt10 to synaptic vesicles, as examined by Syt1 and synapsin co-labeling and by a staining against the vesicular GABA-transporter (vGAT), could not be observed.

The distribution pattern of Syt10 argues for a vesicular localization, which was postulated in PC12 cells stably expressing Syt10-GFP (Saegusa et al., 2002). The

authors proposed that Syt10 is localized to small vesicles and not to LDCVs. Interestingly, analysis of Syt10 dynamics upon depolarization using Syt10-pHluorin revealed that Syt10 is not located on synaptic vesicles (SVs) (Dean et al., 2012a) and overexpression of Syt10 in OB neurons suggested Syt10 to be localized on extremely large IGF1 containing vesicles (Cao et al., 2011; Cao et al., 2013). Taken together, these results suggest that Syt10 is not present on SVs in primary neurons but found on other vesicle types. To exclude that the punctate expression pattern was not due to an overexpression artifact, time lapse imaging experiments with Syt10 fused to a photoconvertable fluorescent tag changing its fluorescence upon photoactivation should be performed. Thereby, immobile aggregates could be distinguished from vesicular structures carrying Syt10.

6.3.2 Syt10 is not a resident Golgi protein

Syt10 was present mainly in the soma and to a lesser extend in neurites. Moreover, Syt10 exhibited a punctate distribution (this thesis) and other Syt isoforms, Syt4, 7 and 9, are located to lysosomes or different endosomal compartments, the Golgi Apparatus and secretory granules (Ahras et al., 2006; Flannery et al., 2010; Haberman et al., 2007; Ibata et al., 2000; Monterrat et al., 2007). Therefore, the aim was to further identify the subcellular localization of Syt10 and thereby potential trafficking steps that require Syt10.

In the present study Syt10-mCherry was observed to be co-localized with a fluorescently tagged Transferrin Receptor (TfR) protein, a well established marker for early endosomes (reviewed by Mayle et al., 2012), mainly in the soma of neurons and not in PC12 cells. Furthermore, Brefeldin A (BFA) was used to study the trafficking of proteins from the Endoplasmatic Reticulum (ER) to the Golgi Apparatus. This drug was described to result in disassembly of the Golgi and to the formation of two intermixing compartments (merged ER-Golgi and fused TGN-early endosomes) (Doms et al., 1989; Fujiwara et al., 1988; Lippincott-Schwartz et al., 1989; Hunziker et al., 1991; Lippincott-Schwartz et al., 1991; Wood et al., 1991), thereby inhibiting transport between the two combined compartments (Lippincott-Schwartz et al., 1991). Following treatment of both cell types with BFA, labeling of the Golgi marker protein 130 (GM130) indeed showed a collapse of the Golgi stacks but not a redistribution of Syt10 protein (chapter 5.4.4). This result indicates that Syt10 is not a resident Golgi protein.

Interpretation of these results becomes even more complicated by the fact that neurons are polarized cells with complex transport pathways, which are distinct in dendrites (TfR-positive endosomes, positive for the early endosome marker (EEA1) and BFA-sensitive) and in axons (TfR-negative endosomes, EEA1-negative and BFA-insensitive) (Mundigl et al., 1993).

Taken together, the observed results may indicate that even though Syt10 was not identified to be a local Golgi protein, it may still be localized to other parts of the ER-Golgi trafficking pathway, i.e. internal transport vesicles. If Syt10 were not glycosylated it would not pass through the Golgi Apparatus on its way to these endosomal structures. To further analyze Syt10 and its putative localization on endosomes, a detailed analysis of all compartments without the use of overexpressed proteins e.g. labeling of early endosomes with Rab5 or EEA1, of recycling endosomes with Rab8 or 11 or of late endosomes with Rab7 or Syt7 will be necessary.

6.3.3 Syt10 partially co-localizes with NPY- or IGF1-containing vesicles in hippocampal or cortical neurons

Recently, it was reported that in OB neurons overexpressed Syt10 and IGF1 co-localize on very large vesicular structures (Cao et al., 2011). Here, it was examined on which types of vesicles Syt10 was localized in cortical or hippocampal neurons. Since Syt10-GFP was expressed in a punctate manner but was not localized on SVs, it was analyzed whether Syt10 is localized to secretory peptide-containing vesicles as marked by overexpression of NPY-GFP. In dendrites and the soma of neurons, only partial overlap of either Syt10-mRFP with NPY-GFP or of untagged Syt10 with NPY-GFP could be detected. This result suggests that Syt10 is present in a subset of secretory peptide vesicles.

Furthermore, in cortical neurons Syt10-GFP and IGF1-mRFP did not exhibit a high degree of co-localization as it was reported for OB neurons (Cao et al., 2011, 2013). To exclude, that a large tag did not affect the correct localization of overexpressed proteins, untagged Syt10 co-transfected with IGF1-HA was analyzed. However, labeling with either of the Syt10 antibodies also revealed little overlap of the Syt10 and IGF1 signals in hippocampal neurons.

In OB neurons, Syt10 serves as a calcium sensor for Ca^{2+}-dependent exocytosis of IGF1. However, it remains still uncertain whether Syt10, after activity-dependent up-

regulation, mediates release of IGF1 in hippocampal or cortical neurons as well. There is evidence that Syt10 function might differ between hippocampal neurons and olfactory bulb neurons as pHluorin-tagged Syt10 was found to mediate activity-dependent exocytosis in olfactory bulb neurons (Cao et al., 2011, 2013) but not in hippocampal neurons (Dean et al., 2012a). Hence, maybe all components of Syt10 vesicles are only present after SE, e.g. following up-regulation of IGF1. Figure 6.3 summarizes the subcellular localization of Syt10 in hippocampal neurons examined so far in the present study.
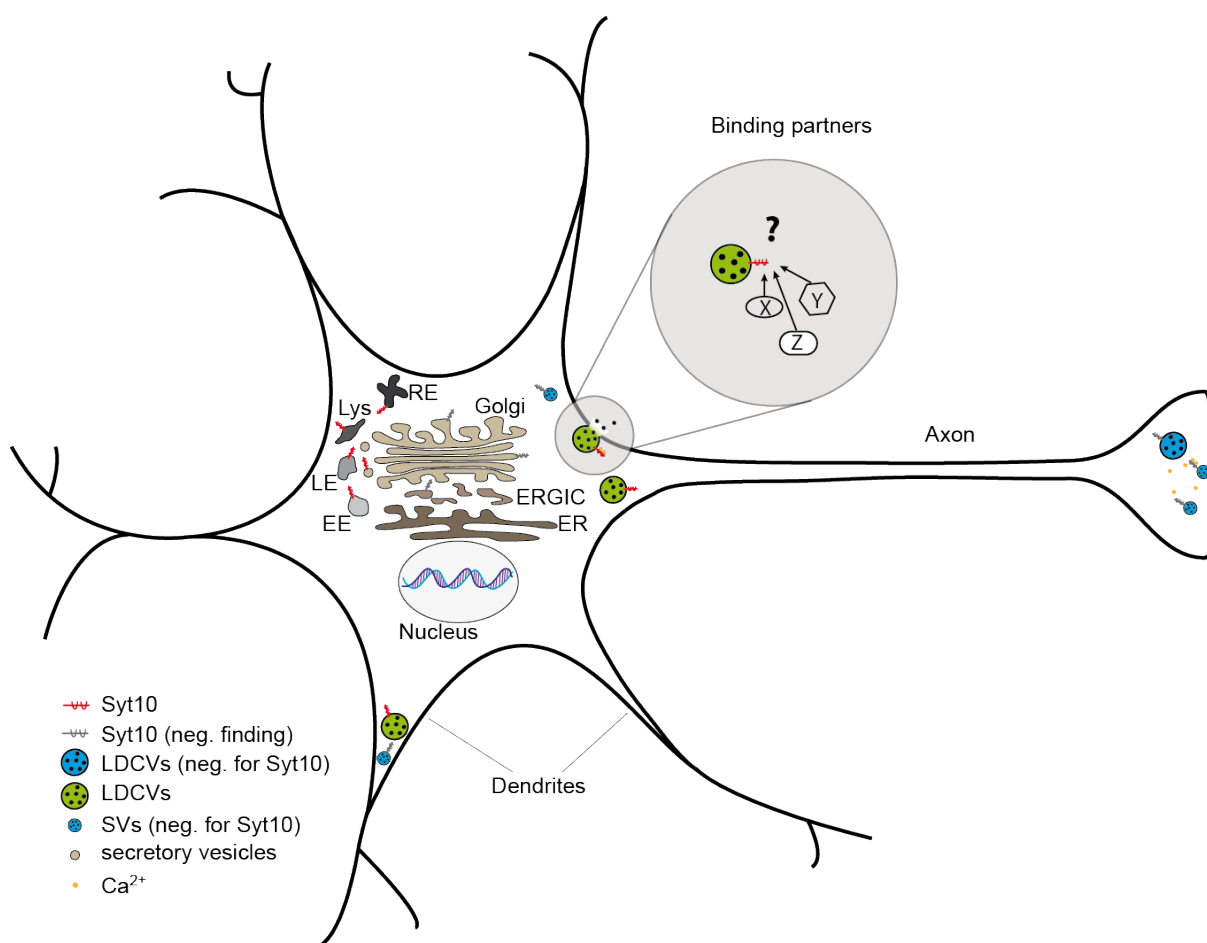
Figure 6.3 Cartoon depicting the subcellular localization of Syt10 in hippocampal neurons. The present study showed Syt10 to be absent from SVs (small, blue vesicles) or LDCVs (large, blue vesicles) in the presynapse. Syt10 was furthermore not identified to be a resident Golgi or ERGIC protein (indicated by grey color). Whether Syt10 can be enriched on endosomes or on neuropeptide containing vesicles (e.g. IGF1) in the soma or in dendrites remains an open question (blue vesicles or red depicted Syt10). Therefore, to unravel the subcellular localization of Syt10 the identification of its binding partners (indicated by X, Y, Z) would be crucial. EE: Early endosome; ER: Endoplasmatic Reticulum; LE: Late Endosome; Lys: Lysosome; RE: Recycling Endosome.

6.3.4 Syt3, 5, 6 and 10 display overlapping and diverging localizations

Due to the high sequence similarity of the Syt subgroup comprising Syts 3, 5, 6 and 10 and their ability to form heterodimers it was hypothesized that they might be

limited to the same subcellular compartments. Therefore, their localization was analyzed after overexpression alone and after co-expression with Syt10 to examine whether they co-localize with Syt10 or if a change of their distribution following co-transfection can be observed. In the present study, Syt3-GFP was observed to be enriched at the plasma membrane of PC12 cells. However, the results of co-expressed Syt3-GFP and Syt10-GFP differed between PC12 cells and neurons. An overlapping Syt3-GFP localization with Syt10-GFP was only found in neurons but not in PC12 cells. Similar to the results observed in the present study, a plasma membrane localization of overexpressed Syt3 in PC12 cells and of endogenous Syt3 in ß-pancreatic cells by immunocytochemistry has been described (Gut et al., 2001; Saegusa et al., 2002).

In line with this thesis it was reported in an earlier study that the localization of Syt3 differs between cell types. It was described to be localized to the plasma membrane in pancreatic ß-cells and neurons but exhibits a granular expression in another insulin-secreting cell line and in somatostatin-secreting cells (Gut et al., 2001). For the results obtained in this thesis it may indicate that even though Syt3 and Syt10 do not co-localize in PC12 cells, they may be found on the same subcellular compartment in neurons.

In the present study, Syt5-GFP fusion protein was found both in the cytosol of PC12 cells and in the soma and dendrites of neurons, with a punctate expression pattern. Whereas high degree of overlapping Syt5-GFP with Syt10-mCherry was observed in the cytosol of PC12 cells co-localization was restricted to only a small area of the soma of neurons. In an earlier study Syt5 was reported to be localized to LDCVs in PC12 cells (Saegusa et al., 2002). Syt10-mCherry was found to be co-localized with NPY-GFP in the soma of neurons (present study) and Syt10 was identified in OB neurons on IGF1 containing vesicles (Cao et al., 2011). Hence, even though Saegusa suggested that Syt10 is present on SLMVs in PC12 cells (Saegusa et al., 2002), it is more likely that in neurons Syt10 might be distributed with Syt5 to LDCVs. Syt6-GFP was observed in the cytosol of PC12 cells and was strongly distributed throughout the soma and dendrites of neurons in a punctate expression pattern. Interestingly, following co-expression with Syt6-mCherry at a ratio of 4:1, the distribution of Syt10-GFP was changed to a more punctate expression pattern observed not only in the soma but also in the branches of neurons. The co-localization of Syt10-GFP and Syt6-mCherry is most likely mediated by

heterodimerization through the conserved cysteine residues and interestingly, Syt10 and Syt6 are both more abundant in response to SE (personal communication T. Mittelstaedt). Consequences of the presence of two Syt isoforms on the same vesicular structure could be an alteration of their functional properties, as has been controversially discussed for Syt1 and Syt9 (Fukuda et al., 2002; Lynch & Martin, 2007). Though in OB neurons, a redundant function of Syt10 with Syts 3, 5 and 6 was not found (Cao et al., 2011). Given that a change in the functional properties of these Syts also depends on the quantity of each variant in the cell, a functional redundancy as a consequence of heterodimerization appears to be plausible.

6.3.5 Characterization of Syt10 N-terminal targeting signals

Localization of a given protein is mostly defined by targeting signal sequences spanning up to 30 amino acids in the N-terminus or by posttranslational modifications, i.e. N- and O-glycosylation or palmitoylation (Han et al., 2004; Flannery et al., 2010; Kwon and Chapman, 2012). To unravel, which targeting signal determines the subcellular localization of Syt10, two approaches were pursued to address this question. Firstly, chimeric proteins were overexpressed in neurons to unravel whether a targeting signal in the N-terminus determines the localization of Syt10. Secondly, as cysteine-containing motifs are the main targets for palmitoylation (Jang et al., 2009; Prescott et al., 2009) and for dimerization (Han et al., 2004) N-terminal cysteines of Syt10 were mutated into alanines to examine if one of these processes is indispensable for the targeting of Syt10.

Chimeric proteins overexpressed in neurons contained the Syt3, 5 or 6 N-terminus and the TMD, the linker, the C_2A and C_2B domains and the C-terminus of Syt10 fused to a GFP-tag. All chimeric proteins were more diffusely distributed in the soma and along the branches than the respective WT variant. Consequently, the localization of none of the chimeric proteins was similar to its full-length variant indicating that the N-termini of the other Syts were not sufficient to switch the Syt-TMD-C_2A-C_2B targeting. However, also the distribution compared to the Syt10 full-length was altered demonstrating that the C-terminus (linker, C_2A, C_2B) was not sufficient for the localization of Syt10.

N-terminal cysteines were mutated into alanines and the distribution of the mutated Syt10-GFP protein was examined by overexpression in neurons. The results suggest that cysteine residues were crucial for the correct trafficking and stability of Syt10-

GFP, since in neurons transfected with mutated constructs large aggregates in the soma and a reduction of Syt10-GFP signal in the branches were observed.

For the most studied isoform of the Syt family, Syt1, it was suggested that the N-terminus contains the targeting signal directing Syt1 to SVs (Han et al., 2004), even though the targeting mechanism has not been resolved unequivocally. It was reported that N- and O-glycosylation are both essential for sorting Syt1 to secretory vesicles (Atiya-Nasagi et al., 2005; Han et al., 2004; Kanno & Fukuda, 2008), although a recent publication suggested that glycosylation is dispensable for the targeting of Syt1 but that a combination of the Syt1 N-terminus and the C2 domains mediate Syt1 targeting (Kwon & Chapman, 2012). In line with this finding it may be hypothesized that there is more than one protein domain needed for the correct localization of the Syt10 protein.

Besides the N-terminus, the linker region of all Syt isoforms is highly variable. Furthermore, this region comprises amino acids that are either palmitoylated or glycosylated by fatty acylation and thereby can play a role in oligomerization or in targeting of Syts (Flannery et al., 2010; Fukuda et al., 2001a; Han et al., 2004; Heindel et al., 2003; Veit et al., 1996). Considering the high variability and the fact that the linker region, together with the C-terminus, is essential for the Golgi localization of Syt4 (Fukuda et al., 2001a), it may be hypothesized that this region together with another Syt10 protein domain might determine the targeting of Syts 3, 5, 6 or 10. Interestingly, Fukuda et al., 2001, suggest that not only the disulfide-bonding contributes to oligomerization of Syt10 but also three cysteine residues between the transmembrane domain and the linker region do (Fukuda et al., 2001b). Correspondingly, two palmitoylation motifs were predicted for the linker region of Syt10.

Recently, it was demonstrated that targeting of Syt7 to lysosomes is accomplished by the formation of a palmitoylation-dependent complex with a member of the transmembrane 4 superfamily, CD63. Co-expressed Syt7-YFP and CFP-CD63 carrying a mutation in the lysosomal targeting motif were not trafficked to lysosomes but accumulated in the plasma membrane. Therefore, identification of binding partners of Syt10 or systematic mutation analyses of Syt protein domains would be required to define the regions responsible for Syt10 targeting or the potential role of palmitoylation.

Besides mediating the targeting of Syt10 by posttranslational modification, the exchange of N-terminal cysteines to alanines may impair the ability of Syt10 to homodimerize. This in turn could directly affect the stability of the protein as this could lead to a misfolded tertiary protein structure. As a consequence, misfolded Syt10 might not be properly processed in the Golgi Apparatus, leading to protein aggregates in this compartment. To examine whether Syt10 protein aggregates accumulate at the Golgi Apparatus, neurons transfected with the mutated constructs could be labeled with GM130. Moreover, analyzing movement of vesicles by live imaging (mentioned in chapter 6.1.1) of wildtype (WT) Syt10 and mutated Syt10 might unravel whether the protein aggregates display an altered stability or turnover of Syt10 protein.

6.4   Spatiotemporal and functional activation of Syt10 following SE

Strong depolarization of primary hippocampal neurons elicited either by KCl or kainate resulted in a strong increase of endogenous Syt10, IGF1 and NPAS4. SE represents a particular strong stimulation *in vivo*. To relate the *in vitro* findings to an *in vivo* situation the spatiotemporal expression patterns of Syt10, IGF1 and NPAS4 were studied in the mouse hippocampus after pilocarpine-induced SE.

6.4.1 Syt10, IGF1 and NPAS4 exhibit distinct spatiotemporal expression patterns after SE

In rats, Syt10 mRNA expression in the piriform cortex and hippocampus is rapidly and transiently induced three and six hours, respectively, following KA-induced SE (Babity et al., 1997). To date, the respective spatiotemporal expression profile in mice has not been examined yet. As a basis for functional studies in mice, C57/Bl6 mice were injected with pilocarpine, sacrificed at different time points and the Syt10, IGF1 and NPAS4 mRNA expression was analyzed via quantitative real-time PCR. Different time points were chosen to reflect distinct stages of epileptogenesis: The acute phase (2 h, 6 h, 12 h), the latency stage (24 h, 36 h, 72 h) and the chronic epileptic phase (28 d). Surprisingly, Syt10 gene expression was different in mice as compared to rats (Babity et al., 1997). In the dentate gyrus Syt10 expression was either unchanged or lower, whereas in the CA3 and CA1 region, Syt10 was more abundant between 12 and 36 h after SE. The strongest induction, however, was

observed in CA1 36 h after SE (Figure 6.4), a 30 h delay compared to the peak induction in rats. In summary, in rats an augmentation in the acute phase (6 h after SE) was observed (Babity et al., 1997) whereas in mice the regions differ and the increase in CA1 and CA3 was shifted towards the latent phase compared to rats (present study). This altered spatiotemporal expression pattern after pilocarpine-induced SE was more likely due to the different species than due to the diverse epilepsy model used, because in unpublished data from pilocarpine-induced SE, rats exhibited a comparable time course of Syt10 mRNA increase to Babity et al. 1997 (Babity et al., 1997; personal communication T. Mittelstaedt).

In OB neurons, IGF1 was suggested to be the cargo of Syt10 vesicles (Cao et al., 2011). Moreover, IGF1 and Syt10 mRNA expression in the native brain exhibit a strikingly similar distribution mainly in the OB (Mittelstaedt et al., 2009; Rotwein et al., 1988). It was therefore hypothesized that if Syt10 would be localized to IGF1 containing vesicles also in the hippocampus, a parallel time course of IGF1 and Syt10 expression could be expected. IGF1 mRNA expression was elevated in all hippocampal subregions at nearly all time points. The expression patterns of IGF1 and Syt10 in the CA3 and CA1 region did not show an exact parallelism, but peak induction of IGF1 seemed to be shifted 24 h later compared to Syt10 (Figure 6.4). Recent reports already showed an up-regulation of IGF1 in mice 2 d and in rats 3 and 7 d after SE, as well as in the chronic phase of pilocarpine-induced SE (Choi et al., 2008; Okamoto et al., 2010). Taken together, the shifted peak induction of IGF1 expression following SE compared to Syt10 could indicate that Syt10 vesicles contain a different cargo than IGF1.

In contrast, NPAS4 mRNA expression was rapidly and strongly stimulated already 2 h after SE (Figure 6.4). This is consistent with previous reports, which described an increase of NPAS4 mRNA 1 h following PTZ-induced seizures (Flood et al., 2004). Conceivably, augmented NPAS4 levels in response to SE mediate the up-regulation of Syt10 expression. The delayed peak of Syt10 gene expression argues in favor for this hypothesis. NPAS4 was reported to regulate activity-dependent inhibitory synapse development (Lin et al., 2008). To date, it remains unresolved, in which neuronal subpopulation Syt10 is expressed in the hippocampus. Given that the excitatory/inhibitory balance is disturbed in epilepsy, NPAS4 might contribute to this imbalance by increasing down-stream target gene expression only in a subpopulation thereby shifting the proportion towards for example more inhibitory synapses.

In the native brain, IGF1, Per1 and Syt10 expression is mainly enriched in the SCN (Bohannon et al., 1988; Sun et al., 1997; Husse et al., 2011), in which circadian rhythms are controlled endogenously (Reppert and Weaver, 1997). Moreover, Per1 has been reported to be expressed in an oscillatory manner in response to light exposure in the SCN (Albrecht et al., 1997; Hastings et al., 1999; Shearman et al., 1997; Shieh et al., 2005; Tei et al., 1997) and in the hippocampus (Reick et al., 2001; Jilg et al., 2010; Gilhooley et al., 2011). Interestingly, the present study suggests that NPAS4 and Per1 can induce Syt10 expression synergistically and it was found that NPAS4, which was up-regulated following SE, caused an increase of endogenous Syt10 levels.

An earlier study already reported an induction of Per1 mRNA and protein expression following seizures (Eun et al., 2011). Therefore, one possible consequence of the endogenous increase of Syt10, IGF1 and NPAS4 after SE may be a disruption in the circadian rhythm of vesicle depletion, and thereby an aggravation of seizures during a specific diurnal phase. Additionally, IGF1 mRNA expression was reported to be lowest during night (Kawai et al., 2010). Furthermore, parts of the synaptic vesicle cycle follow diurnal changes as well. At GABAergic synapses of the SCN, paired-pulse depression is obtained only at day, whereas vGlut sorting to the plasma membrane takes place with a circadian rhythmicity (Gompf and Allen, 2004; Darna et al., 2009).

Correspondingly, several different epilepsy models reported a diurnal tendency for the occurrence of seizures (Quigg 2000, Hellier & Dudek 1999, Tchekalarova 2010). Nevertheless, to clearly identify the role of Syt10 following SE and a putative alteration in seizure frequency or amplitude, a detailed analysis of seizure frequency and onset in the different phases of the day, was analyzed and compared between Syt10 WT and KO mice (personal communication J. Pitsch, data not shown). First analyses of EEG recordings from SE-experienced mice showed, different from WT mice, that the power of all frequency bands from KO mice were significantly increased ictally (during a seizure). This may well suggest that ablation of Syt10 leads to an aggravation of seizures. Furthermore, throughout the night, KO mice generated most seizures out of sleep as compared to WT animals (personal communication J. Pitsch, data not shown).

Taken together, one could hypothesize that under normal conditions, Per1 is expressed in the hippocampus with a circadian rhythm, which is not sufficient to drive

Syt10 oscillatory expression. Moreover, NPAS4 has not been reported to be expressed in an oscillatory manner. However, following SE, induction of Per1 could overrule the rhythmic expression and, together with NPAS4, activate Syt10. There is already evidence that the Per1 peak expression of kindled mice is shifted towards six hours earlier, which correlates with a shift in the sleep homeostasis (Yi et al., 2012). Earlier studies in a rat model of epilepsy reported that more seizures are generated out of an inactive state (Hellier & Dudek, 1999; Quigg et al., 1998), which would be contradictory to this hypothesis. However, there might be a difference in the occurrence of seizures and sleep rhythm between mice and rats and so far, a shift of the activity state following seizures was only examined in rats (Stewart and Leung, 2003). To understand the role of sleep homeostasis after SE and the role of Syt10 in this regard, analysis of sleep and awake cycles of control and SE-experienced mice would be necessary.
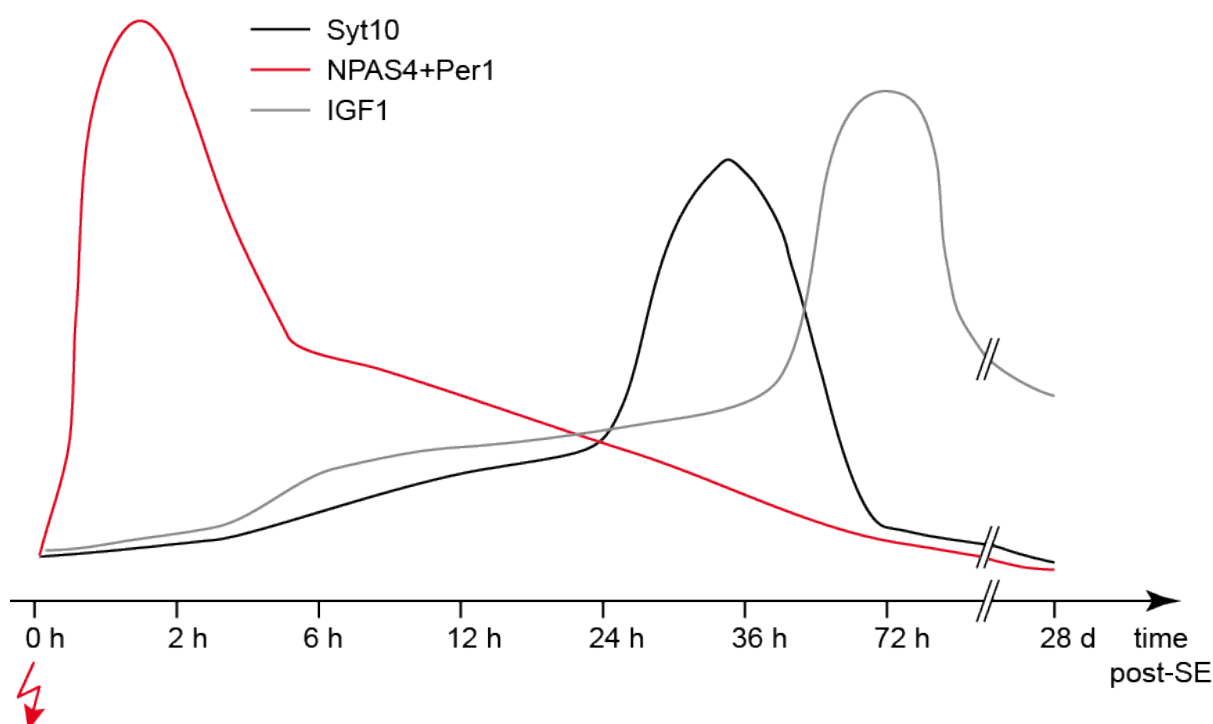
Figure 6.4 Time course of Syt10, IGF1 and NPAS4 expression following SE. Syt10 peak mRNA expression in the CA1 region was reached 36 h after SE (black line). Peak expression of IGF1 mRNA was observed 72h after SE. NPAS4 mRNA expression was up-regulated immediately after SE and as NPAS4 and Per1 synergistically regulate the Syt10 promoter, Per1 might also be constantly increased in this heterodimer as well (red solid line). Time point of SE-induction is symbolized by a red flash.

6.4.2 Role of Syt10 in progenitor cell proliferation in response to SE

One hallmark of epilepsy is an aberrant network reorganization that is also mediated by increased neurogenesis (Parent et al., 1997; Parent et al., 2006; Parent et al.,

2006). Adult neurogenesis occurs in the subgranular zone and in the subventricular zone (Curtis et al., 2012; Eriksson et al., 1998; Ming & Song, 2005). The factors contributing to increased neurogenesis are poorly understood. However, it was suggested that IGF1 promotes adult neurogenesis and mediates progenitor cell proliferation in the subgranular zone 2 d following SE (Choi et al., 2008). As mentioned above, IGF1 was reported to be the cargo of Syt10 vesicles in OB neurons (Cao et al., 2011).

It was therefore hypothesized that if Syt10 would be localized to IGF1 containing vesicles in the hippocampus, a difference in cell proliferation should be obtained if Syt10 is knocked out. To probe this hypothesis Syt10 KO and WT animals were pilocarpine-injected. Two days afterwards mice were injected with BrdU and sacrificed two hours later. First as a control, newly proliferating cells were counted outside the subgranular zone, namely in the granule cell layer and in the hilus. In neither of the two regions a difference between WT and KO was found. As expected, SE-experienced mice exhibited more active cell proliferation in the subgranular zone. Intriguingly, this increase was less in Syt10 KO mice compared to WT mice.

These results support a role for Syt10 in the regulation of IGF1 release after pilocarpine-induced SE. To further validate this finding, the release of IGF1 secretion could be analyzed in hippocampal Syt10 KO cells. The functional consequences of SE-induced subgranular zone neurogenesis vary between studies. One report states that newborn granule cells under epileptic conditions have decreased excitatory and increased inhibitory inputs (Jakubs et al., 2006). Thereby, neurogenesis would increase the threshold for seizure propagation. Other studies suggest that SE-induced neurogenesis goes along with an increase in seizure frequency (McCloskey et al., 2006; Parent et al., 1997; Scharfman et al., 2003).

Administration of intrahippocampal injection of KA causes substantial alterations such as astrogliosis, microgliosis and increased hippocampal neurogenesis. Previous studies described that this injury can be reversed by simultaneous injection of IGF1 into mice and rats as assessed 13 d after KA treatment (Miltiadous et al., 2011; Miltiadous et al., 2010) indicating a neuroprotective function for IGF1. Furthermore, chronic treatment but not acute infusion of mice with IGF1 prevented KA-induced cognitive impairment (Bluthé et al., 2005). In contrast, Choi et al. (2008) reported that increased neuronal cell proliferation 2 d after SE was dependent on IGF1. Therefore, IGF1 may, in the acute phase following SE, mediate neurogenesis to compensate

the extensive neuronal cell loss during SE. Later (in the latent or chronic phase), IGF1 might ameliorate hippocampal neurodegeneration (Miltiadous et al., 2011; Miltiadous et al., 2010) by preventing uncontrolled neurogenesis and thereby diminishing the progression of a hyperexcitable network.

Epileptogenesis is accompanied by the occurrence of reactive astrocytes (astrogliosis) as well as microglia activation. Both phenomena are well documented to contribute to hyperexcitability (Binder & Steinhäuser, 2006; Heinemann et al., 2000; de Lanerolle et al., 2010) and to epileptogenesis, respectively (Borges, 2003). Nevertheless, following induced dentate granule cell injury, IGF1 protein levels in astroglia and microglia and mRNA levels in the hippocampus become augmented (Wine et al., 2009). Different from WT mice, in IGF1 KO mice, this damage relates to a significantly increased CA1 neuronal cell death, suggesting a survival effect of this growth factor.

However, interpreting the functional consequences of altered cell proliferation in Syt10 WT animals following SE is complicated, given that serum IGF1 is transported through the blood-brain-barrier to activated brain areas (Nishijima et al., 2010). Electrical, sensory and behavioral stimulation but not local synthesis increased the IGF1 input in these regions of the brain.

Taken together, due to the multiple factors influencing IGF1 levels further studies will be required to identify the precise role of newly synthesized IGF1 in the hippocampus.

7   Outlook

The results obtained in this study raise several questions that need to be addressed in further experiments.

The next stage of this project would be to fully resolve the signaling cascades mediating Syt10 expression. In this regard, it will be first necessary to unravel if NPAS4 regulates the Syt10 promoter via direct or indirect binding. Next, it should be examined whether the Syt10 promoter is functional *in vivo* using viral gene transfer. If a differential regulation of the promoter is observed in response to SE it should be an intriguing tool to study consequences of epileptic seizures in a specific subset of cells.

In addition, a detailed analysis of subcellular compartments will be required to determine to which vesicular structures Syt10 is localized in the hippocampus after SE and to identify, which proteins regulate the docking of Syt10 containing vesicular compartments. Therefore, the identification of Syt10 binding partners would be mandatory.

Furthermore, it is important to understand the physiological relevance of Syt10 following SE in more detail. It should be analyzed *in vivo* if the Syt10 protein is differentially regulated in a specific subset of cells in response to SE. Given that IGF1 may be secreted by astrocytes as well as by microglia, analyzing differences in Syt10 KO and WT mice with regard to astrogliosis and microgliosis after SE may provide important insights into the physiological role of Syt10 and IGF1 in the progression of epilepsy.

8   Summary

During epileptogenesis multiple cellular and molecular changes occur in the brain resulting in the emergence of recurrent spontaneous seizures. Epileptogenesis encompasses acquired changes leading to neuropathological alterations of circuits and neuronal connections in the brain and to functional modifications of the cellular network. One member of the Synaptotagmin (Syt) gene family that is rapidly and transiently up-regulated in the rat hippocampus early after the experimental induction of SE but is barely detectable in the native brain is Syt10. However, the knowledge about the function of Syt10 in health and disease conditions, especially in the hippocampus, is very limited.

In order to delineate the mechanisms regulating Syt10 gene expression in response to strong electrical stimulation, this study provided the first fundamental bioinformatic and functional characterization of the Syt10 promoter and genomic regulatory regions in different cell types. Conserved regions in the Syt10 gene mediated strong induction of Syt10 promoter activity, particularly in the hippocampal formation. The transcription factor NPAS4 was identified to positively regulate endogenous expression of Syt10 as well as, together with Per1, Syt10 promoter activity. Epilepsy-induced up-regulation of endogenous Syt10 expression was mimicked by induction of membrane depolarization and by application of the convulsant compound kainic acid. A key genomic region underlying depolarization-mediated induction of the Syt10 promoter was clearly identified.

As a way to obtain first insights into the putative function of Syt10, its subcellular distribution was examined in hippocampal neurons and was compared with the related Syt isoforms 3, 5 and 6. Syt10 was identified not to be a resident Golgi protein but partially co-localized with IGF1, which was suggested to be the cargo of Syt10 vesicles in OB neurons, and with NPY, a marker for secretory vesicles. A synaptic localization for Syt10, as analyzed by Syt1 and synapsin labelings, was not identified. These results support the hypothesis that Syt10 is localized to large vesicular structures but not to synaptic vesicles. Next, to identify targeting signals defining the subcellular localization of Syt10 two approaches were used. Mutation of Syt10 N-terminal cysteines known to mediate dimerization indicated the importance of cysteines rather for the stability than for the localization of Syt10. Syt10 chimera

with an exchanged N-terminus by the related Syts 3, 5 and 6 revealed that another domain besides the N-terminus might be important for the Syt10 targeting.

Additionally, first steps have been accomplished regarding the identification of Syt10 containing protein complexes or organelles forming the basis for an isolation of the respective complexes from the hippocampus following status epilepticus (SE).

To date, the role of Syt10 in epileptogenesis remains enigmatic and the spatiotemporal expression profile was only analyzed in rats. Therefore, the time course of Syt10 expression following pilocarpine-induced SE was examined in mice. The strongest induction of Syt10 expression in mice was observed with a 30 hours delay compared to rats. The time course of IGF1 induction did not show an exact parallelism to Syt10 but, as reported for IGF1, Syt10 was observed to be important for SE-induced progenitor cell proliferation as well. These data may suggest that Syt10 plays a critical role in the attenuation of acquired changes during epileptogenesis.

Taken together, the results of this thesis provide novel insights into the key mechanisms regulating Syt10 expression in the hippocampus in the normal and epileptic brain as well as into the subcellular distribution of Syt10 and form the basis for further studies into the precise understanding of the function of Syt10 during epileptogenesis.

9 Appendix
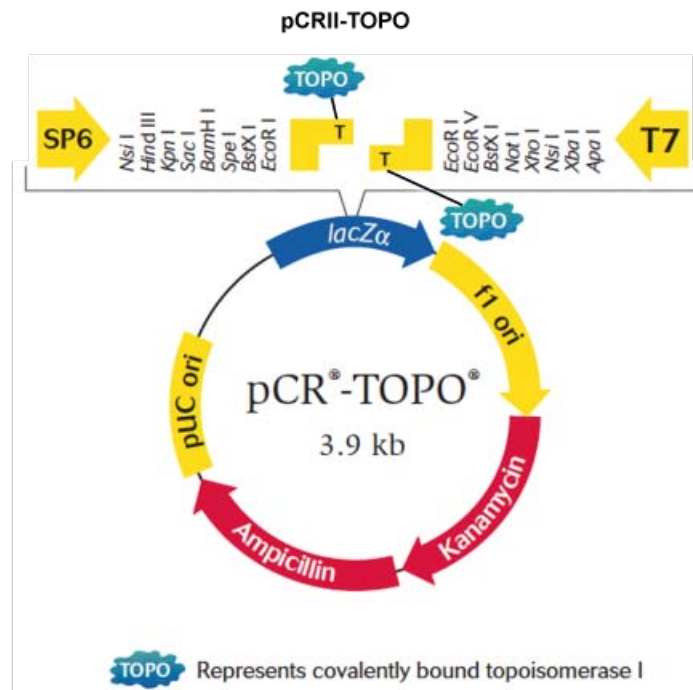
Supplementary figure 1 Circular map of the pCRII TOPO vector. The vector contains an ampicillin and a kanamycin resistance gene, a lacZ gene, a multiple cloning site (MCS) and covalently bound topoisomerase I. Topoisomerase I leads to a ligation of the poly-A strand of the PCR product with the poly-T site of the vector. The MCS comprises sites for commonly used restriction enzymes and the arrows indicate the direction of transcription.
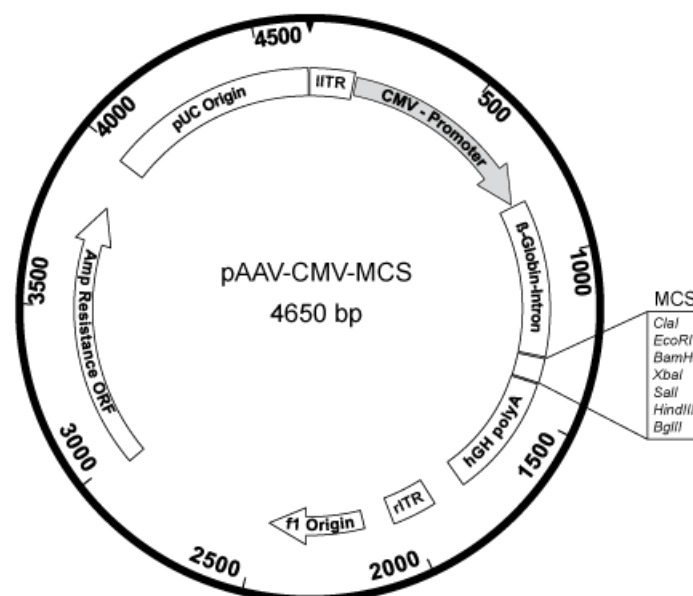
Supplementary figure 2 Circular map of the pAAV-CMV-MCS vector. The vector comprises a cytomegalovirus (CMV) -promoter, with a ß-globin intron, a MCS and a polyadenylation site (poly A). These vector features are flanked by a left inverted terminal repeat (lITR) and a right inverted terminal repeat (rITR) which are needed for the synthesis of recombinant adeno-associated viruses (rAAV) genome. The most commonly used sites for restriction enzymes of the MCS are listed in the order of their appearance. The numbers in the circle are sequence reference points.
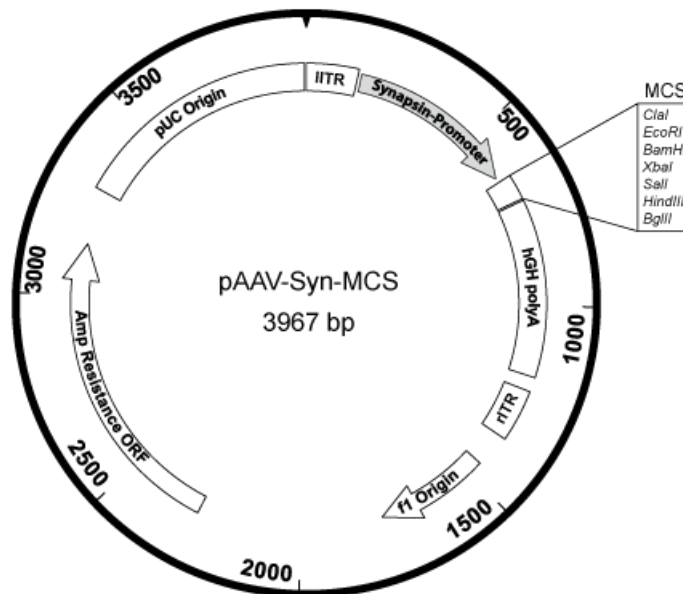
Supplementary figure 3 Circular map of the pSyn-MCS vector. The vector comprises a human synapsin I (Syn I) –promoter, a MCS and a polyadenylation site (poly A). The most commonly used sites for restriction enzymes of the MCS are listed in the order of their appearance. The numbers in the circle are sequence reference points.
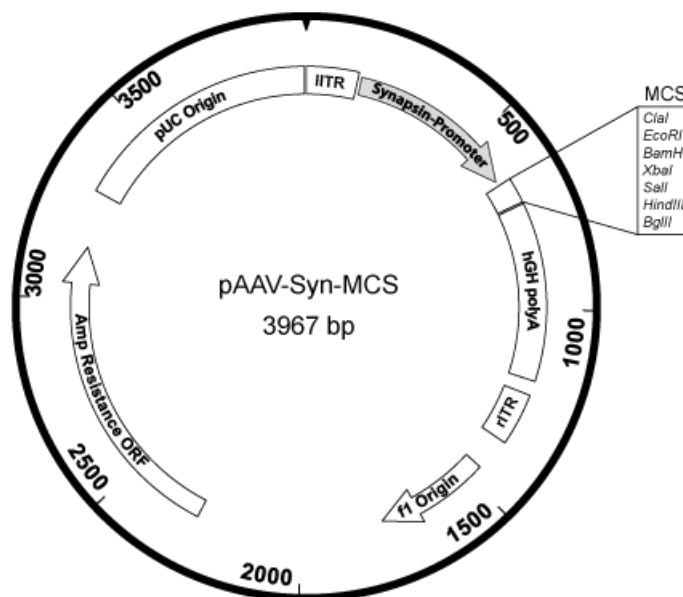
Supplementary figure 4 Circular map of the pAAV-Syn-MCS vector. The vector comprises a human synapsin I (SynI) –promoter, a MCS and a polyadenylation site (poly A). These vector features are flanked by a left inverted terminal repeat (lITR) and a right inverted terminal repeat (rITR) which are needed for the synthesis of recombinant adeno-associated viruses (rAAV) genome. The most commonly used sites for restriction enzymes of the MCS are listed in the order of their appearance. The numbers in the circle are sequence reference points.
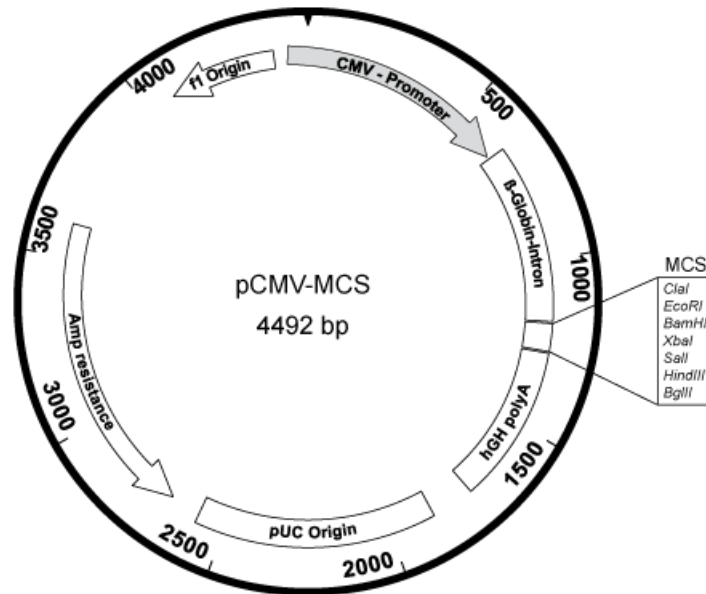
Supplementary figure 5 Circular map of the pCMV-MCS vector. The vector comprises a cytomegalovirus (CMV)–promoter, with a ß-globin intron, a MCS and a polyadenylation site (poly A). The most commonly used sites for restriction enzymes of the MCS are listed in the order of their appearance. The numbers in the circle are sequence reference points.
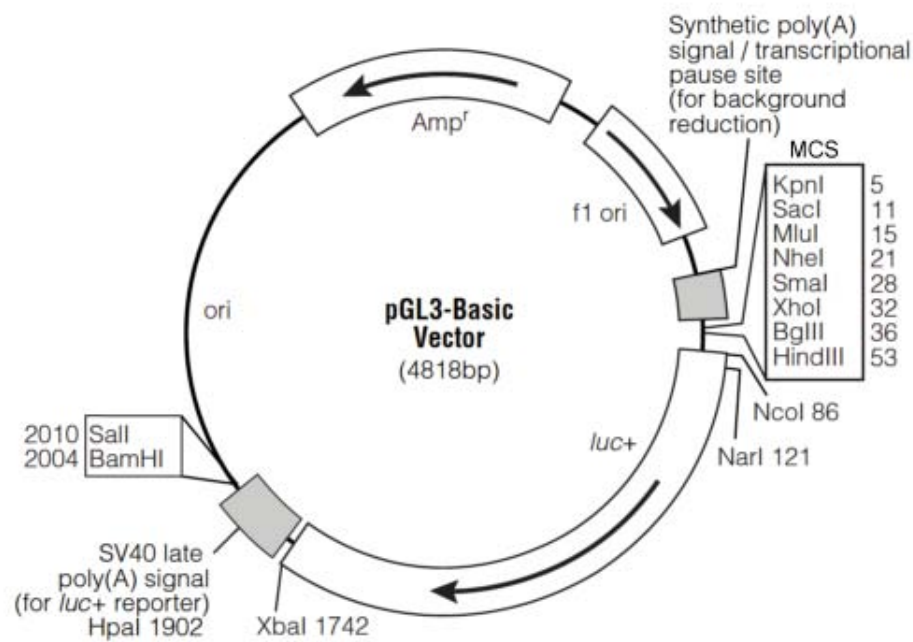

Supplementary figure 6 Circular map of the pGL3-basic vector. The vector comprises an ampicillin resistance (Amp^r) gene, a MCS, and a firefly luciferase gene (luc+). The sites for the most commonly used restriction enzymes are listed in the order of their appearance and the numbers serve as sequence references. Note, that there are three restriction sites behind the luciferase gene (XbaI, BamHI, SalI).

Supplementary table 1: Overrepresented transcription factor binding sites in the Syt10 promoter region of rat, mouse, human and dog

	TF Family	number of matches	Z-Score genome			TF Family	number of matches	Z-Score promoter
Rat (5490 bp)								
1	V$ZF5F	11	8,22		1	V$BPTF	10	5,03
2	V$ZF06	5	4,67		2	V$ZF06	5	4,19
3	V$ZF02	22	4,23		3	V$MEF2	17	3,88
4	V$BPTF	10	3,61		4	V$IRFF	23	3,11
5	V$GLIF	14	3,22		5	V$CAAT	20	3,1
6	V$MYBL	23	2,67		6	V$CHRF	9	2,65
7	V$GRHL	10	2,59		7	V$PDX1	14	2,53
8	V$RREB	8	2,59		8	V$GRHL	10	2,35
9	V$MAZF	9	2,33		9	V$MYBL	23	2,19
10	V$CAAT	20	2,3		10	V$BCL6	12	2,15
Mouse (5413 bp)								
1	V$ZF5F	12	9,69		1	V$FKHD	48	5,04
2	O$TF2B	2	5,88		2	V$CART	39	4,16
3	V$NRF1	5	4,37		3	V$BPTF	9	3,98
4	V$MYBL	27	4,09		4	V$LEFF	27	3,81
5	V$E2FF	17	3,7		5	V$MYBL	27	3,51
6	V$HDBP	2	2,82		6	V$MEF2	16	3,03
7	V$BPTF	9	2,72		7	V$BCDF	16	2,71
8	V$FKHD	48	2,45		8	V$IRFF	21	2,38
9	V$OSRF	5	2,26		9	V$HBOX	31	2,37
10	V$EGRF	15	2,17		10	V$SALL	4	2,22
Human (3116 bp)								
1	V$ZF5F	12	12,1		1	V$NKX1	11	5,15
2	V$NRF1	5	7,57		2	V$FKHD	31	5,02
3	V$EGRF	17	7,17		3	V$PDX1	14	4,4
4	V$E2FF	20	7		4	V$HBOX	26	3,78
5	V$GABF	8	4,55		5	V$GRHL	8	3,52
6	V$ZF07	6	4,06		6	V$GABF	8	3,41
7	O$MTEN	4	3,98		7	V$DLXF	13	3,25
8	V$GRHL	8	3,69		8	V$CART	24	3,21
9	V$CTCF	7	3,5		9	V$LHXF	27	3,19
10	V$WHNF	3	3,11		10	V$HOXF	29	3,16
Dog (3250 bp)								
1	V$ZF5F	11	0,64		1	V$GABF	20	5,81
2	V$NRF1	7	0,25		2	V$HBOX	29	4,6
3	V$E2FF	15	0,41		3	V$HOXC	16	4,38
4	V$GABF	20	5,81		4	V$HOXF	34	4,26
5	V$ZFHX	9	2,46		5	V$CART	28	4,21
6	V$HZIP	3	2,78		6	V$SALL	6	3,98
7	V$RORA	10	3,02		7	V$BRN5	22	3,76
8	V$HOXC	16	4,38		8	V$HOMF	40	3,7
9	V$SALL	6	3,98		9	V$FKHD	27	3,52
10	V$SF1F	5	1,65		10	V$SORY	30	3,4
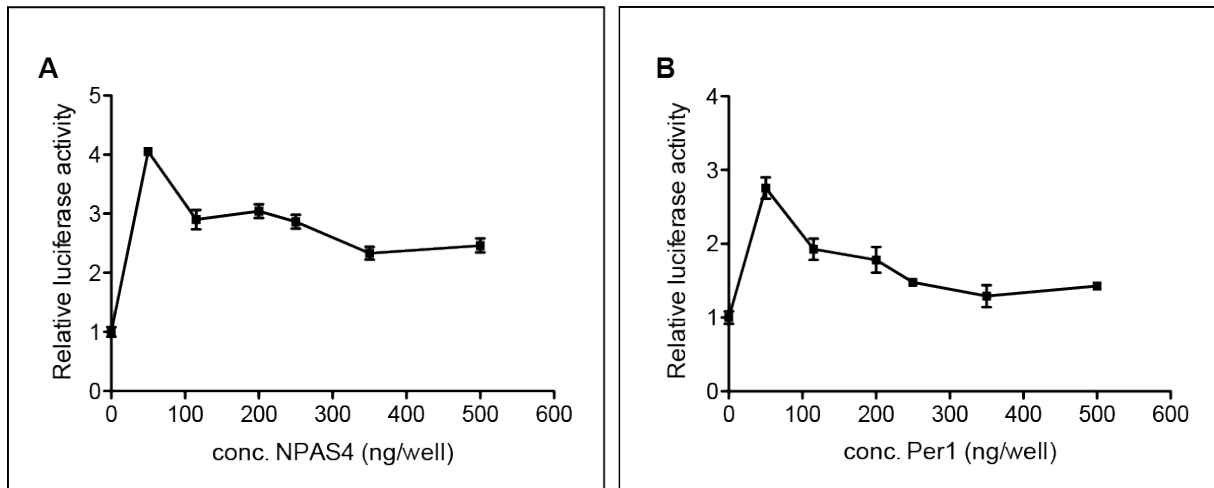
Supplementary figure 7 Saturation curves of the transcription factors NPAS4 and Per1 on the Syt10 promoter. Rat hippocampal neurons were transfected on DIV5 with the promoter fragment -4713 and with different concentrations of the transcription factor NPAS4 or Per1 (0 ng, 50 ng, 120 ng, 200 ng, 250 ng, 350 ng and 500 ng). On DIV7, cells were lysed and luciferase activity was measured. (A) Concentration curve of NPAS4 reveals a saturation of the transcription factor at a concentration of 50 ng. (B) Per1 activation of the Syt10 promoter fragment -4713 is strongest at a concentration of 50 ng. All values were normalized to the basal condition (without transcription factor) and results are presented as mean +/- SEM.
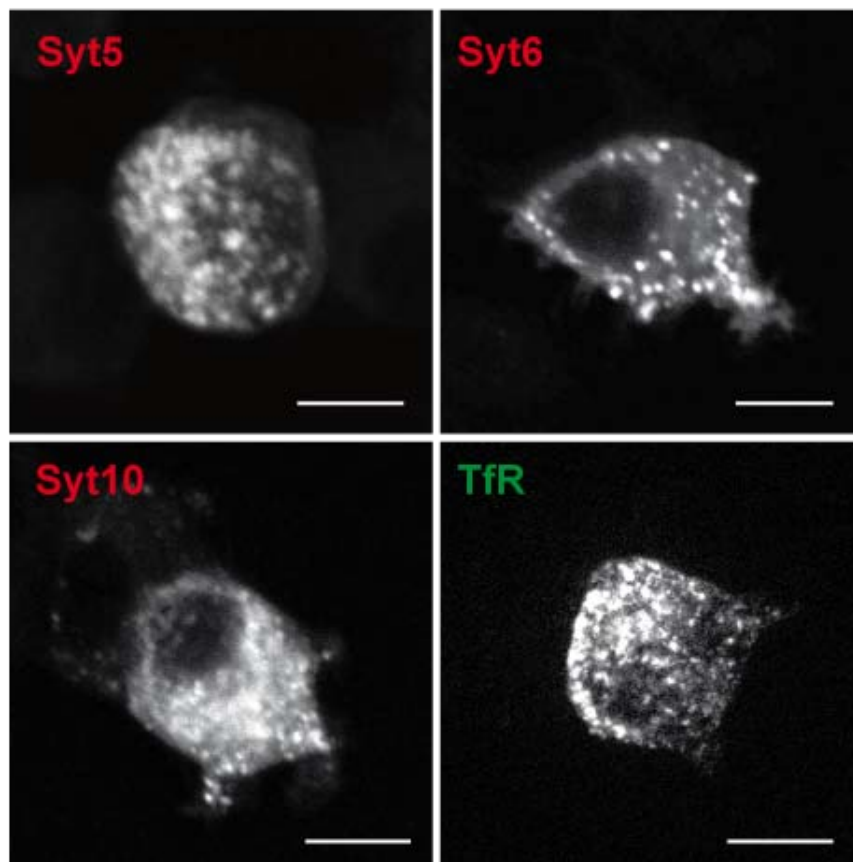
Supplementary figure 8 Single transfected PC12 cells. Upper row: Syt5-mCherry and Syt6-mCherry, lower row: Syt10-mCherry and TfR-GFP. Scale bar: 5 µm.
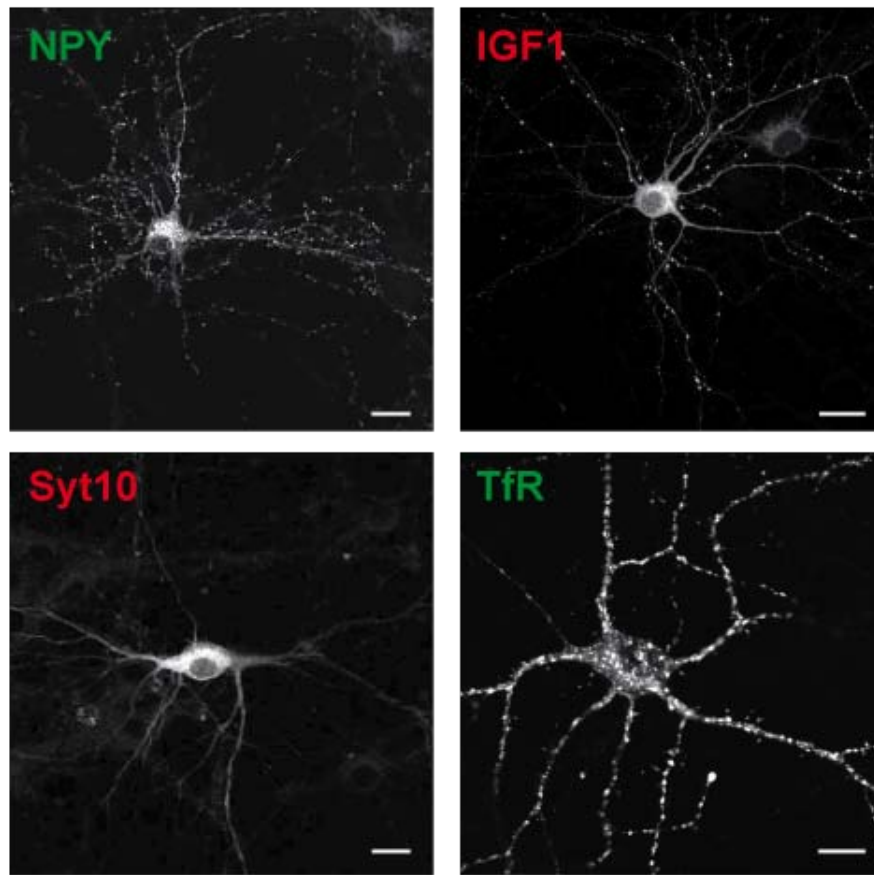
Supplementary figure 9 Single transfected mouse primary neurons. Upper row: NPY-GFP and IGF1-mRFP, lower row: Syt10-mRFP and TfR-GFP. Scale bar: 20 µm.

A
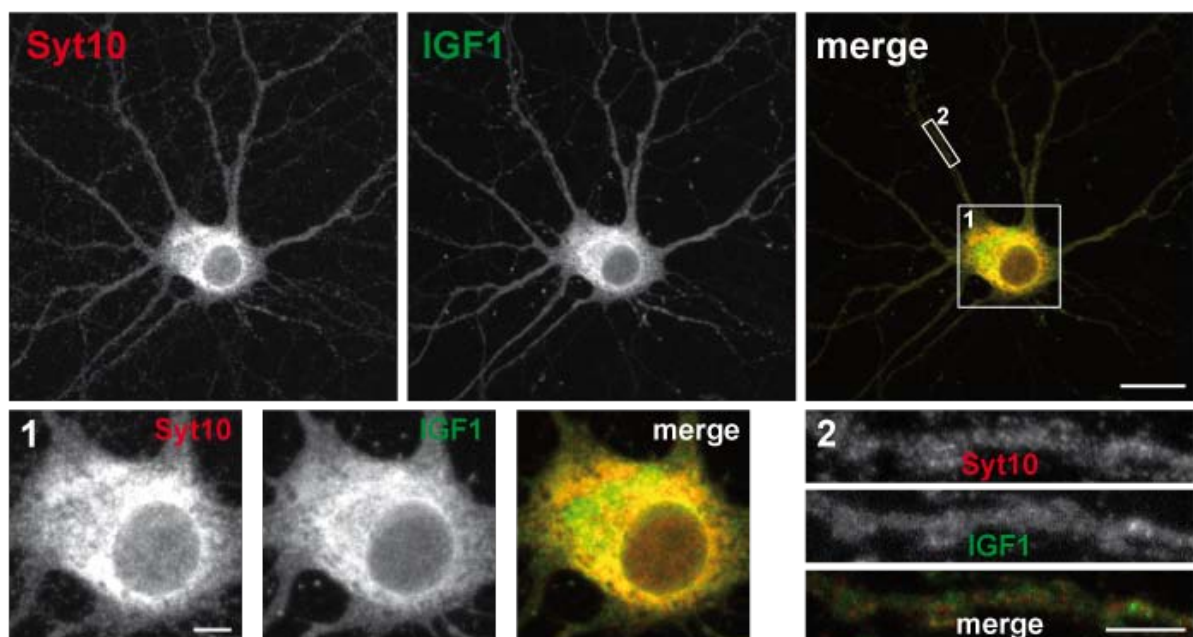
B
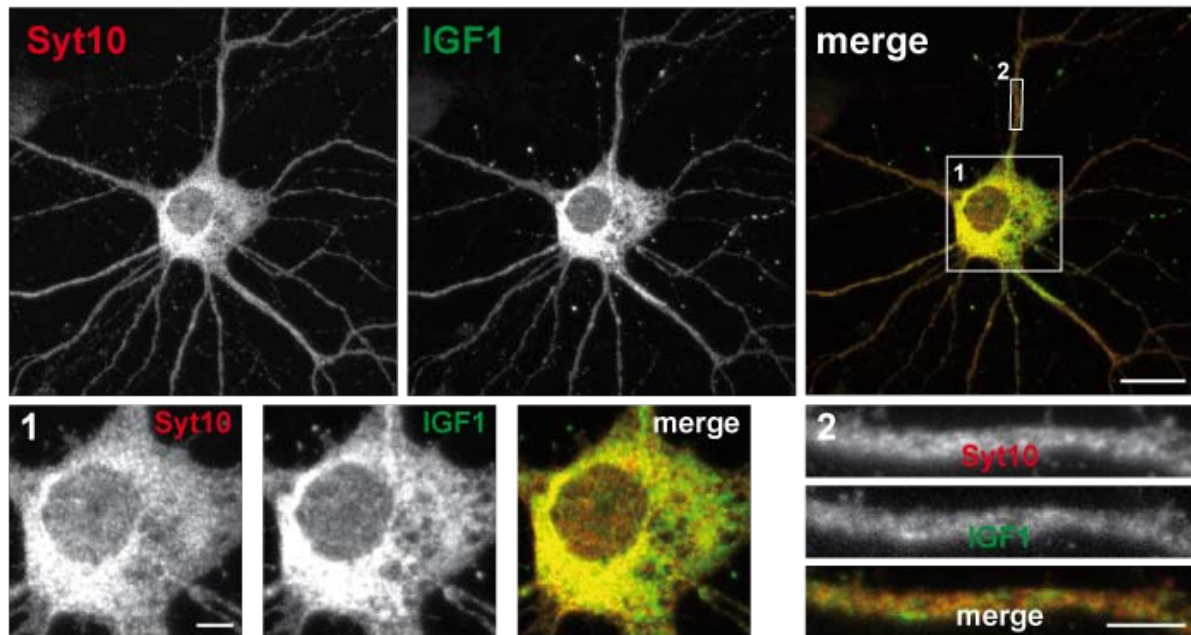
Supplementary figure 10 Co-transfection of untagged Syt10 and IGF1-HA in mouse hippocampal neurons DIV14. (A) Staining with the monoclonal Syt10 antibody 1D3 and a specific HA antibody. Diffuse and weak co-expression of the two proteins in the soma and dendrites. No overlap in the dendrites is obtained. (B) Staining against Syt10 was accomplished by the polyclonal antibody 150 T3 and IGF1 was labeled by a HA-tag specific antibody. A similar distribution of the fluorescence signal was obtained compared with the other Syt10 antibodies. Numbers in the upper right image indicate the boxes with higher magnifications of the soma (1) and one branch (2). Scale bar: 20 µm, magnifications: 5 µm.
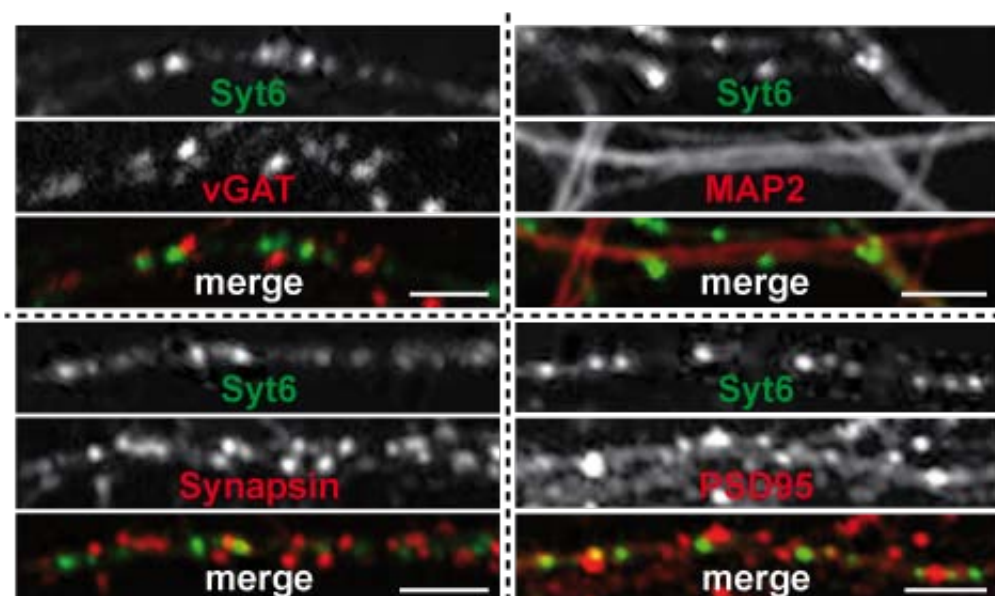
Supplementary figure 11 Subcellular localization of Syt6-GFP in primary neurons DIV13-16. Inhibitory neurons were labeled by vGAT, dendrites by MAP2, presynapses by Synapsin and postsynapses by PSD95. Syt6 was distributed along the dendrites but no overlap with an inhibitory or pre- and postsynaptic marker was observed. Scale bar: 5 µm.
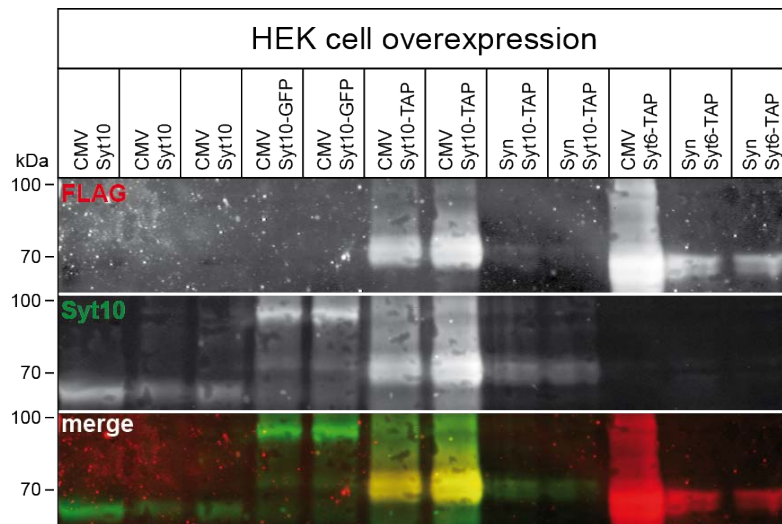
Supplementary figure 12 Immunoblot verifying the size of SF-TAP fusion proteins.
HEK293T cells were either transfected with a SF-TAP-tagged Syt10 or Syt6 construct or with a GFP-tagged or untagged Syt10 plasmid as positive controls for the staining and the size of the protein bands. Protein samples were loaded as duplets (CMV Syt10 as triplets) and were stained with a FLAG antibody (red) and the polyclonal Syt10 antibody 150 T3 (green). Syt10 (62 kDa), Syt10-GFP (90 kDa) and Syt10-TAP (70 kDa) proteins are recognized by the polyclonal antibody 150 T3. The FLAG antibody also recognizes TAP-tagged Syt10. Note that there is less protein present in the sample under the control of the synapsin promoter compared to the CMV promoter due to its lesser activity in HEK293T cells. TAP-tagged Syt6 constructs are translated into proteins of a correct size and are recognized by the FLAG antibody.

10 Abbreviations

Ac	Histone acetylation
AHS	Ammon's horn sclerosis
ANOVA	Analysis of variance
AP2	Clathrin assembly (adapter) protein 2
Ara-C	Arabinofuranosyl cytidine
Arc/Arg3.1	Activity-regulated cytoskeletal protein
B/K protein	Brain/kidney protein
BDNF	Brain-derived neurotrophic factor
BES	N,N-Bis-(2-hydroxyethyl)-2-amino-ethansulfonic acid
BFA	Brefeldin A
bHLH	Basic Helix-loop-helix
bp	Base pairs
BrdU	5-bromo-2'-deoxyuridine
CA1	Cornu Ammonis 1
Ca^{2+}	Calcium
CA3	Cornu Ammonis 3
CA4	Cornu Ammonis 4
Cav3.2	T-type voltage-activated calcium channel
CHAPS	3-[(3-cholamidopropyl)dimethylammonio]-1-propanesulfonate
CMV	Cytomegalovirus
CO2	carbon dioxide
CRE	cAMP response element
CREB	cAMP response element-binding protein
Ctrl	Control
DAPI	4′,6-diamidino-2-phenylindole
DDM	n-Dodecyl-ß-maltoside
DDM	n-Dodecyl-ß-maltoside
DG	Dentate gyrus
DMEM	Dulbecco's modified eagle medium
DMSO	dimethyl sulfoxide
DNA	Desoxyribonucleic acid
DTT	dithiothreitol
E-Syts	extended Syts
EE	early endosome
EEG	Electroencephalography
e.g.	exempli gratia
Egr	Early growth factor
EGTA	ethylene glycol tetraacetic acid

EPL	external plexiform layer
ER	Endoplasmatic Reticulum
ERGIC	ER to Golgi Intermediate Compartment
FCS	fetal calf serum
GABA	Gamma-aminobutyric acid
GCL	Granule cell layer
GFAP	glial fibrillary acidic protein
GFP	Green fluorescent protein
GM130	Golgi matrix protein 130
h	Hour
HAT	Histone acetyltransferase
HAT	sodium hypoxanthine, aminopterin, thymidine
HBS	HEPES buffered saline
HBSS	Hanks buffered salt solution
HBSS	Hank's Buffered Salt Solution
HC	Hippocampus
HCl	hydorchloride
HEBS	HEPES buffered saline
HEK293T	Human embryonic kidney cell line 293T
Hi	Hilus
ICC	Immunocytochemistry
ICH	Immunohistochemistry
i.e.	id est
IGF1	Insulin-like growth factor 1
IMDM	Iscove's Modified Dulbecco's Medium
INR	Initiator
KA	kainic acid
kb	kilo base
KCl	Potassium chloride
kDa	Kilo Dalton
KO	Knockout
l	Liter
LAR	Luciferase
LDCV	Large dense core vesicle
LE	late endosome
Lys	lysosme
MAP2	microtubule-associated protein 2
MCL	mitral cell layer
MCS	Multiple cloning site
MEF2	Myocyte enhancer factor 2
MEM	Minimum essential medium

MgCl$_2$	Magnesium chloride
min	Minute
ml	Milliliter
mm	Millimeter
mM	Millimolar
MOB	mouse olfactory bulb (neurons)
mRNA	Messenger RNA
MTCPs	Multiple C2-transmembrane proteins
Munc13	Mammalian Unc-13 homolog
n-Octyl-ß	n-Octyl-ß-D-glucopyranoside
n-octyl-ß	n-octy-ß-D-glucopyranoside
NaCl	Sodium chloride
NFkB	Nuclear factor 'kappa-light-chain-enhancer' of activated B-cells
ng	Nanogram
NG108-15	Neuroblastoma glioma cell line 108-15
NGS	Normal goat serum
NPAS4	Neuronal PAS domain protein 4
NPY	neuropeptide Y
NSF	N-ethylmaleimide sensitive factor
NTMCs	N-terminal-TM-C2-domain genes
OB	Olfactory bulb
Oligo	Oligonucleotide
P	Phosphorylation
PAS	Period-Arnt-Sim
PBS	Phosphate buffered saline
PC	phosphatidlycholine
PC12	Pheochromocytoma cell line 12
PCR	Polymerase chain reaction
pen/strep	penicillin/streptomycin
Per1	Period1
PFA	Paraformaldehyde
Pfu	Pyrococcus furiosus
PIP$_2$	phosphatidylinositol 4,5-bisphosphate
PM	Plasma membrane
PS	phosphatidylserine
PSD95	postsynaptic density protein 95
rAAV	recombinant adeno-associated virus
RC	rat cortical (neurons)
RE	recycling endosome
REST	repressor element 1-silencing transcription factor
RFP	red fluorescent protein

RH	Rat hippocampal (neurons)
RIM	Rab3 interacting molecule
RNA	Ribonucleic acid
RT-PCR	Reverse transcription PCR
SARE	Synaptic activity response element
s.c.	subcutaneously
SCN	Suprachiasmatic nucleus
SDS	Sodium dodecyl sulfate
SE	Status epilepticus
sec	seconds
SEM	Standar error of mean
SEM	Standard error of mean
SF-TAP	streptavidin/FLAG-tandem affinity purification
Sim	Single-minded
SLMV	synaptic-like microvesicle
SLPs	Syt-like proteins
SNAP-25	Synaptosome-associated protein of 25 kDa
SNARE	N-ethylmaleimide sensitive factor (NSF) -attachment protein receptor
SRE	Serum response element
SRF	Serum response factor
SV	Synaptic vesicle
Syn	Synapsin
Syp	Synaptophysin
Syt	Synaptotagmin
TCF	Ternary complex factor
TfR	Transferrin receptor
TLE	Temporal lobe epilepsy
TMD	Transmembrane domain
TSS	Transcription start site
TX-100	Triton X-100
UCSC	University of california, santa cruz
USF	Upstream regulatory factor
vGAT	vesicular GABA-transporter
WB	Western blot
WT	Wildtype
ZRE	Zeste-like response element
ZW 3-14	Zwittergent 3-14
µl	Microliter
µm	Micrometer
µM	Micromolar

11 References

Adolfsen B, Saraswati S, Yoshihara M, Littleton JT (2004) Synaptotagmins are trafficked to distinct subcellular domains including the postsynaptic compartment. The Journal of cell biology 166:249–260.

Ahras M, Otto GP, Tooze SA (2006) Synaptotagmin IV is necessary for the maturation of secretory granules in PC12 cells. Journal of cell biology 173:241–251.

Albrecht U, Sun ZS, Eichele G, Lee CC (1997) A differential response of two putative mammalian circadian regulators, mper1 and mper2, to light. Cell 91:1055–1064.

Aronica E, Gorter JA (2007) Gene expression profile in temporal lobe epilepsy. The Neuroscientist : a review journal bringing neurobiology, neurology and psychiatry 13:100–108.

Atiya-Nasagi Y, Cohen H, Medalia O, Fukudan M, Sagi-Eisenberg R (2005) O-glycosylation is essential for intracellular targeting of synaptotagmins I and II in non-neuronal specialized secretory cells. Journal of cell science 118:1363–1372.

Babity J, Armstrong J, Plumier J-C, Currie RW, Robertson HA (1997) A novel seizure-induced synaptotagmin gene identified by differential display. Proceedings of the National Academy of Sciences of the United States of America 94:2638–2641.

Balsalobre A, Marcacci L, Schibler U (2000) Multiple signaling pathways elicit circadian gene expression in cultured Rat-1 fibroblasts. Current biology 10:1291–1294.

Baram D, Adachi R, Medalia O (1999) Synaptotagmin II Negatively Regulates Ca2+-triggered Exocytosis of Lysosomes in Mast Cells. The Journal of experimental medicine 189:1649–1658.

Baram D, Mekori Y, Sagi-Eisenberg R (2001) Synaptotagmin regulates mast cell functions. Immunological reviews 179:25–34.

Bausch SB, McNamara JO (2004) Contributions of mossy fiber and CA1 pyramidal cell sprouting to dentate granule cell hyperexcitability in kainic acid-treated hippocampal slice cultures. Journal of neurophysiology 92:3582–3595.

Becker A, Chen J, Zien A (2003) Correlated stage- and subfield-associated hippocampal gene expression patterns in experimental and human temporal lobe epilepsy. European Journal of Neuroscience 18:2792–2802.

Becker AJ, Pitsch J, Sochivko D, Opitz T, Staniek M, Chen C-C, Campbell KP, Schoch S, Yaari Y, Beck H (2008) Transcriptional upregulation of Cav3.2 mediates epileptogenesis in the pilocarpine model of epilepsy. The Journal of neuroscience: the official journal of the Society for Neuroscience 28:13341–13353.

Ben-Ari Y, Lagowska J, Tremblay E, Le Gal La Salle G (1979) A new model of focal status epilepticus: intra-amygdaloid application of kainic acid elicits repetitive secondarily generalized convulsive seizures. Brain research 163:176–179.

Bennett MK, Calakos N, Scheller RH (1992) Syntaxin: a synaptic protein implicated in docking of synaptic vesicles at presynaptic active zones. Science (New York, NY) 257:255–259.

Bi GQ, Alderton JM, Steinhardt RA (1995) Calcium-regulated exocytosis is required for cell membrane resealing. The Journal of cell biology 131:1747–1758.

Binder D, Steinhäuser C (2006) Functional changes in astroglial cells in epilepsy. Glia 54:358–368.

Blackstone C, O'Kane CJ, Reid E (2011) Hereditary spastic paraplegias: membrane traffic and the motor pathway. Nature reviews Neuroscience 12:31–42.

Bluthé R-M, Frenois F, Kelley KW, Dantzer R (2005) Pentoxifylline and insulin-like growth factor-I (IGF-I) abrogate kainic acid-induced cognitive impairment in mice. Journal of neuroimmunology 169:50–58.

Bohannon NJ, Corp ES, Wilcox BJ, Figlewicz DP, Dorsa DM, Baskin DG (1988) Localization of binding sites for insulin-like growth factor-I (IGF-I) in the rat brain by quantitative autoradiography. Brain research 444:205–213.

Borges K (2003) Neuronal and glial pathological changes during epileptogenesis in the mouse pilocarpine model. Experimental Neurology 182:21–34.

Boulaire J, Balani P, Wang S (2009) Transcriptional targeting to brain cells: Engineering cell type-specific promoter containing cassettes for enhanced transgene expression. Advanced drug delivery reviews 61:589–602.

Brooks-Kayal AR, Shumate MD, Jin H, Rikhter TY, Coulter DA (1998) Selective changes in single cell GABA(A) receptor subunit expression and function in temporal lobe epilepsy. Nature medicine 4:1166–1172.

Brose N, Petrenko AG, Südhof TC, Jahn R (1992) Synaptotagmin: a calcium sensor on the synaptic vesicle surface. Science (New York, NY) 256:1021–1025.

Brown H, Meister B, Deeney J, Corkey B (2000) Synaptotagmin III isoform is compartmentalized in pancreatic beta-cells and has a functional role in exocytosis. Diabetes 48:383–391.

Butz S, Fernandez-Chacon R, Schmitz F, Jahn R, Südhof TC (1999) The subcellular localizations of atypical synaptotagmins III and VI. Synaptotagmin III is enriched in synapses and synaptic plasma membranes but not in synaptic vesicles. The Journal of biological chemistry 274:18290–18296.

Cao P, Maximov A, Südhof TC (2011) Activity-dependent IGF-1 exocytosis is controlled by the Ca(2+)-sensor synaptotagmin-10. Cell 145:300–311.

Cao P, Yang X, Südhof TC (2013) Complexin activates exocytosis of distinct secretory vesicles controlled by different synaptotagmins. The Journal of neuroscience : the official journal of the Society for Neuroscience 33:1714–1727.

Chapman ER, Jahn R (1994) Calcium-dependent Interaction of the Cytoplasmic Region of Synaptotagmin with Membranes. The Journal of biological chemistry 269:5735–5741.

Chapman E, Hanson P, An S, Jahn R (1995) Ca 2+ Regulates the Interaction between Synaptotagmin and Syntaxin 1. Journal of Biological Chemistry 270:23667–23671.

Chapman ER (2008) How does synaptotagmin trigger neurotransmitter release? Annual review of biochemistry 77:615–641.

Cheng CM, Cohen M, Tseng V, Bondy CA (2001) Endogenous IGF1 enhances cell survival in the postnatal dentate gyrus. Journal of neuroscience research 64:341–347.

Cho C-H (2012) Molecular mechanism of circadian rhythmicity of seizures in temporal lobe epilepsy. Frontiers in cellular neuroscience 6:1–9.

Choi Y-S, Cho H-Y, Hoyt KR, Naegele JR, Obrietan K (2008) IGF-1 receptor-mediated ERK/MAPK signaling couples status epilepticus to progenitor cell proliferation in the subgranular layer of the dentate gyrus. Glia 56:791–800.

Coppola T, Magnin-Luthi S, Perret-Menoud V, Gattesco S, Schiavo G, Regazzi R (2001) Direct interaction of the Rab3 effector RIM with Ca2+ channels, SNAP-25, and synaptotagmin. The Journal of biological chemistry 276:32756–32762.

Craxton M (2001) Genomic analysis of synaptotagmin genes. Genomics 77:43–49.

Craxton M (2004) Synaptotagmin gene content of the sequenced genomes. BMC genomics 5.

Craxton M (2010) A manual collection of Syt, Esyt, Rph3a, Rph3al, Doc2, and Dblc2 genes from 46 metazoan genomes--an open access resource for neuroscience and evolutionary biology. BMC genomics 11.

Curtis MA, Low VF, Faull RLM (2012) Neurogenesis and progenitor cells in the adult human brain: a comparison between hippocampal and subventricular progenitor proliferation. Developmental neurobiology 72:990–1005.

Dai H, Shin O-H, Machius M, Tomchick DR, Südhof TC, Rizo J (2004) Structural basis for the evolutionary inactivation of Ca2+ binding to synaptotagmin 4. Nature structural & molecular biology 11:844–849.

Darna M, Schmutz I, Richter K, Yelamanchili S V, Pendyala G, Höltje M, Albrecht U, Ahnert-Hilger G (2009) Time of day-dependent sorting of the vesicular glutamate transporter to the plasma membrane. The Journal of biological chemistry 284:4300–4307.

Dashtipour K, Yan X-X, Dinh TT, Okazaki MM, Nadler JV, Ribak CE (2002) Quantitative and morphological analysis of dentate granule cells with recurrent basal dendrites from normal and epileptic rats. Hippocampus 12:235–244.

Davletov BA, Südhof TC (1993) A Single C2 Domain from Synaptotagmin I Is Sufficient for High affinits Ca2+/phospholipid binding. Journal of biological chemistry 268:26386–26390.

De Lanerolle N, Lee T, Spencer D (2010) Astrocytes and epilepsy. Neurotherapeutics 7:424–438.

Dean C, Liu H, Dunning FM, Chang PY, Jackson MB, Chapman ER (2009) Synaptotagmin-IV modulates synaptic function and long-term potentiation by regulating BDNF release. Nature neuroscience 12:767–776.

Dean C, Dunning FM, Liu H, Bomba-Warczak E, Martens H, Bharat V, Ahmed S, Chapman ER (2012a) Axonal and dendritic synaptotagmin isoforms revealed by a pHluorin-syt functional screen. Molecular biology of the cell 23:1715–1727.

Dean C, Liu H, Staudt T, Stahlberg MA, Vingill S, Bückers J, Kamin D, Engelhardt J, Jackson MB, Hell SW, Chapman ER (2012b) Distinct subsets of Syt-IV/BDNF vesicles are sorted to axons versus dendrites and recruited to synapses by activity. The Journal of neuroscience : the official journal of the Society for Neuroscience 32:5398–5413.

Detrait ER, Eddleman C (2000a) Axolemmal Repair Requires Proteins That Mediate Synaptic Vesicle Fusion. Journal of neurobiology 44:382–391.

Detrait ER, Yoo S, Eddleman CS, Fukuda M, Bittner GD, Fishman HM (2000b) Plasmalemmal repair of severed neurites of PC12 cells requires Ca(2+) and synaptotagmin. Journal of neuroscience research 62:566–573.

DiAntonio A, Schwarz T (1994) The effect on synaptic physiology of synaptotagmin mutations in drosophila. Neuron 12:909–920.

Doms RW, Russ G, Yewdell JW (1989) Brefeldin A redistributes resident and itinerant Golgi proteins to the endoplasmic reticulum. The Journal of cell biology 109:61–72.

Elfving B, Bonefeld BE, Rosenberg R, Wegener G (2008) Differential expression of synaptic vesicle proteins after repeated electroconvulsive seizures in rat frontal cortex and hippocampus. Synapse (New York, NY) 62:662–670.

Elger CE (2002) Epilepsy: disease and model to study human brain function. Brain pathology (Zurich, Switzerland) 12:193–198.

Eriksson PS, Perfilieva E, Björk-Eriksson T, Alborn AM, Nordborg C, Peterson DA, Gage FH (1998) Neurogenesis in the adult human hippocampus. Nature medicine 4:1313–1317.

Eun B, Kim HJ, Kim SY, Kim TW, Hong ST, Choi KM, Shim JK, Moon Y, Son GH, Kim K, Kim H, Sun W (2011) Induction of Per1 expression following an experimentally induced epilepsy in the mouse hippocampus. Neuroscience letters 498:110–113.

Falkowski MA, Thomas DDH, Messenger SW, Martin TF, Groblewski GE (2011) Expression, localization, and functional role for synaptotagmins in pancreatic acinar cells. American journal of physiology Gastrointestinal and liver physiology 301:G306–16.

Farnham PJ (2009) Insights from genomic profiling of transcription factors. Nature reviews Genetics 10:605–616.

Ferguson GD, Anagnostaras SG, Silva AJ, Herschman HR (2000) Deficits in memory and motor performance in synaptotagmin IV mutant mice. Proceedings of the National Academy of Sciences of the United States of America 97:5598–5603.

Fernández-Chacón R, Königstorfer A, Gerber SH, García J, Matos MF, Stevens CF, Brose N, Rizo J, Rosenmund C, Südhof TC (2001) Synaptotagmin I functions as a calcium regulator of release probability. Nature 410:41–49.

Fisher R, Van Emde Boas W, Blume W, Elger C, Genton P, Lee P, Engel JJ (2005) Comment on epileptic seizures and epilepsy: definitions proposed by the International League Against Epilepsy (ILAE) and the International Bureau for Epilepsy (IBE). Epilepsia 46:470–472.

Flannery AR, Czibener C, Andrews NW (2010) Palmitoylation-dependent association with CD63 targets the Ca2+ sensor synaptotagmin VII to lysosomes. The Journal of cell biology 191:599–613.

Flavell SW, Greenberg ME (2008) Signaling mechanisms linking neuronal activity to gene expression and plasticity of the nervous system. Annual review of neuroscience 31:563–590.

Flavell SW, Kim T-K, Gray JM, Harmin DA, Hemberg M, Hong EJ, Markenscoff-Papadimitriou E, Bear DM, Greenberg ME (2008) Genome-wide analysis of MEF2 transcriptional program reveals synaptic target genes and neuronal activity-dependent polyadenylation site selection. Neuron 60:1022–1038.

Flood WD, Moyer RW, Tsykin A, Sutherland GR, Koblar SA (2004) Nxf and Fbxo33: novel seizure-responsive genes in mice. The European journal of neuroscience 20:1819–1826.

Fujiwara T, Oda K, Yokota S, Takatsuki A, Ikehara Y (1988) Brefeldin A causes disassembly of the Golgi complex and accumulation of secretory proteins in the endoplasmic reticulum. The Journal of biological chemistry 263:18545–18552.

Fukuda M, Kanno E, Mikoshiba K (1999a) Conserved N-terminal cysteine motif is essential for homo- and heterodimer formation of synaptotagmins III, V, VI, and X. The Journal of biological chemistry 274:31421–31427.

Fukuda M, Mikoshiba K (1999b) A Novel Alternatively Spliced Variant of Synaptotagmin VI Lacking a Transmembrane Domain. Journal of Biological Chemistry 274:31428–31434.

Fukuda M, Ibata K, Mikoshiba K (2001a) A unique spacer domain of synaptotagmin IV is essential for Golgi localization. Journal of neurochemistry 77:730–740.

Fukuda M, Kanno E, Ogata Y, Mikoshiba K (2001b) Mechanism of the SDS-resistant synaptotagmin clustering mediated by the cysteine cluster at the interface between the transmembrane and spacer domains. The Journal of biological chemistry 276:40319–40325.

Fukuda M, Kowalchyk JA, Zhang X, Martin TFJ, Mikoshiba K (2002) Synaptotagmin IX regulates Ca2+-dependent secretion in PC12 cells. The Journal of biological chemistry 277:4601–4604.

Fukuda M (2003a) Molecular cloning, expression and characterization of a novel class of synaptoagmin (Syt XIV) Conserved from Drosophila to humans. Journal of biochemistry 133:641–649.

Fukuda M (2003b) Molecular cloning and characterization of human, rat, and mouse synaptotagmin XV. Biochemical and Biophysical Research Communications 306:64–71.

Fukuda M, Kanno E, Ogata Y, Saegusa C, Kim T, Loh YP, Yamamoto A (2003c) Nerve growth factor-dependent sorting of synaptotagmin IV protein to mature dense-core vesicles that undergo calcium-dependent exocytosis in PC12 cells. The Journal of biological chemistry 278:3220–3226.

Fukuda M, Kanno E, Satoh M, Saegusa C, Yamamoto A (2004a) Synaptotagmin VII is targeted to dense-core vesicles and regulates their Ca2+ -dependent exocytosis in PC12 cells. The Journal of biological chemistry 279:52677–52684.

Fukuda M, Yamamoto A (2004b) Effect of forskolin on Synaptotagmin IV protein trafficking in PC12 cells. Journal of biochemistry 136:245–253.

Gao Z, Reavey-Cantwell J, Young RA, Jegier P, Wolf BA (2000) Synaptotagmin III/VII isoforms mediate Ca2+-induced insulin secretion in pancreatic islet beta - cells. The Journal of biological chemistry 46:36079–36085.

Geppert M, Goda Y, Hammer RE, Li C, Rosahl TW, Stevens CF, Südhof TC (1994) Synaptotagmin I: a major Ca2+ sensor for transmitter release at a central synapse. Cell 79:717–727.

Gilhooley MJ, Pinnock SB, Herbert J (2011) Rhythmic expression of per1 in the dentate gyrus is suppressed by corticosterone: implications for neurogenesis. Neuroscience letters 489:177–181.

Glavan G, Zivin M (2005) Differential expression of striatal synaptotagmin mRNA isoforms in hemiparkinsonian rats. Neuroscience 135:545–554.

Glavan G, Schliebs R, Zivin M (2009) Synaptotagmins in neurodegeneration. Anatomical record (Hoboken, N.J. : 2007) 292:1849-62

Golini RS, Delgado SM, Navigatore Fonzo LS, Ponce IT, Lacoste MG, Anzulovich AC (2012) Daily patterns of clock and cognition-related factors are modified in the hippocampus of vitamin A-deficient rats. Hippocampus 22:1720–1732.

Gompf HS, Allen CN (2004) GABAergic synapses of the suprachiasmatic nucleus exhibit a diurnal rhythm of short-term synaptic plasticity. The European journal of neuroscience 19:2791–2798.

Gorter JA, van Vliet EA, Aronica E, Breit T, Rauwerda H, Lopes da Silva FH, Wadman WJ (2006) Potential new antiepileptogenic targets indicated by microarray analysis in a rat model for temporal lobe epilepsy. The Journal of neuroscience : the official journal of the Society for Neuroscience 26:11083–11110.

Greene LA, Tischler AS (1976) Establishment of a noradrenergic clonal line of rat adrenal pheochromocytoma cells which respond to nerve growth factor. Proceedings of the National Academy of Sciences of the United States of America 73:2424–2428.

Grimberg E (2002) Synaptotagmin III is a critical factor for the formation of the perinuclear endocytic recycling compartment and determination of secretory granules size. Journal of Cell Science 116:145–154.

Guan J, Williams CE, Carina E, Gluckman D (1996) The Effects of Insulin-Like Growth Brain Injury in Adult Rats : Evidence for a Role for IGF. Endocrinology 137:2–7.

Gustavsson N, Han W (2009) Calcium-sensing beyond neurotransmitters: functions of synaptotagmins in neuroendocrine and endocrine secretion. Bioscience reports 29:245–259.

Gustavsson N, Lao Y, Maximov A, Chuang J-C, Kostromina E, Repa JJ, Li C, Radda GK, Südhof TC, Han W (2008) Impaired insulin secretion and glucose intolerance in synaptotagmin-7 null mutant mice. Proceedings of the National Academy of Sciences of the United States of America 105:3992–3997.

Gut A, Kiraly CE, Fukuda M, Mikoshiba K, Wollheim CB, Lang J (2001) Expression and localisation of synaptotagmin isoforms in endocrine beta-cells: their function in insulin exocytosis. Journal of cell science 114:1709–1716.

Haberman Y, Ziv I, Gorzalczany Y, Hirschberg K, Mittleman L, Fukuda M, Sagi-Eisenberg R (2007) Synaptotagmin (Syt) IX is an essential determinant for protein sorting to secretory granules in mast cells. Blood 109:3385–3392.

Han W, Rhee J-S, Maximov A, Lao Y, Mashimo T, Rosenmund C, Südhof TC (2004) N-glycosylation is essential for vesicular targeting of synaptotagmin 1. Neuron 41:85–99.

Hanaya R, Hosoyama H, Sugata S, Tokudome M, Hirano H, Tokimura H, Kurisu K, Serikawa T, Sasa M, Arita K (2012) Low distribution of synaptic vesicle protein 2A and synaptotagimin-1 in the cerebral cortex and hippocampus of spontaneously epileptic rats exhibiting both tonic convulsion and absence seizure. Neuroscience 221:12–20.

Hanus C, Ehlers MD (2008) Secretory outposts for the local processing of membrane cargo in neuronal dendrites. Traffic (Copenhagen, Denmark) 9:1437–1445.

Hastings MH, Field MD, Maywood ES, Weaver DR, Reppert SM (1999) Differential regulation of mPER1 and mTIM proteins in the mouse suprachiasmatic nuclei: new insights into a core clock mechanism. The Journal of neuroscience : the official journal of the Society for Neuroscience 19:RC11.

Hauser E, Freilinger M, Seidl R, Groh C (1996) Prognosis of Childhood Epilepsy in Newly Referred Patients. Journal of Child Neurology 11:201–204.

Heindel U, Schmidt MFG, Veit M (2003) Palmitoylation sites and processing of synaptotagmin I, the putative calcium sensor for neurosecretion. FEBS Letters 544:57–62.

Heinemann U, Gabriel S, Jauch R, Schulze K (2000) Alterations of Glial Cell Function in Temporal Lobe Epilepsy. Epilepsia 41:185–189.

Hellier JL, Dudek FE (1999) Spontaneous motor seizures of rats with kainate-induced epilepsy: effect of time of day and activity state. Epilepsy research 35:47–57.

Hendriksen H, Datson NA, Ghijsen WE, van Vliet EA, da Silva FH, Gorter JA, Vreugdenhil E (2001) Altered hippocampal gene expression prior to the onset of spontaneous seizures in the rat post-status epilepticus model. The European journal of neuroscience 14:1475–1484.

Hirose K, Morita M, Ema M, Mimura J, Hamada H, Fujii H, Saijo Y, Gotoh O, Sogawa K, Fujii-Kuriyama Y (1996) cDNA cloning and tissue-specific expression of a novel basic helix-loop-helix/PAS factor (Arnt2) with close sequence similarity to the aryl hydrocarbon receptor nuclear translocator (Arnt). Molecular and cellular biology 16:1706–1713.

Horton AC, Ehlers MD (2003) Dual modes of endoplasmic reticulum-to-Golgi transport in dendrites revealed by live-cell imaging. The Journal of neuroscience : the official journal of the Society for Neuroscience 23:6188–6199.

Huang Z, Edery I, Rosbash M (1993) PAS is a dimerization domain common to Drosophila period and several transcription factors. Nature 364:259–262.

Huang ZJ, Curtin KD, Rosbash M (1995) PER protein interactions and temperature compensation of a circadian clock in Drosophila. Science (New York, NY) 267:1169–1172.

Hunziker W, Whitney JA, Mellman I (1991) Selective inhibition of transcytosis by brefeldin A in MDCK cells. Cell 67:617–627.

Hurtado-Chong A, Yusta-Boyo MJ, Vergaño-Vera E, Bulfone A, de Pablo F, Vicario-Abejón C (2009) IGF-I promotes neuronal migration and positioning in the olfactory bulb and the exit of neuroblasts from the subventricular zone. The European journal of neuroscience 30:742–755.

Husse J, Zhou X, Shostak A, Oster H, Eichele G (2011) Synaptotagmin10-Cre, a driver to disrupt clock genes in the SCN. Journal of biological rhythms 26:379–389.

Hutagalung A, Novick P (2011) Role of Rab GTPases in membrane traffic and cell physiology. Physiological Reviews 91:119–149.

Hutt DM, Cardullo RA, Baltz JM, Ngsee JK (2002) Synaptotagmin VIII is localized to the mouse sperm head and may function in acrosomal exocytosis. Biology of reproduction 66:50–56.

Huynh DP, Scoles DR, Nguyen D, Pulst SM (2003) The autosomal recessive juvenile Parkinson disease gene product, parkin, interacts with and ubiquitinates synaptotagmin XI. Human molecular genetics 12:2587–2597.

Ibata K, Fukuda M, Hamada T, Kabayama H, Mikoshiba K (2000) Synaptotagmin IV is present at the Golgi and distal parts of neurites. Journal of neurochemistry 74:518–526.

Jakubs K, Nanobashvili A, Bonde S, Ekdahl CT, Kokaia Z, Kokaia M, Lindvall O (2006) Environment matters: synaptic properties of neurons born in the epileptic adult brain develop to reduce excitability. Neuron 52:1047–1059.

Jang D-J, Park S-W, Kaang B-K (2009) The role of lipid binding for the targeting of synaptic proteins into synaptic vesicles. BMB reports 42:1–5.

Jilg A, Lesny S, Peruzki N, Schwegler H, Selbach O, Dehghani F, Stehle JH (2010) Temporal dynamics of mouse hippocampal clock gene expression support memory processing. Hippocampus 20:377–388.

Kanno E, Fukuda M (2008) Increased Plasma Membrane Localization of O-glycosylation-Deficient Mutant of Synaptotagmin I in PC12 Cells. Journal of neuroscience research 86:1036–1043.

Kawai M, Delany AM, Green CB, Adamo ML, Rosen CJ (2010) Nocturnin suppresses igf1 expression in bone by targeting the 3' untranslated region of igf1 mRNA. Endocrinology 151:4861–4870.

Kawashima T, Okuno H, Nonaka M, Adachi-Morishima A, Kyo N, Okamura M, Takemoto-Kimura S, Worley PF, Bito H (2009) Synaptic activity-responsive element in the Arc/Arg3.1 promoter essential for synapse-to-nucleus signaling in activated neurons. Proceedings of the National Academy of Sciences of the United States of America 106:316–321.

Kim T-K, Hemberg M, Gray JM, Costa AM, Bear DM, Wu J, Harmin D a, Laptewicz M, Barbara-Haley K, Kuersten S, Markenscoff-Papadimitriou E, Kuhl D, Bito H, Worley PF, Kreiman G, Greenberg ME (2010) Widespread transcription at neuronal activity-regulated enhancers. Nature 465:182–187.

Klausner RD, Donaldson JG, Lippincott-Schwartz J (1992) Brefeldin A: insights into the control of membrane traffic and organelle structure. The Journal of cell biology 116:1071–1080.

Köhrmann M, Haubensak W, Hemraj I, Kaether C, Lessmann VJ, Kiebler MA (1999) Fast, convenient, and effective method to transiently transfect primary hippocampal neurons. Journal of Neuroscience Research 58:831–835.

Korb E, Finkbeiner S (2011) Arc in synaptic plasticity: from gene to behavior. Trends in neurosciences 34:591–598.

Krüger C, Cira D, Sommer C, Fischer A, Schäbitz W-R, Schneider A (2006) Long-term gene expression changes in the cortex following cortical ischemia revealed by transcriptional profiling. Experimental neurology 200:135–152.

Kwon SE, Chapman ER (2012) Glycosylation is dispensable for sorting of synaptotagmin 1 but is critical for targeting of SV2 and synaptophysin to recycling synaptic vesicles. The Journal of biological chemistry 287:35658–35668.

Laurén HB, Lopez-Picon FR, Brandt AM, Rios-Rojas CJ, Holopainen IE (2010) Transcriptome analysis of the hippocampal CA1 pyramidal cell region after kainic acid-induced status epilepticus in juvenile rats. PloS one 5:e10733.

Lazzell DR, Belizaire R, Thakur P, Sherry DM, Janz R (2004) SV2B regulates synaptotagmin 1 by direct interaction. The Journal of biological chemistry 279:52124–52131.

Lewis JL, Dong M, Earles CA, Chapman ER (2001) The transmembrane domain of syntaxin 1A is critical for cytoplasmic domain protein-protein interactions. The Journal of biological chemistry 276:15458–15465.

Li C (1995) Distinct Ca2+ and Sr2+ binding properties of synaptotagmins. Journal of Biological Chemistry 270:24898–24902.

Li Y, Wang P, Xu J, Gorelick F, Yamazaki H, Andrews N, Desir G V (2007) Regulation of insulin secretion and GLUT4 trafficking by the calcium sensor synaptotagmin VII. Biochemical and biophysical research communications 362:658–664.

Lin Y, Bloodgood BL, Hauser JL, Lapan AD, Koon AC, Kim T-K, Hu LS, Malik AN, Greenberg ME (2008) Activity-dependent regulation of inhibitory synapse development by Npas4. Nature 455:1198–1204.

Lippincott-Schwartz J, Yuan L, Tipper C, Amherdt M, Orci L, Klausner RD (1991) Brefeldin A's effects on endosomes, lysosomes, and the TGN suggest a general mechanism for regulating organelle structure and membrane traffic. Cell 67:601–616.

Lippincott-Schwartz J, Yuan LC, Bonifacino JS, Klausner RD (1989) Rapid redistribution of Golgi proteins into the ER in cells treated with brefeldin A: evidence for membrane cycling from Golgi to ER. Cell 56:801–813.

Littleton JT, Stern M, Perin M, Bellen HJ (1994) Calcium dependence of neurotransmitter release and rate of spontaneous vesicle fusions are altered in Drosophila synaptotagmin mutants. Proceedings of the National Academy of Sciences of the United States of America 91:10888–10892.

Löscher W (2002) Animal models of epilepsy for the development of antiepileptogenic and disease-modifying drugs. A comparison of the pharmacology of kindling and post-status epilepticus models of temporal lobe epilepsy. Epilepsy research 50:105–123.

Lubin FD, Ren Y, Xu X, Anderson AE (2007) Nuclear factor-kappa B regulates seizure threshold and gene transcription following convulsant stimulation. Journal of neurochemistry 103:1381–1395.

Lynch KL, Martin TFJ (2007) Synaptotagmins I and IX function redundantly in regulated exocytosis but not endocytosis in PC12 cells. Journal of cell science 120:617–627.

Lyons MR, Schwarz CM, West AE (2012) Members of the myocyte enhancer factor 2 transcription factor family differentially regulate Bdnf transcription in response to neuronal depolarization. The Journal of neuroscience : the official journal of the Society for Neuroscience 32:12780–12785.

Lyons MR, West AE (2011) Mechanisms of specificity in neuronal activity-regulated gene transcription. Progress in neurobiology 94:259–295.

Machado HB, Liu W, Vician LJ, Herschman HR (2004) Synaptotagmin IV overexpression inhibits depolarization-induced exocytosis in PC12 cells. Journal of neuroscience research 76:334–341.

Majores M, Schoch S, Lie A, Becker AJ (2007) Molecular neuropathology of temporal lobe epilepsy: Complementary appraches in animal models and human disease tissue. Epilepsia 48:4-12

Marquèze B, Berton F, Seagar M (2000) Synaptotagmins in membrane traffic: which vesicles do the tagmins tag? Biochimie 82:409–420.

Martinez I, Chakrabarti S, Hellevik T, Morehead J, Fowler K, Andrews NW (2000) Synaptotagmin VII regulates Ca(2+)-dependent exocytosis of lysosomes in fibroblasts. The Journal of cell biology 148:1141–1149.

Masliah E, Mallory M, Alford M, DeTeresa R, Hansen LA, McKeel DW, Morris JC (2001) Altered expression of synaptic proteins occurs early during progression of Alzheimer's disease. Neurology 56:127–129.

Matsuoka H, Harada K, Nakamura J, Fukuda M, Inoue M (2011) Differential distribution of synaptotagmin-1, -4, -7, and -9 in rat adrenal chromaffin cells. Cell and tissue research 344:41–50.

Matthew W, Tsavaler L, Reichardt L (1981) Identification of a synaptic vesicle-specific membrane protein with a wide distribution in neuronal and neurosecretory tissue. The Journal of cell biology 91:257–269.

Maximov A, Shin O-H, Liu X, Südhof TC (2007) Synaptotagmin-12, a synaptic vesicle phosphoprotein that modulates spontaneous neurotransmitter release. The Journal of cell biology 176:113–124.

Mayle KM, Le AM, Kamei DT (2012) The intracellular trafficking pathway of transferrin. Biochimica et biophysica acta 1820:264–281.

McCloskey DP, Hintz TM, Pierce JP, Scharfman HE (2006) Stereological methods reveal the robust size and stability of ectopic hilar granule cells after pilocarpine-induced status epilepticus in the adult rat. The European journal of neuroscience 24:2203–2210.

Melicoff E, Sansores-Garcia L, Gomez A, Moreira DC, Datta P, Thakur P, Petrova Y, Siddiqi T, Murthy JN, Dickey BF, Heidelberger R, Adachi R (2009) Synaptotagmin-2 controls regulated exocytosis but not other secretory responses of mast cells. The Journal of biological chemistry 284:19445–19451.

Michaut M, De Blas G, Tomes CN, Yunes R, Fukuda M, Mayorga LS (2001) Synaptotagmin VI participates in the acrosome reaction of human spermatozoa. Developmental biology 235:521–529.

Miltiadous P, Stamatakis A, Koutsoudaki PN, Tiniakos DG, Stylianopoulou F (2011) IGF-I ameliorates hippocampal neurodegeneration and protects against cognitive deficits in an animal model of temporal lobe epilepsy. Experimental neurology 231:223–235.

Miltiadous P, Stamatakis A, Stylianopoulou F (2010) Neuroprotective effects of IGF-I following kainic acid-induced hippocampal degeneration in the rat. Cellular and molecular neurobiology 30:347–360.

Ming G, Song H (2005) Adult neurogenesis in the mammalian central nervous system. Annual review of neuroscience 28:223–250.

Mittelstaedt T, Seifert G, Alvárez-Barón E, Steinhäuser C, Becker A, Schoch S (2009) Differential mRNA Expression Patterns of the Synaptotagmin Gene Family in the Rodent Brain. The Journal of comparative neurology 512:514–528.

Miyake K, McNeil PL (1995) Vesicle accumulation and exocytosis at sites of plasma membrane disruption. The Journal of cell biology 131:1737–1745.

Monterrat C, Grise F, Benassy MN, Hémar A, Lang J (2007) The calcium-sensing protein synaptotagmin 7 is expressed on different endosomal compartments in endocrine, neuroendocrine cells or neurons but not on large dense core vesicles. Histochemistry and cell biology 127:625–632.

Mufson E, Counts S, Ginsberg S (2002) Gene expression profiles of cholinergic nucleus basalis neurons in Alzheimer's disease. Neurochemical research 27:1035–1048.

Mundigl O, Matteoli M, Daniell L, Thomas-Reetz a, Metcalf a, Jahn R, De Camilli P (1993) Synaptic vesicle proteins and early endosomes in cultured hippocampal neurons: differential effects of Brefeldin A in axon and dendrites. The Journal of cell biology 122:1207–1221.

Nadler JV (2003) The recurrent mossy fiber pathway of the epileptic brain. Neurochemical research 28:1649–1658.

Nagy G, Kim JH, Pang ZP, Matti U, Rettig J, Südhof TC, Sørensen JB (2006) Different effects on fast exocytosis induced by synaptotagmin 1 and 2 isoforms and abundance but not by phosphorylation. The Journal of neuroscience : the official journal of the Society for Neuroscience 26:632–643.

Nishijima T, Piriz J, Duflot S, Fernandez AM, Gaitan G, Gomez-Pinedo U, Verdugo JMG, Leroy F, Soya H, Nuñez A, Torres-Aleman I (2010) Neuronal activity drives localized blood-brain-barrier transport of serum insulin-like growth factor-I into the CNS. Neuron 67:834–846.

Okamoto OK, Janjoppi L, Bonone FM, Pansani AP, da Silva A V, Scorza FA, Cavalheiro EA (2010) Whole transcriptome analysis of the hippocampus: toward a molecular portrait of epileptogenesis. BMC genomics 11:230.

Ooe N, Saito K, Mikami N (2004) Identification of a novel basic helix-loop-helix-PAS factor, NXF, reveals a Sim2 competitive, positive regulatory role in dendritic-cytoskeleton modulator drebrin gene. Molecular and cellular biology 24:608–616.

Ooe N, Motonaga K, Kobayashi K, Saito K, Kaneko H (2009a) Functional characterization of basic helix-loop-helix-PAS type transcription factor NXF in vivo: putative involvement in an "on demand" neuroprotection system. The Journal of biological chemistry 284:1057–1063.

Ooe N, Saito K, Kaneko H (2009b) Characterization of functional heterodimer partners in brain for a bHLH-PAS factor NXF. Biochimica et biophysica acta 1789:192–197.

Pang ZP, Bacaj T, Yang X, Zhou P, Xu W, Südhof TC (2011) Doc2 supports spontaneous synaptic transmission by a Ca(2+)-independent mechanism. Neuron 70:244–251.

Pang ZP, Südhof TC (2010) Cell biology of Ca2+-triggered exocytosis. Current opinion in cell biology 22:496–505.

Parent JM, Yu TW, Leibowitz RT, Geschwind DH, Sloviter RS, Lowenstein DH (1997) Dentate granule cell neurogenesis is increased by seizures and contributes to aberrant network reorganization in the adult rat hippocampus. The Journal of neuroscience: the official journal of the Society for Neuroscience 17:3727–3738.

Parent JM, Elliott RC, Pleasure SJ, Barbaro NM, Lowenstein DH (2006a) Aberrant seizure-induced neurogenesis in experimental temporal lobe epilepsy. Annals of neurology 59:81–91.

Parent JM, von dem Bussche N, Lowenstein DH (2006b) Prolonged seizures recruit caudal subventricular zone glial progenitors into the injured hippocampus. Hippocampus 16:321–328.

Park H, Poo M (2013) Neurotrophin regulation of neural circuit development and function. Nature reviews Neuroscience 14:7–23.

Pelham HR (1991) Multiple targets for brefeldin A. Cell 67:449–451.

Perin MS, Fried VA, Mignery GA, Jahn R, Südhof TC (1990) Phospholipid binding by a synaptic vesicle protein homologous to the regulatory region of protein kinase C. Nature 345:260-263

Perin MS, Brose N, Jahn R, Südhof TC (1991) Domain structure of synaptotagmin (p65). The Journal of biological chemistry 266:623–629.

Pintchovski SA, Peebles CL, Kim HJ, Verdin E, Finkbeiner S (2009) The serum response factor and a putative novel transcription factor regulate expression of the immediate-early gene Arc/Arg3.1 in neurons. The Journal of neuroscience: the official journal of the Society for Neuroscience 29:1525–1537.

Pitkänen A, Lukasiuk K (2011) Mechanisms of epileptogenesis and potential treatment targets. Lancet neurology 10:173–186.

Pongratz I, Antonsson C (1998) Role of the PAS Domain in Regulation of Dimerization and DNA Binding Specificity of the Dioxin Receptor. Molecular and cellular and cellular biology 18:4079–4088.

Posern G, Treisman R (2006) Actin' together: serum response factor, its cofactors and the link to signal transduction. Trends in cell biology 16:588–596.

Prescott GR, Gorleku OA, Greaves J, Chamberlain LH (2009) Palmitoylation of the synaptic vesicle fusion machinery. Journal of neurochemistry 110:1135–1149.

Pruunsild P, Sepp M, Orav E, Koppel I, Timmusk T (2011) Identification of cis-elements and transcription factors regulating neuronal activity-dependent transcription of human BDNF gene. The Journal of neuroscience : the official journal of the Society for Neuroscience 31:3295–3308.

Quigg M, Straume M, Menaker M, Bertram EH (1998) Temporal distribution of partial seizures: comparison of an animal model with human partial epilepsy. Annals of neurology 43:748–755.

Radhakrishnan A, Stein A, Jahn R, Fasshauer D (2009) The Ca2+ affinity of synaptotagmin 1 is markedly increased by a specific interaction of its C2B domain with phosphatidylinositol 4,5-bisphosphate. The Journal of biological chemistry 284:25749–25760.

Ramamoorthi K, Fropf R, Belfort GM, Fitzmaurice HL, McKinney RM, Neve RL, Otto T, Lin Y (2011) Npas4 regulates a transcriptional program in CA3 required for contextual memory formation. Science (New York, NY) 334:1669–1675.

Reddy A, Caler E, Andrews N (2001) Plasma membrane repair is mediated by Ca2+-Regulated Exocytosis of Lysosomes. Cell 106:157–169.

Reick M, Garcia JA, Dudley C, McKnight SL (2001) NPAS2: an analog of clock operative in the mammalian forebrain. Science (New York, NY) 293:506–509.

Reid CA, Adams BEL, Myers D, O'Brien TJ, Williams DA (2008) Sub region-specific modulation of synchronous neuronal burst firing after a kainic acid insult in organotypic hippocampal cultures. BMC neuroscience 9.

Reppert S, Weaver D (1997) Forward Genetic Approach Strikes Gold : Cloning of a Mammalian Clock Gene. Cell 89:487–490.

Rizo J, Südhof TC (1998) C2-domains, structure and function of a universal Ca2+-binding domain. Journal of Biological Chemistry 273:15879-15882.

Robinson IM, Ranjan R, Schwarz TL (2002) Synaptotagmins I and IV promote transmitter release independently of Ca(2+) binding in the C(2)A domain. Nature 418:336–340.

Rodríguez-Tornos FM, San Aniceto I, Cubelos B, Nieto M (2013) Enrichment of conserved synaptic activity-responsive element in neuronal genes predicts a coordinated response of MEF2, CREB and SRF. PloS one 8:e53848.

Rotwein P, Burgess SK, Milbrandt JD, Krause JE (1988) Differential expression of insulin-like growth factor genes in rat central nervous system. Proceedings of the National Academy of Sciences of the United States of America 85:265–269.

Routbort MJ, Bausch SB, McNamara JO (1999) Seizures, cell death, and mossy fiber sprouting in kainic acid-treated organotypic hippocampal cultures. Neuroscience 94:755–765.

Saegusa C, Fukuda M, Mikoshiba K (2002) Synaptotagmin V is targeted to dense-core vesicles that undergo calcium-dependent exocytosis in PC12 cells. The Journal of biological chemistry 277:24499–24505.

Sansone L, Reali V, Pellegrini L, Villanova L, Aventaggiato M, Marfe G, Rosa R, Nebbioso M, Tafani M, Fini M, Russo MA, Pucci B (2013) SIRT1 silencing confers neuroprotection through IGF-1 pathway activation. Journal of cellular physiology 228:1754-61.

Scharfman HE, Sollas AE, Berger RE, Goodman JH, Pierce JP (2003) Perforant path activation of ectopic granule cells that are born after pilocarpine-induced seizures. Neuroscience 121:1017–1029.

Schivell AE, Batchelor RH, Bajjalieh SM (1996) Isoform-specific, calcium-regulated interaction of the synaptic vesicle proteins SV2 and synaptotagmin. The Journal of biological chemistry 271:27770–27775.

Schivell AE, Mochida S, Kensel-Hammes P, Custer KL, Bajjalieh SM (2005) SV2A and SV2C contain a unique synaptotagmin-binding site. Molecular and cellular neurosciences 29:56–64.

Schonn J-S, Maximov A, Lao Y, Südhof TC, Sørensen JB (2008) Synaptotagmin-1 and -7 are functionally overlapping Ca2+ sensors for exocytosis in adrenal chromaffin cells. Proceedings of the National Academy of Sciences of the United States of America 105:3998–4003.

Scolnick J, Cui K, Duggan C, Xuan S (2008) Role of IGF Signaling in Olfactory Sensory Map Formation and Axon Guidance. Neuron 57:847–857.

Selvamani A, Sathyan P, Miranda RC, Sohrabji F (2012) An antagomir to microRNA Let7f promotes neuroprotection in an ischemic stroke model. PloS one 7:e32662.

Shearman LP, Zylka MJ, Weaver DR, Kolakowski LF, Reppert SM (1997) Two period homologs: circadian expression and photic regulation in the suprachiasmatic nuclei. Neuron 19:1261–1269.

Shieh K-R, Yang S-C, Lu X-Y, Akil H, Watson SJ (2005) Diurnal rhythmic expression of the rhythm-related genes, rPeriod1, rPeriod2, and rClock, in the rat brain. Journal of biomedical science 12:209–217.

Simantov R, Crispino M, Hoe W, Broutman G, Tocco G, Rothstein JD, Baudry M (1999) Changes in expression of neuronal and glial glutamate transporters in rat hippocampus following kainate-induced seizure activity. Brain research Molecular brain research 65:112–123.

Sørensen JB, Fernández-Chacón R, Südhof TC, Neher E (2003) Examining synaptotagmin 1 function in dense core vesicle exocytosis under direct control of Ca2+. The Journal of general physiology 122:265–276.

Steinhardt RA, Bi G, Alderton JM (1994) Cell membrane resealing by a vesicular mechanism similar to neurotransmitter release. Science (New York, NY) 263:390–393.

Stevens CF, Sullivan JM (2003) The synaptotagmin C2A domain is part of the calcium sensor controlling fast synaptic transmission. Neuron 39:299–308.

Stewart LS, Leung LS (2003) Temporal lobe seizures alter the amplitude and timing of rat behavioral rhythms. Epilepsy & Behavior 4:153–160.

Striegel AR, Biela LM, Evans CS, Wang Z, Delehoy JB, Sutton RB, Chapman ER, Reist NE (2012) Calcium binding by synaptotagmin's C2A domain is an essential element of the electrostatic switch that triggers synchronous synaptic transmission. The Journal of neuroscience : the official journal of the Society for Neuroscience 32:1253–1260.

Südhof TC (2002) Synaptotagmins: why so many? The Journal of biological chemistry 277:7629–7632.

Südhof TC (2012) Calcium control of neurotransmitter release. Cold Spring Harbor perspectives in biology 4:a011353.

Sugita S, Han W, Butz S, Liu X, Fernández-Chacón R, Lao Y, Südhof TC (2001) Synaptotagmin VII as a plasma membrane Ca(2+) sensor in exocytosis. Neuron 30:459–473.

Sugita S, Shin O-H, Han W, Lao Y, Südhof TC (2002) Synaptotagmins form a hierarchy of exocytotic Ca(2+) sensors with distinct Ca(2+) affinities. The EMBO journal 21:270–280.

Sun ZS, Albrecht U, Zhuchenko O, Bailey J, Eichele G, Lee CC (1997) RIGUI, a putative mammalian ortholog of the Drosophila period gene. Cell 90:1003–1011.

Sze C-I, Bi H, Kleinschmidt-DeMasters BK, Filley CM, Martin LJ (2000) Selective regional loss of exocytotic presynaptic vesicle proteins in Alzheimer's disease brains. Journal of the Neurological Sciences 175:81–90.

Tabuchi A, Sakaya H, Kisukeda T, Fushiki H, Tsuda M (2002) Involvement of an upstream stimulatory factor as well as cAMP-responsive element-binding protein in the activation of brain-derived neurotrophic factor gene promoter I. The Journal of biological chemistry 277:35920–35931.

Tauck DL, Nadler J V (1985) Evidence of functional mossy fiber sprouting in hippocampal formation of kainic acid-treated rats. The Journal of neuroscience : the official journal of the Society for Neuroscience 5:1016–1022.

Tei H, Okamura H, Shigeyoshi Y, Fukuhara C, Ozawa R, Hirose M, Sakaki Y (1997) Circadian oscillation of a mammalian homologue of the Drosophila period gene. Nature 389:512–516.

Tinnes S, Schäfer MKE, Flubacher A, Münzner G, Frotscher M, Haas C a (2011) Epileptiform activity interferes with proteolytic processing of Reelin required for dentate granule cell positioning. FASEB journal : official publication of the Federation of American Societies for Experimental Biology 25:1002–1013.

Tocco G, Bi X, Vician L, Lim I (1996) Two synaptotagmin genes Syt1 and Syt4 are differentially regulated in adult brain and during postnatal development following kainic acid-induced seizures. Molecular brain research. Molecular brain research 40:229-39

Tucker WC, Chapman ER (2002) Role of synaptotagmin in Ca2+-triggered exocytosis. The Biochemical journal 366:1–13.

Ubach J, Zhang X, Shao X, Südhof TC, Rizo J (1998) Ca2+ binding to synaptotagmin: how many Ca2+ ions bind to the tip of a C2-domain? The EMBO journal 17:3921–3930.

Van Loo KMJ, Schaub C, Pernhorst K, Yaari Y, Beck H, Schoch S, Becker AJ (2012) Transcriptional regulation of T-type calcium channel CaV3.2: bi-directionality by early growth response 1 (Egr1) and repressor element 1 (RE-1) protein-silencing transcription factor (REST). The Journal of biological chemistry 287:15489–15501.

Veit M, Söllner TH, Rothman JE (1996) Multiple palmitoylation of synaptotagmin and the t-SNARE SNAP-25. FEBS letters 385:119–123.

Vician L, Lim IK, Ferguson G, Tocco G, Baudry M, Herschman HR (1995) Synaptotagmin IV is an immediate early gene induced by depolarization in PC12 cells and in brain. Proceedings of the National Academy of Sciences of the United States of America 92:2164–2168.

Vinet AF, Fukuda M, Descoteaux A (2008) The exocytosis regulator synaptotagmin V controls phagocytosis in macrophages. Journal of immunology (Baltimore, Md : 1950) 181:5289–5295.

Voets T, Moser T, Lund PE, Chow RH, Geppert M, Südhof TC, Neher E (2001) Intracellular calcium dependence of large dense-core vesicle exocytosis in the absence of synaptotagmin I. Proceedings of the National Academy of Sciences of the United States of America 98:11680–11685.

Von Poser C, Ichtchenko K, Shao X (1997) The evolutionary pressure to inactivate. A subclass of synaptotagmins with an amino acid substitution that abolishes Ca2+ binding. Journal of Biological Chemistry 272:14314–14319.

Walther W, Stein U (1996) Cell type specific and inducible promoters for vectors in gene therapy as an approach for cell targeting. Journal of molecular medicine (Berlin, Germany) 74:379–392.

Wang C-T, Lu J-C, Bai J, Chang PY, Martin TFJ, Chapman ER, Jackson MB (2003) Different domains of synaptotagmin control the choice between kiss-and-run and full fusion. Nature 424:943–947.

Wang CT, Grishanin R, Earles CA, Chang PY, Martin TF, Chapman ER, Jackson MB (2001) Synaptotagmin modulation of fusion pore kinetics in regulated exocytosis of dense-core vesicles. Science (New York, NY) 294:1111–1115.

Wang P, Chicka M (2005) Synaptotagmin VII Is Targeted to Secretory Organelles in PC12 Cells, Where It Functions as a High-Affinity Calcium Sensor. Molecular and cellular biology 25:8693–8702.

Wang Z, Chapman ER (2010) Rat and Drosophila synaptotagmin 4 have opposite effects during SNARE-catalyzed membrane fusion. The Journal of biological chemistry 285:30759–30766.

Wieser HG, Häne A (2004) Antiepileptic drug treatment in seizure-free mesial temporal lobe epilepsy patients with hippocampal sclerosis following selective amygdalohippocampectomy. Seizure : the journal of the British Epilepsy Association 13:534–536.

Wine RN, McPherson CA, Harry GJ (2009) IGF-1 and pAKT signaling promote hippocampal CA1 neuronal survival following injury to dentate granule cells. Neurotoxicity research 16:280–292.

Wood SA, Park JE, Brown WJ (1991) Brefeldin A causes a microtubule-mediated fusion of the trans-Golgi network and early endosomes. Cell 67:591–600.

Xiao Z, Gong Y, Wang X-F, Xiao F, Xi Z-Q, Lu Y, Sun H-B (2009) Altered expression of synaptotagmin I in temporal lobe tissue of patients with refractory epilepsy. Journal of molecular neuroscience : MN 38:193–200.

Xu J, Mashimo T, Südhof TC (2007) Synaptotagmin-1, -2, and -9: Ca(2+) sensors for fast release that specify distinct presynaptic properties in subsets of neurons. Neuron 54:567–581.

Yang JW, Czech T, Felizardo M, Baumgartner C, Lubec G (2006) Aberrant expression of cytoskeleton proteins in hippocampus from patients with mesial temporal lobe epilepsy. Amino acids 30:477–493.

Yao J, Kwon SE, Gaffaney JD, Dunning FM, Chapman ER (2012) Uncoupling the roles of synaptotagmin I during endo- and exocytosis of synaptic vesicles. Nature neuroscience 15:243–249.

Ye B, Zhang Y, Song W, Younger SH, Jan LY, Jan YN (2007) Growing dendrites and axons differ in their reliance on the secretory pathway. Cell 130:717–729.

Yi P-L, Chen Y-J, Lin C-T, Chang F-C (2012) Occurrence of epilepsy at different zeitgeber times alters sleep homeostasis differently in rats. Sleep 35:1651–1665.

Yokota N, Uchijima M, Nishizawa S, Namba H, Koide Y, Kontos HA (2001) Identification of Differentially Expressed Genes in Rat Hippocampus After Transient Global Cerebral Ischemia Using Subtractive cDNA Cloning Based on Polymerase Chain Reaction Editorial Comment. Stroke 32:168–174.

Yoo B, Cairns N (2001) Synaptosomal Proteins, Beta-Soluble N-Ethylmaleimide-Sensitive Factor Attachment Protein (Beta-SNAP), Gamma-SNAP and Synaptotagmin I in Brain of Patients with Down Syndrome and Alzheimer ' s Disease. Dementia and geriatric cognitive disorders 12:219–225.

Zaromytidou A-I, Miralles F, Treisman R (2006) MAL and ternary complex factor use different mechanisms to contact a common surface on the serum response factor DNA-binding domain. Molecular and cellular biology 26:4134–4148.

Zeng K, Wang X, Wang Y, Yan Y (2009) Enhanced synaptic vesicle traffic in hippocampus of phenytoin-resistant kindled rats. Neurochemical research 34:899–904.

Zhang JZ, Davletov BA, Südhof TC, Anderson RG (1994) Synaptotagmin I is a high affinity receptor for clathrin AP-2: implications for membrane recycling. Cell 78:751–760.

Zhang Q, Fukuda M, Van Bockstaele E, Pascual O, Haydon PG (2004) Synaptotagmin IV regulates glial glutamate release. Proceedings of the National Academy of Sciences of the United States of America 101:9441–9446.

Zhang S-J, Zou M, Lu L, Lau D, Ditzel DAW, Delucinge-Vivier C, Aso Y, Descombes P, Bading H (2009) Nuclear calcium signaling controls expression of a large gene pool: identification of a gene program for acquired neuroprotection induced by synaptic activity. PLoS genetics 5:e1000604.

Zhang Z, Bhalla A, Dean C, Chapman ER, Jackson MB (2009) Synaptotagmin IV: a multifunctional regulator of peptidergic nerve terminals. Nature neuroscience 12:163–171.

Zhang Z, Zhang Z, Jackson MB (2010) Synaptotagmin IV modulation of vesicle size and fusion pores in PC12 cells. Biophysical journal 98:968–978.

Zhao E, Li Y, Fu X, Zeng L, Zeng H, Jin W, Chen J, Yin G, Qian J, Ying K, Xie Y, Zhao RC, Mao Y (2003) Cloning and Characterization of Human Synaptotagmin 10 Gene. DNA Sequence - The Journal of Sequencing and Mapping 14:393–398.

12   Acknowledgments

The realization of my PhD thesis would not have been possible without the help and support of others. Therefore, I wish to express my gratitude to all people who contributed to this work.

I am indebted to my thesis director Prof. Dr. Susanne Schoch for offering me the opportunity to do my PhD in her lab and for her patient guidance, enthusiastic encouragement and supportive critiques of this research work.

I would like to express my gratitude to Prof. Dr. Albert Haas for his willingness to be my supervisor. I would like to show my appreciation to Prof. Dr. Albert Becker and Prof. Dr. Jörg Höhfeld for their time as part of my thesis committee. I acknowledge the very helpful suggestions and comments of Prof. Dr. Heinz Beck and Prof. Dr. Dirk Dietrich.

Many thanks to all members of AG Schoch and Becker especially to Sabine for the preparation of primary neuronal cultures, to Lioba and Daniela for their kind assistance with brain slices, animals and viruses. I am very thankful to Elena for the great help during my first year and to Ramona for her help during my last year. Additionally, many thanks to Jule for her help with mice. Furthermore, I am much obliged to my office neighbor and friend Karen for her support, her advices for my work, for proofreading my thesis and for the great time in our office. Many thanks to my friends Katharina and Eva for sharing this time with me and for the funny hours in- and outside the lab. In addition, many thanks go to AG Beck and AG Dietrich for interesting retreats and seminars.

I deeply wish to thank my family and friends, especially my parents, for their support, their patience and their honest interest in my thesis. Many thanks to my cousin, Annette, for inspiring me to study biology and for sharing this whole time with me and of course for proofreading my thesis.

And of course I particularly thank Patrick for his constant and lovely encouragement throughout good and hard times during the last years, his critical interest in my work and for proofreading my thesis.